



BIOCHEMICAL ADAPTATIONS IN HOST-PARASITE INTERACTIONS

Michiel L. Bexkens

Biochemical Adaptations in Host-Parasite Interactions

Michiel Leendert Bexkens

Biochemical Adaptations in Host-Parasite Interactions

Biochemische aanpassingen in gastheer-parasiet interacties

Proefschrift

ter verkrijging van de graad van doctor aan de
Erasmus Universiteit Rotterdam
op gezag van de
rector magnificus

Prof.dr. R.C.M.E. Engels

en volgens besluit van het College voor Promoties.
De openbare verdediging zal plaatsvinden op

9 september 2020 om 13.30 uur

door

Michiel Leendert Bexkens
geboren te Breda

ISBN: 978-94-6402-447-0
Cover: Ilse Modder | www.ilsemodder.nl
Lay-out: Ilse Modder | www.ilsemodder.nl
Print: Gildeprint, Enschede | www.gildeprint.nl



© All rights reserved. No part of this book may be reproduced, stored in a retrieval system, or transmitted, in any form or by any means, electronic, mechanical, photocopying, recording or otherwise, without the prior written permission of the copyright holder.

Erasmus University Rotterdam



PROMOTIECOMMISSIE

Promotoren: Prof. dr. H.A. Verbrugh
 Prof. dr. A.G.M. Tielens

Overige leden: Prof. dr. B.M. Bakker
 Prof. dr. C.H. Hokke
 Prof. dr. Y.B. de Rijke

Copromotor: Dr. J.J. van Hellemond

CONTENTS

Chapter 1.	Introduction	11
Chapter 2.	The unusual properties of lactate dehydrogenase of <i>Schistosoma mansoni</i> play a distinct role in metabolic adaptations that occur during the life cycle of this parasite	33
Chapter 3.	<i>Schistosoma mansoni</i> does not and cannot oxidise fatty acids, but these are used for biosynthetic purposes instead	77
Chapter 4.	A mono-acyl phospholipid (20:1 lyso-PS) activates Toll-Like Receptor 2/6 hetero-dimer	109
Chapter 5.	<i>Schistosoma mansoni</i> infection affects the proteome and lipidome of circulating extracellular vesicles in the host	125
Chapter 6.	Lipids are the preferred substrate of the protist <i>Naegleria gruberi</i> , relative of a human brain pathogen	147
Chapter 7.	Summarizing discussion	169
Appendices.	Dutch Summary / Nederlandse samenvatting	189
	Curriculum Vitae	196
	PhD Portfolio	197
	List of Publications	198
	Dankwoord	200



CHAPTER 1

Introduction

ON PARASITES, PARASITISM AND PARASITIC DISEASE

In our lives, we will all encounter parasites, be it aware or unaware. In biomedical sciences parasitism is usually defined as “living in or on an organism of another species (the host) while benefiting by deriving nutrients at the other's expense”. Although pathogenic viruses, bacteria, and fungi can have a parasitic life-style, only parasitic protists (unicellular eukaryotes) and metazoa (multi-cellular eukaryotes) are classified as parasites. Collectively, the global burden of parasitic diseases is gigantic, as it is estimated that parasitic diseases cause close to a million deaths per year and that over 15% of the global population suffers from one or more parasitic diseases (Hotez, Alvarado et al. 2014, Pullan, Smith et al. 2014). In addition, it is estimated that half of the humans who ever lived, have died from a parasitic disease (Drisdelle 2011).

In Western Europe, the disease course of parasitic infections is usually not life-threatening in humans with a properly functioning immune system. In high-income, industrialized countries human exposure to parasites is often limited to a relatively small set of parasites, such as lice, fleas, ticks, pinworms (*Enterobius vermicularis*) and the parasitic protozoa *Giardia lamblia*. The burden of parasitic diseases in Western Europe is limited and predominantly caused by parasitic protozoa of the genus *Cryptosporidium*, *Giardia*, *Toxoplasma*, and *Trichomonas* (Flegr, Prandota et al. 2014, Torgerson, Devleesschauwer et al. 2015).

On a global scale, man is not as fortunate, as it is estimated that over 90% of the population is infected with one or more parasites (Brooker 2010, Hotez, Alvarado et al. 2014, Pullan, Smith et al. 2014, Torgerson, Devleesschauwer et al. 2015). Humans are permissive hosts for over 350 species of parasites (Ashford and Crewe 2003), ranging from small unicellular protists such as *Giardia lamblia* (ca. 10 micrometers) to the intestinal tapeworm *Taenia saginata* that can be as long as 20 meters. Clearly, parasites come in many shapes and sizes.

THE INTRICACY OF COMBATING PARASITES

Eradication or reduction of the disease burden of parasitic infections has proven difficult for several reasons. First, treatment of infected patients aimed at killing the parasite within the human host is hampered by the limited availability of drugs in endemic low and middle-income countries and by the increase in drug-resistant parasites (Wang, Wang et al. 2012, Hong 2018). Second, most parasites can re-infect the same host

organism, because the host does not become immune to the parasite after clearance of the infection upon treatment. This is particularly important for parasitic diseases because most parasites have complicated life-cycles involving many developmental life-cycle stages in two or more hosts. Hence, if the fight against parasitic diseases involves treatment of only one of the host species of the parasite's life cycle (e.g., humans), these hosts quickly become re-infected from the remaining parasite reservoir present in the environment or in the other host species of the parasite. Therefore, it is crucial to block the transmission cycle in order to eradicate a parasitic infection. This often involves active surveillance and treatment of infected patients in combination with actions that prevent reinfection, such as sanitation and safe drinking water for fecal- orally transmitted infections or removal of the vector that transmits the disease. As an example, the treatment and (near) eradication of parasitic guinea worm (*Dracunculus medinensis*) offers a compelling case where the combination of intervention measures was very successful. One year after the infection, adult female guinea worms induce a blister on the skin, generally on the lower parts of legs. As the blister causes a severe burning sensation upon rupturing, the infected patient will attempt to cool this blister in water. When the lesion comes into contact with water, the female guinea worm releases many larvae that can subsequently infect their secondary host; a copepod, a microscopic crustacean that lives in freshwater. The parasite will then develop within the copepod into larvae that can infect humans, in case they swallow the infected copepod. By the introduction of clean-water techniques, i.e., boiling or sieving water before consumption, or drinking water through specially prepared straws, the transmission cycle of this parasitic disease could be interrupted. Thanks to a great effort by many organizations, this parasite is one of the first that is now close to global eradication (Cleveland, Eberhard et al. 2019). However, many more parasite species remain, and despite our best efforts, humans are still plagued by many parasitic diseases. Modern medicine has advanced tremendously over the last 50 years (Brugmans, Thienpont et al. 1971, Gonnert and Andrews 1977, Chabala, Mroziak et al. 1980, Liao 2009) but significant gaps in our knowledge regarding parasites and parasitic diseases are still present. After several millennia of co-evolution, several mechanisms have evolved in parasites by which they successfully avoid to be expelled by the immune system of their hosts (Yazdanbakhsh and Sacks 2010), while other parasites are becoming resistant to the most commonly used drugs (Vanaerschot, Huijben et al. 2014). These traits, combined with the ease of (global) travel, and the advent of global climate change, appear to herald in a new golden age for parasites. This poses us with a challenge: how can we tip the balance in our favor in the fight against parasites?

FINDING THE RIGHT TARGET TO COMBAT PARASITES

From the above-described definition of what parasites are, it can be deduced that a magic bullet against all parasites will be hard to find. Although parasites are a very diverse group of organisms, they do share common traits that might be exploited as their weakness. The most obvious unifying theme that parasites share is the host, without whom the parasites cannot survive. The host provides the parasite with all they require. This does not only include nutrients for energy demands but also molecules that can be used for biosynthetic purposes, such as proteins, and lipids for membrane synthesis.

In parasites, biosynthetic pathways have often become redundant, as parasites directly obtain the required building blocks from their host. For this reason, many anabolic pathways are not an ideal target for anti-parasitic drug development, because these processes are often not used or not essential to the parasite. On the other hand, energy metabolism is crucial for all organisms, because adenosine triphosphate (ATP), which plays in a central role in energy metabolism, cannot be directly obtained from the host and must be (re)generated by the parasite itself. This makes the energy metabolism of the parasite an attractive target for drug intervention, especially as the processing of substrates for energy metabolism in parasites often occurs differently from that in humans/mammals. A striking difference in energy metabolism exists between humans/mammals and parasites. Whereas mammals fully oxidize their substrates for energy metabolism, most parasites use fermentative processing of their substrates. Instead of completely oxidizing their substrates to carbon dioxide via Krebs cycle activity, parasites excrete partly oxidized end-products, such as lactate, acetate, succinate and propionate (Tielens 1994). These differences in metabolic pathways used for energy metabolism offer targets for potential drug interventions to interfere with parasite metabolism, but not with that of the host. This thesis focuses on the energy metabolism of two important parasites, *Schistosoma mansoni* and *Naegleria fowleri*, and the biochemical adaptations of these parasites to live and survive within their host.

SCHISTOSOMA MANSONI, A BLOOD DWELLING PARASITE

Schistosoma mansoni is a parasitic flatworm that causes the human disease schistosomiasis, also known as bilharzia, named after the German physician Dr. Theodor Billharz in 1851. Next to *S. mansoni* several other *Schistosoma* species exist that can infect humans, among which *Schistosoma haematobium* is the most prevalent one. *S. mansoni* has a complex life-cycle that requires a minimum of 10 weeks to complete and

comprises many developmental stages in two distinct hosts (Fig. 1). Adult schistosomes pair up for life and the female worm resides within a cleft of the male schistosome, from which its name was deduced; “schisto-soma”, meaning split-body. Adult schistosomes are blood-dwelling flukes and despite this challenging habitat in which the parasite is exposed to all components of the immune system of the host, the average life span of adult schistosomes is 5 to 10 years with cases reported up to 30 years (Gryseels, Polman et al. 2006, Colley, Bustinduy et al. 2014). The female worms produce eggs of which it is estimated that about 50% is excreted with the feces. The other half of the produced eggs will get trapped in tissues of host, mainly gut and liver tissue. These trapped eggs cause inflammation and tissue damage, which finally results in granuloma formation and tissue fibrosis. The eggshells are rigid structures highly resistant to proteolytic breakdown (deWalick, Bexkens et al. 2011). *Schistosoma* eggs have even been identified in conserved bodies of over 1000's year-old and in pre-historic latrines (Kloos and David 2002, Anastasiou, Lorentz et al. 2014). This pathology explains why schistosomiasis is often asymptomatic at first, but upon time the increasing amounts of trapped eggs will cause organ dysfunction and disease.

Schistosomiasis causes a devastating disease burden of 1.5 million years lived with disability, with over 220 million people at risk of infection, and resulting in approximately 100.000 deaths a year (McManus, Dunne et al. 2018). Treatment is straightforward because the drug praziquantel is efficient, cheap and therefore commonly available in endemic areas. In 2017 over 100 million people received praziquantel either as a treatment for symptomatic schistosomiasis or as a preventive treatment. Unfortunately, a *Schistosoma* infection does not result in protection against a subsequent infection, and therefore, repeated exposure results in infection by an increased number of schistosomes. For this reason, in high endemic areas schistosomiasis is combatted by repeated mass drug administration programs providing praziquantel to the entire population (Doenhoff, Hagan et al. 2009, Gray, McManus et al. 2010, Secor and Montgomery 2015). Despite the massive drug administration programs, schistosomiasis is still a very prevalent disease with an enormous disease burden, which shows that interruption of the transmission cycle (by providing sanitation and hygiene) is crucial for the eradication of this disease. However, as this will for several reasons probably not be achievable in low-income countries, mass drug administration will remain the cornerstone to reduce the disease burden in the near future. The expected downside of mass-drug administration is the inadvertent rise of drug-resistance in schistosomes (Utzinger, Raso et al. 2009, Crellen, Walker et al. 2016). This means that new drugs or interventions are required to continue the battle against schistosomiasis. Therefore, fundamental research is required to identify new targets for anti-schistosomal drug

design. As explained above, energy metabolism is essential for all organisms, and thus also for schistosomes.

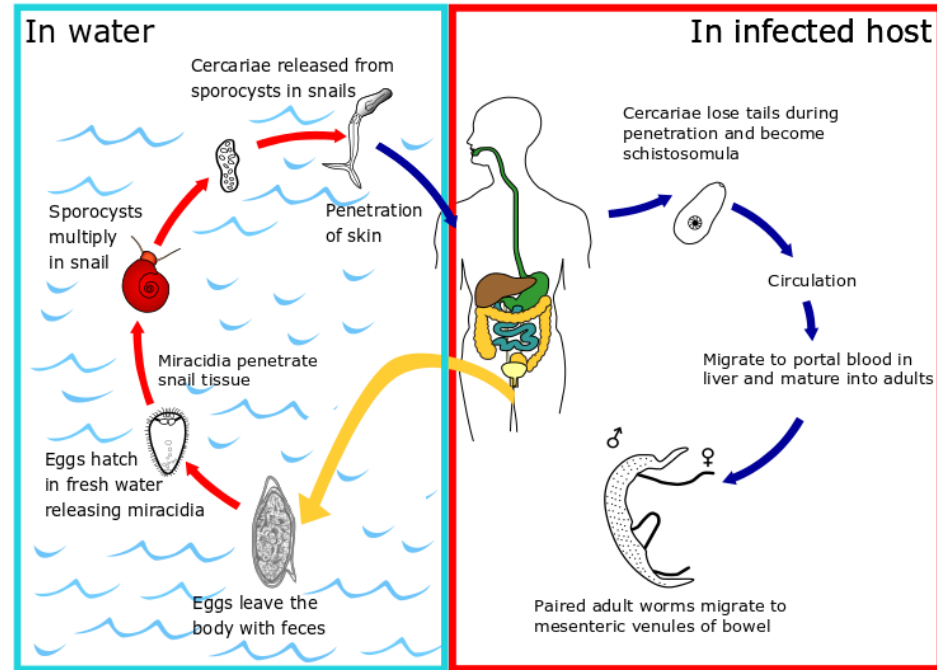


Figure 1. Life cycle of *Schistosoma mansoni*. Eggs are excreted with feces and upon contact with freshwater the eggs hatch and release miracidia. This free-living stage then needs to find and penetrate its intermediate host, a freshwater snail of the genus *Biomphalaria*. After infecting the snail host, the miracidium will develop into sporocysts that after several weeks will produce cercariae that are released from the snail. The free-living cercariae are infectious to humans, as they can penetrate human skin during water contact. After penetration of the skin, cercariae transform into schistosomula which migrate via the venous circulation to the lungs and after a short period via the heart to liver. After migration through the liver, male and female parasites form pairs and mature into adult worms that reside in the mesenteric veins. The female worm produces over 300 eggs a day (one egg, every five minutes) which are deposited in the wall of the mesenteric veins in an effort to reach the intestine to be excreted. Figure from CDC/DPDx, modified.

Residing in the mesenteric veins of the host, provides *S. mansoni* with ideal nutrient conditions; ample availability of glucose, lipids, proteins, and oxygen. In addition, waste products of parasite metabolism can be expelled by the parasite to be cleaned up by the host. Adult schistosomes are fully dependent on carbohydrates (glucose) for their energy metabolism, and although oxygen is available in the mesenteric veins, adult schistosomes are considered to be homo-lactic fermenters as they degrade

most of their glucose by anaerobic glycolysis to lactate. However, a small part of the pyruvate that is generated from glucose by glycolysis is not converted into lactate but instead imported into the mitochondria to be fully oxidized to carbon dioxide by Krebs cycle activity and oxidative phosphorylation (Fig. 2). Hence, *S. mansoni* has the metabolic capacity to degrade carbohydrates either aerobically (via the Krebs cycle) or anaerobically (fermentation to lactate). As complete oxidation of carbohydrates by Krebs cycle activity and oxidative phosphorylation results in ca. 15 fold more ATP production when compared to fermentation to lactate, ATP production in adult schistosomes is still for a large part dependent on oxygen (van Oordt, van den Heuvel et al. 1985). In contrast to adult worms, the free-living stages miracidia and cercariae cannot take up nutrients from their environment (freshwater), and therefore, these stages rely entirely on the limited energy stores, and thus they cannot afford an inefficient energy metabolism. Hence, free-living stages fully oxidize glucose from their glycogen stores into carbon dioxide.

During the development from cercaria to adult worm, the parasite thus shifts from an aerobic to an anaerobic type of energy metabolism. Previous research demonstrated that in schistosomula, this shift depends on the external glucose concentration, as schistosomula incubated in low glucose concentrations degraded glucose into carbon dioxide and in the presence of high glucose concentrations into lactate (Horemans, Tielens et al. 1992). These results showed that the energy metabolism of schistosomula could reversibly and instantaneously be switched from aerobic to anaerobic metabolism depending on the externally available glucose concentration. However, the molecular mechanism by which this interesting phenomenon could be explained is still unresolved.

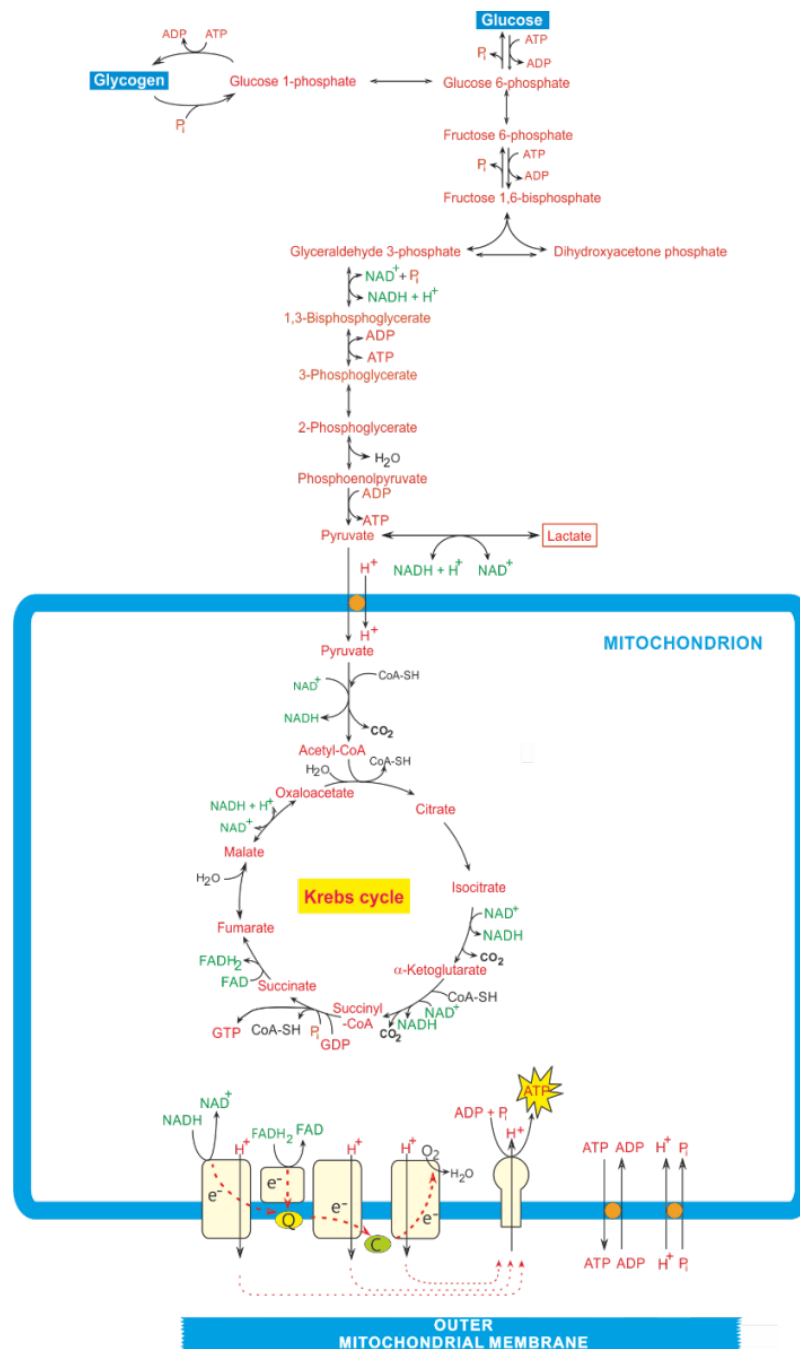


Figure 2. Schematic overview of the energy metabolism of *Schistosoma mansoni*. The energy metabolism of *S. mansoni* relies on carbohydrates, either glucose or glycogen (blue box). Glycolysis is performed after which pyruvate is either converted (anaerobically) to lactate or shuttled into the mitochondria. Here a functional Krebs cycle is present and aerobic processing of pyruvate to carbon dioxide can occur. Subsequent oxidative phosphorylation allows the regeneration of ATP.

NAEGLERIA SPP

Naegleria species are free-living unicellular flagellates with a global distribution (De Jonckheere 2004). This amoeba has three stages in its life cycle: trophozoites, cysts, and a flagellated form (Fig. 3). The trophozoite stage of this amoeba is the replicating stage that can move by the use of pseudopodia. In this stage, it feeds mainly on bacteria. When facing harsher conditions, *Naegleria* has two options. First, it can transform into a flagellate form, which is a swimming stage with increased movement speed to find better conditions elsewhere. Second, it can transform into a cyst stage, which is a dormant stage that can survive for many years even under poor conditions, to later emerge when conditions have improved. Over 40 different *Naegleria* sub-species exist, which can be grouped into eight sub-types based on their genomic content. *Naegleria* species can be found in fresh-water with a temperature range of 0-46 degrees Celsius, depending on their geographic distribution (De Jonckheere 2011).

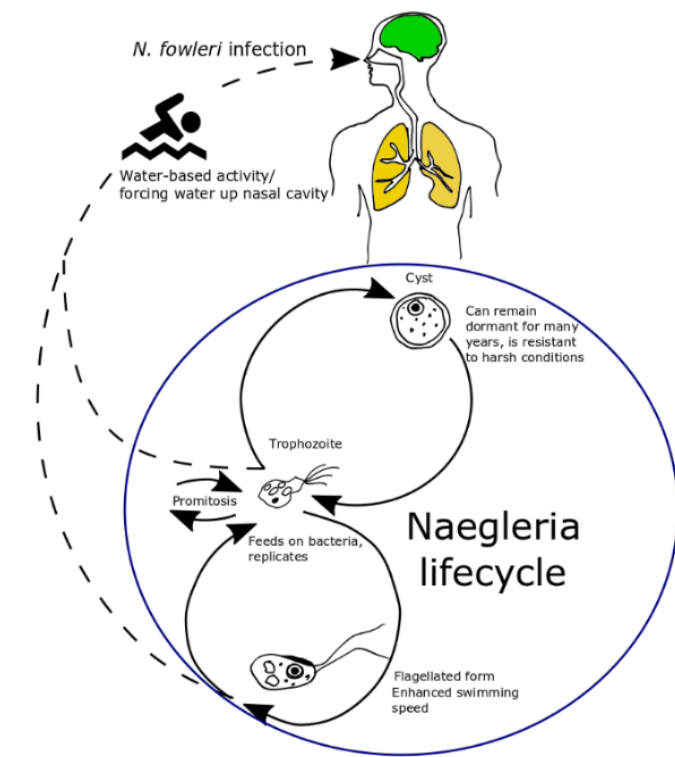


Figure 3. Life cycle stages of *Naegleria fowleri*. *N. fowleri* can be considered to be a facultative parasite, as it also has a complete free-living, self-supporting life cycle. The replicating trophozoite stage of the amoeba feeds mostly on bacteria. In case of unfavorable conditions, the trophozoite can transform to a cyst, and remain dormant for extended periods. Another possibility for the trophozoite is to transform into a flagellated form which has increased motility to migrate to an environment with better conditions. Infection of humans occurs mostly after nasal uptake of contaminated water.

Naegleria fowleri is of particular interest as it is the only subspecies of *Naegleria* known to be infectious to humans. This subspecies of *Naegleria* thrives in freshwater of about 26–46°C and is commonly found near hot springs and bodies of warm natural water. Human infection is thought to occur via the nose, and is often associated with the forceful entry of contaminated water in the nasal cavity i.e., snorting water, falling during water skiing, though merely swimming in these waters can be dangerous (Fig. 3). Children are more often infected than adults, probably because they spend more time playing in water. Members of various religious communities are at special risk to acquire an *N. fowleri* infection (Barnett, Kaplan et al. 1996), as certain religions prescribe ingesting water through the nose to cleanse (wudu), or immersion baptism to cleanse the body. If this water is contaminated with *N. fowleri*, a risk of infection exists (Ghanchi, Khan et al. 2016). Another confounding risk-factor is the behavior associated with the common cold, devices such as neti-pots, or other tools to rinse out the nasal cavities, can cause risk of infection with *N. fowleri* if the water used is contaminated (Yoder, Straif-Bourgeois et al. 2012). Even though *N. fowleri* resides mostly in warm water tropical and subtropical areas, *N. fowleri* has also been detected in milder climates, as continuously warm water (>26°C) is found in natural waters used by factories for cooling purposes. Also, global warming is expected to increase the suitable habitats for *N. fowleri* even more (Diaz 2010, O'Reilly, Sharma et al. 2015, Cooper, Aouthmany et al. 2019) (Fig. 4).

After infection with *N. fowleri* a rapidly progressing disease is initiated that leads to primary amoebic meningoencephalitis (PAM). Fever, headache, neck stiffness, nausea, and vomiting are the most common symptoms, but as these are frequently associated with bacterial meningitis PAM is often misdiagnosed and broad-spectrum antibiotics are given that are ineffective against the amoeba. The classical way to diagnose an *N. fowleri* infection is microscopic inspection of a wet mount of cerebrospinal fluid (CSF). Nowadays, PCR-based detection of the amoeba in CSF is also available in specialized health centers. When PAM is properly diagnosed, specific treatment can be started. However, a highly efficacious treatment is still lacking, and therefore, the mortality rate of PAM is extremely high (over 95%)(Capewell, Harris et al. 2015, Cope and Ali 2016). Therefore, new drugs are urgently needed for effective treatment of PAM.

Recently the core genome of *Naegleria gruberi*, a close relative of *N. fowleri*, was characterized and thereby more insight has been gained into the metabolism of these unusual amoebae (Fritz-Laylin, Prochnik et al. 2010). This study suggested that *N. gruberi* was capable of functioning both aerobically and anaerobically, as genes were identified that encoded all enzymes of the Krebs cycle, a plant-like alternative oxidase and a hydrogenase. Although the combination of all these traits alone warrants more

research to these micro-organisms to determine their place in the evolutionary tree of life, it is also of interest to study in more detail in order to identify new drug targets for PAM as *N. gruberi* is a model organism for *N. fowleri*.

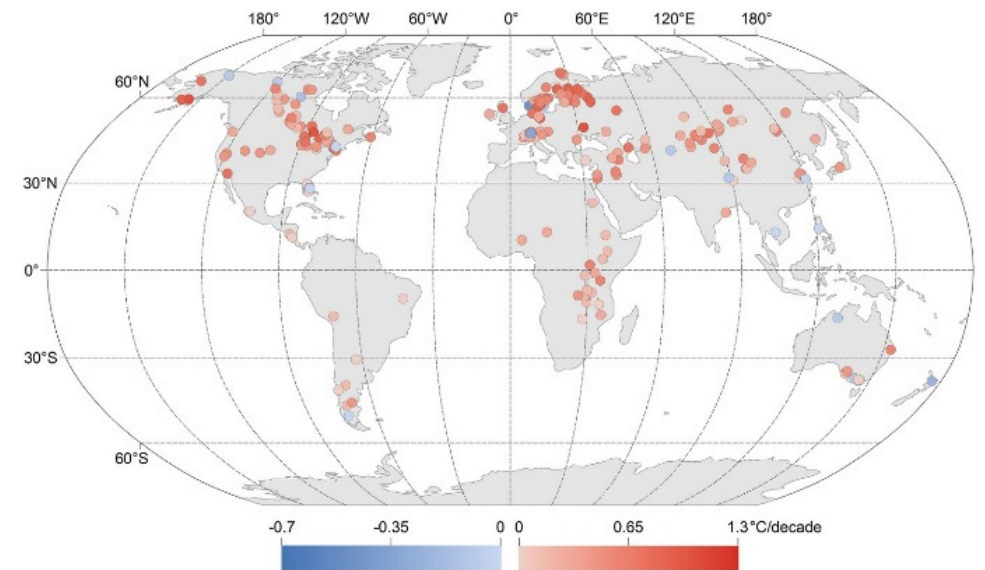


Figure 4. Changes in water temperature in freshwater lakes and spring water sources around the global. Colors indicate temperature change per decade, followed over a 25 year period (1985–2009). Red dots indicate an increase in temperature and blue dots a decrease. This map illustrates the increase in the temperature of freshwater, particularly in the northern hemisphere, thereby potentially increasing the number of suitable habitats for *N. fowleri*.

HOST-PARASITE INTERACTIONS

With the description of all these perilous parasites, one may begin to worry that humans are merely helpless hosts. However, exposure to parasites does not always result in an infection, as the host has several immunological mechanisms to defend itself against pathogens. The first and most important defense mechanism is the skin, as it is water-repellent and provides the first barrier against unwanted intrusion by parasites. Unfortunately, this is not always as effective, parasites such as *Plasmodium* (the causative agent of malaria) use a special tool (the proboscis of a mosquito) to penetrate this barrier. Other parasites such as the cercariae of *Schistosoma* species have special glands filled with enzymes they can release to break down the upper parts of the skin to cross this barrier and gain access to the human body. The other important physical barrier is the mucosa of the gastrointestinal and urinary tract. Many parasite species infect humans by passive oral uptake of dormant stages that can withstand proteolytic degradation in the stomach to reach the intestines. This environment is attractive as it is rich in nutrients and not so challenging in terms of immunological host responses when compared to tissue or blood-dwelling parasites.

PROTECTION AGAINST PATHOGENS

In current literature three types of immunity have been defined; Type 1, providing defense against intracellular pathogens; Type 2, providing defense against helminths, allergens, venoms; Type 3, providing defense versus extracellular bacteria and fungi (Annunziato, Romagnani et al. 2015). Primary recognition of pathogens is performed by the innate immune system, which uses pattern recognition receptors (PRRs) to identify pathogen-associated molecular patterns (PAMPs). Currently, five classes of PRRs have been defined; C-type lectin receptors, nucleotide-binding oligomerization domain leucine-rich repeat-containing receptors (NOD-like receptors), retinoic acid-inducible gene I protein (RIG-I) helicase receptors, cytosolic dsDNA sensors and Toll-like receptors (TLRs) (Ashour 2015). These TLRs are an important and well-studied class of PRRs.

TLRs are present on multiple types of immune cells, such as T-cells, B-cells and dendritic cells, as well as on epithelial cells. TLR 1, 2, 4, 6 and 10 are involved in lipid and lipopeptide recognition, while TLR 5 and 11 recognize proteins and TLR 3, 7, 8, and 9 detect nucleic acids (Ashour 2015). Activation of TLRs is followed by the recruitment of the myddosome complex, which consists of several proteins such as MyD88, IRAK4 and IRAK1. This complex can then activate TRAF6 (All TLRs) or TRAF3 (TLR3 as

well as endocytosed TLR4/CD14 complex). Activation of TRAF6 will ultimately result in the activation of NF- κ B, which then upregulates the expression of pro-inflammatory cytokines, such as IL-6, IL-1 β , IL-12, IL-23 or TGF- β . These cytokines can induce the differentiation of naive lymphocytes to cytotoxic t-lymphocytes, Th1, Th2, or Th17 cells, dependent on which cytokines are released (De Nardo 2015). The cytokines mentioned play a part in the innate immune system and can be called level 1 cytokines, as part of the primary immune system. If the immune system remains activated, i.e. the threat is not neutralized, then the differentiated lymphocytes can release so-called level 2 cytokines, which can act on macrophages, neutrophils and B-cells. This is however a much stronger immune response, which can also have damaging effects to surrounding host tissues (Iwasaki and Medzhitov 2015).

Helminths provoke a type 2 immune response, of which the complete mechanism has not yet been fully elucidated. Helminths are far too large to be phagocytosed by immune cells, such as macrophages. During infection by helminths so-called excretory/secretory (ES) antigens are released by the parasite, which are postulated to influence immune cells of the host (Hewitson, Grainger et al. 2009, White and Artavanis-Tsakonas 2012). Over the years, not only the immune system of the host evolved, the parasites did as well. Hence, host and parasite co-evolved and most parasites still manage to avoid to be expelled by the host. However, for long term survival in the host, it is important for the parasite not to reduce the fitness of the host such that the life-span of the host will be reduced, as this will also limit parasite life-span and thus the amount of progeny the parasite can produce. Hence, successful parasitism is the result of millennia of co-evolution and a delicate balance between benefits for the parasite and being too harmful for the host. Therefore, the parasite has to ensure both parasite and host survival, while at the same time creating optimal conditions for transmission.

The parasitic helminth *S. mansoni* is an intriguing example of complex parasite-host interactions in which offspring production is maximalized and pathology is minimalized. Previous research has demonstrated that *S. mansoni* affects the host immune system by excreting products that skew the immune response (Dunne and Cooke 2005). After infection by cercariae and during the migratory phase of the schistosomula stage, the host reacts initially with a T-helper 1 type of immune response, in which CD4⁺ T-helper cells produce cytokines (such as interleukin 2, IL-2, and interferon-gamma, IFN- γ) to activate macrophages, CD8⁺ T-cells and dendritic cells. The Th-1 type of immune response leads to an increased cell-mediated response, which is typically directed against intracellular bacteria and protozoa. After approximately 6 weeks the worms have matured and the first eggs are deposited. At that time the Th-1 type of immune

response is skewed into a Th-2 immune response. Th2 helper cells lead to a humoral immune response, which is typically directed against extracellular parasites, such as helminths. Th2 helper cells produce specific effector cytokines, such as IL-4 and IL-5, which leads to the outgrowth of eosinophils, basophils, mast cells and B cells that produce IgE antibodies. IL-5 produced by the CD4⁺ T-cells will activate eosinophils to attack helminths. The sudden shift in host immune response from a Th-1 type response into a Th-2 type response is induced by excretion products of the *S. mansoni* egg. Of these excretion products the glycoprotein Omega-1, turned out to be the crucial factor for the induction of a Th2-type of immune response (Everts, Perona-Wright et al. 2009).

Next to the induction of a Th-2 type of immune response, the schistosomal infection also induces a regulatory T-cell response, which is characterized by increased levels of regulatory T-cells (also known as suppressor T-cells), which are classically associated with immune-suppression (Dunne and Cooke 2005). The regulatory T-cell response suppresses the induction of effector T-cells and thereby it reduces the immune reaction which is thought to be critical for *S. mansoni* to establish a long term infection in its host. One of the molecules in *S. mansoni* to play a critical role in the induction of a regulatory T-cell response was identified by van der Kleij et al. in 2002. This molecule, 20:1 lyso-phosphatidylserine, was identified following the purification and analysis of lipid fractions from adult worms. It was shown that addition of the lipid fractions containing lyso-phosphatidylserine to an *in vitro* culture of host immune cells (dendritic cells), induced attenuation of the effector T-cells, making them less responsive to other stimuli. This immune modulating is of interest not only because it is likely to be involved in parasite survival, but also because the inducing factors might be applied in diseases in which an unwanted immune response occurs, such as auto-immune diseases. This brings us to another challenge for science, can we use the good parts from parasites and leave out the bad and the ugly?

SCOPE OF THE THESIS

In this thesis, multiple novel insights into the molecular mechanisms involved in host-parasite interactions are presented. The main topic is the energy metabolism of *S. mansoni* and its interaction with the immune system of the host.

In **Chapter 2**, lactate dehydrogenase (LDH), the pivotal enzyme of *S. mansoni* is discussed. This enzyme was first investigated by Mansour and Bueding over 70 years ago, and these authors already notified the peculiarities of schistosomal LDH

as they stated that “The kinetics of lactic dehydrogenase of *Schistosoma mansoni* are compared to those of rabbit muscle. Differences in the pH optima and in some dissociation constants suggest that these two enzymes are not identical” (Mansour and Bueding 1953). In **Chapter 2** the unusual kinetic properties of LDH from *S. mansoni* are described. Subsequently, these determined kinetic properties and parameters were used to prepare a custom-designed metabolic model to assess both the effect of the external glucose concentration on the switch from aerobic to anaerobic energy metabolism as well as the role of the specific kinetic properties of schistosomal LDH in this switch. These results suggested that the specific features of schistosomal LDH are crucial for the parasite to cope with the rapid changes in glucose concentration in the environments it encounters during its life cycle.

For a long time adult schistosomes were considered to be homo-lactic fermenters and to be entirely dependent on carbohydrates (glucose) for their energy metabolism. Recently, however, following indirect evidence it was postulated that degradation of fatty acids (lipids) by beta-oxidation is essential for egg production by the female schistosome (Huang, Freitas et al. 2012). As these observations contradicted previous investigations of our research group, we performed a comprehensive study towards lipid metabolism in schistosomes. For this, schistosomes were incubated with radioactively ¹⁴C- labeled lipids, after which the metabolic fate of the lipids was traced. The results are described in **Chapter 3** and showed that although schistosomes do not and cannot oxidize fatty acids, these are essential for anabolic processes involved in egg production.

The role that lipids can play in host-parasite interactions is further discussed in **Chapter 4**. Here is reported the results of a study in which we have synthesized phospholipids identical to those that were reported to be produced by *S. mansoni* and to affect host immune cells such that a regulatory T-cell response was induced (Van der Kleij, Latz et al. 2002). The developed biosynthetic method allowed us not only to confirm that 20:1 lyso-PS can activate TLR2, it also allowed the synthesis of lysophospholipid variants to determine the most potent lysophospholipid agonist for TLR2. The developed biosynthetic method to produce these lysophospholipids opens the possibility for future studies on therapeutic applications of these molecules to induce suppression of undesirable immune reactions, such as allergy.

Since these special lysophospholipids are known to be present in large amounts in the outer-surface of adult schistosomes, it is tempting to speculate that these lysophospholipids are excreted and affect the host immune cells *in vivo*. However, previous studies demonstrated that these schistosome-specific lysophospholipids could

not be detected in blood plasma of infected hosts (Retra, deWalick et al. 2015). Since lysophospholipids are amphipathic molecules, they will easily insert into membranes of surrounding cells or possibly also in extracellular vesicles that are also present in blood plasma. Since extracellular vesicles play an important role in intercellular communication (Raposo and Stoorvogel 2013, Yanez-Mo, Siljander et al. 2015), we have isolated these small extracellular vesicles from host blood and determined the lipid and protein content of these vesicles. **Chapter 5** describes the results of this study, which demonstrated that both the lipid and protein composition of circulating extracellular vesicles differ between hamsters (*Mesocricetus auratus*) infected with *S. mansoni* and non-infected ones. These results suggest that extracellular vesicles can play a role in the complex host-schistosome interaction.

Our knowledge of carbohydrate and lipid metabolism was applied to a different parasite, with a fascinating metabolism, *Naegleria fowleri*. Recently, the core genome of the *N. fowleri* model organism, *Naegleria gruberi* was published and several interesting hypotheses were postulated on the oxygen requirements of *Naegleria* (Fritz-Laylin, Prochnik et al. 2010). Using the model organism *N. gruberi* we analyzed the metabolic capacities, substrate preferences, and end-product formation under various (an)aerobic conditions of these amoebae. The results are presented in **Chapter 6** and showed that lipids are the preferred substrate of the amoeba. A, so far, unprecedented feature among eukaryotes.

Finally, in the summarizing discussion in **Chapter 7**, the implications are discussed and recommendations for further research are proposed.

REFERENCES

- Anastasiou, E., K. O. Lorentz, G. J. Stein and P. D. Mitchell (2014). "Prehistoric schistosomiasis parasite found in the Middle East." *The Lancet Infectious Diseases* **14**(7): 553-554.
- Annunziato, F., C. Romagnani and S. Romagnani (2015). "The 3 major types of innate and adaptive cell-mediated effector immunity." *Journal of Allergy and Clinical Immunology* **135**(3): 626-635.
- Artemisinin structure research group, g. (1977). "A new type of sesquiterpene lactone—artemisinin." *Chinese Science Bulletin* **22**: 142.
- Ashford, R. and W. Crewe (2003). *Parasites of Homo sapiens: An Annotated Checklist of the Protozoa, Helminths and Arthropods for which we are Home*, CRC Press.
- Ashour, D. S. (2015). "Toll-like receptor signaling in parasitic infections." *Expert Review of Clinical Immunology* **11**(6): 771-780.
- Barnett, N. D. P., A. M. Kaplan, R. J. Hopkin, M. A. Saubolle and M. F. Rudinsky (1996). "Primary amoebic meningoencephalitis with *Naegleria fowleri*: clinical review." *Pediatric neurology* **15**(3): 230-234.
- Brooker, S. (2010). "Estimating the global distribution and disease burden of intestinal nematode infections: adding up the numbers--a review." *International Journal for Parasitology* **40**(10): 1137-1144.
- Brugmans, J. P., D. C. Thienpont, I. van Wijngaarden, O. F. Vanparijs, V. L. Schuermans and H. L. Lauwers (1971). "Mebendazole in Enterobiasis Radiochemical and Pilot Clinical Study in 1,278 Subjects." *Journal of the American Medical Association* **217**(3): 313-316.
- Capewell, L. G., A. M. Harris, J. S. Yoder, J. R. Cope, B. A. Eddy, S. L. Roy, G. S. Visvesvara, L. M. Fox and M. J. Beach (2015). "Diagnosis, Clinical Course, and Treatment of Primary Amoebic Meningoencephalitis in the United States, 1937-2013." *Journal of Pediatric Infectious Disease Society* **4**(4): e68-75.
- Chabala, J. C., H. Mrozk, et al. (1980). "Ivermectin, a new broad-spectrum antiparasitic agent." *Journal of Medicinal Chemistry* **23**(10): 1134-1136.
- Cleveland, C. A., M. L. Eberhard, et al. (2019). "A search for tiny dragons (*Dracunculus medinensis* third-stage larvae) in aquatic animals in Chad, Africa." *Scientific Reports* **9**(1): 375.
- Colley, D. G., A. L. Bustinduy, E. Secor and C. H. King (2014). "Human schistosomiasis." *Lancet* **383**(9936): 2253-2264.
- Cooper, A. M., S. Aouthmany, K. Shah and P. P. Rega (2019). "Killer amoebas: Primary amoebic meningoencephalitis in a changing climate." *Journal of the American Academy of PAs* **32**(6): 30-35.
- Cope, J. R. and I. K. Ali (2016). "Primary Amebic Meningoencephalitis: What Have We Learned in the Last 5 Years?" *Curr Infect Dis Rep* **18**(10): 31.
- Crellen, T., M. Walker, P. H. L. Lamberton, N. B. Kabatereine, E. M. Tukahebwa, J. A. Cotton and J. P. Webster (2016). "Reduced efficacy of praziquantel against *Schistosoma mansoni* is associated with multiple rounds of mass drug administration." *Clinical Infectious Diseases* **63**(9): 1151-1159.
- De Jonckheere, J. F. (2004). "Molecular definition and the ubiquity of species in the genus *Naegleria*." *Protist* **155**(1): 89-103.
- De Jonckheere, J. F. (2011). "Origin and evolution of the worldwide distributed pathogenic amoeboflagellate

- Naegleria fowleri*." *Infection Genetics and Evolution* **11**(7): 1520-1528.
- De Nardo, D. (2015). "Toll-like receptors: Activation, signalling and transcriptional modulation." *Cytokine* **74**(2): 181-189.
- deWalick, S., M. L. Bexkens, et al. (2011). "The proteome of the insoluble *Schistosoma mansoni* eggshell skeleton." *International Journal for Parasitology* **41**(5): 523-532.
- Diaz, J. H. (2010). "Increasing intracerebral infections caused by free-living amebae in the United States and worldwide." *Journal of Neuroparasitology* **1**: 23-32.
- Doenhoff, M. J., P. Hagan, et al. (2009). "Praziquantel: its use in control of schistosomiasis in sub-Saharan Africa and current research needs." *Parasitology* **136**(13): 1825-1835.
- Drisdelle, R. (2011). *Parasites: Tales of Humanity's Most Unwelcome Guests*, University of California Press.
- Dunne, D. W. and A. Cooke (2005). "A worm's eye view of the immune system: consequences for evolution of human autoimmune disease." *Nature Reviews Immunology* **5**: 420-426.
- Everts, B., G. Perona-Wright, et al. (2009). "Omega-1, a glycoprotein secreted by *Schistosoma mansoni* eggs, drives Th2 responses." *Journal of Experimental Medicine* **206**(8): 1673-1680.
- Fleg, J., J. Prandota, M. Sovičková and Z. H. Israeli (2014). "Toxoplasmosis – A Global Threat. Correlation of Latent Toxoplasmosis with Specific Disease Burden in a Set of 88 Countries." *Plos One* **9**(3): e90203.
- Fritz-Laylin, L. K., S. E. Prochnik, et al. (2010). "The genome of *Naegleria gruberi* illuminates early eukaryotic versatility." *Cell* **140**(5): 631-642.
- Ghanchi, N. K., E. Khan, A. Khan, W. Muhammad, F. R. Malik and A. Zafar (2016). "*Naegleria fowleri* Meningoencephalitis Associated with Public Water Supply, Pakistan, 2014." *Emerging infectious diseases* **22**(10): 1835-1837.
- Gonnert, R. and P. Andrews (1977). "Praziquantel, a new board-spectrum antischistosomal agent." *Zeitschrift der Parasitenkunde* **52**(2): 129-150.
- Gray, D. J., D. P. McManus, Y. Li, G. M. Williams, R. Bergquist and A. G. Ross (2010). "Schistosomiasis elimination: lessons from the past guide the future." *Lancet Infectious Diseases* **10**(10): 733-736.
- Gryseels, B., K. Polman, J. Clerinx and L. Kestens (2006). "Human schistosomiasis." *Lancet* **368**(9541): 1106-1118.
- Hewitson, J. P., J. R. Grainger and R. M. Maizels (2009). "Helminth immunoregulation: the role of parasite secreted proteins in modulating host immunity." *Molecular and Biochemical Parasitology* **167**(1): 1-11.
- Hong, S. T. (2018). "Albendazole and Praziquantel: Review and Safety Monitoring in Korea." *Infection & chemotherapy* **50**(1): 1-10.
- Horemans, A. M. C., A. G. M. Tielens and S. G. van den Bergh (1992). "The reversible effect of glucose on the energy metabolism of *Schistosoma mansoni* cercariae and schistosomula." *Molecular and Biochemical Parasitology* **51**(1): 73-79.
- Hotez, P. J., M. Alvarado, et al. (2014). "The Global Burden of Disease Study 2010: Interpretation and Implications for the Neglected Tropical Diseases." *PLoS neglected tropical diseases* **8**(7).
- Huang, S. C.-C., T. C. Freitas, E. Amiel, B. Everts, E. L. Pearce, J. B. Lok and E. J. Pearce (2012). "Fatty Acid Oxidation Is Essential for Egg Production by the Parasitic Flatworm *Schistosoma mansoni*." *Plos*

Pathogens **8**(10).

- Iwasaki, A. and R. Medzhitov (2015). "Control of adaptive immunity by the innate immune system." *Nature Immunology* **16**(4): 343-353.
- Kloos, H. and R. David (2002). "The paleoepidemiology of schistosomiasis in ancient Egypt." *Human Ecology Review*: 14-25.
- Mansour, T. E. and E. Bueding (1953). "Kinetics of lactic dehydrogenases of *Schistosoma mansoni* and of rabbit muscle." *British Journal of Pharmacology* **8**(4): 431-434.
- McManus, D. P., D. W. Dunne, M. Sacko, J. Utzinger, B. J. Vennervald and X.-N. Zhou (2018). "Schistosomiasis." *Nature Reviews Disease Primers* **4**(1): 13.
- O'Reilly, C. M., S. Sharma, et al. (2015). "Rapid and highly variable warming of lake surface waters around the globe." *Geophysical Research Letters* **42**(24): 10,773-710,781.
- Pullan, R. L., J. L. Smith, R. Jasrasaria and S. J. Brooker (2014). "Global numbers of infection and disease burden of soil transmitted helminth infections in 2010." *Parasites & Vectors* **7**(1): 37.
- Raposo, G. and W. Stoorvogel (2013). "Extracellular vesicles: Exosomes, microvesicles, and friends." *The Journal of Cell Biology* **200**(4): 373-383.
- Retra, K., S. deWalick, M. Schmitz, M. Yazdanbakhsh, A. G. M. Tielens, J. F. H. M. Brouwers and J. J. van Hellemond (2015). "The tegumental surface membranes of *Schistosoma mansoni* are enriched in parasite-specific phospholipid species." *International journal for parasitology* **45**(9-10): 629-636.
- Secor, W. E. and S. P. Montgomery (2015). "Something old, something new: is praziquantel enough for schistosomiasis control?" *Future medicinal chemistry* **7**(6): 681-684.
- Tielens, A. G. M. (1994). "Energy generation in parasitic helminths." *Parasitology today* **10**(9): 346-352.
- Torgerson, P. R., B. Devleeschauwer, et al. (2015). "World Health Organization Estimates of the Global and Regional Disease Burden of 11 Foodborne Parasitic Diseases, 2010: A Data Synthesis." *Plos Medicine* **12**(12): e1001920.
- Utzinger, J., G. Raso, S. Brooker, D. de Savigny, M. Tanner, N. Ornberg, B. H. Singer and E. K. N'Goran (2009). "Schistosomiasis and neglected tropical diseases: towards integrated and sustainable control and a word of caution." *Parasitology* **136**(13): 1859-1874.
- Van der Kleij, D., E. Latz, et al. (2002). "A novel host-parasite lipid cross-talk - Schistosomal lyso-phosphatidylserine activates Toll-like receptor 2 and affects immune polarization." *Journal of Biological Chemistry* **277**(50): 48122-48129.
- van Oordt, B. E. P., J. M. van den Heuvel, A. G. M. Tielens and S. G. van den Bergh (1985). "The energy production of the adult *Schistosoma mansoni* is for a large part aerobic." *Molecular and Biochemical Parasitology* **16**(2): 117-126.
- Vanaerschot, M., S. Huijben, F. Van den Broeck and J.-C. Dujardin (2014). "Drug resistance in vectorborne parasites: multiple actors and scenarios for an evolutionary arms race." *FEMS Microbiology Reviews* **38**(1): 41-55.
- Wang, W., L. Wang and Y.-S. Liang (2012). "Susceptibility or resistance of praziquantel in human schistosomiasis: a review." *Parasitology Research* **111**(5): 1871-1877.

- White, R. R. and K. Artavanis-Tsakonas (2012). "How helminths use excretory secretory fractions to modulate dendritic cells." Virulence **3**(7): 668-677.
- Yanez-Mo, M., P. R. M. Siljander, et al. (2015). "Biological properties of extracellular vesicles and their physiological functions." Journal of extracellular vesicles **4**: 27066.
- Yazdanbakhsh, M. and D. L. Sacks (2010). "Why does immunity to parasites take so long to develop?" Nature reviews Immunology **10**(2): 80-81.
- Yoder, J. S., S. Straif-Bourgeois, et al. (2012). "Primary Amebic Meningoencephalitis Deaths Associated With Sinus Irrigation Using Contaminated Tap Water." Clinical Infectious Diseases **55**(9): e79-e85.



CHAPTER 2

The unusual properties of lactate dehydrogenase of *Schistosoma mansoni* play a distinct role in metabolic adaptations that occur during the life cycle of this parasite

Michiel L. Bexkens¹, Olivier M.F. Martin², Jos M. van den Heuvel³, Marion G.J. Schmitz³, Bas Teusink², Jurgan R. Haanstra², Jaap J. van Hellemond¹, Malcolm D. Walkinshaw⁴, Aloysius G.M. Tielens^{1,3}

1. Department of Medical Microbiology and Infectious Diseases, Erasmus MC, Rotterdam, The Netherlands
2. Systems Biology Lab, AIMMS, Vrije Universiteit Amsterdam, Amsterdam, The Netherlands
3. Department of Biochemistry and Cell Biology, Faculty of Veterinary Medicine, Utrecht University, Utrecht, The Netherlands
4. The Centre for Translational and Chemical Biology, School of Biological Sciences, The University of Edinburgh, Edinburgh, United Kingdom

Supplementary data associated with this article:

- Figures S1-S4
- Building the kinetic model
- Description of the kinetic model

Manuscript in preparation

ABSTRACT

Here we show that lactate dehydrogenase (LDH) from *Schistosoma mansoni* has peculiar properties for a eukaryotic LDH. Schistosomal LDH (SmLDH) isolated from schistosomes, as well as the recombinantly expressed protein, is strongly inhibited by ATP, which is released by fructose-1,6-bisphosphate (FBP).

In the conserved FBP/anion binding site we identified two residues in SmLDH (Val187 and Tyr190) that differ from the conserved residues in LDHs of other eukaryotes, but are identical to conserved residues in FBP-sensitive LDHs of prokaryotes.

3D-models were generated to compare the structure of SmLDH with other LDHs. These models indicated that residues Val187 and especially Tyr190 play a crucial role in the interaction of FBP with the anion pocket of SmLDH. These 3D-models of SmLDH are consistent with a competitive model of SmLDH inhibition in which ATP (inhibitor) and FBP (activator) compete for binding in a well-defined anion pocket. The model of bound ATP predicts a distortion of the nearby key catalytic residue His195, resulting in enzyme inhibition.

To investigate a possible physiological role of this allosteric regulation of LDH in schistosomes we made a kinetic model in which the allosteric regulation of the glycolytic enzymes can be varied. The model showed that inhibition of LDH by ATP prevents fermentation to lactate in the free-living stages in water and ensures oxidation of the endogenous glycogen reserves via the Krebs cycle. This prevents the untimely depletion of these glycogen reserves, the only fuel of the free-living cercariae. The release of this ATP inhibition of LDH by FBP prevents glycolysis to run wild when *S. mansoni* cercariae are confronted with a sudden large increase in glucose availability upon penetration of the final host. Apparently, the LDH of *S. mansoni* is adapted and very suitable to deal with the variation in glucose availability the parasite encounters during its life cycle.

HIGHLIGHTS

- Lactate dehydrogenase (LDH) of *S. mansoni* is allosterically regulated
- The active site of LDH from *S. mansoni* closely resembles that of prokaryotic LDH
- ATP inhibits LDH of *S. mansoni*, and this inhibition can be released by FBP
- LDH inhibition by ATP is an advantage in the free-living stages of *S. mansoni*
- Release of the ATP inhibition by FBP is crucial for survival in the final host

INTRODUCTION

The lifecycle of *S. mansoni* comprises free-living and parasitic stages which encounter environmental conditions that differ in substrate availability. The free-living stages of *S. mansoni*, cercariae and miracidia, use as energy source their endogenous glycogen stores, which are largely aerobically degraded via the Krebs cycle to CO₂, while generating ATP mainly via oxidative phosphorylation (Bruce, Weiss et al. 1969, Van Oordt, Tielens et al. 1989, Tielens, Van de Pas et al. 1991). Adult *S. mansoni* worms on the other hand live in the bloodstream of the final host, humans. They consume glucose present in the bloodstream of this host and produce mainly lactate (Bueding 1950, Tielens, Van Oordt et al. 1989). This switch in the energy metabolism of *S. mansoni* from an aerobic metabolism to lactate fermentation occurs immediately after penetration of the final host by the cercariae and is caused by the sudden increase in the availability of glucose (Horemans et al. 1991; Horemans et al. 1992). The yeast *Saccharomyces cerevisiae* is also known to use a fermentative metabolism when glucose is in excess which suppresses respiration, a metabolic feature that is generally referred to as the Crabtree effect (Pronk et al. 1996).

Lactate dehydrogenase (LDH) catalyzes the interconversion of pyruvate and lactate. LDH is one of the best characterized enzymes in terms of protein evolution, folding, catalytic mechanism, stability, and three-dimensional structure and this enzyme has been purified and characterized in archae, eukaryotes and prokaryotes (Birkoft, Fernley et al. 1982, Madern 2002). Here we focus on a eukaryotic fructose 1,6-bisphosphate (FBP) sensitive LDH discovered in the human parasitic helminth *Schistosoma mansoni* (Tielens, 1997). Its structural characteristics are compared with prokaryotic FBP-sensitive LDHs and the canonical eukaryotic orthologues that are not FBP-sensitive.

NADH-dependent L-lactate dehydrogenases (L-LDH, EC 1.1.1.27) catalyze the reversible reduction of pyruvate to lactate with the simultaneous oxidation of NADH to NAD⁺. The NADH-dependent L-LDHs form together with NAD(P)H-dependent L-malate dehydrogenases (L-MDH) a large super family of dehydrogenases which have been very well characterized. NADH-dependent L-LDHs are tetrameric enzymes where each subunit functions independently and cooperativity between the catalytic sites is not observed. The active site of each subunit consists of a well-defined pocket. The side chains of Arg171, Gln102 and Thr250 form direct hydrogen bonds with the pyruvate substrate¹. Other key catalytic residues including His195, Asp 168 and Asp53 line

¹ Throughout this paper, numbering of the amino acids in LDH is according to Eventoff et al., 1977.

the pocket and facilitate transfer of electrons from the coenzyme NADH to pyruvate. Despite a relatively low amino acid sequence identity, considerable structural identity is observed between the crystal structures of LDH and MDH (Goward and Nicholls 1994). Many prokaryote NADH-dependent L-LDHs are allosterically activated by FBP, an intermediate of glycolysis (Garvie 1980, Iwata and Ohta 1993, Fushinobu, Kamata et al. 1996). A few preliminary findings of FBP-sensitivity of LDH in eukaryotes were reported, but these have never been pursued (Lloyd 1983, Brennan, Holder et al. 1995, Tielens 1997). The allosteric regulation of L-LDHs of prokaryotes on the other hand has been studied extensively (Iwata and Ohta 1993, Iwata, Kamata et al. 1994, Fushinobu, Kamata et al. 1996) and these LDHs all consist of four identical monomers arranged around what are conventionally known as the *P*, *Q* and *R* axes (Adams, Liljas et al. 1973). Each monomer has one active site and the tetramer has two allosteric FBP-binding sites, each situated at the interface between two monomers, which correspond to the so-called anion-binding sites of the vertebrate enzymes (Grau, Trommer et al. 1981, Wigley, Gamblin et al. 1992).

In the FBP-binding site of prokaryotic LDHs, an FBP molecule interacts with four positively charged residues, Arg173 and His188 of two juxtaposed subunits, thereby stabilizing the tetramer by forming a bridge between the subunits (Wigley, Gamblin et al. 1992, Iwata, Kamata et al. 1994). Eukaryotic LDHs, on the other hand, have an N-terminal extension of about 13-20 residues, which is absent in prokaryotic LDHs (Adams, Liljas et al. 1973, Iwata, Kamata et al. 1994). This N-terminal extension forms an extended conformation, wraps around the adjacent subunit in the tetramer and provides an alternative mechanism for stabilizing the tetrameric quaternary structure of eukaryotic L-LDHs (Read, Winter et al. 2001).

It has been suggested that in prokaryotes a system evolved that enables LDH to be fully active only when FBP levels are high, which is in times of high glucose availability (Wigley, Gamblin et al. 1992). Under less favorable conditions, LDH activity is reduced and pyruvate, instead of being converted to lactate and then excreted, passes mainly into the Krebs cycle, which results in more ATP per glucose degraded. In this paper we propose such a metabolic switch orchestrated by allosterically regulated LDH is not exclusive to prokaryotes but exists also in *S. mansoni*. The sensitivity of SmLDH to ATP and FBP prevents not only the inefficient fermentation of the endogenous glycogen reserves of the free-living stages but also prevents a fatal accumulation of glycolytic intermediates which would otherwise occur after penetration of the final host, caused by the presence of high glucose levels in this new environment.

MATERIAL AND METHODS

Chemicals

All chemicals used were from Sigma Aldrich, St. Louis, Missouri, United states of America unless otherwise indicated.

Purification of native lactate dehydrogenase from adult *S. mansoni* worms

Adult *S. mansoni* worms (Puerto Rican Strain) were harvested from Golden Hamsters, 6-7 weeks post-infection. After isolation, adult worms were washed in ice-cold buffer A which consisted of 25 mM imidazole, 1 mM EDTA, 50 mM glucose and 20 mM thioglycerol. Worms were homogenized with an ultra-turrax in 5 ml buffer A supplemented with 0.25 mM NADH and 2 mM FBP. The homogenate was sonicated on ice 10 times intermittently for 15 seconds, with a 10 second rest in between pulses and subsequently centrifuged for 30 minutes at 48,000*g*, 4°C. The supernatant was filtered over a fine mesh and taken up in a final volume of 20 ml buffer A supplemented with 0.25 mM NADH and 2 mM FBP. This sample was applied to a DEAE column, which was eluted with buffer A. The fractions containing LDH activity were pooled and NADH, FBP and NaCl were added to reach final concentrations of 0.25 mM, 2 mM and 0.5 M respectively.

A DEAE-sepharose 4B affinity column was prepared via the following procedure, AH-sepharose 4B was soaked in 0.5 M NaCl, washed over a filter with 300ml 0.5 M NaCl followed by 100 ml H₂O. Potassium oxalate (1.1 g) was dissolved in 5 ml water and added to the sepharose. N-(3-Dimethylaminopropyl)-N'-ethylcarbodiimide hydrochloride (EDC-HCl) was dissolved (0.9 g in 1.5 ml H₂O), and added while keeping the pH at 7.5 for 75 minutes. The reaction was continued for 48 hours while shaking gently. The sepharose was washed with acetate-buffer (0.1 M acetate, 0.5 M NaCl, pH 4) before being washed with Tris/HCl buffer (0.1 M Tris/HCl, 0.5 M NaCl, pH8) and was washed with acetate-buffer once more. The column was rinsed with buffer A supplemented with 0.5 M NaCl, 0.25 mM NADH and 2 mM FBP prior to loading the *S. mansoni* sample. The column was then rinsed with 30 ml of the same buffer before starting the elution. Elution buffer was the same buffer but now without NADH. Fractions of 1 ml were collected and screened for LDH activity.

Recombinant expression of r-SmLDH

For recombinant expression of the *S. mansoni* protein lactate dehydrogenase (r-SmLDH), cDNA was prepared from RNA isolated from adult *S. mansoni* worms (Puerto Rico strain) as described earlier (Van Grinsven, Van Hellemond et al. 2009). In short, worms were snap frozen and ground up in liquid nitrogen, and dissolved in TRIzol reagent (Invitrogen, Breda, The Netherlands). Total RNA was extracted following the manufacturer's instructions

and cDNA was prepared using oligo-dT primers and ImProm-II™ Reverse Transcriptase (Promega, Leiden, The Netherlands). This cDNA was used as target in a polymerase chain reaction (PCR) with the primers SmLDHFwd (5'- **aagctagc**atgtcatctatatgcgatgt-3') and SmLDHRev (5'- **ggatcc**taatggatggtgatggtgccattgatccccgttat-3'). These primers contained two restriction sites, **BamHI** and **NheI** (indicated in **bold** in the forward and reverse primer respectively) and a *6xHIS motif*, (underlined in the reverse primer). A fragment of 1063 base pairs was amplified and inserted in the PGEM T-EZ plasmid (Promega) after which the ligated plasmid was transformed in Top10 *E. coli* cells (Invitrogen). Plasmids were screened with direct colony PCR and restriction analysis using EcoRI Fastdigest (Thermo Fisher Scientific, Breda, The Netherlands). Plasmid DNA was isolated from positive clones and the SmLDH insert was cloned in the PET11c plasmid(vector) by BamHI+NheI digestion and subsequent ligation with T4 ligase (Promega). Ligated plasmids were transformed in BL21(DE3)pLysS *E. coli* for protein expression after which they were sequenced and verified by aligning them to the SmLDH sequence with accession number Smp_038950, retrieved from the Sanger SchistoDB. Additionally, the sequence was translated and verified to match Uniprot entrance number G4VQZ5. The *S. mansoni* genome contains one other gene coding for L-LDH, Smp_038960, which codes for a protein 332 amino acids long, that is overall 94.3% identical to the protein encoded by Smp_038950, and 100% identical in the region between the amino acids 59 and 305, that contains all catalytic domains and regulatory sites.

Purification of Recombinant LDH

Recombinant LDH (r-SmLDH) was purified from *E. coli* using Ni-NTA Fast Kit with nickel charged agarose beads following manufacturer's instructions (Qiagen, Hilden, Germany). After induction of expression by 1 mM IPTG (Thermo Fisher Scientific, Breda, The Netherlands) for 24 hours, bacteria were pelleted by centrifugation at 4,000g for 30 minutes at 4°C, supernatants removed and the pellets were stored at -20°C until further use. To purify the recombinant protein, the pellets were thawed and lysed in 1 ml lysis buffer. The lysates were spun down at 15,000g for 10 minutes at 4°C. Supernatants were transferred to a clean tube and 250 µl Ni-NTA beads (Qiagen) added. After 1 hour shaking gently at 4°C, the beads were washed 10 times using the provided washing buffer. Elution buffer, 1 ml, was applied to the beads. Supernatant was removed after 15 minutes incubation, after which β-mercapto-ethanol was added to a final concentration of 0.5 mM to inhibit oxidation of SmLDH. Samples were taken prior to addition of β-mercapto-ethanol to determine the protein concentration by a Lowry method as described by (Bensadoun and Weinstein 1976) using bovine serum albumin as a standard.

Alignments

Amino acid sequences of multiple well characterized LDH enzymes (P0CW93, Q27888, Q95028, Q839C1, P13491, G4VQZ5, P00341, P26283, P16115) were retrieved from Uniprot in FASTA-format. An alignment was produced with ClustalW2, and scored for similarity using Boxshade server version 3.21.

Enzyme kinetics of SmLDH

The enzyme kinetics of native and recombinant SmLDH were determined by an enzyme assay monitoring at 22° C the oxidation of NADH to NAD⁺ at 340nm. The assay buffer consisted of 100 mM Tris-HCl pH 7.4, 0.125 mM NADH (Roche, Basel, Switzerland), 1 mM MgCl₂, 0-2 mM Fructose-1,6-bisphosphate (FBP) and/or 0-5 mM ATP. Stock solutions of FBP and ATP were prepared in 100 mM Tris-HCl pH 7.4. In all experiments a steady baseline was reached prior to starting the reaction by the addition of pyruvate (16 mM final concentration or otherwise as indicated). As a control, LDH from rabbit muscle (Roche) was tested under identical conditions. All measurements were performed in triplicate, except for those performed with LDH purified from adult worms, because of the very limited availability of that sample.

Model building of SmLDH

Two tetrameric models of smLDH were produced using the MODELLER program (Eswar, Webb et al. 2006). One model used as a template the protein X-ray structure of human B lactate dehydrogenase complexed with NAD⁺ and 4-hydroxy-1,2,5-oxadiazole-3-carboxylic acid (PDB code 1t2f). The second model was built using the X-ray structure of *Bacillus subtilis* LDH complexed with FBP and NAD⁺ (PDB code, 3PQD) as a template. The rms fit between the two tetramer models using all 1249 Ca atoms (excluding the N-terminal 30 residues) was calculated using the program SUPERPOSE (Winn, Ballard et al. 2011) gave a mean displacement of 1.7 Å. Docking studies of ATP and FBP binding to the anion pocket in the model SmLDH structure were carried out using Autodock Vina (Trott and Olson, 2010).

Kinetic modeling of the carbohydrate metabolism in *S. mansoni*

An existing yeast glycolysis model was modified to the stoichiometry of *S. mansoni* carbohydrate metabolism. Where possible, *S. mansoni* values for enzyme parameters were used. As a starting point we used the Van Eunen yeast glycolysis model (Van Eunen et al., 2012), which itself is based on the Teusink yeast model (Teusink et al., 2000). A full description of the construction of the model as well as the final model are presented in the Supplementary data.

RESULTS

Enzyme activity of LDH purified from adult worms

Stimulation of LDH by FBP is common in prokaryotes but has never been characterized in eukaryotes. We investigated the kinetics of SmLDH purified from adult worms to study the effects of FBP on this enzyme. As several FBP-sensitive bacterial LDHs are inhibited by ATP, we also tested the influence of ATP on the activity of SmLDH (Figure 1, left panel). Purified SmLDH was sensitive to inhibition by ATP: 2.5 mM ATP inhibited the enzyme activity by 50%. At physiological concentrations of 5 mM ATP, only 14% of the enzyme activity remained. Addition of 2 mM FBP reversed the inhibition incurred by ATP, and at 2.5 mM ATP restored enzyme activity close to 100% of normal activity (Figure 1, left panel). In the absence of ATP, FBP also acted as an activator of SmLDH. At a concentration of 2 mM, FBP increased the specific activity of SmLDH to about 175% (Figure 1, left panel). LDH from rabbit muscle was tested as a control under identical conditions and was not sensitive to ATP nor to FBP (Figure 1, right panel).

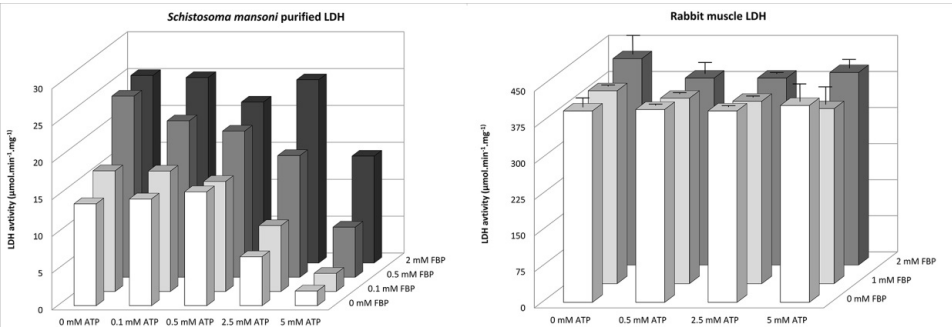


Figure 1. The effects of FBP (0-2 mM) and ATP (0-5 mM) on the lactate dehydrogenase activity of *S. mansoni* and rabbit muscle.
Left panel shows the activity of LDH affinity-purified from adult *S. mansoni* worms
Right panel shows the activity of commercially available LDH from rabbit muscle, each column represents the average of three measurements + SD.

Abbreviations: FBP, Fructose-1,6-bisphosphate; LDH, Lactate Dehydrogenase; ATP, Adenosine-triphosphate

Alignment of LDHs

In view of the kinetic properties of SmLDH which resemble those of the FBP-sensitive LDHs of prokaryotes, we hypothesized that this peculiar FBP-sensitive eukaryotic LDH might structurally resemble prokaryotic LDH. Therefore, we looked more closely at the

amino-acid sequence of SmLDH and compared it to known FBP-sensitive and non-sensitive LDHs. SmLDH (G4VQZ5 Uniprot) was aligned against several prokaryotic and eukaryotic LDHs (Supplementary Figure S1).

At first glance, SmLDH seemed to resemble standard eukaryotic LDHs. SmLDH features a 15-amino acids N-terminal extension, common in eukaryotic LDHs, which acts as an extended structure of each of the four monomers and interacts with the neighbouring subunit, stabilizing the (enzymatically active) relaxed state conformation of non-allosteric LDHs (Iwata, Kamata et al. 1994). Furthermore, the universally conserved polar residues Asp168, Arg171 and His195 that play an important role in substrate binding and catalytic action are present in SmLDH (Figures 2a and 2b). However, the SmLDH residues of the conserved FBP/anion binding site, show some interesting similarities and differences when compared with common eukaryotic LDHs; while all eukaryotic LDHs have Cys187 and Trp190 residues, SmLDH has Val187 and Tyr190. Intriguingly, the latter two are the same residues that are present in FBP-sensitive prokaryotic LDHs (Figure 2a).

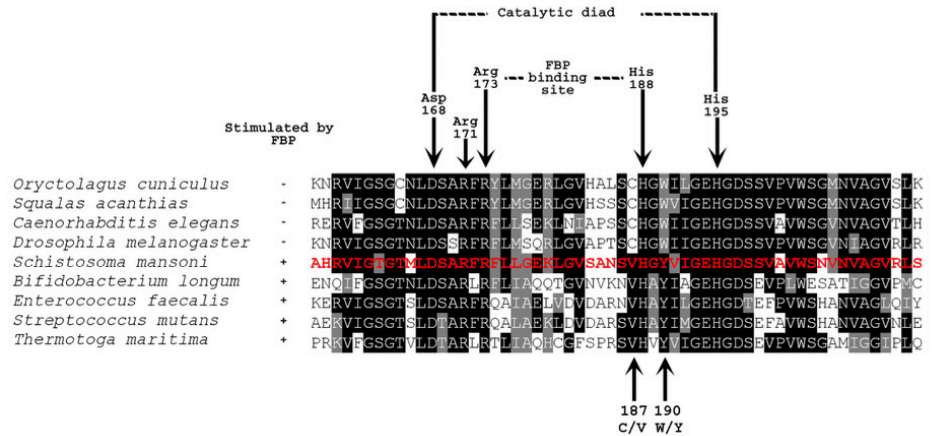


Figure 2a. Multiple species alignment of LDH
Alignment of several different LDHs, marked with black arrows (top) are highly conserved amino acids around the active site. Above the sequence of *S. mansoni*, 4 sequences are shown of LDHs of eukaryotes, while the 4 sequences underneath are from prokaryotic, FBP-sensitive LDHs. Black arrows (bottom) indicate amino acids 187 and 190 where the schistosomal amino acids are identical to the prokaryotic FBP-sensitive ones. Black shading indicates identity, gray shading indicates similarity.

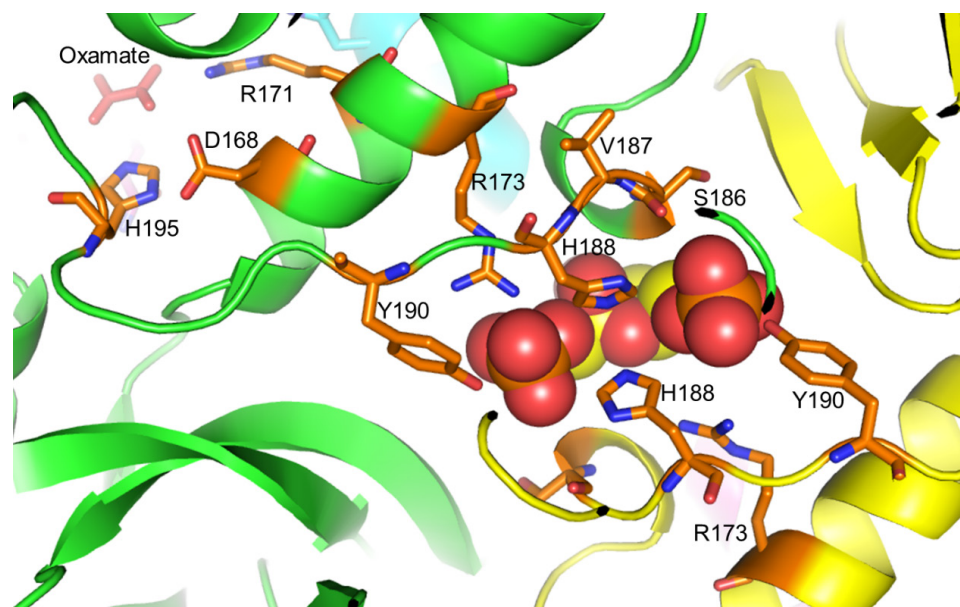


Figure 2b. View of the FBP binding pocket and lactate binding site in the SmLDH structure (modelled on the human LDH(1t2f) crystal structure)

The view is parallel to the 2-fold axis relating two chains (green and yellow) of the LDH tetramer. FBP is shown as spheres, and sidechains within 5 Å of the modelled FBP are drawn as sticks as are the key catalytic residues R171, D168 and H195. Both the oxamate ion which mimics the lactate substrate and FBP are from the R-state LDH structure from *Bifidobacterium longum* (1LDH) and positioned by a least squares fit of all Ca atoms.

Enzyme activity of recombinant *S. mansoni* lactate dehydrogenase

We expressed schistosomal LDH as a recombinant protein to allow a more thorough characterization of the kinetic properties of SmLDH. The kinetic parameters V_{max} and K_m were determined and the influence of ATP and FBP was investigated. The recombinant SmLDH (r-SmLDH) was catalytically active and had similar enzymatic properties as the purified native SmLDH. Addition of FBP increased the affinity of the recombinant enzyme for pyruvate, the $K_m(\text{pyruvate})$ decreased from 2.7 mM at 0 mM FBP to 1.1 mM in the presence of 0.5 mM FBP (Figure 3). The V_{max} decreased slightly (~20%) from 79 to 63 $\mu\text{mol}\cdot\text{min}^{-1}\cdot\text{mg}^{-1}$ at increasing FBP concentrations (Figure 3). Similar to the native SmLDH, addition of ATP had a strong inhibitory effect on r-SmLDH and decreased the V_{max} from 34 $\mu\text{mol}\cdot\text{min}^{-1}\cdot\text{mg}^{-1}$ (0 mM ATP) to 14 $\mu\text{mol}\cdot\text{min}^{-1}\cdot\text{mg}^{-1}$ (0.5 mM ATP), while the $K_m(\text{Pyruvate})$ remained constant at around 2.5 mM (Figure 4). These results revealed that addition of ATP had a more pronounced effect on the V_{max} of r-SmLDH while addition of FBP more strongly influenced the $K_m(\text{pyruvate})$.

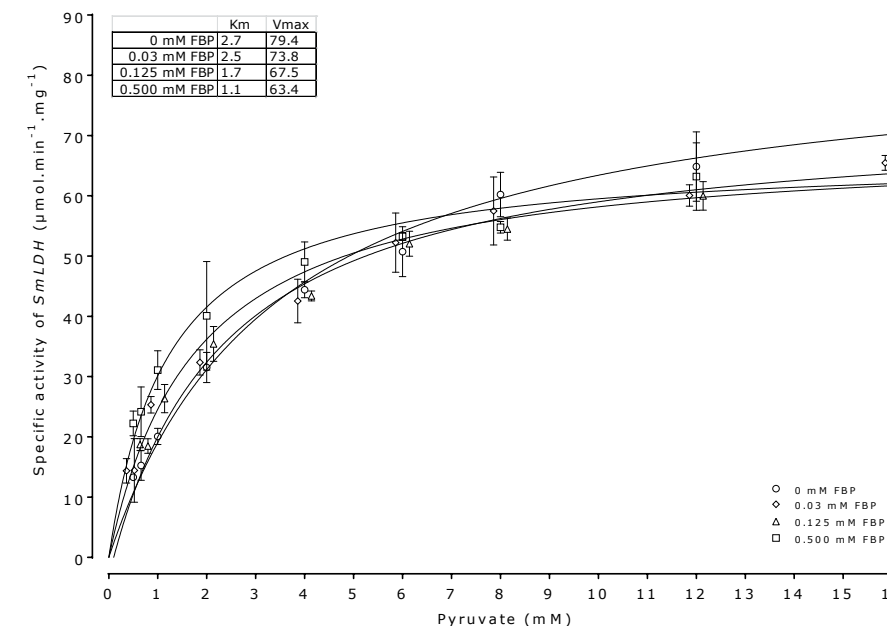


Figure 3. The effect of FBP on the $K_m(\text{pyruvate})$ of recombinant *S. mansoni* LDH

Enzymatic activity of r-SmLDH was determined at different pyruvate concentrations [0.5–16 mM] and FBP concentrations [0–0.5 mM]. The K_m (mM) and V_{max} ($\mu\text{mol}\cdot\text{min}^{-1}\cdot\text{mg}^{-1}$) were determined via direct linear plot. All measurements were performed in triplicate, shown is the average \pm SD.

Three dimensional structural alignment of lactate dehydrogenase

To investigate whether the observed differences in kinetic properties between SmLDH and canonical eukaryotic LDHs can be explained by the structural differences between these enzymes caused by the known differences in primary structures, we produced two tetrameric models of SmLDH with the MODELLER program using two different crystal structures as templates; human B-LDH (hLDH) and *Bacillus subtilis* LDH (BsLDH), which is FBP-sensitive. The two resulting tetrameric model structures of SmLDH are very similar both in the active site and in the allosteric FBP binding site. Comparison of the active site of SmLDH with those of hLDH and BsLDH showed no significant differences, which is not very surprising as the catalytic and substrate binding residues are highly conserved in all LDHs, prokaryotic as well as eukaryotic (Figure 2a).

The allosteric site also showed very few differences between the models based on bacterial and human LDH. An overlay of the SmLDH model with the human LDH structure (PDB code: 1t2f) highlights the side chain differences in the allosteric pocket that result in SmLDH and bacterial LDHs being regulated by FBP compared to the FBP-insensitive

eukaryotic LDHs (Figure 5).

Val187 faces into a very hydrophobic environment (Leu175, Leu180, Val182) which is quite well conserved between prokaryotes and eukaryotes (Figure 2a). X-ray structures of eukaryote LDHs show Cys187 filling that same pocket without any significant conformational change. The Tyr190Trp mutation would be expected to hamper FBP binding as (based on the modelled side chain positions) there would be a loss of the favourable Tyr hydrogen bonds with the phosphate groups at either end of FBP (with a modelled distance of $\approx 2.6 \text{ \AA}$). In contrast, a best model of the large hydrophobic side chain of Trp190 makes unfavourably short van der Waals contacts of less than 3.8 \AA with the phosphates.

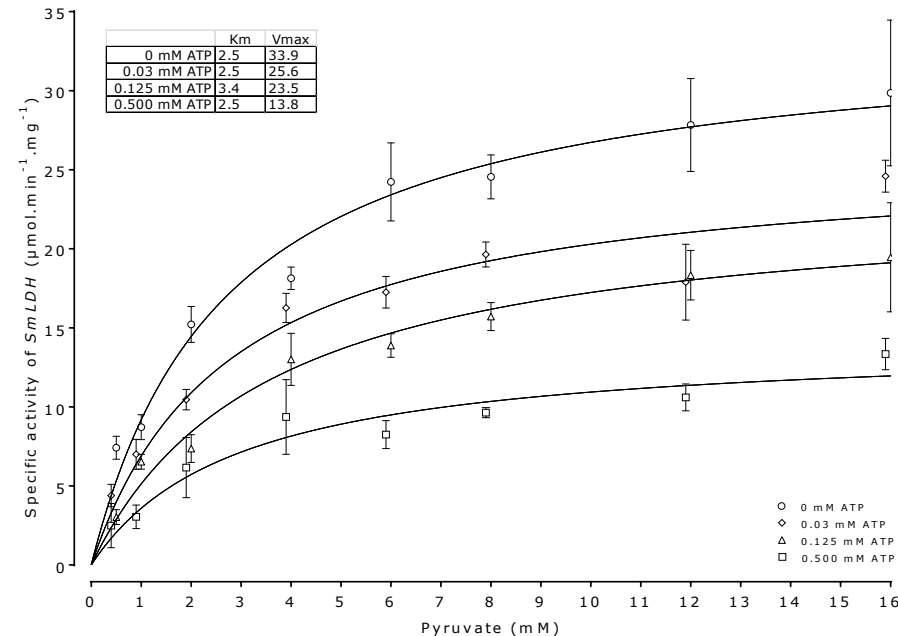


Figure 4. The effect of ATP on the Vmax and Km(pyruvate) of recombinant *S. mansoni* LDH
Enzymatic activity of r-SmLDH was determined at different pyruvate concentrations [0.5-16 mM] and ATP concentrations [0-0.5 mM]. The Km (mM) and Vmax (μmol.min⁻¹.mg⁻¹) were determined via direct linear plot. All measurements were performed in triplicate, shown is the average \pm SD.

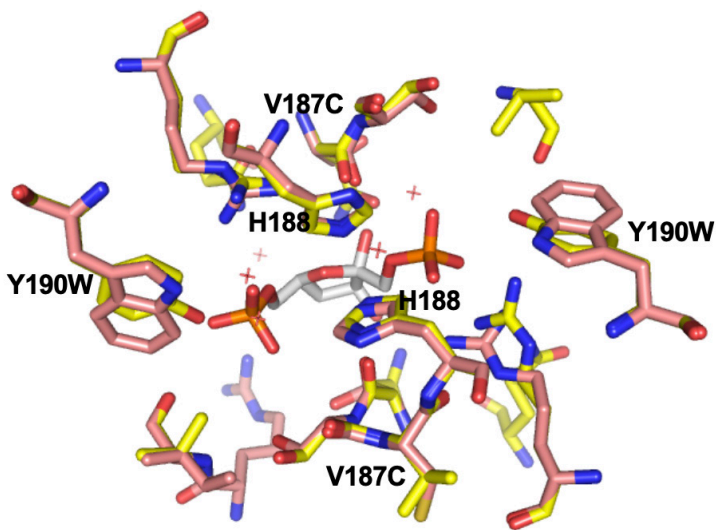


Figure 5. Allosteric site of schistosomal LDH modelled on human LDH
Overlay of model SmLDH (yellow) threaded on X-ray structure of human LDH (PDB code 1t2f) salmon. FBP is from the bacillus structure and residues were selected that were within 5 \AA from the modelled FBP viewed down the approximate 2-fold rotation axis relating two chains of the tetramer.

An overlay of the BsLDH structure (pdb code 3PQD) onto the model of the native SmLDH showed that the FBP molecule identified in 3PQD could be accommodated in the anion pocket without any steric clashes. To investigate the potential binding modes of FBP in the anion pocket of SmLDH, the docking program Vina (Trott & Olson, 2010) was used to identify a number of energetically favourable poses similar to that identified in the BsLDH crystal structure. Vina was also used to explore the possibility that ATP could bind in the same anion pocket and compete with FBP. A number of energetically favourable poses were identified showing that indeed the SmLDH model could easily accommodate ATP (Supplementary Figure S2).

SmLDH has an N-terminal extension of 15 residues in common with the eukaryotic LDHs. This tail sequence does show some amino acid differences compared with the majority of eukaryotic sequences (Supplementary Figure S1). A model of this N-terminal tail based on the hLDH structure (1T2F) was generated suggesting that the tail could behave in the same way as in hLDH by wrapping round and stabilizing the tetramer (not shown).

Kinetic modeling of the carbohydrate metabolism in *S. mansoni*

To investigate what could be the physiological role of the allosteric regulation of schistosome LDH in the different environmental conditions that the parasite encounters,

we created a kinetic model of eukaryotic glycolysis in which we varied the allosteric regulation on LDH. Kinetic models of parasite glycolysis have been successfully used previously to investigate the metabolic role of the glycosome in *Trypanosoma brucei* (Bakker et al., 2000; Haanstra et al., 2008). We decided to adjust the well-established glycolysis model of the eukaryote *Saccharomyces cerevisiae* (Teusink et al., 2000; Van Heerden et al., 2014), because not enough kinetic data are available for all the schistosome enzymes to construct a complete schistosome glycolysis model. We removed reactions from the yeast model that are not used in schistosomes and added glycogen metabolism, a Krebs cycle, respiration and an allosterically regulated LDH that was parameterised on *in vitro* kinetic data for schistosome LDH (see metabolic scheme in Figure 6).

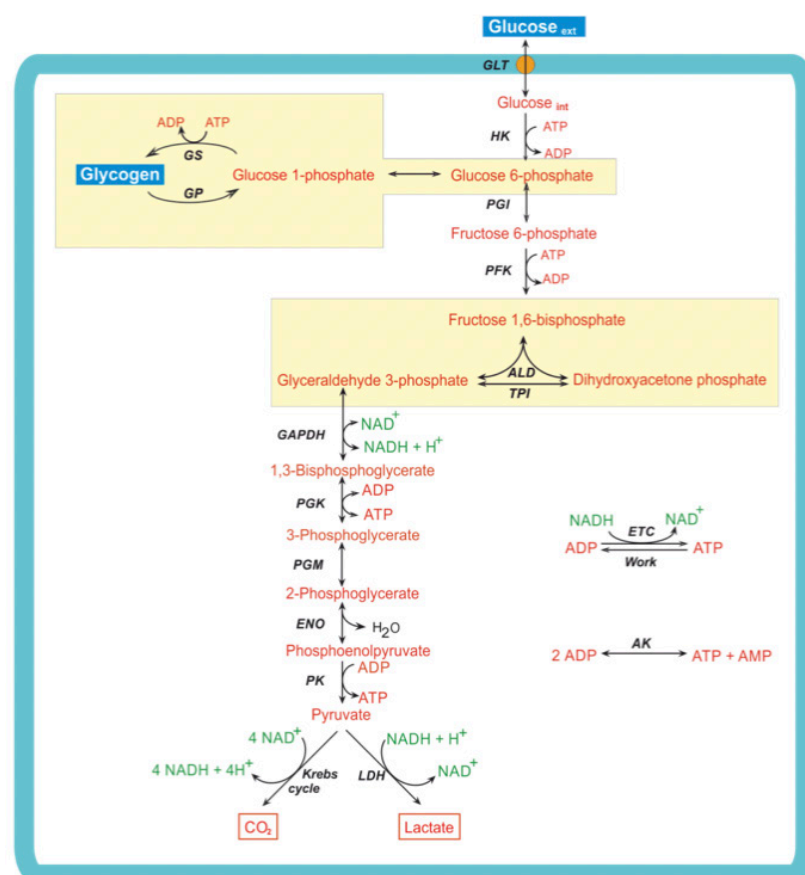


Figure 6. Metabolic scheme of glucose and glycogen degradation by *S. mansoni*.

The two colored areas in this scheme indicate that the reactions in that area are modelled in the kinetic model as one single reaction.

Abbreviations: AK, adenylate kinase; ALD, aldolase; ENO, enolase; ETC, electron transport chain; GAPDH, glyceraldehyde 3-phosphate dehydrogenase; GLT, glucose transporter; GP, glycogen phosphorylase;

GS, glycogen synthase; HK, hexokinase; LDH, lactate dehydrogenase; PFK, phosphofructo kinase; PGI, phosphoglucose isomerase; PGK, phosphoglycerate kinase; PGM, phosphoglycerate mutase; PK, pyruvate kinase; TPI, triosephosphate isomerase

Where available, kinetic parameters were adjusted to values measured in schistosomes. To handle the limited available information on enzyme parameters, we explicitly took parameter uncertainty into account in our analysis, as was also previously done for a model of *T. brucei* glycolysis (Achcar et al., 2012). In every analysis we made 1000 versions of the model. Each model has slightly different values for each of the parameters as they were randomly selected from a normal distribution with a standard deviation of 15-30% around the value reported in the literature (dependent on the source – schistosome or other eukaryotes - see Supplementary data for more details). In addition, we also started each model from different concentrations of intermediary metabolites. To probe the role of the inhibition by ATP and activation by FBP, we made three model versions that have one of the two modes of allosteric regulation of LDH or both: The 'Schisto'-model has inhibition of LDH by ATP as well as activation by FBP, while in the 'FBP'-model LDH is only regulated (activated) by FBP and in the 'ATP'-model LDH is only regulated (inhibited) by ATP.

We first analysed the three models in freshwater conditions: no glucose is available and glycogen is the sole carbon source. Supplementary Figure S3 shows the steady-state values for all metabolites and rates in the models. The three models mostly had similar steady-state levels for metabolites and rates, but there was a clear difference for the rates of LDH (Figure 7A) and the Krebs cycle (Figure 7B). The FBP-model has a higher vLDH and a lower vTCA, resulting in a lower ATP yield (Figure 7C). Clearly, the Schisto-model and the ATP-model, which both have ATP inhibition of LDH, degraded the glycogen more to carbon dioxide via the Krebs cycle than happened in the FBP model. This suggests that ATP inhibition of LDH is essential to prevent fermentation of the endogenous glycogen reserve to lactate. There does not seem to be a metabolic function for FBP activation of LDH when the parasite lives in freshwater conditions and is solely dependent on glycogen as carbon source.

Next, we switched the three models from a steady state in freshwater (no glucose) to 5.5 mM glucose and did a time-course for rates and metabolites (Supplementary Figure S4). Lack of FBP activation of LDH in the ATP-model led to accumulating levels of intracellular FBP upon the increase in glucose at t=0 (Figure 7A). The rate of LDH (vLDH; Figure 7B) shows that upon this sudden increase in glucose, the ATP-model was unable to increase vLDH as high as the other two models. The FBP-model reached an even higher rate of LDH than the Schisto-model, but apparently the rate that LDH could reach in the Schisto-model is sufficient to limit the increase of FBP to levels well below 10 mM. The

FBP accumulation in the ATP-model was the result of an imbalance in the rates of upper glycolysis (vHK-vPFK, see vPFK in Figure 8C) and lower glycolysis (vGAPDH-vPYK, see vGAPDH in Figure 8D). In steady state the flux through lower glycolysis should be twice as high as through upper glycolysis. This is because at the aldolase (ALD) step, the glycolytic intermediate gets split into two molecules that both end up as glyceraldehyde 3-phosphate (GAP). Instead, in the 'ATP' model the upper part of glycolysis was too fast and the lower part could not follow the pace: vPFK is similar to vGAPDH, while for a steady state vGAPDH would need to be twice as high. This imbalance can explain the accumulation of an intermediate between these steps (FBP in Figure 8A). A possible explanation for this imbalance comes from crosstalk between LDH and GAPDH via the NAD⁺/NADH ratio. In the reaction catalysed by LDH, electrons of NADH are used to ferment pyruvate to lactate. A lower rate of LDH lowers the NAD⁺/NADH ratio (Fig 8E) which will decrease the rate of GAPDH (Figure 8D). Overall, these results indicate that the FBP activation of LDH is important to cope with a sudden increase in glucose availability, but only in the context of an LDH that is inhibited by ATP. Inhibition of LDH by ATP, on the other hand, is an advantage in *S. mansoni* as it prevents in the free-living stages fermentation of the glycogen reserves to lactate.

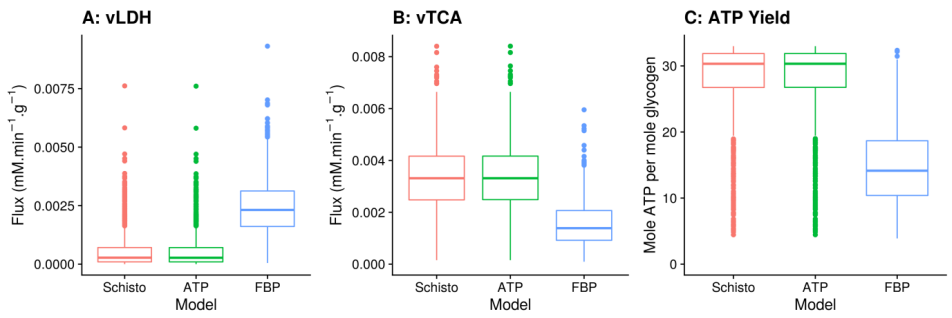


Figure 7. Steady state enzyme rates (v) at 0 mM extracellular glucose in *S. mansoni* models with LDHs with different allosteric properties. The three models: Schisto = smLDH with its allosteric properties (inhibition by ATP and activation by FBP), ATP = LDH with only ATP inhibition, FBP = LDH with only activation by FBP. Data for these boxplots were obtained by simulating 1000 models: for each model the parameters values were sampled from probability distributions (see Methods). If a steady-state solution was flagged as invalid, a time course of 7 days was done and the last value was recorded. Abbreviations: LDH, Lactate dehydrogenase; TCA, Tricarboxylic acid cycle

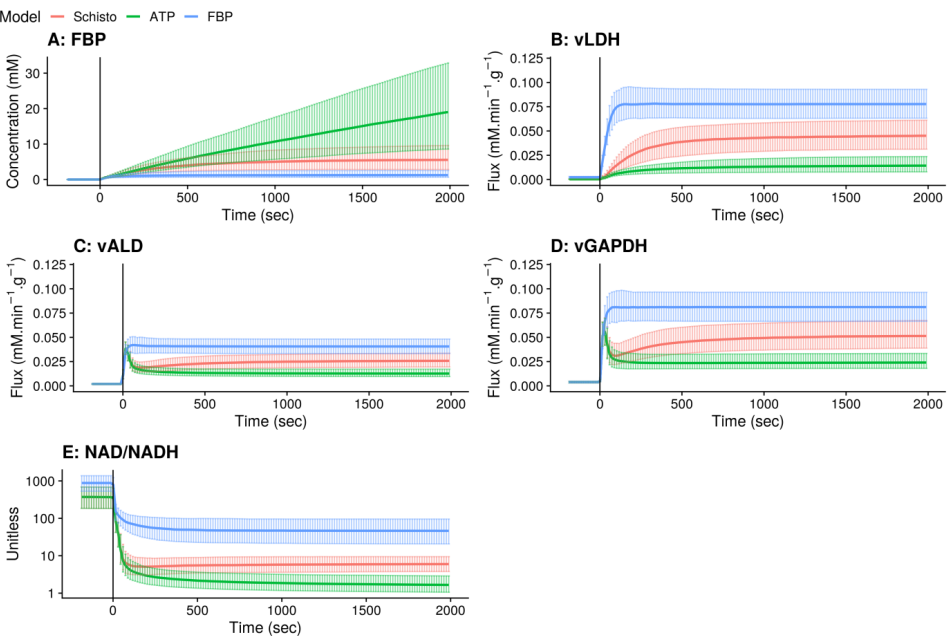


Figure 8. Effect of a sudden shift from 0 mM to 5.5 mM extracellular glucose in *S. mansoni* models with LDHs with different allosteric properties. Schisto = smLDH with its allosteric properties, ATP = LDH with only ATP inhibition, FBP = LDH with only activation by FBP. Data for these graphs were obtained by simulating 1000 models: for each model the parameters values were sampled from probability distributions (see methods). Shown is the median (solid line) with their 25% and 75% quantiles (shading). From a steady-state at 0 mM of extracellular glucose, at t=0 s the extracellular glucose concentration was set to 5.5 mM and a time-course was simulated for 2000 seconds.

Abbreviations:ALD, Aldolase; FBP, Fructose 1,6-bisphosphate; GAPDH, Glyceraldehyde 3-phosphate dehydrogenase; LDH, Lactate dehydrogenase; NAD(H), Nicotinamide adenine dinucleotide;

DISCUSSION

Here we present a detailed study of a eukaryotic LDH that is regulated by ATP and FBP. By combining data collected from affinity purified LDH of *S. mansoni* and from recombinant expression of this enzyme we demonstrated that this type of regulation is not restricted to prokaryotic LDH, in which it is a common trait to be regulated by FBP. (Garvie 1980, Iwata and Ohta 1993, Fushinobu, Kamata et al. 1996).

In all tetrameric L-LDHs the active site of each subunit is well conserved across all species. The residues Arg171, His195, Arg109 and Gln102 bind directly to the substrate

and position it over the nicotinamide ring of the NADH cofactor which binds in a Rossmann-fold, a conserved protein domain consisting of six stranded parallel β sheets and four associated α helices. After binding of the coenzyme followed by binding of the substrate, a protein conformational change occurs in which a highly conserved flexible loop (residues 97 to 123) folds down over the active-site pocket to bind the substrate and protect catalytically important residues from the solvent (Abad-Zapatero, Griffith et al. 1987, Goward and Nicholls 1994). The His195 and Asp168 residues are conserved in all LDHs and this pair forms a proton relay system in the active site and allow the imidazole ring of the histidine to act as both an acid and a base (Goward and Nicholls 1994) (Figures 2a and 2b). The catalytically crucial proton donor residue His195 sits at the tip of a loop (residues 186-202) which also includes the key residues involved in binding FBP, namely Tyr190, His188 and Ser186 (Figure 2b). It is likely that any distortion of this loop would disturb the positioning of the catalytic His and affect enzyme activity.

Our comparison of the kinetic properties of LDH from rabbit muscle with the purified enzyme from adult *S. mansoni* worms and the recombinant version of it, revealed that whereas rabbit LDH was unaffected by FBP and ATP, both preparations of the schistosomal enzyme were strongly inhibited by ATP and stimulated by FBP, the latter especially when the enzyme is inhibited by ATP.

In prokaryotic LDHs that are sensitive to FBP, binding of FBP causes a shift from the tense (inactive) to the relaxed (active) state of the enzyme. There are two anion pockets in each LDH tetramer and they lie between two protomers related to each other by a 2-fold rotational axis. The conserved residues lining this pocket (marked in Figure 2b) are Arg173, His188 and Tyr190 from protomer 'A' and the identical residues from the 2-fold related protomer 'B'. This results in a deep symmetrical electropositive cavity. Binding of the (approximately 2-fold symmetrical) FBP stabilizes the prokaryotic LDH tetramers in an enzymatically active (R-state) conformation (Wigley, Gamblin et al. 1992, Iwata, Kamata et al. 1994).

As we (Figure 1) and others have shown (Garvie 1980, Brennan, Holder et al. 1995), FBP has no effect on the catalytic activity of common eukaryotic LDH despite the presence of a deep and well defined anion binding pocket. It is intriguing that the anion pocket is also quite well conserved in eukaryotic LDH but is not occupied by FBP. However, of the over forty eukaryotic LDH X-ray structures available in the protein database www.rcsb.org (Berman, Westbrook et al. 2000) the anion pocket is frequently occupied by a variety of anions including small sulfate or phosphate ions or larger organic anions

including citrate. The three carboxyl groups of citrate have been shown in a number of enzyme structures to provide a potential mimic for the three phosphates of ATP (Wenger, Klinglmayr et al. 2013, Georgescu, Moynié et al. 2014, Chandran, Prabu et al. 2015). This suggests that the inhibition of SmLDH and many bacterial LDHs by ATP could be the result of direct competition of FBP and ATP binding to the anion pocket; a suggestion further supported by our docking studies (Supplementary Figure S2). The direct competition of ATP with FBP also fits with the available enzymatic data showing that FBP can compete out ATP and restore activity (Figure 1A) while titrating in even large amounts of substrate could not compete off the ATP (Figure 4). Hence, we propose that ATP is binding in the allosteric pocket.

It was shown that addition of the N-terminal extension from mouse testes LDH to *T. thermophilus* LDH causes the prokaryotic enzyme to be partially active without FBP present (Iwata, Kamata et al. 1994). It was also shown that removal of the N-terminal extension from rabbit LDH causes an increased sensitivity to sub-optimal pH and temperatures, indicating the importance and stabilizing function of this N-terminal extension (Zheng, Guo et al. 2004). SmLDH has an N-terminal extension, but is nevertheless stimulated by FBP and inhibited by ATP. Our model of the anion binding pocket showing the steric effect of the Tyr190Trp mutation probably explains the ability of SmLDH to bind FBP and to be activated by FBP. The schistosomal N-extension is comparable in length to other eukaryotic LDHs, but the sequence is not well conserved with other eukaryotes (Supplementary Figure S1). Presumably the SmLDH extension plays some role in stabilizing the tetramer but may not provide the same level of stabilization seen in other eukaryotes.

We studied the role of allosteric regulation via a model, rather than *in vivo*, as genetic manipulation of this multi-cellular parasite is still impossible. Our modeling studies on glycolysis in *S. mansoni* showed that the regulation of LDH activity is important, because of the variable glucose availability the parasite encounters during its life cycle. It is at this moment not possible to construct a schistosome model in an ideal way as the kinetic properties are not known for all enzymes involved. However, even with the available data, modeling provided new insights by explicitly taking parameter uncertainty into account. We show in our analyses that applying uncertainty of the parameters within realistic ranges did not change the overall outcome of the simulations.

The observed accumulation of FBP if glucose becomes available, has been observed before in other organisms and kinetic models have been used to understand this phenomenon. In *T. brucei* the glycosome is needed to protect accumulation of hexose-

phosphates (Haanstra et al., 2008) – the explanation there is that without allosteric regulation of HK and PFK the cell needs a glycosome to separate the ATP consuming reactions from the ATP producing ones. In yeast, a TPS-1 mutant cannot survive a sudden access to glucose (van Heerden et al., 2014). In that case a trehalose cycle is used to hydrolyse ATP in order to maintain a phosphate-pool that GAPDH needs to be sufficiently active.

The for eukaryotes rather unique regulatory mechanism of the LDH of *S. mansoni* suits very well the changes in the environments the parasite encounters during its life cycle. These environments differ greatly in glucose availability. The two free living stages live in water and oxidize their very limited endogenous glycogen stores completely to carbon dioxide for the production of ATP by oxidative phosphorylation. The inhibition of schistosomal LDH by ATP is an advantage for the parasite, as it prevents the wasteful fermentation of the glycogen reserves to lactate. Substrates for the two parasitic stages, on the other hand, are provided by the host and a wasteful fermentative metabolism producing lactate is of no concern to the parasite. The FBP activation of schistosomal LDH is important to cope with the sudden increase in glucose availability, but only in the context of an LDH that is inhibited by ATP.

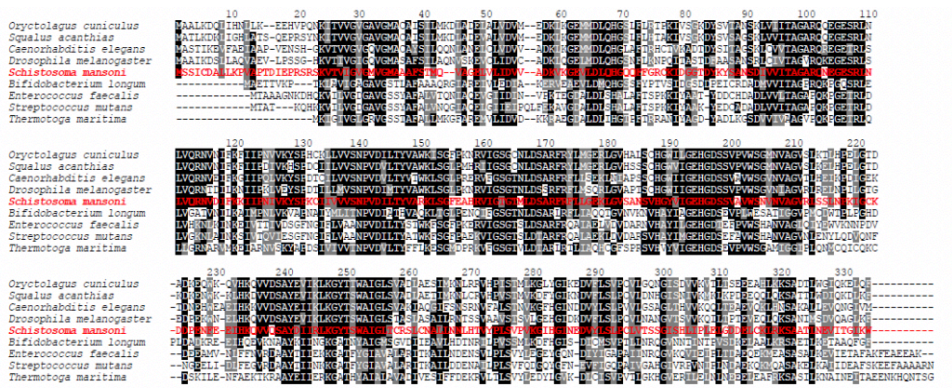
The *S. mansoni* LDH is ideal to facilitate the delicate orchestration of these switches in energy metabolism. The homolactic type of energy metabolism of *S. mansoni* (and of closely related trematodes such as *Schistosoma japonicum*, *Clonorchis sinensis* and *Opisthorchis viverrini*) that relies predominantly on LDH, is an interesting drug target, especially as small molecular inhibitors directed against LDH are already being investigated as possible drugs against cancer cell metabolism (Le, Cooper et al. 2010, Porporato, Dhup et al. 2011).

REFERENCES

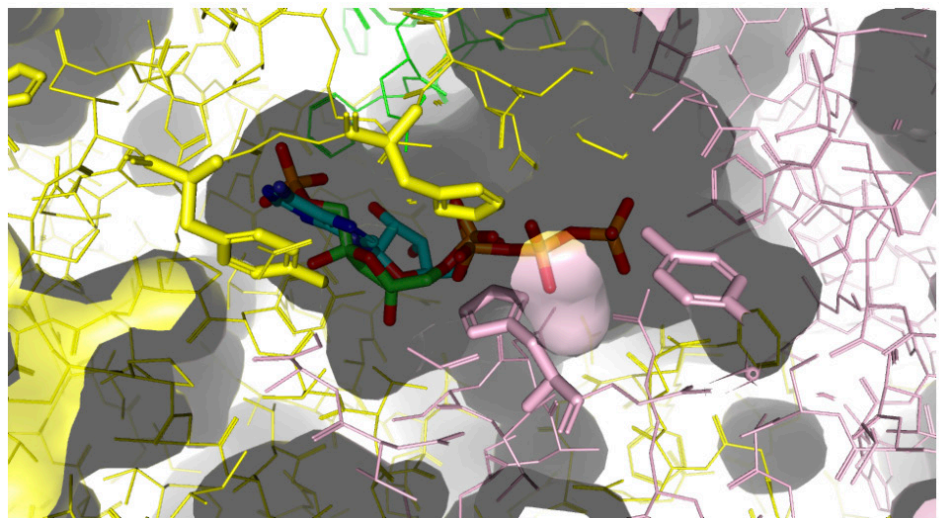
- Abad-Zapatero, C., J. P. Griffith, J. L. Sussman and M. G. Rossmann (1987). "Refined crystal structure of dogfish M 4 apo-lactate dehydrogenase." *Journal of Molecular Biology* **198**(3): 445-467.
- Achcar, F., E. J. Kerkhoven, B. M. Bakker, M. P. Barrett, R. Breitling and C. SilicoTryp (2012). "Dynamic modelling under uncertainty: the case of *Trypanosoma brucei* energy metabolism." *PLoS computational biology* **8**(1): e1002352.
- Adams, M. J., A. Liljas and M. G. Rossmann (1973). "Functional anion binding sites in dogfish M4 lactate dehydrogenase." *Journal of Molecular Biology* **76**(4): 519-528.
- Bakker, B. M., F. I. C. Mensonides, B. Teusink, P. van Hoek, P. A. M. Michels and H. V. Westerhoff (2000). "Compartmentation protects trypanosomes from the dangerous design of glycolysis." *Proceedings of the National Academy of Sciences* **97**(5): 2087-2092.
- Bensadoun, A. and D. Weinstein (1976). "Assay of proteins in the presence of interfering materials." *Analytical Biochemistry* **70**(1): 241-250.
- Berman, H. M., J. Westbrook, Z. Feng, G. Gilliland, T. N. Bhat, H. Weissig, I. N. Shindyalov and P. E. Bourne (2000). "The Protein Data Bank." *Nucleic Acids Research* **28**(1): 235-242.
- Birkoft, J., R. Fernley, R. Bradshaw and L. Banaszak (1982). "Amino acid sequence homology among the 2-hydroxyacid dehydrogenase: mitochondrial and cytoplasmique malate dehydrogenase form a homologous system with lactate dehydrogenase." *Proceedings of the National Academy of Sciences of the United States of America* **79**: 6166-6170.
- Brennan, S., J. Holder and J. Baldwin (1995). "An unusual fructose 1,6-bisphosphate-activated lactate dehydrogenase from the ascidian *Pyura stolonifera*." *Comparative Biochemistry and Physiology - Part B*, **110**(4): 689-695.
- Bruce, J. I., E. Weiss, M. A. Stirewalt and D. R. Lincicome (1969). "*Schistosoma mansoni*: Glycogen content and utilization of glucose, pyruvate, glutamate, and citric acid cycle intermediates by cercariae and schistosomules." *Experimental Parasitology* **26**(1): 29-40.
- Bueding, E. (1950). "Carbohydrate metabolism of *Schistosoma mansoni*." *Journal of General Physiology* **33**(5): 475-495.
- Chandran, A. V., J. R. Prabu, A. Nautiyal, K. N. Patil, K. Muniyappa and M. Vijayan (2015). "Structural studies on *Mycobacterium tuberculosis* RecA: Molecular plasticity and interspecies variability." *Journal of Bioscience* **40**(1): 13-30.
- Eswar, N., B. Webb, M. A. Marti-Renom, M. S. Madhusudhan, D. Eramian, M. y. Shen, U. Pieper and A. Sali (2006). "Comparative protein structure modeling using Modeller." *Current Protocols in Bioinformatics*: **15**(1), 5-6.
- Fushinobu, S., K. Kamata, S. Iwata, H. Sakai, T. Ohta and H. Matsuzawa (1996). "Allosteric Activation of L-Lactate Dehydrogenase Analyzed by Hybrid Enzymes with Effector-sensitive and -insensitive Subunits." *Journal of Biological Chemistry* **271**(41): 25611-25616.
- Garvie, E. I. (1980). "Bacterial lactate dehydrogenases." *Microbiological Reviews* **44**(1): 106-139.

- Georgescauld, F., L. Moynié, J. Habersetzer and A. Dautant (2014). "Structure of *Mycobacterium tuberculosis* nucleoside diphosphate kinase R80N mutant in complex with citrate." *Acta Crystallographica. Section E. Structural Biology Communications*. **70**(1): 40-43.
- Goward, C. R. and D. J. Nicholls (1994). "Malate dehydrogenase: A model for structure, evolution, and catalysis." *Protein Science* **3**(10): 1883-1888.
- Grau, U. M., W. E. Trommer and M. G. Rossmann (1981). "Structure of the active ternary complex of pig heart lactate dehydrogenase with S-lac-NAD at 2.7 Å resolution." *Journal of Molecular Biology* **151**(2): 289-307.
- Haanstra, J. R., M. Stewart, V.-D. Luu, A. van Tuijl, H. V. Westerhoff, C. Clayton and B. M. Bakker (2008). "Control and Regulation of Gene Expression quantitative analysis of the expression of phosphoglycerate kinase in bloodstream form *Trypanosoma brucei*." *Journal of Biological Chemistry* **283**(5): 2495-2507.
- Heerden, J. H. V., M. T. Wortel, et al. (2014). "Fatal attraction in glycolysis: how *Saccharomyces cerevisiae* manages sudden transitions to high glucose." *Microbial cell (Graz, Austria)* **1**(3): 103-106.
- Horemans, A. M. C., A. G. M. Tielens and S. G. van den Bergh (1992). "The reversible effect of glucose on the energy metabolism of *Schistosoma mansoni* cercariae and schistosomula." *Molecular and Biochemical Parasitology* **51**(1): 73-79.
- Horemans, A. M. C., A. G. M. Tielens and S. G. Van den Bergh (1991). "The transition from an aerobic to an anaerobic energy metabolism in transforming *Schistosoma mansoni* cercariae occurs exclusively in the head." *Parasitology* **102**(2): 259-265.
- Iwata, S., K. Kamata, S. Yoshida, T. Minowa and T. Ohta (1994). "T and R states in the crystals of bacterial L-lactate dehydrogenase reveal the mechanism for allosteric control." *Nature Structural & Molecular Biology*. **1**(3): 176-185.
- Iwata, S. and T. Ohta (1993). "Molecular Basis of Allosteric Activation of Bacterial L-Lactate Dehydrogenase." *Journal of Molecular Biology*. **230**(1): 21-27.
- Le, A., C. R. Cooper, et al. (2010). "Inhibition of lactate dehydrogenase A induces oxidative stress and inhibits tumor progression." *Proceedings of the National Academy of Sciences of the United States of America*. **107**(5): 2037-2042.
- Lloyd, G. M. (1983). "A fructose bisphosphate activated lactate dehydrogenase in the liver fluke *Fasciola hepatica*." *Molecular and Biochemical Parasitology* **7**(3): 237-246.
- Madern, D. (2002). "Molecular Evolution Within the L-Malate and L-Lactate Dehydrogenase Super-Family." *Journal of Molecular Evolution* **54**(6): 825-840.
- Porporato, P. E., S. Dhup, R. K. Dadhich, T. Copetti and P. Sonveaux (2011). "Anticancer Targets in the Glycolytic Metabolism of Tumors: A Comprehensive Review." *Frontiers in pharmacology* **2**: 49.
- Pronk, J. T., H. Yde Steensma and J. P. van Dijken (1996). "Pyruvate metabolism in *Saccharomyces cerevisiae*." *Yeast* **12**(16): 1607-1633.
- Read, J. A., V. J. Winter, C. M. Eszes, R. B. Sessions and R. L. Brady (2001). "Structural basis for altered activity of M- and H-isozyme forms of human lactate dehydrogenase." *Proteins* **43**(2): 175-185.
- Teusink, B., J. Passarge, et al. (2000). "Can yeast glycolysis be understood in terms of in vitro kinetics of the constituent enzymes? Testing biochemistry." *European Journal of Biochemistry* **267**(17): 5313-5329.
- Tielens, A. G. M. (1997). Biochemistry of trematodes. *Advances in Trematode Biology*. B. Fried and T. K. Graczyk, CRC Press, Boca Raton, Florida: 309-343.
- Tielens, A. G. M., F. A. M. Van de Pas, J. M. Van den Heuvel and S. G. Van den Bergh (1991). "The aerobic energy metabolism of *Schistosoma mansoni* miracidia." *Molecular and Biochemical Parasitology* **46**(1): 181-184.
- Tielens, A. G. M., B. E. P. Van Oordt and S. G. Van den Bergh (1989). "Carbohydrate metabolism in adult schistosomes of different strains and species." *International Journal for Parasitology* **19**(4): 447-449.
- Trott, O. and A. J. Olson (2010). "AutoDock Vina: Improving the speed and accuracy of docking with a new scoring function, efficient optimization, and multithreading." *Journal of Computational Chemistry* **31**(2): 455-461.
- van Eunen, K., J. A. L. Kiewiet, H. V. Westerhoff and B. M. Bakker (2012). "Testing biochemistry revisited: how in vivo metabolism can be understood from in vitro enzyme kinetics." *PLoS computational biology* **8**(4): e1002483.
- Van Grinsven, K. W. A., J. J. Van Hellemond and A. G. M. Tielens (2009). "Acetate:succinate CoA-transferase in the anaerobic mitochondria of *Fasciola hepatica*." *Molecular and Biochemical Parasitology* **164**(1): 74-79.
- Van Oordt, B. E. P., A. G. M. Tielens and S. G. Van den Bergh (1989). "Aerobic to anaerobic transition in the carbohydrate-metabolism of *Schistosoma mansoni* cercariae during transformation in vitro." *Parasitology* **98**: 409-415.
- Wenger, J., E. Klinglmayr, C. Fröhlich, C. Eibl, A. Gimeno, M. Hessenberger, S. Puehringer, O. Daumke and P. Goettig (2013). "Functional Mapping of Human Dynamin-1-Like GTPase Domain Based on X-ray Structure Analyses." *PLOS ONE* **8**(8): e71835.
- Wigley, D. B., S. J. Gamblin, J. P. Turkenburg, E. J. Dodson, K. Piontek, H. Muirhead and J. J. Holbrook (1992). "Structure of a ternary complex of an allosteric lactate dehydrogenase from *Bacillus stearothermophilus* at 2.5 Å resolution." *Journal of Molecular Biology* **223**(1): 317-335.
- Winn, M. D., C. C. Ballard, et al. (2011). "Overview of the CCP4 suite and current developments." *Acta Crystallographica D* **67**(4): 235-242.
- Zheng, Y., S. Guo, Z. Guo and X. Wang (2004). "Effects of N-Terminal Deletion Mutation on Rabbit Muscle Lactate Dehydrogenase." *Biochemistry* **69**(4): 401-406.

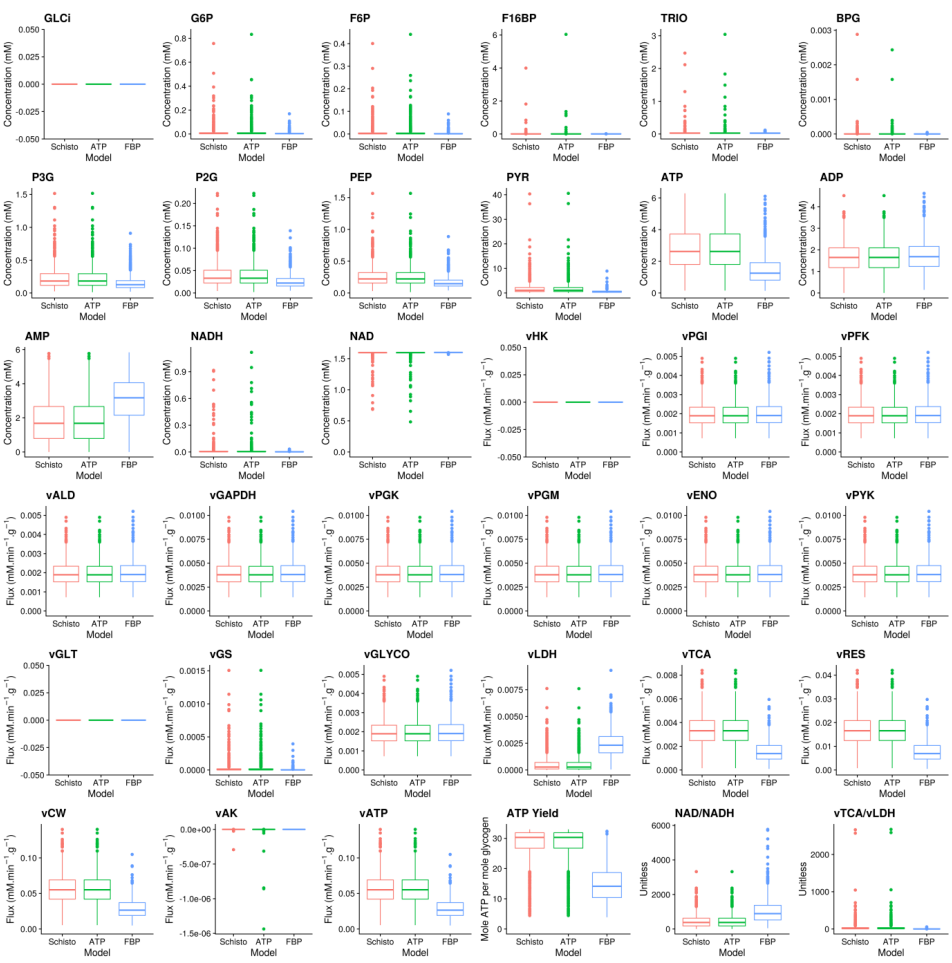
SUPPLEMENTARY FIGURES



Supplementary Figure S1. Multiple species alignment of LDH
Alignment of several different LDHs. Above the sequence of *S. mansoni* 4 sequences are shown of LDHs of eukaryotes, while the 4 sequences underneath are from prokaryotic, FBP-sensitive LDH. These are the complete LDH proteins of the same organisms of which the catalytic and allosteric sites are shown in figure 2a. Black shading indicates identity, gray shading indicates similarity.

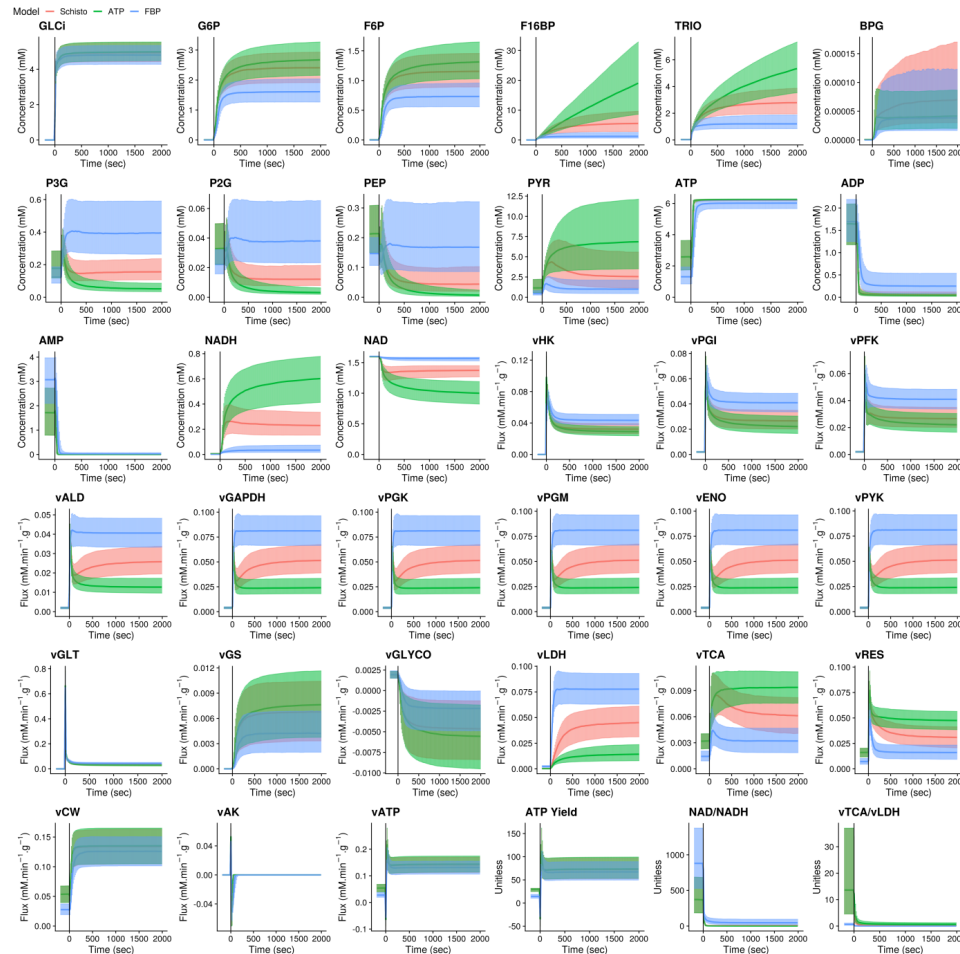


Supplementary Figure S2. Docking of ATP in the FBP binding site of SmlDH



Supplementary Figure S3
Steady state concentrations and enzyme rates (v) at 0 mM extracellular glucose in *S. mansoni* models with LDHs with different allosteric properties. The three models: Schisto = smLDH with its allosteric properties (inhibition by ATP and activation by FBP), ATP = LDH with only ATP inhibition, FBP = LDH with only activation by FBP. Distribution were obtained by simulating 1000 models: for each model the parameters values were sampled within their confidence intervals. If a steady-state solution was flagged as invalid, a time course of 7 days was done and the last value was recorded.

Abbreviations: ADP, Adenosine-diphosphate; AMP, Adenosine-monophosphate; ATP, Adenosine-triphosphate; BPG, 1,3-biphosphoglycerate; F16BP, Fructose 1,6-bisphosphate; F6P, Fructose-6-phosphate; G6P, Glucose-6-phosphate; GLCI, Glucose intracellular; NAD, Nicotinamide adenine dinucleotide; NADH, Nicotinamide adenine dinucleotide reduced; P2G, Phospho-2-glycerate; P3G, Phospho-3-glycerate; PEP, Phosphoenolpyruvate; PYR, Pyruvate; TRIO, Triosephosphate isomerase; vAK, Adenylate kinase; vALD, Aldolase; vCW, Cellular work; vENO, Enolase; vGAPDH, Glyceraldehyde 3-phosphate dehydrogenase; vGLT, Glucose transporter; vGLYCO, Glycogen breakdown; vGS, Glycogen synthase; vHK, Hexokinase; vLDH, Lactate dehydrogenase; vPFK, Phosphofructo kinase; vPGI, Phosphoglucose isomerase; vPGK, Phosphoglycerate kinase; vPGM, Phosphoglycerate mutase; vPYK, Pyruvate kinase; vRES, Respiration; vTCA, Tricarboxylic acid cycle



Supplementary Figure S4

Effect of a sudden shift from 0 mM to 5.5 mM extracellular glucose in *S. mansoni* models with LDHs with different allosteric properties. Schisto = smLDH with its allosteric properties, ATP = LDH with only ATP inhibition, FBP = LDH with only activation by FBP. Distribution were obtained by simulating 1000 models: for each model the parameters values were sampled within their confidence intervals. From a steady-state at 0 mM of extracellular glucose, at t=0 s the extracellular glucose concentration was set to 5.5 mM and a time-course was simulated for 2000 seconds. Abbreviations are the same as in Fig S3.

SUPPLEMENTARY DATA 1

Building the kinetic model of Schistosoma metabolism

Model language and simulation software

Models were built in the PySCeS Model Description Language [1] and are available upon request. Simulations were done in the open-source software PySCeS (version 0.9.3) [1]. Our analysis made use of the iPython console [2], Jupyter Notebooks [3], and the Python modules numpy [4], scipy [5] and pandas [6]. All plots were made in R [7] with help from the ggplot2 [8] and data.table [9] packages.

Model construction

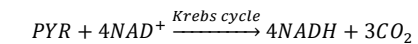
General modifications to an existing yeast glycolysis model.

We used the van Eunen [10] yeast glycolysis model as a starting point, which itself is based on the Teusink yeast model [11].

The van Eunen model [10] was modified as follows:

1. The reactions concerning trehalose and glycerol were removed because there is no evidence that these exist in *Schistosoma mansoni*.
2. In the van Eunen model, pyruvate is converted to succinate, acetate and ethanol [10]. In *Schistosoma mansoni*, pyruvate is converted into carbon dioxide through the Krebs cycle and into lactate through fermentation [12] and therefore these changes were made:

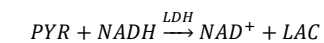
- a. The reactions concerning succinate, acetate, and ethanol were removed.
- b. The Krebs cycle was modeled by the following lumped reaction



Its rate is modelled by an irreversible two-substrate Michaelis-Menten equation ("model description" eq. 2.14).

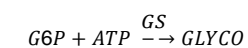
- c. Fermentation of pyruvate to lactate by lactate dehydrogenase (LDH) was included

with this reaction:



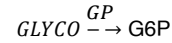
Because *Schistosoma mansoni* LDH has a complicated regulation we derived a new rate equation with the use of kinetic data (see section "Deriving a rate equation and parameters for smLDH")

3. Free-living cercariae live in freshwater where they have no access to extracellular glucose and depend on glycogen breakdown for their energy production. Once cercariae penetrate the human body, they gain access to the high extracellular glucose concentration environment of blood and start synthesizing glycogen [13, 14]. While glycogen synthesis and glycogenolysis consist of multiple reactions, we modelled them as two separate, simple linear reactions. Glycogen synthesis was modelled as



With a rate equation based on mass action kinetics (model description eq. 2.2)

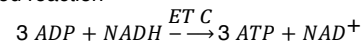
Glycogen phosphorylation was modelled as



With a rate equation based on mass action kinetics (model description eq. 2.3)

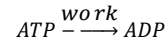
Note that when the glycogen concentration is fixed (i.e. in steady state analyses), this reaction has a fixed rate.

4. Yeast hexokinase is inhibited by trehalose-6-phosphate. There is no evidence of such regulation in *Schistosoma mansoni*. However, glucose-6-phosphate is a known competitive inhibitor with respect to ATP [14, 15]. We modeled this using an irreversible two-substrate Michaelis-Menten rate equation with competitive inhibition (model description eq. 2.4) with Michaelis-Menten constants taken from [15].
5. Because we were unable to solve for steady state using the kinetic parameters of *Saccharomyces cerevisiae* for glyceraldehyde-3-phosphate dehydrogenase (data not shown), we replaced its rate equation and parameters of the unicellular parasite *Trypanosoma brucei* as described in [16] (see model description eq. 2.8)
6. Contrary to the Teusink et al. study [11], van Eunen et al. [10] were not interested in the dynamics of AMP, ADP, and ATP and fixed the concentration of these metabolites. Because LDH of *Schistosoma mansoni* is allosterically regulated by ATP, we had no a priori reason to believe that ATP dynamics are not relevant in the metabolic switch. For this reason, the concentration of AMP, ADP, and ATP were unfixed. Accordingly, ATP synthesis from NADH (respiration), ATP degradation (work), and adenylate kinase (AK) were included in our model
 - a. Respiration (ATP synthesis with electron from the oxidation of NADH) was modelled via a lumped reaction



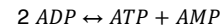
With an irreversible mass action rate equation (model description eq. 2.15)

- b. ATP expenditure (work) was modelled by



With mass action kinetics (model description eq. 2.16)

- c. Adenylate kinase (AK) was modelled as



With reversible mass action kinetics (model description eq. 2.17)

Deriving a rate equation and parameters for smLDH

Data used

Kinetics of LDH were studied by Bexkens et al. (this manuscript) by measuring initial lactate production rates for different initial substrate and allosteric modulators concentrations. In total, six experiments were performed:

1. varying pyruvate (0.5–16 mM) and ATP (0–0.5 mM), fixed NADH (0.125 mM), no FBP;
2. varying pyruvate (0.5–16 mM) and FBP (0–0.5 mM), fixed NADH (0.125 mM), no ATP;
3. varying NADH (0.01–0.13 mM) and ATP (0–1.5 mM), fixed pyruvate (16 mM), no FBP;
4. varying NADH (0.01–0.13 mM) and FBP (0–2 mM), fixed pyruvate (16 mM), no ATP;
5. varying ATP (0–5 mM), fixed pyruvate (16 mM), NADH (0.125 mM), FBP (2.0 mM);

6. varying FBP (0–2 mM), fixed pyruvate (16 mM), NADH (0.125 mM), ATP (2.5 mM).

Because LDH is stable for only about four hours, it had to be purified every day resulting in different specific activities for experiments. A correction factor was thus applied to the data so that a concentration of 16 mM pyruvate, 0.125 mM NADH, 0 mM ATP and 0 mM FBP would have a specific activity of 100 mM/min/g for all experiments.

Rate equation

STEP 1 – STARTING FROM A NON-ALLOSTERICALLY REGULATED ENZYME

NADH-dependent L-LDHs are tetrameric enzymes that catalyze the conversion of pyruvate to lactate with concomitant oxidation of NADH. Each monomer possesses one catalytic site that functions independently, that is, no cooperativity was observed [17]. This implies that we can study each monomer independently. Moreover, LDHs are known to follow a compulsory order ternary-complex mechanism with coenzyme binding first and unbinding last [18]. Based on this, we first derived a rate equation for a non-allosterically regulated enzyme [19]:

$$v_{LDH} = \frac{V_m \frac{NADH}{K_{INADH}} \frac{PYR}{K_{mPYR}}}{1 + \frac{NADH}{K_{INADH}} + \frac{PYR}{K_{mPYR}} + \frac{NADH PYR}{K_{INADH} K_{mPYR}}} \quad (\text{Eq. 1})$$

STEP 2 – INCLUDING ALLOSTERIC REGULATION

The LDH of *Schistosoma mansoni* is allosterically inhibited by ATP and activated by FBP [20]. Experimental data suggests that allosteric modulators affect the K_m of LDH for pyruvate [21] and that the K_m for NADH is unchanged [22]. For this reason, we assumed that only K_m for pyruvate would be modulated by ATP and FBP. We now define K_{mPYR}^0 to be the Michaelis-Menten constant for pyruvate in the absence of any allosteric modulator as:

$$K_{mPYR} = \frac{K_{mPYR}^0}{\alpha} \quad (\text{Eq. 2})$$

The α quantifies the strength of the allosteric regulation. We can put equations 1 and 2 together to come to an equation that includes allosteric regulation:

$$v_{LDH} = \frac{V_m \frac{NADH}{K_{INADH}} \frac{PYR \alpha}{K_{mPYR}^0}}{1 + \frac{NADH}{K_{INADH}} + \frac{PYR \alpha}{K_{INADH} K_{mPYR}^0} + \frac{NADH PYR \alpha}{K_{INADH} K_{mPYR}^0}} \quad (\text{eq. 3})$$

We then investigated different equations for α , each for different mechanisms of allosteric regulation: independence between allosteric sites or dependent allosteric sites. Each of the two mechanism for α were investigated in combination with Eq. 3, by fitting the parameters of the equations in COPASI 4.19 (Build 140) [23] using simulated annealing with the following parameters: start temperature: 1.0; cooling factor: 0.85; tolerance: 10^{-6} ; random number generator: 1; seed: 0. Parameters estimates were identified by minimizing the sum of squared between the measured (see “Data used” above) and the predicted rates. By using both the quantitative descriptors of the fits and plotting of the equations with the data, we identified the α based on dependent allosteric sites with all ATP-bound enzyme molecules inactive to be the best for the WT smLDH ($\beta=\gamma=\delta=0$). The general equation for the α considering dependent allosteric sites has the following equation:

$$\alpha = \frac{1 + \beta \frac{ATP}{K_A} + \gamma \frac{(ATP K_A)^2}{(1 + ATP K_A + FBP K_F)^2} + \delta \frac{ATP K_A FBP K_F}{(1 + ATP K_A + FBP K_F)^2} + \epsilon \frac{FBP K_F}{(1 + ATP K_A + FBP K_F)^2} + \zeta \frac{(FBP K_F)^2}{(1 + ATP K_A + FBP K_F)^2}}{(1 + ATP K_A + FBP K_F)^2} \quad (\text{eq. 4})$$

Through this equation, the α depends on the concentration of allosteric modulators ATP and FBP, on thermodynamic equilibrium constants denoted K_A and K_F , but also on parameters reflecting the strength of activation and inhibition denoted by Greek letters.

STEP 3 - PARAMETERS FOR LDH

From the parameter analysis we derived the parameters for smLDH following the procedure described in the section “Parameters of the model” below. The only exception is the V_m -value. Because the specific activity of an enzyme depends on the enzyme concentration and its environment, the estimated value of V_m of LDH was discarded and replaced by the one in [24].

Stoichiometry of the model

Reactions and differential equations

These can be found in “model description” sections 1 and 5

Parameters of the model

All parameters are listed in section 3 of “model description”. In the subsections below we describe our choices.

Starting points

REACTIONS WITH PARAMETERS AVAILABLE (EITHER FROM SCHISTOSOMES OR THE ORIGINAL YEAST MODEL)

Specific activities of many glycolytic enzymes during the worm stage have been measured [24]. Although we were attempting to model the cercaria stage, we assumed that the specific activities of enzymes at the cercaria stage are closer to those of the worm stage than those of yeast. Accordingly, we have replaced the V_m of all glycolytic enzymes by the values found in [24].

As in *Saccharomyces cerevisiae*, glucose transporters of *Schistosoma mansoni* use facilitate diffusion to import extracellular glucose. Michaelies-Menten constants of these transporters are estimated to be between 0.6 and 2.2 mM with a mean value of 2.0 mM [25]. For the glucose transported rate equation, vGLT, the K_m was thus set to 2.0 mM. Its V_m was estimated using fluxes reported in [20].

The pyruvate kinase rate equation was parameterised based on unpublished data from the Tielens lab. L_0 was not estimated because it had a high standard deviation in the estimation procedure (i.e., changing its value does not change the fit significantly). K_{mADP} was not estimated because it was not varied in the experiment.

For other parameters the values from the yeast model were used.

REACTIONS WITH NO MEASURED PARAMETERS

Creating a model for *Schistosoma mansoni* glycolysis required introducing reactions for which parameters were neither measured in *Saccharomyces cerevisiae* nor in *Schistosoma mansoni*. These reactions were glycogen synthesis (vGS), glycogen degradation (vGP), Krebs cycle (vKrebs), respiration (vRES), work (vwork) and adenylate kinase (vAK).

Their parameters were estimated within the glycolytic model using data found in the *Schistosoma mansoni* literature.

DATA USED TO ESTIMATE THESE PARAMETERS

The first dataset was the lactate, CO₂ and glycogen fluxes as measured by [20] in the head of the cercaria in presence of 0.05 mM or 5.5 mM extracellular glucose. Measurements were converted from $\text{nmol}\cdot\text{h}^{-1}\cdot\text{mg}^{-1}$ into $\text{mM}\cdot\text{min}^{-1}\cdot\text{g}^{-1}$ by multiplying fluxes by $10^{-3}/6$ and setting the cytosolic compartment volume to 1L. A steady state simulation was used to predict these fluxes.

The second dataset was the mean glycogen amount over time in 0 mM extracellular glucose as measured by Lawson and Wilson [13]. However, because glycogen was measured in grams, and not in glucose-units, their raw measurements were not directly usable. Nonetheless, the authors stated that glycogen degradation follows a negative exponential model, $G(t) = G_0 \cdot e^{-kt}$ where $G(t)$ is the amount or concentration of glycogen at time t and where k is the decay rate. The unit of k is inverse

time and is thus independent of the unit used for glycogen. For this reason, we used this model to approximate dynamics of glycogen concentration. A time-course simulation predicted these concentrations for a simulation length of 24 hours with 101 steps. A decay rate $k=0.089 \text{ h}^{-1}$ was used.

ERROR FUNCTION

The different datasets (see above) have different numbers of datapoints (6 vs 101) and the standard deviations of the flux measurements were not uniform. To solve this, we used the following error function was used:

$$\rho(J, G, \theta) = \sum_i \frac{(j_i(\theta) - J_i)^2}{\sigma_i^2} + \frac{1}{G_0 n} \sum_{i=0}^{n=100} (\hat{G}_i(\theta) - G_i)^2 \quad (\text{Eq 6})$$

where J_i is one of flux measured by Horemans et al [20] with standard deviation σ_i and $j_i(\theta)$ J is the corresponding predicted flux from our steady-state model with parameters θ , G_i is the glycogen concentration obtained from the negative exponential model from Lawson and Wilson [13] and $\hat{G}_i(\theta)$ the corresponding predicted concentration from our time-course model with parameters simulated using n steps.

Finally, to avoid solutions that were biologically unlikely, ρ was set to infinity when:

1. metabolite concentrations were above 20 mM at steady-state or during time-course;
2. absolute reaction rates were above $1 \text{ mM}\cdot\text{min}^{-1}$ at steady-state or during time-course;
3. ATP concentration was below 3 mM during the first 10 hours of the time-course simulation.

The first two constraints are based on what we believe to be biologically unlikely. The last constraint was set because Lawson and Wilson reported that cercariae live for at least 10 hours at 25°C [13].

OPTIMISATION ALGORITHM

We used a Bayesian approach to estimate the posterior probability of parameters θ given the two datasets J and G described above. We used this formula:

$$P(\theta|J, G) = \frac{P(J, G|\theta) P(\theta)}{P(J, G)}$$

Here, the prior probability $P(\theta)$ can be used to define constraints for kinetics parameters. In this study, all prior distributions were uniform. Minimum and maximum values of uniform distributions are reported in Table 1.

Standard evaluation of the posterior thus requires the evaluation of its likelihood, which is, alas, not available for our simulation-based model. In order to resolve this, Approximate Bayesian Computation (ABC) methods were used. These are based on approximating the posterior using an error measure ρ and a threshold ϵ :

$$P(\theta|J, G) \approx P(\theta|\rho(J, G, \theta) \leq \epsilon)$$

This algorithm is implemented in the `abcpmc` module for Python [26] which was used in this study. The algorithm had the following parameters:

1. population size: 1000;
2. number of iterations: 20;
3. starting value epsilon threshold: 0.25;
4. percentile of the sorted errors: 75.

Parameter sampling

There is always some uncertainty on the parameters. Measurements are never perfect (as reflected by their error margin) and for some parameters we did not even have values for *Schistosoma mansoni*. To explicitly include this uncertainty [16], parameters were sampled from probability

distributions. For each result 1000 models were created by sampling parameters from the following distributions:

- Parameters fitted as described in section “Deriving a rate equation and parameters for smLDH” and were sampled from their estimated posterior distribution.
- Schistosoma mansoni* parameters were sampled from a normal distribution. Its mean was the value found in the literature and its standard deviation was set to 15% of the value. Most reported standard deviations of kinetic parameters in the literature appear to be within 10% to 20% percent the value of the parameter [16].
- Saccharomyces cerevisiae* and *Trypanosoma brucei* parameters were also sampled from a normal distribution. Its mean was the value found in the literature and its standard deviation was set to 30% of the value. Although this decision is arbitrary, increasing the standard deviation up to around 60% of the value did not influence our conclusions.

Models that lack allosteric regulation by ATP or FBP

The goal of this study was to investigate possible roles for the allosteric regulation of LDH in the orchestration of the schistosomal metabolic switch. To do so, we compared models with LDHs having different allosteric properties. This was achieved by changing parameters reflecting the strength of activation and inhibition in Eq.4. More specifically, we studied three glycolytic models with LDHs having different allosteric properties:

- smLDH: A wildtype LDH that is inhibited by ATP and activated by FBP (with parameters $\beta=0$, $\gamma=0$, $\delta=0$, $\epsilon=1.021\cdot10^6$, $\zeta=2.146\cdot10^{11}$);
- ATP: An LDH that is only inhibited by ATP ($\beta=\gamma=0$; $\delta=\epsilon=\zeta=1$);
- FBP: An LDH that is only activated by FBP ($\beta=\gamma=\delta=1$; $\epsilon=1.021\cdot10^6$, $\zeta=2.146\cdot10^{11}$)

Initial concentrations of external substrates and internal substrates/intermediates

The initial conditions can be found in “model description” section 4. We checked whether different initial concentrations would change the conclusions and it did not.

Steady state and timecourse simulations

One thousand models with sampled parameters (see Parameter sampling) were generated, and either a steady-state analysis or a time course was computed. Steady states flagged as invalid by PySCeS were discarded and a time-course of a duration of seven days was run and the last value was recorded as the steady-state solution. This value was chosen because no more variations could be observations by plotting concentrations over time for a model parametrized by the mean value of the posterior distribution of unmeasured parameters.

Tables

Table 1 Prior uniform distribution minimum and maximum values of parameters specified in ABC PMC algorithm.

Reaction	Parameter	Minimum	Maximum	Unit
V _{GLT}	V _m	0.1	2.5	mM·min ⁻¹
V _{GS}	k	0.005	0.01	mM·min ⁻¹
V _{GP}	k	0.001	0.003	min ⁻¹
V _{TCA}	V _m	0.1	2.5	mM·min ⁻¹
V _{TCA}	K _{mPYR}	0.1	30.0	mM
V _{TCA}	K _{mNAD}	0.1	30.0	mM
V _{RES}	k	0.1	1.5	mM·min ⁻¹
V _{CW}	k	0.05	0.15	mM
V _{AK}	k ₁	0.5	2.5	mM·min ⁻¹
V _{AK}	k ₂	0.5	2.5	mM·min ⁻¹

References

[1] Olivier, B.G., Rohwer, J.M., Hofmeyr, J.H. (2005) Modelling cellular systems with PySCeS. *Bioinformatics*, 21 560-561.

[2] Perez, F., Granger, B.E. (2007) IPython: A system for interactive scientific computing. *Comput Sci Eng*, 9 21-29.

[3] Kluyver, T., Ragan-Kelley, B., Pérez, F., Granger, B., Bussonnier, M., Frederic, J., Kelley, K., Hamrick, J., Grout, J., Corlay, S., *et al.*, Jupyter Notebooks – a publishing format for reproducible computational workflows, Positioning and Power in Academic Publishing: Players, Agents and Agendas, IOS Press Ebooks2016.

[4] Walt, S.v.d., Colbert, S.C., Varoquaux, G. (2011) The NumPy Array: A Structure for Efficient Numerical Computation. *Comput Sci Eng*, 13 22-30.

[5] Jones, E., Oliphant, T., Peterson, P. (2001) SciPy: Open Source Scientific Tools for Python.

[6] McKinney, W. (2011) pandas: a Foundational Python Library for Data Analysis and Statistics. Python High Performance Science Computer.

[7] Team, R.C. (2016) R: A language and environment for statistical computing [Computer software manual]. Vienna, Austria. 2016.

[8] Wickham, H. (2009) ggplot2: Elegant Graphics for Data Analysis. Springer Publishing Company, Incorporated

[9] Dowle, M., Srinivasan, A., Short, T., Lianoglou, S. (2017) data. table: Extension of data. frame. R package version, 1.

[10] van Eunen, K., Kiewiet, J.A., Westerhoff, H.V., Bakker, B.M. (2012) Testing biochemistry revisited: how in vivo metabolism can be understood from in vitro enzyme kinetics. *PLoS computational biology*, 8 e1002483.

[11] Teusink, B., Passarge, J., Reijenga, C., Esgalhado, E., van der Weijden, C., Schepper, M., Walsh, M., Bakker, B., van Dam, K., Westerhoff, H., *et al.* (2000) Can yeast glycolysis be understood in terms of in vitro kinetics of the constituent enzymes? Testing biochemistry. *European journal of biochemistry / FEBS*, 267 5313-5329.

[12] Bueding, E. (1950) Carbohydrate metabolism of *Schistosoma mansoni*. *J Gen Physiol*, 33 475-495.

[13] Lawson, J.R., Wilson, R.A. (1980) The survival of the cercariae of *Schistosoma mansoni* in relation to water temperature and glycogen utilization. *Parasitology*, 81 337-348.

[14] Tielens, A.G., van den Heuvel, J.M., van Mazijk, H.J., Wilson, J.E., Shoemaker, C.B. (1994) The 50-kDa glucose 6-phosphate-sensitive hexokinase of *Schistosoma mansoni*. *J Biol Chem*, 269 24736-24741.

[15] Armstrong, R.L., Wilson, J.E., Shoemaker, C.B. (1996) Purification and characterization of the hexokinase from *Schistosoma mansoni*, expressed in *Escherichia coli*. *Protein Expr Purif*, 8 374-380.

[16] Achcar, F., Kerkhoven, E.J., SilicoTryp, C., Bakker, B.M., Barrett, M.P., Breitling, R. (2012) Dynamic modelling under uncertainty: the case of *Trypanosoma brucei* energy metabolism. *PLoS computational biology*, 8 e1002352.

[17] Goward, C.R., Nicholls, D.J. (1994) Malate dehydrogenase: a model for structure, evolution, and catalysis. *Protein Sci*, 3 1883-1888.

[18] Shoemark, D.K., Cliff, M.J., Sessions, R.B., Clarke, A.R. (2007) Enzymatic properties of the lactate dehydrogenase enzyme from *Plasmodium falciparum*. *FEBS J*, 274 2738-2748.

[19] Cornish-Bowden, A. (2004) Fundamentals of Enzyme Kinetics. 3rd ed., Portland Press, London,

[20] Horemans, A.M., Tielens, A.G., van den Bergh, S.G. (1992) The reversible effect of glucose on the energy metabolism of *Schistosoma mansoni* cercariae and schistosomula. *Mol Biochem Parasitol*, 51

[21] Iwata, S., Kamata, K., Yoshida, S., Minowa, T., Ohta, T. (1994) T and R states in the crystals of bacterial L-lactate dehydrogenase reveal the mechanism for allosteric control. *Nat Struct Biol*, 1

[22] van Niel, E.W., Palmfeldt, J., Martin, R., Paese, M., Hahn-Hagerdal, B. (2004) Reappraisal of the regulation of lactococcal L-lactate dehydrogenase. *Appl Environ Microbiol*, 70 1843-1846.

[23] Hoops, S., Sahle, S., Gauges, R., Lee, C., Pahle, J., Simus, N., Singhal, M., Xu, L., Mendes, P., Kummer,(2006) COPASI--a COmplex PAthway Simulator. *Bioinformatics*, 22 3067-3074.

[24] Shapiro, T.A., Talalay, P. (1982) *Schistosoma mansoni*: mechanisms in regulation of glycolysis. *Exp Parasitol*, 54 379-390.

[25] Skelly, P.J., Tielens, A.G., Shoemaker, C.B. (1998) Glucose Transport and Metabolism in Mammalian-stage Schistosomes. *Parasitol Today*, 14 402-406.

[26] Akeret, J., Refregier, A., Amara, A., Seehars, S., Hasner, C. (2015) Approximate Bayesian computation for forward modeling in cosmology. *Journal of Cosmology and Astroparticle Physics*, 2015 043-043.

SUPPLEMENTARY DATA 2

DESCRIPTION OF THE KINETIC MODEL

1 Reactions

Name	Reaction Equation
vGLT	$GLCe \rightleftharpoons GLCi$
vGS	$G6P + ATP \longrightarrow GLYCO$
vGP	$GLYCO \longrightarrow G6P$
vHK	$GLCi + ATP \xrightleftharpoons{G6P} G6P + ADP$
vPGI	$G6P \rightleftharpoons F6P$
vPFK	$F6P + ATP \xrightarrow{F26BP,AMP} F16BP + ADP$
vALD	$F16BP \rightleftharpoons 2\ TRIO$
vGAPDH	$TRIO + NAD \rightleftharpoons BPG + NADH$
vPGK	$BPG + ADP \rightleftharpoons P3G + ATP$
vPGM	$P3G \rightleftharpoons P2G$
vENO	$P2G \rightleftharpoons PEP$
vPK	$PEP + ADP \xrightleftharpoons{F16P} PYR + ATP$
vLDH	$PYR + NADH \xrightleftharpoons{ATP, F16BP} LAC + NAD$
vKrebs	$PYR + 4\ NAD \longrightarrow 3\ CO_2 + 4\ NADH$
vRES	$3\ ADP + NADH \longrightarrow 3\ ATP + NAD$
vWork	$ATP \longrightarrow ADP$
vAK	$2\ ADP \longrightarrow AMP + ATP$

Table 1: List of reactions. Abbreviations: 2PG: 2-phosphoglycerate, 3PG: 3-phosphoglycerate, AK: adenylate kinase (EC 2.7.4.3), ALD: aldolase (EC 4.1.2.13), BPG: 1,3-bisphosphoglycerate, DHAP: dihydroxyacetone phosphate, ENO: enolase (EC 4.2.1.11), F16BP: fructose-1,6-bisphosphate, F26BP: fructose-2,6-bisphosphate, F6P: fructose-6-phosphate, G6P: glucose-6-phosphate, GAP: glyceraldehyde 3-phosphate, GAPDH: glyceraldehyde-3-phosphate dehydrogenase (EC 1.2.1.12), GLCe: extracellular glucose, GLCi: intracellular glucose, GLT: glucose transport, GP glycogen phosphorylase (EC 2.4.1.1), GS glycogen synthase (EC 2.4.1.11), GLYCO: glycogen, HK: hexokinase (EC 2.7.1.1), LAC: lactate, LDH lactate dehydrogenase (EC 1.1.1.27), PFK: phosphofructokinase (EC 2.7.1.11), PEP: phosphoenolpyruvate, PGI: phosphoglucose isomerase (EC 5.3.1.9), PGK: 3-phosphoglycerate kinase (EC 2.7.2.3), PGM: phosphoglycerate mutase (EC 5.4.2.1), PK: pyruvate kinase (EC 2.7.1.40), PYR: pyruvate, RES: respiration, Krebs: Krebs cycle.

2 Rate Equations

2.1 Glucose Transport

$$v_{GLT} = \frac{\frac{V_m}{K_{mGLC}} \left(GLC_e - \frac{GLC_i}{K_{eq}} \right)}{1 + \frac{GLC_e}{K_{mGLC}} + \frac{GLC_i}{K_{mGLC}} + \frac{0.91 GLC_e GLC_i}{K_{mGLC} K_{mGLC}}}$$

2.2 Glycogen Synthesis

$$v_{GS} = k G6P ATP$$

2.3 Glycogen Degradation

$$v_{GP} = k GLYCO$$

2.4 Hexokinase

$$v_{HK} = \frac{V_m \frac{\frac{GLC_i}{K_{mGLC}} ATP}{K_{mATP} \left(1 + \frac{G6P}{K_{iG6P}} \right)}}{1 + \frac{GLC_i}{K_{mGLC}} + \frac{ATP}{K_{mATP} \left(1 + \frac{G6P}{K_{iG6P}} \right)}}$$

2.5 Glucose-6-phosphate Isomerase

$$v_{PGI} = \frac{\frac{V_m}{K_{mG6P}} \left(G6P - \frac{F6P}{K_{eq}} \right)}{1 + \frac{G6P}{K_{mG6P}} + \frac{F6P}{K_{mF6P}}}$$

2.6 Phosphofructokinase

$$v_{PFK} = \frac{V_m g_R \frac{F6P}{K_{mF6P}} \frac{ATP}{K_{mATP}} \left(1 + \frac{F6P}{K_{mF6P}} + \frac{ATP}{K_{mATP}} + g_R \frac{F6P}{K_{mF6P}} \frac{ATP}{K_{mATP}} \right)}{\left(1 + \frac{F6P}{K_{mF6P}} + \frac{ATP}{K_{mATP}} + g_R \frac{F6P}{K_{mF6P}} \frac{ATP}{K_{mATP}} \right)^2 + L \left(1 + C_{ATP} \frac{ATP}{K_{mATP}} \right)^2}$$

$$L = L_0 \left(\frac{1 + C_{iATP} \frac{ATP}{K_{iATP}}}{1 + \frac{ATP}{K_{iATP}}} \right)^2 \left(\frac{1 + C_{AMP} \frac{AMP}{K_{mAMP}}}{1 + \frac{AMP}{K_{mAMP}}} \right)^2 \left(\frac{1 + \frac{C_{F26BP} F26BP}{K_{mF26BP}} + \frac{C_{F16BP} F16BP}{K_{mF16BP}}}{1 + \frac{F26BP}{K_{mF26BP}} + \frac{F16BP}{K_{mF16BP}}} \right)^2$$

2.7 Aldolase

$$v_{ALD} = \frac{\frac{V_m}{K_{mF16BP}} \left(F16BP - \frac{K_{eq} TPI}{1 + K_{eq} TPI} \frac{TRIO - TRIO}{K_{eq}} \right)}{1 + \frac{F16BP}{K_{mF16BP}} + \frac{K_{eq} TPI}{1 + K_{eq} TPI} \frac{TRIO}{K_{mGAP}} + \frac{1}{1 + K_{eq} TPI} \frac{TRIO}{K_{mDHAP}} + \frac{K_{eq} TPI}{1 + K_{eq} TPI} \frac{TRIO}{K_{mGAP}} \frac{1}{1 + K_{eq} TPI} \frac{TRIO}{K_{mDHAP}} + \frac{F16BP}{K_{mGAP}} \frac{K_{eq} TPI}{1 + K_{eq} TPI} \frac{TRIO}{K_{mF16BP}}}$$

2.8 Glyceraldehyde-3-Phosphate Dehydrogenase

$$v_{GAPDH} = \frac{V_m \frac{TRIO}{K_{mGAP}} \frac{K_{eq} TPI}{1 + K_{eq} TPI} \frac{NAD}{K_{mNAD}} \left(1 - \frac{BPG NADH}{K_{eq} TRIO \frac{K_{eq} TPI}{1 + K_{eq} TPI} NAD} \right)}{\left(1 + \frac{BPG}{K_{mBPG}} + \frac{TRIO}{K_{mGAP}} \frac{K_{eq} TPI}{1 + K_{eq} TPI} \right) \left(1 + \frac{NADH}{K_{mNADH}} + \frac{NAD}{K_{mNAD}} \right)}$$

2.9 Phosphoglycerate Kinase

$$v_{PGK} = \frac{V_m \left(\frac{K_{eq} BPG ADP}{K_{mBPG} K_{mATP}} - \frac{P3G ATP}{K_{mP3G} K_{mATP}} \right)}{\left(1 + \frac{BPG}{K_{mBPG}} + \frac{P3G}{K_{mP3G}} \right) \left(1 + \frac{ATP}{K_{mATP}} + \frac{ADP}{K_{mADP}} \right)}$$

2.10 Phosphoglycerate Mutase

$$v_{PGM} = \frac{\frac{V_m}{K_{mP3G}} \left(P3G - \frac{P2G}{K_{eq}} \right)}{1 + \frac{P3G}{K_{mP3G}} + \frac{P2G}{K_{mP2G}}}$$

2.11 Enolase

$$v_{ENO} = \frac{\frac{V_m}{K_{mP2G}} \left(P2G - \frac{PEP}{K_{eq}} \right)}{1 + \frac{P2G}{K_{mP2G}} + \frac{PEP}{K_{mPEP}}}$$

2.12 Pyruvate Kinase

$$v_{PK} = \frac{\frac{V_m PEP}{K_{mPEP}} \left(1 + \frac{PEP}{K_{mPEP}} \right)^{n-1}}{L_0 \left(\frac{1 + \frac{ATP}{K_{mATP}}}{1 + \frac{ATP}{K_{mF16BP}}} \right)^n + \left(1 + \frac{PEP}{K_{mPEP}} \right)^n} \frac{ADP}{ADP + K_{mADP}}$$

2.13 Lactate Dehydrogenase

$$v_{LDH} = \frac{V_m \frac{NADH}{K_{iNADH}} \frac{PYR \alpha}{K_m^{PYR}}}{1 + \frac{NADH}{K_{iNADH}} + \frac{PYR \alpha}{K_{iNADH} K_m^{PYR}} + \frac{NADH PYR \alpha}{K_{iNADH} K_m^{PYR}}}$$
$$\alpha = \frac{1}{(1 + ATP K_A + FBP K_F)^2} + \frac{\beta ATP K_A}{(1 + ATP K_A + FBP K_F)^2} + \frac{\gamma (ATP K_A)^2}{(1 + ATP K_A + FBP K_F)^2} + \frac{\delta ATP K_A FBP K_F}{(1 + ATP K_A + FBP K_F)^2} + \frac{\epsilon FBP K_F}{(1 + ATP K_A + FBP K_F)^2} + \frac{\zeta (FBP K_F)^2}{(1 + ATP K_A + FBP K_F)^2}$$

2.14 Krebs Cycle

$$v_{Krebs} = \frac{\frac{V_m PYR}{K_m PYR} \frac{NAD}{K_m NAD}}{1 + \frac{PYR}{K_m PYR} + \frac{NAD}{K_m NAD}}$$

2.15 Respiration

$$v_{RES} = k NADH ADP$$

2.16 Cellular Work

$$v_{Work} = k ATP$$

2.17 Adenylate Kinase

$$v_{AK} = k_1 ADP^2 - k_2 AMP ATP$$

3 Kinetic Parameters

Reaction	Parameter	Value	Reference
v_{GLT}	K_{eq}	1.0	[9]
v_{GLT}	K_{mGLC}	2.0	[8]
v_{HK}	K_{iG6P}	0.193	[2]
v_{HK}	K_{mATP}	0.927	[2]
v_{HK}	K_{mGLCi}	0.128	[2]
v_{HK}	V_m	0.086	[7]
v_{PGI}	K_{eq}	0.538	[5]
v_{PGI}	K_{mF6P}	0.1	[5]
v_{PGI}	K_{mG6P}	1.4	[9]
v_{PGI}	V_m	2.24	[7]
v_{PFK}	C_{F16BP}	0.397	[9]
v_{PFK}	C_{F26BP}	0.0174	[9]
v_{PFK}	C_{iATP}	100.0	[9]
v_{PFK}	C_{AMP}	0.0845	[9]
v_{PFK}	C_{ATP}	3.0	[9]
v_{PFK}	g_R	5.12	[9]
v_{PFK}	K_{mAMP}	0.0995	[9]
v_{PFK}	K_{iATP}	0.65	[9]
v_{PFK}	K_{mATP}	0.3	[6]
v_{PFK}	K_{mF16BP}	0.111	[9]
v_{PFK}	K_{mF26BP}	0.000682	[9]
v_{PFK}	K_{mF6P}	0.4	[6]
v_{PFK}	L_0	0.66	[9]
v_{PFK}	V_m	0.42	[7]
v_{ALD}	K_{eq}	0.069	[9]
v_{ALD}	K_{mDHAP}	2.4	[9]
v_{ALD}	K_{mF16BP}	0.3	[9]
v_{ALD}	K_{mGAP}	2.0	[9]
v_{ALD}	K_{mGAPi}	10.0	[9]
v_{ALD}	V_m	0.225	[7]
v_{ALD}, v_{GAPDH}	K_{eqTPI}	0.045	[9]
v_{GAPDH}	K_{eq}	0.044	[1]
v_{GAPDH}	K_{mBPG}	0.1	[1]
v_{GAPDH}	K_{mGAP}	0.15	[1]
v_{GAPDH}	K_{mNAD}	0.45	[1]
v_{GAPDH}	K_{mNADH}	0.02	[1]
v_{GAPDH}	V_m	0.845	[7]
v_{PGK}	K_{eq}	3200.0	[9]
v_{PGK}	K_{mADP}	0.2	[9]
v_{PGK}	K_{mATP}	0.3	[9]
v_{PGK}	K_{mBPG}	0.003	[9]
v_{PGK}	K_{mP3G}	0.53	[9]
v_{PGK}	V_m	0.185	[7]

Reaction	Parameter	Value	Reference
v_{PGM}	K_{eq}	0.19	[9]
v_{PGM}	K_{mP2G}	0.08	[9]
v_{PGM}	K_{mP3G}	1.2	[9]
v_{PGM}	V_m	1.04	[7]
v_{ENO}	K_{eq}	6.7	[9]
v_{ENO}	K_{mP2G}	0.04	[9]
v_{ENO}	K_{mPEP}	0.5	[9]
v_{ENO}	V_m	0.616	[7]
v_{PK}	K_{mADP}	0.28	[4]
v_{PK}	K_{mATP}	0.374665	Estimated from [4]
v_{PK}	K_{mF16BP}	0.176541	Estimated from [4]
v_{PK}	K_{mPEP}	0.091	[4]
v_{PK}	V_m	2.020	[7]
v_{PK}	n	4.0	[9]
v_{PK}	L_0	62.3852	Estimated from [4]
v_{LDH}	V_m	1.24	[7]
v_{LDH}	K_A	2.8799	Estimated from [3]
v_{LDH}	K_F	1.007e-06	Estimated from [3]
v_{LDH}	β	0	Estimated from [3]
v_{LDH}	γ	0	Estimated from [3]
v_{LDH}	δ	0	Estimated from [3]
v_{LDH}	ϵ	1.02121e+06	Estimated from [3]
v_{LDH}	ζ	2.14614e+11	Estimated from [3]
v_{LDH}	K_{mPYR}^O	0.934103	Estimated from [3]
v_{LDH}	K_{iNADH}	0.430032	Estimated from [3]
v_{LDH}	K_{mNADH}	0.0313658	Estimated from [3]

2: List of reaction parameters. Units: V_m mM.min⁻¹.g⁻¹ K_m and K_i : mM. Abbreviations: PK: pyruvate kinase (EC 2.7.4.3), ALD: aldolase (EC 4.1.2.13), Work: cellular work, ENO: enolase 1), GAPDH: glyceraldehyde-3-phosphate dehydrogenase (EC 1.2.1.12), GLT: glucose transport, glycogen phosphorylase (EC 2.4.1.1), GS glycogen synthase (EC 2.4.1.11), HK: hexokinase 1), LDH lactate dehydrogenase (EC 1.1.1.27), PFK: phosphofructokinase (EC 2.7.1.11), PGI: phosphoglucoicose isomerase (EC 5.3.1.9), PGK: 3-phosphoglycerate kinase (EC 2.7.2.3), PGM: phosphoglycerate kinase (EC 5.4.2.1), PK: pyruvate kinase (EC 2.7.1.40), RES: respiration, Krebs: Krebs cycle.

4 Initial Species Concentrations

Species	Compartment	Value	Fixed
ADP	cytosol	0.911	
AMP	cytosol	0.264	
ATP	cytosol	5.125	
LAC	cytosol	0.0	x
BPG	cytosol	$2.025 \cdot 10^{-5}$	
CO ₂	cytosol	0.0	x
F16BP	cytosol	3.276	
F26BP	cytosol	0.014	x
F6P	cytosol	0.286	
G6P	cytosol	0.582	
GLCe	extracellular	0.0, 0.05 or 5.5 †	x
GLCi	cytosol	0.0	
GLYCO	cytosol	9.44 or 17.6 ‡	
NAD	cytosol	1.212	
NADH	cytosol	0.388	
P2G	cytosol	0.238	
P3G	cytosol	1.483	
PEP	cytosol	1.431	
PYR	cytosol	0.427	
TRIO	cytosol	2.22	

Table 3: Values are in mM and correspond to steady-state of steady-state model with extracellular glucose set to 0.0 mM. † Extracellular glucose concentration was varied. ‡ Glycogen concentration is set to 17.6 mM in time-course model and to 9.44 mM in steady-state model. Abbreviations: 2PG: 2-phosphoglycerate, 3PG: 3-phosphoglycerate, BPG: 1,3-bisphosphoglycerate, DHAP: dihydroxyacetone phosphate, F16BP: fructose-1,6-bisphosphate, F26BP: fructose-2,6-bisphosphate, F6P: fructose-6-phosphate, G6P: glucose-6-phosphate, GAP: glyceraldehyde 3-phosphate, GLCe: extracellular glucose, GLCi: intracellular glucose, GLYCO: glycogen, LAC: lactate, PEP: phosphoenolpyruvate, PYR: pyruvate.

5 Differential Equations

$$\begin{aligned}
\frac{dADP}{dt} &= v_{HK} + v_{PFK} + v_{Work} + v_{GS} - v_{PGK} - v_{PK} - 3v_{RES} - 2v_{AK} \\
\frac{dAMP}{dt} &= v_{AK} \\
\frac{dATP}{dt} &= v_{PGK} + v_{PK} + 3v_{RES} - v_{HK} - v_{PFK} - v_{Work} - v_{GS} + v_{AK} \\
\frac{dBPG}{dt} &= v_{GAPDH} - v_{PGK} \\
\frac{dF16BP}{dt} &= v_{PFK} - v_{ALD} \\
\frac{dF6P}{dt} &= v_{PGI} - v_{PFK} \\
\frac{dG6P}{dt} &= v_{HK} + v_{GLYCO} - v_{PGI} \\
\frac{GLYCO}{dt} &= \begin{cases} v_{GS} - v_{GP} & \text{in time-course model} \\ 0 & \text{in steady-state model} \end{cases} \\
\frac{dGLCi}{dt} &= v_{GLT} - v_{HK} \\
\frac{dNAD}{dt} &= v_{LDH} + v_{RES} - v_{GAPDH} - 4v_{Krebs} \\
\frac{dNADH}{dt} &= v_{GAPDH} + 4v_{Krebs} - v_{LDH} - v_{RES} \\
\frac{dP2G}{dt} &= v_{PGM} - v_{ENO} \\
\frac{dP3G}{dt} &= v_{PGK} - v_{PGM} \\
\frac{dPEP}{dt} &= v_{ENO} - v_{PK} \\
\frac{dPYR}{dt} &= v_{PK} - v_{Krebs} - v_{LDH} \\
\frac{dTRIO}{dt} &= 2v_{ALD} - v_{GAPDH}
\end{aligned}$$

6 References

1. Achcar, F. et al. Dynamic Modelling under Uncertainty: The Case of *Trypanosoma brucei* Energy Metabolism. PLOS Computational Biology 8 (2012).
2. Armstrong, R. L., Wilson, J. E. & Shoemaker, C. B. Purification and Characterization of the Hexokinase from *Schistosoma mansoni* Expressed in *Escherichia coli*. Protein Expression and Purification 8, 374–380 (1996).
3. Bexkens, M. L. et al. This manuscript (2020).
4. Brazier, J. B. & Jaffe, J. J. Two types of pyruvate kinase in schistosomes and filariae. Comparative Biochemistry and Physiology Part B: Comparative Biochemistry 44, 145–155 (1973).
5. Bueding, E. & MacKinnon, J. A. Studies of the Phosphoglucose Isomerase of *Schistosoma mansoni*. Journal of Biological Chemistry 215, 507–513 (1955).
6. Bueding, E. & Mansour, J. M. The Relationship Between Inhibition of Phosphofructokinase Activity and the Mode of Action of Trivalent Organic Antimonials on *Schistosoma mansoni*. British Journal of Pharmacology and Chemotherapy 12, 159–165 (1957).
7. Shapiro, T. A. & Talalay, P. *Schistosoma mansoni*: Mechanisms in regulation of glycolysis. Experimental Parasitology 54, 379–390 (1982).
8. Skelly, P. J., Stein, L. D. & Shoemaker, C. B. Expression of *Schistosoma mansoni* genes involved in anaerobic and oxidative glucose metabolism during the cercaria to adult transformation. Molecular and Biochemical Parasitology 60, 93–104 (1993).
9. Van Eunen, K., Kiewiet, J. A. L., Westerhoff, H. V. & Bakker, B. M. Testing Biochemistry Revisited: How In Vivo Metabolism Can Be Understood from In Vitro Enzyme Kinetics. PLOS Computational Biology 8 (2012).



CHAPTER 3

Schistosoma mansoni does not and cannot oxidise fatty acids, but these are used for biosynthetic purposes instead

Michiel L. Bexkens ^a, Mirjam M. Mebius ^a, Martin Houweling ^b,
Jos F. Brouwers ^b, Aloysius G.M. Tielens ^{a, b}, Jaap J. van Hellemond ^{a,*}

- a) Dept. Medical Microbiology & Infectious Diseases, Erasmus MC, University Medical Center Rotterdam, Rotterdam, the Netherlands
- b) Dept. Biochemistry & Cell Biology, Fac. Veterinary Medicine, Utrecht University, Utrecht, the Netherlands

ABSTRACT

Adult schistosomes, parasitic flatworms that cause the tropical disease schistosomiasis, have always been considered to be homolactic fermenters and, in their energy metabolism, strictly dependent on carbohydrates. However, more recent studies suggested that fatty acid β -oxidation is essential for egg production by adult female *Schistosoma mansoni*. To address this conundrum, we performed a comprehensive study on the lipid metabolism of *S. mansoni*. Incubations with [^{14}C]-labelled fatty acids demonstrated that adults, eggs and miracidia of *S. mansoni* did not oxidize fatty acids, as no $^{14}\text{CO}_2$ production could be detected. We then re-examined the *S. mansoni* genome using the genes known to be involved in fatty acid oxidation in six eukaryotic model reference species. This showed that the earlier automatically annotated genes for fatty acid oxidation were in fact incorrectly annotated. In a further analysis we could not detect any genes encoding β -oxidation enzymes, which demonstrates that *S. mansoni* cannot use this pathway in any of its lifecycle stages. The same was true for *S. japonicum* and all other schistosome species that have been sequenced. Absence of β -oxidation, however, does not imply that fatty acids from the host are not metabolized by schistosomes. Adult schistosomes can use and modify fatty acids from their host for biosynthetic purposes and incorporate those in phospholipids and neutral lipids. Female worms deposit large amounts of these lipids in the eggs they produce, which explains why interference with the lipid metabolism in females will disturb egg formation, even though fatty acid β -oxidation does not occur in schistosomes. Our analyses of *S. mansoni* further revealed that during the development and maturation of the miracidium inside the egg, changes in lipid composition occur which indicate that fatty acids deposited in the egg by the female worm are used for phospholipid biosynthesis required for membrane formation in the developing miracidium.

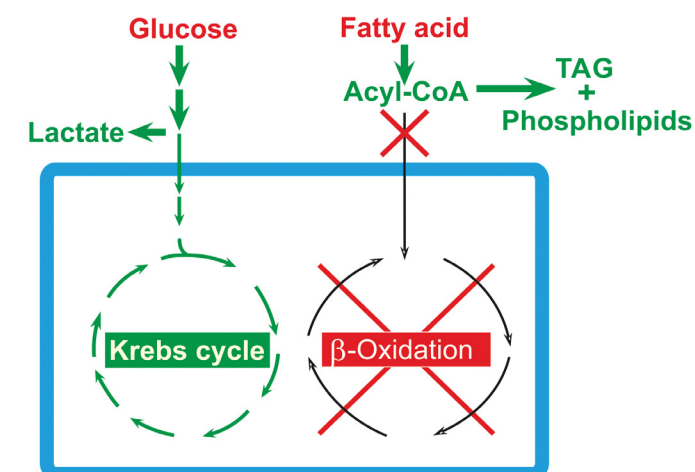
Keywords

Beta-oxidation, Energy metabolism, Helminths, Lipid metabolism, Schistosomiasis, Genome analysis

Highlights

- *Schistosoma mansoni* adults, eggs and miracidia do not oxidize fatty acids
- In-depth re-analysis of the *S. mansoni* genome revealed no enzymes for β -oxidation
- Host fatty acids are used by *S. mansoni* for biosynthetic purposes
- Schistosomes use host fatty acids for egg production
- Lipids play a role during the maturation of eggs

Metabolism of *S. mansoni*



INTRODUCTION

The blood dwelling parasite *Schistosoma mansoni* is a causative agent of the neglected tropical disease schistosomiasis that affects over 200 million people worldwide (Colley et al., 2014). Throughout the life-cycle of this helminth, *S. mansoni* encounters various environments and adapts its energy metabolism accordingly. The free-living stages, cercariae and miracidia, live on their endogenous glycogen stores which they completely oxidize to carbon dioxide using Krebs cycle activity and oxidative phosphorylation (Van Oordt et al., 1989; Tielens et al., 1991). Within the mammalian host, adult *S. mansoni* reside in the mesenteric veins, where male and female worms live paired and acquire everything they need directly from the blood of the host. These adult schistosomes have a mainly fermentative metabolism as only a small part of the glucose obtained from the host is fully oxidized to carbon dioxide using Krebs cycle activity and oxidative phosphorylation, while the major part is degraded to lactate and excreted as such (Bueding, 1950; Schiller et al., 1975; van Oordt et al., 1985). Lipids are also obtained from the host. The lipid metabolism of schistosomes is rather compromised, as schistosomes cannot synthesize sterols or free fatty acids de novo and must use complex precursors from the host (Brouwers et al., 1997). Until recently it was generally accepted that schistosomes do not catabolize lipids for ATP production. However, in 2009 the genome of *S. mansoni* was published, including an automated annotation which indicated that genes for all enzymes used in β -oxidation of fatty acids are present

(Berriman et al., 2009). Automated annotations of genomes are, however, inherently prone to mis annotations and are therefore continuously revised. Currently, several of the *S. mansoni* genes earlier annotated as coding for fatty acid β -oxidation enzymes are no longer annotated as such in GeneDB and in databases such as Biocyc.org, WormBase and the KEGG (Kyoto Encyclopedia of Genes and Genomes) database.

In 2012 Huang et al. (2012) reported that oxidation of fatty acids acquired from the host is essential for egg production by female *S. mansoni* worms. Thereafter fatty acid β -oxidation has received a lot of attention and most general reports on schistosomiasis now state that fatty acid oxidation is essential for egg production in female schistosomes (Colley et al., 2014; Guigas and Molofsky, 2015; Pearce and Huang, 2015; Oliveira et al., 2016). Subsequently, the postulated fatty acid β -oxidation process was a subject of studies on gene expression in schistosomes (Buro et al., 2013; Li et al., 2017) and of studies that aimed to identify novel drugs for schistosomiasis (Edwards et al., 2015; Timson, 2016).

However, the assumption that fatty acid oxidation occurs in schistosomes is still controversial as fatty acid oxidation has never been demonstrated directly in *S. mansoni*, nor in any other parasitic trematode for that matter (Rumjanek and Simpson, 1980; Saz, 1981; Frayha and Smyth, 1983). This prompted us to perform a comprehensive analysis of the lipid metabolism of *S. mansoni*. We incubated adult worm pairs as well as eggs and miracidia with [14 C]-labelled glucose and [14 C]-labelled fatty acids to determine the metabolic fate of these substrates in *S. mansoni*. Furthermore, a genomic analysis was performed to examine the possible presence of genes in the *S. mansoni* genome encoding enzymes involved in oxidation of fatty acids. To further investigate the role of fatty acids in eggs we performed a lipidome analysis of eggs during their development.

MATERIALS AND METHODS

Parasites and chemicals

A Puerto Rican strain of *S. mansoni* was maintained in Golden hamsters with animal ethics approval (license EUR1860-11709). Animal care and maintenance were in accordance with institutional and governmental guidelines. Adult *S. mansoni* worms were isolated from isoflurane anaesthetized hamsters 7 weeks p.i. Worms were collected from the portal vein following heart perfusion with S_{20} medium (20 mM HEPES, 85 mM NaCl, 5.4 mM KCl, 0.7 mM Na_2HPO_4 , 1 mM MgSO_4 , 1.5 mM CaCl_2 , 25 mM NaHCO_3 and 20 mM glucose pH 7.4) (Tielens and van den Bergh, 1987). *Schistosoma mansoni* eggs were obtained from livers of infected hamsters. These livers were homogenized in 1.8% (w/v) NaCl using a MACS

homogenizer (Miltenyi Biotec, San Diego, USA). The liver homogenate was treated with 1% trypsin in 1.8% NaCl (BD, New Jersey, USA) for 1 h at 37°C, after which eggs were isolated by filtration over three sieves with decreasing mesh sizes (Dresden and Payne, 1981). The eggs were collected and rinsed with sterile water. When indicated, the total isolated egg fraction was separated into immature and mature eggs via Percoll density centrifugation by the method described by Ashton et al. (2001). All chemicals used were from Sigma Aldrich, St. Louis, MO, USA unless otherwise specified.

Metabolic incubations

Schistosoma mansoni worms (10 pairs per incubation) were incubated in 25 ml Erlenmeyer flasks for 2.5 h at 37°C, 95% O_2 , 5% CO_2 in 5 ml of S_5^+ medium (20 mM HEPES, 85 mM NaCl, 5.4 mM KCl, 0.7 mM Na_2HPO_4 , 1 mM MgSO_4 , 1.5 mM CaCl_2 , 25 mM NaHCO_3 , 5 mM glucose and 1% (v/v) delipidated BSA pH 7.4). All incubations were started with the addition of one of the labelled substrates (all from PerkinElmer, Boston, MA, USA): D-[6- 14 C] glucose (5 mM, 5 μCi), [1- 14 C] octanoic acid (210 μM , 5 μCi) or [1- 14 C] oleic acid (210 μM , 5 μCi). Radioactive incubations were stopped by acidification of the medium to pH 2 by addition of HCl through the septum of the sealed Erlenmeyer flask. Carbon dioxide was trapped for 1.5 h in 200 μl of 4M KOH in a center well suspended above the incubation medium. Afterwards, the trapping solution was transferred to a vial containing water and Luma gel (Lumac*LCS, Groningen, The Netherlands), after which radioactivity was measured in a scintillation counter. Worm pairs were removed from the incubation medium and stored at -20 °C until further analysis. The acidified supernatant was neutralized by the addition of 6 M NaOH. The labelled metabolic end products in the supernatant were analyzed by anion exchange chromatography on a Dowex 1X8, 100–200 mesh column (Serva) (60 \times 1.1 cm) in chloride form (Tielens et al., 1981). The column was eluted successively with 200 ml of 5 mM HCl and 130 ml of 0.2 M NaCl. All fractions were collected and radioactivity was measured in Luma gel. All values were corrected for blank incubations.

Schistosoma mansoni eggs ($4.3 \cdot 10^4$ – $6.2 \cdot 10^4$) were freshly isolated from infected livers and subsequently transferred to a 25 ml Erlenmeyer flask containing 5 ml of a 1 mM glucose solution supplemented with 100 μg of penicillin and 100 units of streptomycin per ml. After addition of D-[6- 14 C] glucose (5 mM, 5 μCi) or [1- 14 C] octanoic acid (210 μM , 5 μCi) eggs were incubated for 20 h at 22°C while shaking gently at 125 rpm. Incubations were stopped and analyzed as described above.

Analysis of incorporated lipids after metabolic incubation

To analyze the incorporation of radioactively labeled fatty acids into complex lipids by

S. mansoni worms and eggs, lipids were extracted from incubated worms and eggs according to the method of Bligh and Dyer (1959). Prior to the lipid extraction, eggs were disrupted by sonication and adult worms were homogenized by a Teflon potter. The isolated lipid fraction was subsequently split into neutral lipids and phospholipids by dissolving the total lipid fraction in chloroform, after which it was loaded on a 2 ml silica gel 60 column (8 cm tall, 0.5 cm in diameter) equilibrated in chloroform. Neutral lipids were eluted with chloroform, followed by elution of phospholipids with methanol. The lipid composition of the neutral lipid and phospholipid fractions was further analyzed by thin layer chromatography (TLC) on Silica G by the methods of Freeman and West (1966) and Skipski et al. (1962), respectively. After separation of distinct lipid classes by TLC, the plates were dried and placed in iodine vapor to visualize lipid spots, which were subsequently scraped off. The collected silica was suspended in 1 ml of H₂O and 3 ml of Luma gel were added before radioactivity was measured in a scintillation counter.

Lipidome analysis of immature and mature eggs

Approximately 1000 freshly isolated *S. mansoni* eggs were stained with Nile red lipophilic stain (1 mg/ml) for 20 min, shaking at 1200 rpm at 25 °C in 1 ml of 0.9% (w/v) NaCl. After staining, the eggs were washed twice with 1 ml 0.9% (w/v) NaCl and mounted for microscopy. Phase contrast images were captured at 200x magnification. For each bright field image, a corresponding fluorescent exposure was recorded. Eggs were classified by size and developmental stage as described by Jurberg et al. (2009).

In order to analyze the lipid content in immature and mature eggs, lipids were extracted as described in Section 2.3. Subsequently, the phospholipid content in mature and immature eggs was quantified by the method of Rouser et al. (1970), and the ratio of phospholipids over neutral lipids as well as the lipid species composition was determined by Liquid Chromatography coupled to Mass Spectrometry (LCMS). The extracted lipids were loaded on a hydrophilic interaction liquid chromatography (HILIC) column (2.6 µm HILIC 100 Å, 50 x 4.6 mm, Phenomenex, Torrance, CA, USA) and eluted at a flow rate of 1 mL/min with a gradient from acetonitrile/acetone (9:1, v/v) to acetonitrile/H₂O (7:3, v/v) with 10 mM ammonium formate. Both elution solutions also comprised 0.1% (v/v) formic acid. The column outlet of the LC was connected to a heated electrospray ionization (HESI) source of an LTQ-XL mass spectrometer (ThermoFisher Scientific, Waltham, MA, USA). Full scan spectra were collected from m/z 450–1050 at a scan speed of three scans/s. For analysis, the data were converted to mzXML format and analyzed using XCMS version 1.52.0 running under R version 3.4.3 (Smith et al., 2006; R Development Core Team: A language and environment for statistical computing. R Foundation for Statistical Computing, 2016). Principle Component Analysis (PCA) provided by the R

package *pcaMethods* (Stacklies et al., 2007) was used to visualize the multidimensional LC-MS data.

Identification strategy to detect genes possibly encoding enzymes required for fatty acid oxidation in the *S. mansoni* genome

In order to detect genes within the *S. mansoni* genome that are possibly involved in fatty acid oxidation, genes known to be involved in fatty acid oxidation (KEGG pathway 00071) were retrieved from six model reference species: *Caenorhabditis elegans*, *Crassostrea gigas*, *Danio rerio*, *Drosophila melanogaster*, *Homo sapiens* and *Mus musculus*. The protein sequences of these genes were used as a query in a forward BlastP search against the *S. mansoni* genome with an E-value cut-off of 10⁻²⁰. This forward BlastP search resulted in the identification of 14 *S. mansoni* protein sequences. These proteins possibly involved in lipid metabolism were further investigated by the following annotation strategy. First, using the Multiple Sequence Comparison by Log-Expectation (MUSCLE) algorithm (Edgar, 2004), the corresponding proteins of these identified *S. mansoni* genes were aligned to the amino acid sequences of the best hit from the forward BlastP query with the six model organisms. Second, these alignments were further investigated to determine whether obvious conserved regions in the proteins of the model organisms are present in the corresponding schistosomal proteins. Third, the *S. mansoni* proteins were used as a query in a reversed BlastP search against the six model organisms to check their identity and to verify whether the model organism contains a protein with more similarity to the schistosomal protein than the one used in the forward BlastP where only the proteins involved in fatty acid oxidation were used as a query. As a control we also searched in the *S. mansoni* genome for the presence of the enzymes of KEGG pathways 00010 (glycolysis and gluconeogenesis) and 00020 (Citrate Cycle).

RESULTS

The lipid metabolism of *S. mansoni* adult worms and that of eggs and miracidia was studied by incubations with ¹⁴C-labelled fatty acids, after which the metabolic fate of these fatty acids was determined by analysis of ¹⁴C-labelled excreted end products to detect catabolic processes and by analysis of ¹⁴C-labelled lipids to detect incorporation of fatty acids in anabolic processes. Normal physiological functioning of *S. mansoni* can only be studied in paired worms as female worms need males for normal functioning. Female-specific gene expression is dependent on pairing with male worms. To maintain female vitelline cell development there must be direct contact between the male and the

female, and they cease egg laying after removal of the accompanying male (Loverde et al., 2004). Therefore we intentionally studied paired worms as our radioactive method is sensitive enough to detect fatty acid oxidation even if it would occur to a significant extent in female worms only.

Lipid metabolism in adult *S. mansoni* worm pairs

In order to use fatty acids for the production of ATP, fatty acids must be oxidized to carbon dioxide, as fatty acids are too reduced to be fermented. To detect fatty acid oxidation by adult *S. mansoni* worm pairs, the worms were incubated with [1-¹⁴C] oleic acid, or with [1-¹⁴C] octanoic acid, a medium chain-length fatty acid that easily crosses membranes. After these incubations we analyzed the formation of ¹⁴CO₂. We could not detect any fatty acid oxidation by adult *S. mansoni* worm pairs, as the production of ¹⁴C-labeled CO₂ from [1-¹⁴C] octanoic acid as well as from [1-¹⁴C] oleic acid was below the detection limit of 0.05 nmol of CO₂ per h (Table 1). In a simultaneously performed control experiment with [6-¹⁴C] glucose, approximately 60 nmol of CO₂ were produced per h by 10 worm pairs, which is comparable with earlier studies (Tielens et al., 1989). This result showed that the parasites were metabolically active and that if production of ¹⁴C-labelled CO₂ from fatty acids had occurred, it would have been detected by our assay system. All together these results showed that the adult worms did not oxidize fatty acids under standard incubation conditions.

Previous research has shown that *S. mansoni* cannot synthesize lipids de novo, and therefore, adult worms take up fatty acids from their environment, after which the fatty acids can be modified by elongation before incorporation in triacylglycerol (TAG) species and phospholipids (Meyer et al., 1970; Brouwers et al., 1997). To investigate the anabolic fate of the exogenous supplied ¹⁴C-labeld fatty acids in adult *S. mansoni* worms, we determined the incorporation of [1-¹⁴C] octanoic acid and [1-¹⁴C] oleic acid into phospholipids and neutral lipids by adult worm pairs in the above mentioned incubations. This showed that adult worm pairs incorporated oleic acid in both neutral lipids and phospholipids, at rates of approximately 16 nmol and 5.5 nmol per h per 10 worm pairs, respectively (Table 1). Incorporation of octanoic acid was not detected (Table 1). From these results and earlier reports (Meyer et al., 1970; Brouwers et al., 1997), it can be concluded that the lipid metabolism of *S. mansoni* adult worms is fairly limited because adult worms do not de novo synthesize nor oxidize fatty acids. Adult schistosomes have to obtain fatty acids from their environment and can modify those, after which they are used as building blocks for the synthesis of phospholipids and neutral lipids such as TAG.

Table 1. Analysis of end product formation and/or incorporation of labelled substrate in neutral lipids and phospholipids by *Schistosoma mansoni* worms or eggs plus miracidia. Organisms were incubated with labelled glucose or fatty acid for up to 20 h, after which an end product formation was analyzed in the headspace or supernatant of the incubation. *S. mansoni* worms or eggs and miracidia were then analyzed for incorporation of labelled substrate.

Substrate	End product formation		Incorporation of labelled substrate	
	CO ₂ (nmol/h)	Lactate (nmol/h)	Neutral lipids (nmol/h)	Phospholipids (nmol/h)
	worms ^a	worms ^a	worms ^a	worms ^a
[6- ¹⁴ C]-Glucose	62.3 ± 10.4 ^c	534 ± 74 ^c	eggs + miracidia ^b	eggs + miracidia ^b
[1- ¹⁴ C]-Octanoic Acid	N.D.	na	0.49 ^e	0.19 ^f
[1- ¹⁴ C]-Oleic Acid	N.D.	na	33.81 ^g	N.D.
			na	5.51 ± 2.39 ^c
				na

^a10 worm pairs per incubation
^bValues are expressed per 50,000 (eggs + miracidia)
^cAll values represent the mean in nmol per hour per 10 worm pairs and S.D. of three independent experiments.
^dMean of two independent experiments (6.98 and 7.28)
^eMean of two independent experiments (0.53 and 0.44)
^fMean of two independent experiments (0.19 and 0.18)
^gMean of two independent experiments (29.9 and 37.73)
N.D., not detectable, below detection limit of assay
na, not analyzed.

Lipid metabolism of *S. mansoni* eggs and miracidia

We also investigated the lipid metabolism of *S. mansoni* eggs and miracidia by incubation of isolated *S. mansoni* eggs in water with trace amounts of ^{14}C -labeled substrates. Although eggs were isolated from liver tissue in 1.8 % (w/v) NaCl and in the dark, a situation in which only a few eggs will hatch and release miracidia (Xu and Dresden, 1990), the subsequent metabolic incubation was performed in water and during the 20 h incubation a substantial part of the eggs hatched and released miracidia into the medium. Therefore, the results of these incubations reflect in fact the combined metabolic activities of eggs plus miracidia. The *S. mansoni* eggs plus miracidia were incubated with $[1-^{14}\text{C}]$ oleic acid, $[1-^{14}\text{C}]$ octanoic acid and with $[6-^{14}\text{C}]$ glucose. After overnight incubation the production of $^{14}\text{CO}_2$ was determined, but *S. mansoni* eggs plus miracidia did not produce detectable amounts of $^{14}\text{CO}_2$ from the ^{14}C -labelled fatty acids, whereas in the simultaneously performed control incubation with $[6-^{14}\text{C}]$ glucose 7.1 nmol of CO_2 was produced per h per 50,000 organisms (Table 1).

Since the supplied ^{14}C -labeled fatty acids were not used for fatty acid oxidation by *S. mansoni* eggs and miracidia, we analyzed whether the incubated eggs and miracidia had taken up $[1-^{14}\text{C}]$ octanoic acid and incorporated it in complex lipids. This revealed that octanoic acid was incorporated in neutral lipids at a rate of 34 nmol per h per 50,000 *S. mansoni* eggs plus miracidia (Table 1). The incubations performed in parallel with $[6-^{14}\text{C}]$ -glucose demonstrated that not only fatty acids were incorporated into neutral- as well as into phospholipids, but intermediates of glucose metabolism were also incorporated (Table 1). As *S. mansoni* cannot synthesize fatty acids de novo, the incorporation of ^{14}C -label from glucose in lipids is most likely the result of elongation of fatty acids with acetyl-CoA or of the incorporation of glycerol-3-phosphate as a backbone for TAG or phospholipid biosynthesis. These results showed that *S. mansoni* eggs and/or miracidia take up fatty acids and are capable of incorporating those in complex lipids, but they do not oxidize fatty acids to CO_2 .

To perform a more in-depth analysis of the lipid metabolism of the *S. mansoni* egg during development, freshly isolated eggs were separated into mature and immature eggs (Ashton et al., 2001), after which we analyzed the distribution and composition of phospholipids and neutral lipids in the immature and the mature egg fraction. Microscopic analysis of Nile red stained *S. mansoni* eggs showed a differential distribution and content of lipids during the development of the egg (Fig. 1). Immature eggs (Fig. 1A-D) contained many large lipid droplets, which disappeared during maturation of the egg (Fig. 1G-H), suggesting that the amount of neutral lipids decreased during development. To analyze the changes in lipid composition during maturation in more detail, the lipid

composition in the immature and the mature eggs was analyzed by LC-MS. A significant difference in the phospholipid content in immature versus mature eggs was observed, as the phospholipid content almost doubled from 3.2 pmol to 5.2 pmol of fatty acids per egg after maturation and the amount of neutral lipids decreased, although this difference was not significant (Fig. 2). PCA of the lipidomic data demonstrated that the lipid composition between mature and immature eggs differed substantially (Fig. 3A), as the relative abundance of many different lipid species from all lipid classes differs between mature and immature eggs (Fig. 3B). For instance, the phosphatidylserine species (40:4) and phosphatidylinositol species (38:4) were more abundantly present in immature eggs, whereas the phosphatidylcholine species 34:1 and 36:1 were more abundantly present in mature eggs. However, no significant differences in the overall phospholipid class distribution, fatty acid chain length and degree of unsaturation were observed (data not shown). All together, these results showed that the lipidome of *S. mansoni* eggs changes during egg development.

Analysis of lipid metabolism at a genomic level

As the investigated stages of *S. mansoni* apparently did not oxidize fatty acids under standard incubation conditions, the question arises whether *S. mansoni* has the genomic capacity to do so at all. To investigate the possible presence of genes in the *S. mansoni* genome which could encode the enzymes required for fatty acid oxidation, we queried the *S. mansoni* genome using genes known to be involved in fatty acid oxidation. Genes annotated in KEGG map00071 "fatty acid degradation" were retrieved from six well characterized model organisms: *C. elegans*, *C. gigas*, *D. rerio*, *D. melanogaster*, *H. sapiens* and *M. musculus*. This forward BlastP search resulted in the identification of 15 *S. mansoni* protein sequences. Of these 15 *S. mansoni* proteins, two identifiers were protein isoforms of the same gene, leaving 14 *S. mansoni* genes that might encode enzymes involved in fatty acid oxidation (Table 2). Ten of these 14 genes seemed to encode acyl-CoA synthetases. Of the four remaining genes, three genes seemed to code for homologs of mitochondrial β -oxidation enzymes (acyl-CoA dehydrogenase, enoyl-CoA hydratase and 3-keto-acyl CoA thiolase) and the protein encoded by the last gene seemed to be a homolog of both carnitine palmitoyl transferase 1 and 2 (CPT-1 and CPT-2). However, the similarity of these last four *S. mansoni* proteins to their corresponding proteins in the six model organisms is probably low, as the E-values were rather high ($10^{-20} > E > 10^{-80}$, Supplementary Tables S1, S2). Using this approach, no schistosomal protein was found with a significant homology to 3-hydroxyacyl-CoA dehydrogenase (enzyme 6 in Fig. 4).

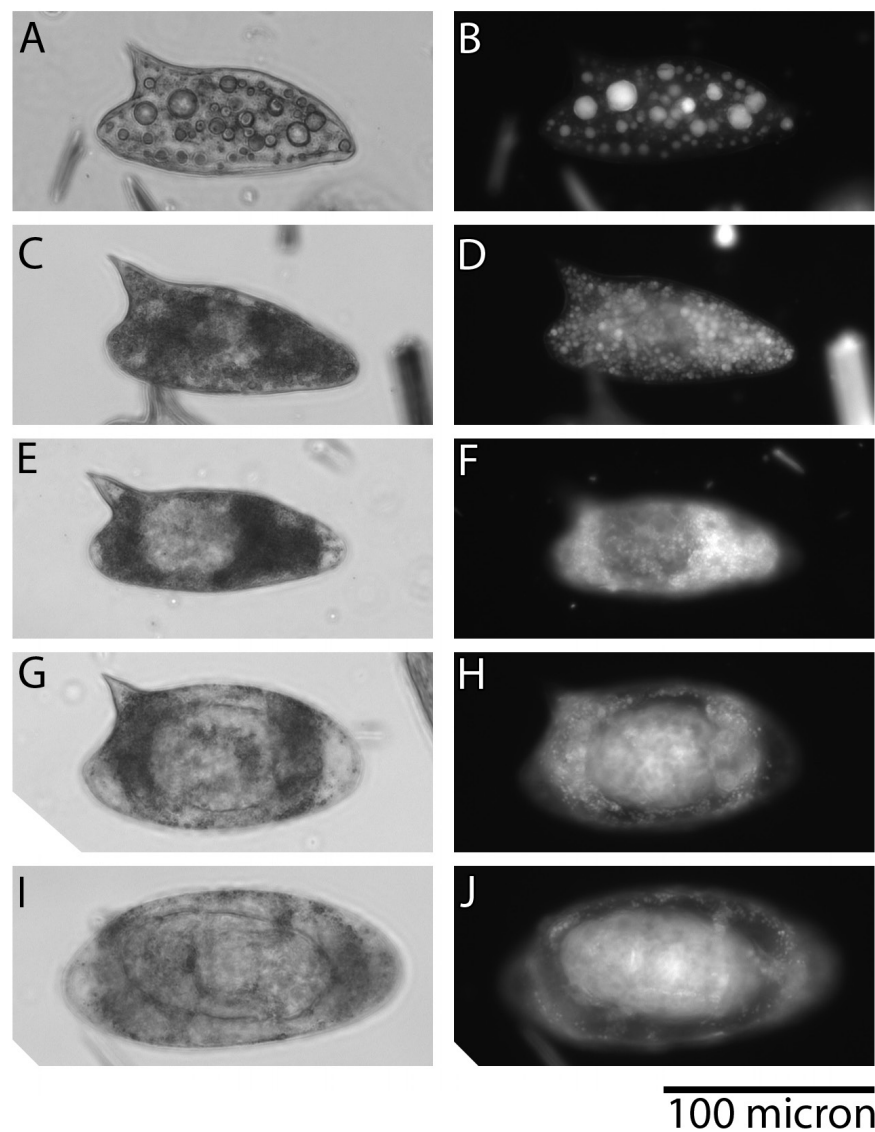


Figure 1. Differential distribution of lipids in developing *Schistosoma mansoni* eggs. Freshly isolated live *S. mansoni* eggs were stained with Nile Red lipophilic stain, after which representative phase contrast images (A, C, E, G and I) and their corresponding fluorescent images of Nile Red lipophilic stain (B, D, F, H and J) were taken. Eggs are placed in order of maturation; from immature eggs at the top to fully mature eggs with a moving miracidium at the bottom of the figure.

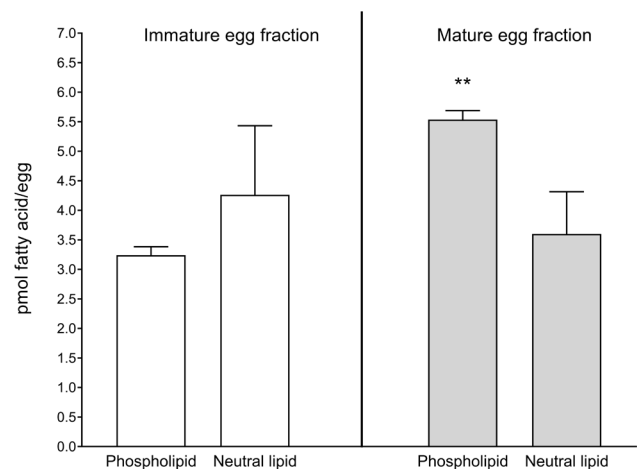


Figure 2. The amount of fatty acids in phospholipids and neutral lipids in *Schistosoma mansoni* eggs changes during maturation. The phospholipid and neutral lipid content of *S. mansoni* eggs were analyzed in immature and mature eggs and expressed as picomoles of fatty acid per lipid fraction. Shown is the average and S.D. of three independent experiments, each performed in duplicate. ** A one-tailed paired t-test showed a statistically significant increase in the phospholipid content (pmol per egg) of mature eggs versus immature eggs ($P < 0.0054$).

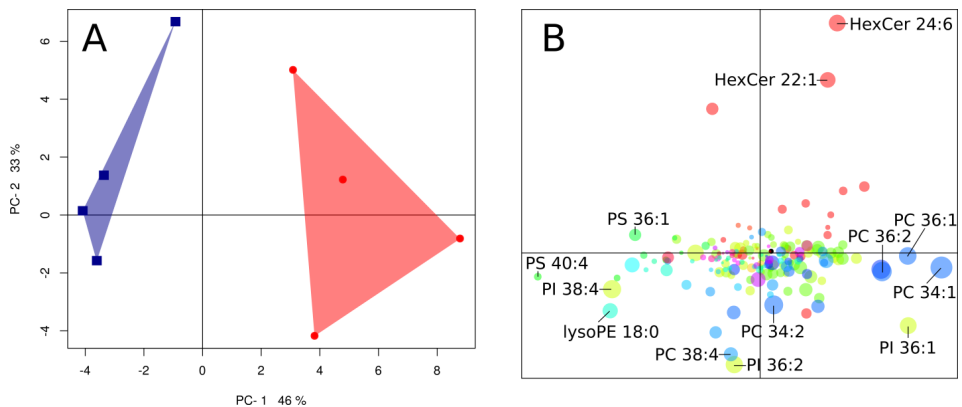


Figure 3. Lipidome analysis of mature and immature *Schistosoma mansoni* eggs. (A) Principal Component Analysis (PCA) on the lipidomic data of mature (blue) and immature (red) eggs revealed different lipid fingerprints for both, as could be concluded from their distinct and non-overlapping score plots. The value of Principal Component 1 (PC-1, representing 46% of total data variance) was found to correspond with the maturation state of the eggs and shows that the difference between mature and immature eggs is reflected in many different lipid species from all major phospholipid classes. (B) Lipids with positive loadings on PC-1 (e.g. PC 34:1, PI 36:1) were more abundant in immature eggs, lipids with negative loadings on PC-1 (e.g. PS 40:4, PI 38:4) were more abundant in mature eggs. HexCer, hexosylceramide; PC, phosphatidylcholine; PE, phosphatidylethanolamine; PI, phosphatidylinositol; PS, phosphatidylserine.

To further investigate whether or not the retrieved schistosomal genes really encode the corresponding enzymes involved in fatty acid oxidation, we aligned the found schistosomal proteins with the best hit for each model organism (Supplementary Fig. S1). The alignments for the identified *S. mansoni* genes possibly encoding acyl-CoA synthetases (Fig. 4, enzyme 1) indicated that these *S. mansoni* proteins are true homologues of acyl-CoA synthetases, because the identified *S. mansoni* proteins were highly similar to the ones that encode acyl-CoA synthetases in the six model organisms (Supplementary Fig. S1). However, the alignments of the other five retrieved proteins showed low homology to the corresponding proteins of the six model organisms and regions highly conserved in the proteins of the model organisms seemed to be missing in the schistosomal proteins (Supplementary Fig. S1).

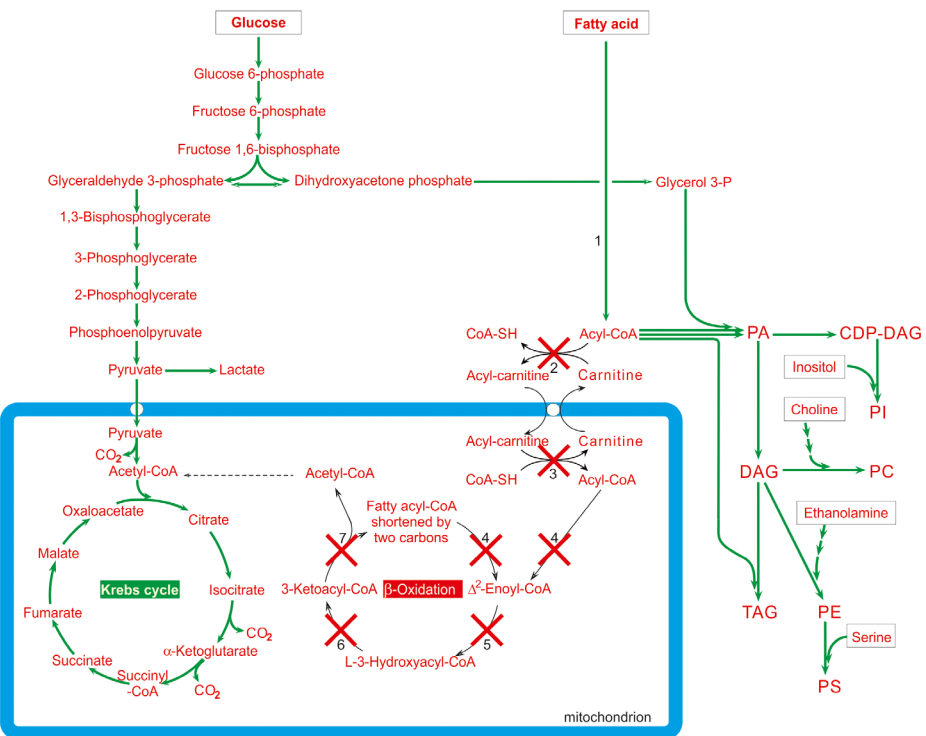


Figure 4. Metabolic map of the glucose and fatty acid metabolism of *Schistosoma mansoni*. Shown are the glycolytic pathway, Krebs cycle, fatty acid β -oxidation and the anabolic processes of triacylglycerol (TAG) and phospholipid synthesis. Genes encoding the enzymes for glycolysis, Krebs cycle and the anabolic processes are present (green arrows), while genes encoding enzymes for fatty acid β -oxidation are absent in the genome of *S. mansoni* (red crosses). CDP-DAG, cytidine diphosphate diacylglycerol; DAG, diacylglycerol; PA, phosphatidic acid; PC, phosphatidylcholine; PE, phosphatidylethanolamine; PI, phosphatidylinositol; PS, phosphatidyl serine. Boxed substrates are supplied by the host. Enzymes: 1, Acyl-CoA synthetase; 2, Carnitine-palmitoyltransferase 1; 3, Carnitine-palmitoyltransferase 2; 4, Acyl-CoA dehydrogenase; 5, Enoyl-CoA hydratase; 6, 3-hydroxyacyl-CoA dehydrogenase; 7, 3-ketoacyl-CoA thiolase.

We further analyzed these alignments to investigate whether known conserved regions in the proteins in question are indeed absent in the corresponding schistosomal proteins. To this end we produced aligned barcodes of each enzyme where a black bar is produced only when an amino acid is identical in *all* six model organisms and these bar codes were then compared with the found schistosomal proteins (Fig. 5). This analysis clearly showed that the schistosomal acyl-CoA synthetases are indeed highly similar to the ones of the model organisms, as their barcodes are real look-a-likes of those of the model organisms. In contrast, the 100% conserved regions in the model organisms of the other five proteins are not mirrored in the schistosomal ones, despite the large gaps the algorithm introduced in three schistosomal proteins (2-4) to produce the best alignment.

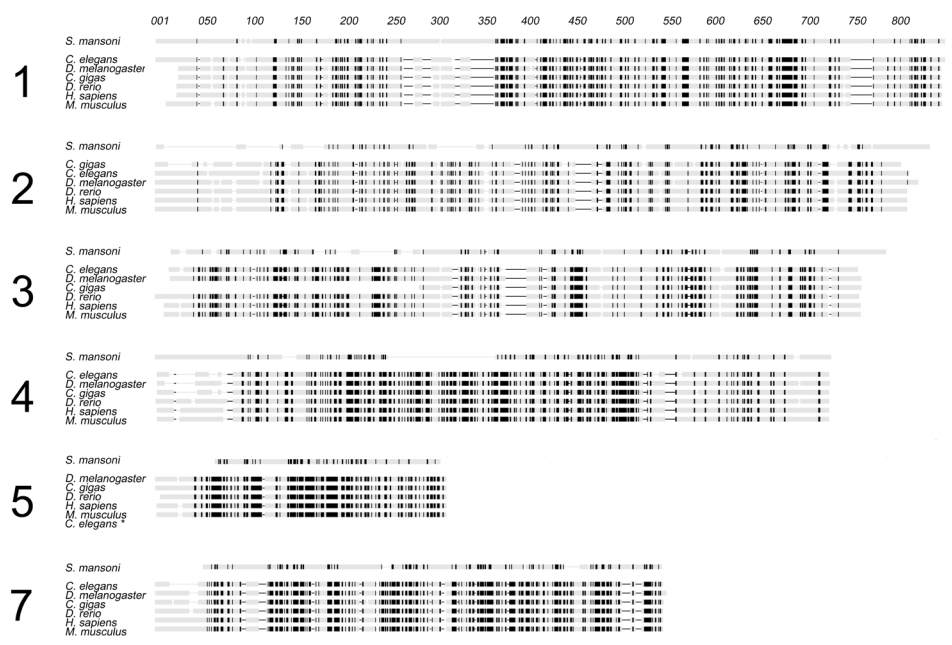


Figure 5. Barcode alignment of *Schistosoma mansoni* proteins against proteins involved in fatty acid oxidation. Conserved residues (100% identity) present throughout all six model organisms (*Caenorhabditis elegans*, *Drosophila melanogaster*, *Crassostrea gigas*, *Danio rerio*, *Homo sapiens*, *Mus musculus*) have been marked as black bars after which it was analyzed whether these residues were also identical in the most similar *S. mansoni* sequences. The resulting barcode shows conserved domains present or absent in *S. mansoni* proteins. The large numbers on the left correspond with the numbering used in Fig. 4 and Table 2. For enzyme number 6, 3-hydroxyacyl-CoA dehydrogenase, no protein with significant homology was detected within the *S. mansoni* genome. The complete alignment is shown in Supplementary Fig. S1. *no gene found with significant homology.

As a final check in this genomic analysis, we performed a reverse BlastP query where the found schistosomal proteins were used in a BlastP search against the six model organisms to investigate whether the model organisms contain a protein with a higher similarity to the schistosomal protein than the protein used in the forward BlastP where only the enzymes involved in fatty acid oxidation were used as a query. This reverse BlastP search revealed that the presumed schistosomal acyl-CoA synthetases indeed show the best homology to the acyl-CoA synthetases of the model organisms (Table 2). However, this reversed BlastP analysis also revealed that the presumed homologs of three β -oxidation enzymes, and CPT-1 and CPT-2, were in fact coding for other proteins, or were at least more similar to those other proteins than to the enzymes involved in fatty acid oxidation (Table 2).

As a positive control, the same genomic analysis was performed for KEGG pathway 00010 (glycolysis and gluconeogenesis) and KEGG pathway 00020 (Citrate Cycle), pathways that are both present in *S. mansoni*. This analysis demonstrated that genes could be detected in the *S. mansoni* genome for all enzymes of both pathways. In addition, the identified *S. mansoni* genes were highly homologous to their corresponding genes in the six model organisms, as demonstrated by the low E-values ($E < 10^{-80}$, not shown).

All together, the results of this genomic analysis showed that the *S. mansoni* genome contains genes coding for acyl-CoA synthetases, which are enzymes that activate fatty acids by coupling those to coenzyme-A (Fig. 4, enzyme number 1). The resulting acyl-CoAs are the beginning of several anabolic pathways that are known to be present in *S. mansoni* (Fig. 4). The genome of *S. mansoni*, however, does not contain genes with a reasonable homology to genes encoding enzymes for fatty acid β -oxidation in the six model organisms. In addition, no genes were found for the two enzymes required for import of fatty acids into the mitochondrion: the cytosolic CPT-1 and mitochondrial CPT-2. This is in itself no longer surprising: an import system for fatty acids is superfluous when the mitochondria contain no enzymes for fatty acid β -oxidation. We also performed this analysis on the published whole genomes of *Schistosoma japonicum*, *Schistosoma haematobium*, *Schistosoma mattheei*, *Schistosoma rodhaini*, *Schistosoma curassoni* and *Schistosoma margrebowiei*, which led to the same result, i.e. none of those parasites possess enzymes for fatty acid β -oxidation (not shown).

Table 2. Analysis and comparison of BlastP results with genome annotations of genes coding for enzymes present in the *Schistosoma mansoni* (Smp) genome. A BlastP analysis was performed using proteins known to be involved in fatty acid oxidation in six model organisms. Results were then ordered by enzyme numbers 1-7 as in Figure 4, representing steps in lipid metabolism and beta-oxidation. Identified genes were compared with earlier studies and analyzed using NCBI SMARTblast.

Enzyme	Enzyme code	Potential homologs identified	Earlier ID (Berriman et al., 2009)	Best hit of reversed BlastP against model organisms	Enzyme code of best hit
1. Acyl-CoA synthetase	EC 6.2.1.3	Smp_103160.1 Smp_103160.2 Smp_175090.1 Smp_175090.2 Smp_175090.3 Smp_266800.1 Smp_125560.1 Smp_209040.1 Smp_165850.1 Smp_244300 Smp_146190	Smp_103160 Smp_175090	Acyl-CoA synthetase Acyl-CoA synthetase Acyl-CoA synthetase Acyl-CoA synthetase Acyl-CoA synthetase Acyl-CoA synthetase Acyl-CoA synthetase choline O-acetyltransferase	EC 6.2.1.3
2. CPT-1	EC 2.3.1.21		Not mentioned		EC 2.3.1.6
3. CPT-2	EC 2.3.1.21		Not mentioned		
4. Acyl-CoA dehydrogenase	EC 1.3.8.-	Smp_122930	Smp_122930	acyl-CoA dehydrogenase family member 9	EC 1.3.99.-
5. Enoyl-CoA hydratase	EC 4.2.1.17	Smp_024930	Smp_024930	enoyl-CoA hydratase domain-containing protein 3	-
6. 3-hydroxyacyl-CoA dehydrogenase	EC 1.1.1.35	ng	Smp_151030	-	-
7. 3-ketoacyl-CoA thiolase	EC 2.3.1.16	Smp_267310	Smp_197330	acetyl-CoA acetyltransferase, cytosolic	EC 2.3.1.9

CPT, carnitine palmitoyl transferase; ng, no gene found with significant homology ($E > 10^{-20}$)

DISCUSSION

In this study we performed a comprehensive analysis of the lipid metabolism of *S. mansoni* with a special focus on the debated presence or absence of fatty acid β -oxidation in adult worms. Metabolic incubations with the [^{14}C]-labelled fatty acids octanoic acid (C8:0) and oleic acid (C18:1) were used to examine the metabolic fate of fatty acids taken up by adult worms and eggs plus miracidia. In addition to a physiologically relevant fatty acid (oleic acid), octanoic acid was studied as well, due to its high bio-availability as it is a medium-chain fatty acid that can pass through membranes relatively easily and independent of carnitine shuttles (Schönfeld and Wojtczak, 2016). These experiments showed that fatty acids are taken up from the environment and are subsequently incorporated in complex lipids such as TAG and phospholipid species, which is an observation that is in agreement with multiple earlier publications (Meyer et al., 1970; Saz, 1970; Rumjanek and Simpson, 1980; Frayha and Smyth, 1983; Brouwers et al., 1997). Despite the high sensitivity of our assay in which radioactive fatty acids were used, we could not detect the production of carbon dioxide from fatty acids, neither by adult worms nor by eggs and miracidia. This showed that these *S. mansoni* stages do not oxidize fatty acids, which confirms an earlier study which demonstrated that miracidia consume their glycogen reserves but not their endogenous TAG stores (Tielens et al., 1991).

As our present study showed that fatty acids were not oxidized, we re-examined whether schistosomes possess the necessary enzymes to do so. In the first automated genome annotation in 2009, it was reported that the genes for the enzymes required for fatty acid β -oxidation are present in the genome of *S. mansoni* (Berriman et al., 2009). Our analysis to resolve the possible presence of genes coding for fatty acid β -oxidation enzymes in *S. mansoni* demonstrated that the genes coding for enzymes required for fatty acid β -oxidation are absent in the *S. mansoni* genome. This discrepancy with earlier results is caused by the inherent impreciseness of the automated annotation performed earlier. The earlier identified genes indeed encode enzymes related to lipid metabolism with some of the conserved domains present in enzymes required for fatty acid β -oxidation, but these conserved domains are also present in enzymes involved in other processes such as lipid binding and biosynthetic thiolase reactions. The presence of these shared domains explains why these proteins were earlier accidentally annotated as being involved in β -oxidation of fatty acids (Berriman et al., 2009). During the review process of this manuscript, an analysis of all available genomes of helminths was published by the International Helminth Genomes Consortium. In that new analysis it is also concluded that schistosomes indeed lack genes of the enzymes necessary for β -oxidation of fatty

acids (Coghlan et al., 2019). Genes coding for acyl-CoA synthetases, on the other hand, are present in the genome of *S. mansoni*, but these enzymes activate fatty acids by coupling those to coenzyme-A and the resulting acyl-CoAs are the beginning of several anabolic pathways that are known to be present in *S. mansoni* (Fig. 4).

As *S. mansoni* does not possess the enzymes necessary for fatty acid oxidation, how is it then possible that experiments seemed to indicate that fatty acid oxidation is essential for egg production by female *S. mansoni* (Huang et al., 2012)? That study used inhibitors and RNA interference (RNAi) to study fatty acid metabolism, while none of the experiments provides direct evidence for fatty acid oxidation, i.e. production of carbon dioxide from fatty acids. The first set of experiments showed that fecund female schistosomes use oxidative phosphorylation and that this process is essential for egg production. Oxidative phosphorylation by itself, however, is no indication for fatty acid oxidation. It has been shown earlier that in adult *S. mansoni* the degradation of glucose to carbon dioxide via Krebs cycle activity and oxidative phosphorylation produces at least one-third of the ATP produced by glucose breakdown, the remainder is produced during the production of lactate, the major end product which is excreted (Van Oordt et al., 1985). This explains why tampering with oxidative phosphorylation has a profound effect on energy consuming processes such as egg laying and vice versa: interference with energy consuming processes will affect oxidative phosphorylation. The second type of experiments was related to CPT1 (enzyme 2 in Fig. 4), an essential component of the pathway used for the import of fatty acids into mitochondria. This enzyme can be inhibited by etomoxir and it was observed that addition of this inhibitor resulted in a decrease in the oxygen consumption rate and in a decrease in the production of eggs in vitro (Huang et al., 2012). However, *S. mansoni* does not possess CPT1 (Figs. 4, 5; Supplementary Table S3) and etomoxir is known to inhibit not only CPT1 but also diacylglycerol acyltransferase (Xu et al., 2003), an anabolic enzyme catalyzing the final reaction in the synthesis of TAG, a process known to occur in schistosomes (Fig. 4). The importance of this enzyme for female schistosomes in the process of egg laying is discussed further below. In the third type of experiments RNAi and an inhibitor were used to study the effect of a decrease in activity of two enzymes on the rate of oxygen consumption and egg laying. The observation that inhibition or RNAi of acyl-CoA synthetase (enzyme 1 in Fig. 4) influences egg laying and oxygen consumption by female *S. mansoni* is not surprising in view of the importance of anabolic processes that occur during this energy consuming process. A correlation between activity of acyl-CoA activity and egg laying is therefore no indication for fatty acid oxidation. The observed slight inhibition of egg laying after RNAi of acyl-CoA dehydrogenase (enzyme 4 in Fig 4) is enigmatic as schistosomes do not possess a gene for that enzyme (Fig. 4, 5;

Table 1; Supplementary Table S3). As a fourth line of evidence for the occurrence and importance of fatty acid oxidation in egg-laying females, the presence of large lipid reserves in the vitellarium of fecund females is mentioned, together with the observation that the decline of these lipid reserves correlates with egg laying and the rate of oxygen consumption. These observations are, however, no indication for fatty acid oxidation and are the result of the use of lipid by female schistosomes to stuff it into the eggs. The role of lipids in the process of egg laying by the female and also during the further development of the egg is discussed below.

As fatty acids do not function in schistosomes as substrate for β -oxidation and therefore have no role as fuel in ATP production, the question arises as to what their real function in *S. mansoni* is. In general, fatty acids are present in cells, mainly in two forms: they can be stored as TAGs and they are used as building blocks of phospholipids and glycolipids. In this respect it should be realized that female worms produce approximately 350 eggs per day (Cheever et al., 1994) and each egg contains fatty acids present in TAG and phospholipids (Fig. 2). Hence, the female worm not only requires energy and amino acids for egg production, it also requires substantial amounts of fatty acids, and therefore their daily uptake and digestion of red blood cells is approximately eight times higher than that of males (Lawrence, 1973; Cheever et al., 1994; Skelly et al., 2014). These ideas are in agreement with an earlier report of Newport and Weller (1982) who demonstrated that fatty acids are an absolute requirement for egg laying. The main lipid constituent of the immature egg is TAG (Fig. 2), which is synthesized from diacylglycerol by the enzyme diacylglycerol acyltransferase (Smp_158510). Expression of this gene was shown to be strongly (10x) upregulated in fecund females in a bi-sex infection, in comparison with virgin females in a single sex infection (Fitzpatrick et al., 2005; Anderson et al., 2015; Lu et al., 2017). By whole mount in situ hybridization and RNA-seq it was shown that this enzyme is expressed exclusively in the vitellarium, which is the site of egg production (Wang and Collins, 2016). These results showed that female worms expel a large amount of fatty acids in lipids present in the excreted eggs and explains why fatty acids are essential for egg production. Fatty acids are essential components that, although they cannot be synthesized by the parasite itself, are used in anabolic processes. This explains why anabolic lipid metabolism in the female worm is crucial for egg production and why interference with it or with ATP generating processes such as oxidative phosphorylation will affect egg production (Huang et al., 2012).

As it was shown that fatty acids are essential for egg production and that interference with lipid metabolism affects egg production (Huang et al., 2012), we investigated the lipidome of eggs during maturation. As mature and immature eggs can be separated by

density (Ashton et al., 2001), it is likely that a change in lipid composition occurs during egg development. Microscopic evaluation of developing eggs revealed that immature eggs contain many large lipid droplets (Fig. 1), which confirms earlier observations (Neill et al., 1988). Mature eggs, on the other hand, have far less lipid droplets and instead more cellular membranes were stained (Fig. 1). The lipidomes of mature and immature eggs was then analyzed by LCMS, which demonstrated that mature eggs contain significantly more phospholipids than immature eggs. On the other hand, mature eggs contained less neutral lipids, albeit not significantly so. These observed changes in lipid composition of eggs prompted us to postulate that TAG in lipid droplets in the immature egg serves as a fatty acid storage that is used during egg maturation for phospholipid biosynthesis, which is needed for the formation of new membranes in the dividing cells of the developing miracidium.

In addition to the increase in phospholipid content, the phospholipid composition changes during egg maturation. The lipidomic 'finger print' of immature eggs was shown to be different from that of mature eggs, as indicated by the distinct and non-overlapping score plots in the PCA (Fig. 3A). The corresponding PCA loadings plot (Fig. 3B) showed that the difference between mature and immature eggs was reflected in many different lipid species from all phospholipid classes. These results showed that lipid metabolism is important during egg maturation as the lipid composition is substantially adjusted during development.

In conclusion, our results show that *S. mansoni* adults take up fatty acids and incorporate those in phospholipids and neutral lipids such as TAG. Use of fatty acids by female schistosomes in these anabolic processes is crucial for egg production as the secreted eggs contain large amounts of fatty acids provided by the host. However, adult worms, eggs and miracidia do not oxidize fatty acids, and therefore, fatty acid catabolism does not occur and thus does not contribute to ATP production. Genome analysis showed that previously postulated genes for fatty acid β -oxidation were incorrectly annotated or attributed and that *S. mansoni* in fact lacks genes encoding the enzymes required for fatty acid β -oxidation. Hence, *S. mansoni* does not and cannot oxidize fatty acids (nor can *S. japonicum* or any other schistosome species that has been sequenced).

Acknowledgements

This research did not receive any specific grants from funding agencies in the public, commercial, or not-for-profit sectors.

REFERENCES

- Anderson, L., M. S. Amaral, et al. (2015). "Schistosoma mansoni Egg, Adult Male and Female Comparative Gene Expression Analysis and Identification of Novel Genes by RNA-Seq." *PLoS neglected tropical diseases* **9**(12): e0004334.
- Ashton, P. D., R. Harrop, B. Shah and R. A. Wilson (2001). "The schistosome egg: development and secretions." *Parasitology* **122**(3): 329-338.
- Berriman, M., B. J. Haas, et al. (2009). "The genome of the blood fluke *Schistosoma mansoni*." *Nature* **460**(7253): 352-U365.
- Bligh, E. G. and W. J. Dyer (1959). "A rapid method of total lipid extraction and purification." *Canadian Journal of Physiology and Biochemistry* **37**(8): 911-917.
- Brouwers, J., I. M. B. Smeenk, L. M. G. vanGolde and A. G. M. Tielens (1997). "The incorporation, modification and turnover of fatty acids in adult *Schistosoma mansoni*." *Molecular and Biochemical Parasitology* **88**(1-2): 175-185.
- Brouwers, J. F. H. M., I. M. B. Smeenk, L. M. G. van Golde and A. G. M. Tielens (1997). "The incorporation, modification and turnover of fatty acids in adult *Schistosoma mansoni*." *Molecular and Biochemical Parasitology* **88**(1): 175-185.
- Bueding, E. (1950). "Carbohydrate metabolism in *Schistosoma mansoni*." *The Journal of General Physiology* **33**(5): 475-495.
- Buro, C., K. C. Oliveira, Z. Lu, S. Leutner, S. Beckmann, C. Dissous, K. Cailliau, S. Verjovski-Almeida and C. G. Grevelding (2013). "Transcriptome Analyses of Inhibitor-treated Schistosome Females Provide Evidence for Cooperating Src-kinase and TGF beta Receptor Pathways Controlling Mitosis and Eggshell Formation." *Plos Pathogens* **9**(6):e1003448
- Cheever, A. W., J. G. Macedonia, J. E. Mosimann and E. A. Cheever (1994). "Kinetics of egg production and egg excretion by *Schistosoma mansoni* and *S. japonicum* in mice infected with a single pair of worms." *The American journal of tropical medicine and hygiene* **50**(3): 281-295.
- Coghlan, A., R. Tyagi, et al. (2019). "Comparative genomics of the major parasitic worms." *Nature genetics* **51**(1): 163-174.
- Colley, D. G., A. L. Bustinduy, E. Secor and C. H. King (2014). "Human schistosomiasis." *Lancet* **383**(9936): 2253-2264.
- Dresden, M. H. and D. C. Payne (1981). "A sieving method for the collection of schistosome eggs from mouse intestines." *Journal for Parasitology* **67**(3): 450-452.
- Edgar, R. C. (2004). "MUSCLE: multiple sequence alignment with high accuracy and high throughput." *Nucleic Acids Research* **32**(5): 1792-1797.
- Edwards, J., M. Brown, E. Peak, B. Bartholomew, R. J. Nash and K. F. Hoffmann (2015). "The Diterpenoid 7-Keto-Semperviol, Derived from *Lycium chinense*, Displays Anthelmintic Activity against both *Schistosoma mansoni* and *Fasciola hepatica*." *PLoS neglected tropical diseases* **9**(3).
- Fitzpatrick, J. M., D. A. Johnston, G. W. Williams, D. J. Williams, T. C. Freeman, D. W. Dunne and K. F. Hoffmann (2005). "An oligonucleotide microarray for transcriptome analysis of *Schistosoma mansoni* and its application/use to investigate gender-associated gene expression." *Molecular and Biochemical Parasitology* **141**(1): 1-13.
- Frayha, G. J. and J. D. Smyth (1983). Lipid Metabolism in Parasitic Helminths. *Advances in Parasitology*. J. R. Baker and R. Muller, Academic Press. **22**: 309-387.
- Freeman, C. P. and D. West (1966). "Complete separation of lipid classes on a single thin-layer plate." *Journal of Lipid Research* **7**(2): 324-327.
- Guigas, B. and A. B. Molofsky (2015). "A worm of one's own: how helminths modulate host adipose tissue function and metabolism." *Trends in Parasitology* **31**(9): 435-441.
- Huang, S. C.-C., T. C. Freitas, E. Amiel, B. Everts, E. L. Pearce, J. B. Lok and E. J. Pearce (2012). "Fatty Acid Oxidation Is Essential for Egg Production by the Parasitic Flatworm *Schistosoma mansoni*." *Plos Pathogens* **8**(10).
- Jurberg, A. D., T. Gonçalves, et al. (2009). "The embryonic development of *Schistosoma mansoni* eggs: proposal for a new staging system." *Development genes and evolution* **219**(5): 219.
- Lawrence, J. D. (1973). "The ingestion of red blood cells by *Schistosoma mansoni*." *Journal of Parasitology* **59**(1): 60-63.
- Li, Q., N. Zhao, M. Liu, H. M. Shen, L. Huang, X. J. Mo, B. Xu, X. M. Zhang and W. Hu (2017). "Comparative Analysis of Proteome-Wide Lysine Acetylation in Juvenile and Adult *Schistosoma japonicum*." *Frontiers in Microbiology* **8**.
- Loverde, P., E. Niles, A. Osman and W. Wu (2011). "*Schistosoma mansoni* male-female interactions." *Canadian Journal of Zoology* **82**: 357-374.
- Lu, Z., F. Sessler, N. Holroyd, S. Hahnel, T. Quack, M. Berriman and C. G. Grevelding (2017). "A gene expression atlas of adult *Schistosoma mansoni* and their gonads." *Scientific data* **4**: 170118.
- Meyer, F., H. Meyer and E. Bueding (1970). "Lipid metabolism in the parasitic and free-living flatworms, *Schistosoma mansoni* and *Dugesia dorotocephala*." *Biochimica et biophysica acta* **210**(2): 257-266.
- Neill, P. J. G., J. H. Smith, B. L. Doughty and M. Kemp (1988). "The ultrastructure of the *Schistosoma mansoni* egg." *The American journal of tropical medicine and hygiene* **39**(1): 52-65.
- Newport, G. R. and T. H. Weller (1982). "Deposition and maturation of eggs of *Schistosoma mansoni* in vitro: importance of fatty acids in serum-free media." *The American journal of tropical medicine and hygiene* **31**(2): 349-357.
- Oliveira, M. P., J. B. Correa Soares and M. F. Oliveira (2016). "Sexual Preferences in Nutrient Utilization Regulate Oxygen Consumption and Reactive Oxygen Species Generation in *Schistosoma mansoni*: Potential Implications for Parasite Redox Biology." *PLOS ONE* **11**(7): e0158429.
- Pearce, E. J. and S. C.-C. Huang (2015). "The metabolic control of schistosome egg production." *Cellular Microbiology* **17**(6): 796-801.
- Rouser, G., S. Fleischer and A. Yamamoto (1970). "Two dimensional thin layer chromatographic separation of polar lipids and determination of phospholipids by phosphorus analysis of spots." *Lipids* **5**(5): 494-496.
- Rumjanek, F. D. and A. J. G. Simpson (1980). "The incorporation and utilization of radiolabelled lipids by adult

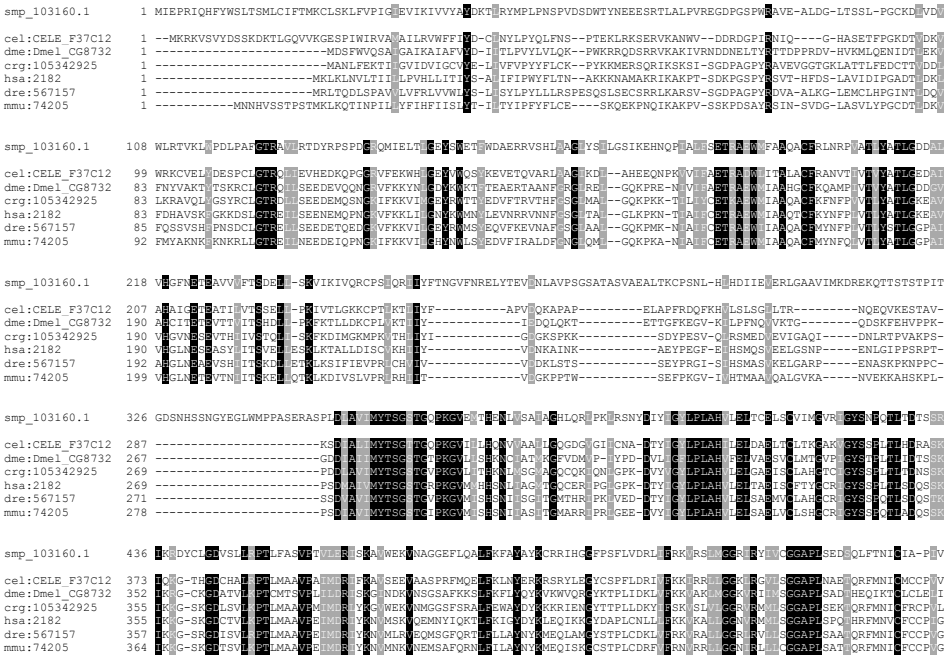
- Schistosoma mansoni* in vitro." Molecular and Biochemical Parasitology **1**(1): 31-44.
- Saz, H. J. (1970). "Comparative energy metabolisms of some parasitic helminths." The Journal of parasitology **56**(4): 634-642.
- Saz, H. J. (1981). "Energy metabolisms of parasitic helminths: adaptations to parasitism." Annual Review of Physiology **43**(1): 323-341.
- Schiller, E. L., E. Bueding, V. M. Turner and J. Fisher (1975). "Aerobic and anaerobic carbohydrate metabolism and egg production of *Schistosoma mansoni* in vitro." The Journal of parasitology: 385-389.
- Schönfeld, P. and L. Wojtczak (2016). "Short- and medium-chain fatty acids in energy metabolism: the cellular perspective." Journal of Lipid Research **57**(6): 943-954.
- Skelly, P. J., A. A. Da'dara, X.-H. Li, W. Castro-Borges and R. A. Wilson (2014). "Schistosome Feeding and Regurgitation." Plos Pathogens **10**(8).
- Skipski, V. P., R. F. Peterson and M. Barclay (1962). "Separation of phosphatidyl ethanolamine, phosphatidyl serine, and other phospholipids by thin-layer chromatography." Journal of Lipid Research **3**(4): 467-470.
- Smith, C. A., E. J. Want, G. O'Maille, R. Abagyan and G. Siuzdak (2006). "XCMS: processing mass spectrometry data for metabolite profiling using nonlinear peak alignment, matching, and identification." Analytical chemistry **78**(3): 779-787.
- Stacklies, W., H. Redestig, M. Scholz, D. Walther and J. Selbig (2007). "pcaMethods—a bioconductor package providing PCA methods for incomplete data." Bioinformatics **23**(9): 1164-1167.
- Tielens, A. G. M., F. A. M. van de Pas, J. M. van den Heuvel and S. G. van den Bergh (1991). "The aerobic energy metabolism of *Schistosoma mansoni* miracidia." Molecular and Biochemical Parasitology **46**(1): 181-184.
- Tielens, A. G. M. and S. G. van den Bergh (1987). "Glycogen metabolism in *Schistosoma mansoni* worms after their isolation from the host." Molecular and Biochemical Parasitology **24**(3): 247-254.
- Tielens, A. G. M., P. Van der Meer and S. G. Van den Bergh (1981). "The aerobic energy metabolism of the juvenile *Fasciola hepatica*." Molecular and Biochemical Parasitology **3**(4): 205-214.
- Tielens, A. G. M., B. E. P. van Oordt and S. G. van den Bergh (1989). "Carbohydrate metabolism in adult schistosomes of different strains and species." International journal for parasitology **19**(4): 447-449.
- Timson, D. J. (2016). "Metabolic Enzymes of Helminth Parasites: Potential as Drug Targets." Current Protein & Peptide Science **17**(3): 280-295.
- Van Oordt, B. E. P., A. G. M. Tielens and S. G. Van Den Bergh (1989). "Aerobic to anaerobic transition in the carbohydrate metabolism of *Schistosoma mansoni* cercariae during transformation in vitro." Parasitology **98**(03): 409.
- van Oordt, B. E. P., J. M. van den Heuvel, A. G. M. Tielens and S. G. van den Bergh (1985). "The energy production of the adult *Schistosoma mansoni* is for a large part aerobic." Molecular and Biochemical Parasitology **16**(2): 117-126.
- Wang, J. and J. J. Collins, III (2016). "Identification of new markers for the *Schistosoma mansoni* vitelline lineage." International journal for parasitology **46**(7): 405-410.
- Xu, F. Y., W. A. Taylor, J. A. Hurd and G. M. Hatch (2003). "Etomoxir mediates differential metabolic channeling

of fatty acid and glycerol precursors into cardiolipin in H9c2 cells." Journal of Lipid Research **44**(2): 415-423.

Xu, Y.-Z. and M. H. Dresden (1990). "The hatching of schistosome eggs." Experimental parasitology **70**(2): 236-240.

SUPPLEMENTARY FILES

1. Acyl-CoA synthetase



Supplementary Fig. S1. MUSCLE alignment of *Schistosoma mansoni* (smp) proteins, shaded using BOXSHADE server to indicate similarity (gray) and identity (black). The *S. mansoni* proteins identified in the forward BlastP search were aligned to the best hit, per model organism (cel, *Caenorhabditis elegans*; dme, *Drosophila melanogaster*; crg, *Crassostrea gigas*; hsa, *Homo sapiens*; dre, *Danio rerio*; mmu, *Mus musculus*). The enzyme number corresponds to the number in Fig. 4. For the identification of conserved regions within the six model organisms, proteins were aligned and shaded. All identifiers are from the KEGG (Kyoto Encyclopedia of Genes and Genomes) database and can be retrieved at <https://genome.jp>

Supplementary Table S1. Query genes used for the identification of genes involved in fatty acid oxidation *Schistosoma mansoni*. Column A lists all KEGG (Kyoto Encyclopedia of Genes and Genomes) orthology terms used in KEGG Map 00071 “fatty acid oxidation”. Column B lists all the KEGG orthology terms related to mitochondrial beta-oxidation. For these genes, relevant gene products were downloaded from the six model organisms; *Homo sapiens*, *Mus musculus*, *Danio rerio*, *Drosophila melanogaster*, *Caenorhabditis elegans* and *Crassostrea gigas*.

All KEGG terms from map 00071	KEGG terms used in our BlastP search	
K00001		E1.1.1.1+ adh; alcohol dehydrogenase
K00022	K00022	HADH; 3-hydroxyacyl-CoA dehydrogenase
K00121		frmA+ ADH5+ adhC; S-(hydroxymethyl)glutathione dehydrogenase / alcohol dehydrogenase
K00128		ALDH; aldehyde dehydrogenase (NAD+)
K00149		ALDH9A1; aldehyde dehydrogenase family 9 member A1
K00232		E1.3.3.6+ ACOX1+ ACOX3; acyl-CoA oxidase
K00248		ACADS+ bcd; butyryl-CoA dehydrogenase
K00249	K00249	ACADM+ acd; acyl-CoA dehydrogenase
K00252		GCDH+ gcdH; glutaryl-CoA dehydrogenase
K00255	K00255	ACADL; long-chain-acyl-CoA dehydrogenase
K00493		E1.14.14.1; unspecific monooxygenase
K00496		alkB1_2+ alkM; alkane 1-monooxygenase
K00529		hcaD; 3-phenylpropionate/trans-cinnamate dioxygenase ferredoxin reductase component
K00626		E2.3.1.9+ atoB; acetyl-CoA C-acetyltransferase
K00632	K00632	fadA+ fadI; acetyl-CoA acyltransferase
K01692	K01692	paaF+ echA; enoyl-CoA hydratase
K01782	K01782	fadJ; 3-hydroxyacyl-CoA dehydrogenase / enoyl-CoA hydratase / 3-hydroxybutyryl-CoA epimerase
K01825	K01825	fadB; 3-hydroxyacyl-CoA dehydrogenase / enoyl-CoA hydratase / 3-hydroxybutyryl-CoA epimerase / enoyl
K01897	K01897	ACSL+ fadD; long-chain acyl-CoA synthetase
K01909		mbtM; long-chain-fatty-acid--
K04072		adhE; acetaldehyde dehydrogenase / alcohol dehydrogenase
K05297		rubB+ alkT; rubredoxin--NAD+ reductase
K05939		aas; acyl-
K06445	K06445	fadE; acyl-CoA dehydrogenase
K07425		CYP4A; long-chain fatty acid omega-monooxygenase
K07508	K07508	ACAA2; acetyl-CoA acyltransferase 2
K07509	K07509	HADHB; acetyl-CoA acyltransferase
K07511	K07511	ECHS1; enoyl-CoA hydratase
K07513	K07513	ACAA1; acetyl-CoA acyltransferase 1
K07514	K07514	EHHADH; enoyl-CoA hydratase / 3-hydroxyacyl-CoA dehydrogenase / 3+2-trans-enoyl-CoA isomerase
K07515	K07515	HADHA; enoyl-CoA hydratase / long-chain 3-hydroxyacyl-CoA dehydrogenase
K07516	K07516	fadN; 3-hydroxyacyl-CoA dehydrogenase
K07517		ECI1_2; Delta3-Delta2-enoyl-CoA isomerase
K08765	K08765	CPT1A; carnitine O-palmitoyltransferase 1+ liver isoform
K08766	K08766	CPT2; carnitine O-palmitoyltransferase 2
K09478	K09478	ACADSB; short/branched chain acyl-CoA dehydrogenase
K09479	K09479	ACADVL; very long chain acyl-CoA dehydrogenase
K10527	K10527	MFP2; enoyl-CoA hydratase/3-hydroxyacyl-CoA dehydrogenase
K13238		ECI1+ DCI; Delta3-Delta2-enoyl-CoA isomerase

Supplementary Table S1 continued.

All KEGG terms from map 00071	KEGG terms used in our BlastP search	
K13239		ECI2+ Peci; Delta3-Delta2-enoyl-CoA isomerase
K13767	K13767	fadB; enoyl-CoA hydratase
K13951		ADH1_7; alcohol dehydrogenase 1/7
K13952		ADH6; alcohol dehydrogenase 6
K13953		adhP; alcohol dehydrogenase+ propanol-preferring
K13954		yiaY; alcohol dehydrogenase
K13980		ADH4; alcohol dehydrogenase 4
K14085		ALDH7A1; aldehyde dehydrogenase family 7 member A1
K14338		cypD_E+ CYP102A2_3; cytochrome P450 / NADPH-cytochrome P450 reductase
K15013	K15013	ACSBG; long-chain-fatty-acid--CoA ligase ACSBG
K15401		CYP86A1; long-chain fatty acid omega-monooxygenase
K18857		ADH1; alcohol dehydrogenase class-P
K18880		ECI3+ HCD1; Delta3-Delta2-enoyl-CoA isomerase
K19523	K19523	CPT1B; carnitine O-palmitoyltransferase 1+ muscle isoform
K19524	K19524	CPT1C; carnitine O-palmitoyltransferase 1+ brain isoform
K20495		CYP704B1; long-chain fatty acid omega-monooxygenase
K21738		alkT; rubredoxin---NAD+ reductase
K22567		nroR; rubredoxin---NAD+ reductase
K22887		CYP52M1; long-chain fatty acid omega-monooxygenase

Supplementary Table S2. Results from a forward homology search in the genome of *Schistosoma mansoni*. Columns A-C show the KEGG (Kyoto Encyclopedia of Genes and Genomes) ID, KEGG term and KEGG name of the query protein used. Columns D-F show the Refseq ID, GeneDB ID and the Gene DB annotated name for the identified *S. mansoni* gene. Column G shows the E-value from the BlastP search, which denotes the statistical significance of the identified gene/protein hit. (Supplementary Table S1 and S2 available on <https://parasitology-online.org/thesis/>)

Supplementary S2. available online at. <https://doi.org/10.1016/j.ijpara.2019.03.005>

Supplementary Table S3. Summarized results from forward and reversed BlastP searches. Shown are the proteins of the six model organisms most similar to a *Schistosoma mansoni* protein retrieved by a BlastP search. For the reverse BlastP search against the six model organisms, the *S. mansoni* sequence retrieved in the forward BlastP search was used as a query. From each species of the six model organism, the gene identifier is shown, as well as the KEGG (Kyoto Encyclopedia of Genes and Genomes) orthology term and the enzyme name with enzyme code. cel, *Caenorhabditis elegans*; dme, *Drosophila melanogaster*; crg, *Crassostrea gigas*; hsa, *Homo sapiens*; dre, *Danio rerio*; mmu, *Mus musculus*.

1. Acyl-CoA synthetase

Forward BlastP	KEGG Orthology term	Enzyme name
cel CELE_F37C12.7	K01897	long-chain acyl-CoA synthetase [EC 6.2.1.3]
dme Dmel_CG8732	K01897	long-chain acyl-CoA synthetase [EC 6.2.1.3]
crg 105342925	K01897	long-chain acyl-CoA synthetase [EC 6.2.1.3]
hsa 2182	K01897	long-chain acyl-CoA synthetase [EC 6.2.1.3]
dre 567157	K01897	long-chain acyl-CoA synthetase [EC 6.2.1.3]
mmu 74205	K01897	long-chain acyl-CoA synthetase [EC 6.2.1.3]

Retrieved ID from <i>S. mansoni</i> genome		
smm smp_103160.1	K01897	long-chain acyl-CoA synthetase [EC 6.2.1.3]

Reverse BlastP	KEGG Orthology term	Enzyme name
smm smp_103160.1	K01897	long-chain acyl-CoA synthetase [EC 6.2.1.3]
Best hit from each model organism		
cel CELE_F37C12.7	K01897	long-chain acyl-CoA synthetase [EC 6.2.1.3]
dme Dmel_CG8732	K01897	long-chain acyl-CoA synthetase [EC 6.2.1.3]
crg 105342925	K01897	long-chain acyl-CoA synthetase [EC 6.2.1.3]
hsa 2182	K01897	long-chain acyl-CoA synthetase [EC 6.2.1.3]
dre 567157	K01897	long-chain acyl-CoA synthetase [EC 6.2.1.3]
mmu 74205	K01897	long-chain acyl-CoA synthetase [EC 6.2.1.3]

2 and 3. Carnitine palmitoyl transferase (CPT) 1 and 2

Forward BlastP (CPT1)	KEGG Orthology term	Enzyme name
crg 105319102	K08765	carnitine O-palmitoyltransferase 1 [EC 2.3.1.21]
cel CELE_Y46G5A.17	K08765	carnitine O-palmitoyltransferase 1 [EC 2.3.1.21]
dme Dmel_CG12891	K08765	carnitine O-palmitoyltransferase 1 [EC 2.3.1.21]
dre 558088	K08765	carnitine O-palmitoyltransferase 1 [EC 2.3.1.21]
hsa 1374	K08765	carnitine O-palmitoyltransferase 1 [EC 2.3.1.21]
mmu 12894	K08765	carnitine O-palmitoyltransferase 1 [EC 2.3.1.21]

Retrieved ID from <i>S. mansoni</i> genome		
smm Smp_146910	K00623	choline O-acetyltransferase [EC 2.3.1.6]

Forward BlastP (CPT2)	KEGG Orthology term	Enzyme name
cel CELE_R07H5.2	K08766	carnitine O-palmitoyltransferase 2 [EC 2.3.1.21]
dme Dmel_CG2107	K08766	carnitine O-palmitoyltransferase 2 [EC 2.3.1.21]
crg 105343773	K08766	carnitine O-palmitoyltransferase 2 [EC 2.3.1.21]
dre 100005717	K08766	carnitine O-palmitoyltransferase 2 [EC 2.3.1.21]
hsa 1376	K08766	carnitine O-palmitoyltransferase 2 [EC 2.3.1.21]
mmu 12896	K08766	carnitine O-palmitoyltransferase 2 [EC 2.3.1.21]

Retrieved ID from <i>S. mansoni</i> genome		
smm Smp_146910	K00623	choline O-acetyltransferase [EC 2.3.1.6]

Reverse Blast	KEGG Orthology term	Enzyme name
smm Smp_146910	K00623	choline O-acetyltransferase [EC 2.3.1.6]
Best hit from each model organism		
dme Dmel_CG12345	K00623	choline O-acetyltransferase [EC 2.3.1.6]
cel CELE_cha-1	K00623	choline O-acetyltransferase [EC 2.3.1.6]
dre 100170938	K00623	choline O-acetyltransferase [EC 2.3.1.6]
mmu 12647	K00623	choline O-acetyltransferase [EC 2.3.1.6]
hsa 1103	K00623	choline O-acetyltransferase [EC 2.3.1.6]
crg 105343100	K00623	choline O-acetyltransferase [EC 2.3.1.6]

4. Enoyl-CoA hydratase

Forward BlastP	KEGG Orthology term	Enzyme name
dme Dmel_CG6543	K07511	enoyl-CoA hydratase [EC 4.2.1.17]
crg 105341094	K07511	enoyl-CoA hydratase [EC 4.2.1.17]
dre 368912	K07511	enoyl-CoA hydratase [EC 4.2.1.17]
hsa 1892	K07511	enoyl-CoA hydratase [EC 4.2.1.17]
mmu 93747	K07511	enoyl-CoA hydratase [EC 4.2.1.17]

Retrieved ID from <i>S. mansoni</i> genome		
smm Smp_024930	No KO	

Reverse Blast	KEGG Orthology term	Enzyme name
smm Smp_024930	No KO	
Best hit from each model organism		
dme Dmel_CG6984	No KO	CG6984; uncharacterized protein
cel CELE_F38H4.8	No KO	Enoyl-CoA Hydratase
crg 105343205	No KO	enoyl-CoA hydratase domain-containing protein 3
dre 780842	No KO	enoyl-CoA hydratase domain-containing protein 3
mmu 67856	No KO	enoyl-CoA hydratase domain-containing protein 3
hsa 79746	No KO	enoyl-CoA hydratase domain-containing protein 3

5. Acyl-CoA dehydrogenase

Forward BlastP	KEGG Orthology term	Enzyme name
cel CELE_E04F6.5	K09479	very long chain acyl-CoA dehydrogenase [EC 1.3.8.9]
dme Dmel_CG7461	K09479	very long chain acyl-CoA dehydrogenase [EC 1.3.8.9]
crg 105344745	K09479	very long chain acyl-CoA dehydrogenase [EC 1.3.8.9]
dre 573723	K09479	very long chain acyl-CoA dehydrogenase [EC 1.3.8.9]
hsa 37	K09479	very long chain acyl-CoA dehydrogenase [EC 1.3.8.9]
mmu 11370	K09479	very long chain acyl-CoA dehydrogenase [EC 1.3.8.9]

Retrieved ID from <i>S. mansoni</i> genome		
smm Smp_122930	K15980	acyl-CoA dehydrogenase family member 9 [EC 1.3.99.-]

Reverse Blast	KEGG Orthology term	Enzyme name
smm Smp_122930	K15980	acyl-CoA dehydrogenase family member 9 [EC 1.3.99.-]
Best hit from each model organism		
dme Dmel_CG7461	K09479	very long chain acyl-CoA dehydrogenase [EC 1.3.8.9]
cel CELE_E04F6.5	K09479	acyl-CoA dehydrogenase family member 9 [EC 1.3.99.-]
crg 105348563	K15980	acyl-CoA dehydrogenase family member 9 [EC 1.3.99.-]
dre 724002	K15980	acyl-CoA dehydrogenase family member 9 [EC 1.3.99.-]
mmu 229211	K15980	acyl-CoA dehydrogenase family member 9 [EC 1.3.99.-]
hsa 28976	K15980	acyl-CoA dehydrogenase family member 9 [EC 1.3.99.-]

7. 3-keto-acyl thiolase

Forward Blast	KEGG Orthology term	Enzyme name
cel CELE_F53A2.7	K07508	3-keto-acyl thiolase [EC 2.3.1.16]
dme Dmel_CG4600	K07508	3-keto-acyl thiolase [EC 2.3.1.16]
dre 406325	K07508	3-keto-acyl thiolase [EC 2.3.1.16]
hsa 10449	K07508	3-keto-acyl thiolase [EC 2.3.1.16]
mmu 52538	K07508	3-keto-acyl thiolase [EC 2.3.1.16]

Retrieved ID from <i>S. mansoni</i> genome		
smm smp_267310 1	K00626	acetyl-CoA acyltransferase [EC 2.3.1.9]

Reverse Blast	KEGG Orthology term	Enzyme name
smm smp_267310 1	K00626	acetyl-CoA acyltransferase [EC 2.3.1.9]
Best hit from each model organism		
cel CELE_F53A2.7	K07508	acetyl-CoA acyltransferase 2 [EC 2.3.1.16]
dme Dmel_CG9149	K00626	acetyl-CoA acyltransferase [EC 2.3.1.9]
crg 105348136	K00626	acetyl-CoA acyltransferase [EC 2.3.1.9]
dre 30643	K00626	acetyl-CoA acyltransferase [EC 2.3.1.9]
hsa 39	K00626	acetyl-CoA acyltransferase [EC 2.3.1.9]
mmu 110460	K00626	acetyl-CoA acyltransferase [EC 2.3.1.9]

Muscle alignment of *S. mansoni* proteins, shaded using BOXSHADE server to indicate similarity (gray) and identity (black). The *S. mansoni* proteins identified from the forward BlastP search were aligned to the best hit, per species. For the identification of conserved region within the six model organisms proteins were aligned and shaded without the *S. mansoni* sequence. Identifiers are from the KEGG database and can be retrieved at <https://genome.jp>



CHAPTER 4

A mono-acyl phospholipid (20:1 lyso-PS)
activates Toll-Like Receptor 2/6 hetero-dimer

Michiel L. Bexkens ^a, Martin Houweling ^b, Peter C. Burgers ^c, Theo M. Luider ^c, Aloysius G.M. Tielens ^{a,b}, Jaap J. van Hellemond ^a

- a. Department of Medical Microbiology and Infectious Diseases, Erasmus Medical Center, Rotterdam, the Netherlands.
- b. Department of Biochemistry and Cell Biology, Faculty of Veterinary Medicine, Utrecht University, Utrecht, the Netherlands.
- c. Department of Neurology, Laboratory of Neuro-Oncology, Erasmus Medical Center, Rotterdam, the Netherlands.

ABSTRACT

Toll-like receptor 2 (TLR2) is an important pattern recognition receptor on the surface of host immune cells that binds a variety of ligands that are released by microorganisms as well as by damaged or dying host cells. According to the current concept, TLR2/1 and TLR2/6 heterodimers are activated by tri- or di-acylated ligands, respectively. However, also mono-acyl phospholipid containing lipid fractions derived from parasites, were reported to be able to activate TLR2. In order to provide conclusive evidence for the TLR2 activating capacity of mono-acyl phospholipids derived from pathogens, we developed a biosynthetic method to produce several mono-acyl-phospholipid variants that could be examined for their TLR2 activating capacity. These investigations demonstrated that 1-(11Z-eicosenoyl)-glycero-3-phosphoserine 20:1 (20:1 lyso-PS) is a true agonist of the TLR2/6 heterodimer and that its polar head group as well as the length of the acyl chain are crucial for TLR2 activation. In silico modelling further confirmed 20:1 mono-acyl PS as a ligand for TLR2/6 heterodimer, as multiple hydrogen bonds are formed between the polar head of 20:1 mono-acyl PS and amino acid residues of both TLR2 and TLR6. As 20:1 mono-acyl PS can now be prepared in higher quantities by the developed biosynthetic method, future studies can be performed to further assess the functions of 20:1 mono-acyl PS as an immunological mediator.

Keywords

Schistosoma mansoni, lysophospholipid, mono-acyl phosphatidylserine, Toll-like receptor-2 ligand, innate immunity.

Highlights

- A straightforward biochemical synthesis was developed to generate specific lyso-phospholipids
- 20:1 lyso-PS is a true agonist of the TLR2/6 hetero-dimer
- Both chainlength and the headgroup of 20:1 lyso-PS determine this interaction

INTRODUCTION

Pattern recognition receptors on the surface of host immune cells fulfil a crucial function in the innate immune response, as these receptors sense the presence of distinct pathogen associated molecular patterns (PAMPs) that are released by micro-organisms as well as by damaged or dying host cells (Uematsu and Akira 2006, Beutler 2009). Among these pattern recognition receptors, Toll-like Receptors (TLR) are an important class that comprises multiple analogues in varying numbers in distinct organisms. The transmembrane TLRs, TLR1 to TLR6 and TLR11, consist of an extracellular domain containing leucine-rich repeats that recognize distinct PAMPs and an intracellular toll-interleukin1 (IL-1) receptor (TIR) domain required for downstream signaling that regulates the expression of pro-inflammatory cytokines (Uematsu and Akira 2006, Beutler 2009). TLR2 is probably the best studied TLR and its importance in the host immune response to many infectious diseases has been shown by various TLR2 knock-out mice studies (van Bergenhenegouwen, Plantinga et al. 2013). In addition, TLR2 is of interest because it is a unique TLR as it needs, unlike other TLRs, to form heterodimers with TLR1 or TLR6 to initiate downstream signaling (Ozinsky, Underhill et al. 2000).

Over the years a wide variety of TLR2 ligands has been identified from many distinct microorganisms (Oliveira-Nascimento, Massari et al. 2012, van Bergenhenegouwen, Plantinga et al. 2013). Most identified TLR2 ligands are lipoproteins or polysaccharides to which two or three fatty acyl chains are attached. Further analysis showed that ligands that bind and activate TLR2/1 heterodimers are often tri-acylated ligands, whereas those that activate TLR2/6 are often di-acylated (Beutler, Jiang et al. 2006, Uematsu and Akira 2006, Oliveira-Nascimento, Massari et al. 2012, van Bergenhenegouwen, Plantinga et al. 2013). In contrast to this general concept, only very few pathogen-derived TLR2-ligands have been reported that contain a single hydrophobic side chain. The lipid fraction of the blood-dwelling fluke *Schistosoma mansoni* containing 1-(eicosenoyl)-glycero-3-phosphoserine (20:1 lyso-PS), was the first mono-acyl phospholipid shown to be able to activate TLR2 (Van der Kleij, Latz et al. 2002). Next, indirect evidence obtained by in vivo studies using TLR2 knock-out mice, suggested that purified lipid fractions of *S. mansoni* containing mono-acyl phosphatidylcholine (PC) species might be an agonist for TLR2 as well (Magalhaes, Almeida et al. 2010). Later on, it was reported that mono-acyl PC species could trigger TLR2- as well as TLR4 mediated signalling in TLR-transfected HEK-293 cells, but in that study contradictory results were found as mono-acyl PC also counteracted the lipopolysaccharide-induced signalling via TLR4 in isolated macrophages (Carneiro, Iacurra et al. 2013). These three reports, which were mainly based on studies using purified lipid fractions from *S. mansoni*, are so far the

only published evidence for mono-acylated molecules derived from pathogens that can activate TLR2. This raises the question whether mono-acylated phospholipids are true activating ligands of TLR2, or that the observed TLR2 activation was induced by other minor components inevitably present in purified fractions of biological origin?

To further investigate the activation of TLR2 by mono-acyl PS, we now developed a biosynthetic method to produce 20:1 mono-acyl PS, as well as other mono-acyl-phospholipid variants with either a different polar head-group or different acyl-chains varying in number of carbon atoms. This biosynthetic method allowed us to study the activating effect on TLR2 of specific mono-acyl PS molecules, instead of using mixtures of mono-acyl PS molecules present in isolated fractions of schistosomes.

For binding and activation by bacterial lipopeptides, TLR2 has to form heterodimers with TLR1 or TLR6 (Uematsu and Akira 2006, Oberg, Juricke et al. 2011, van Bergenhenegouwen, Plantinga et al. 2013). Therefore, we also investigated the TLR2 heterodimer combination that is activated by mono-acyl PS. Finally, we have generated an *in silico* model to study the interaction between mono-acyl PS and the involved TLR 2/6 heterodimer, which allowed structural comparison with the FSL-1, a synthetic di-acyl lipoprotein and known activator of the TLR2/6 heterodimer.

EXPERIMENTAL PROCEDURES

Synthesis of mono-acyl phospholipids

Specific mono-acyl phospholipids were produced from commercially available di-acyl-phospholipid precursors by the following procedure. Different glycerophosphocholines (PC) species were purchased from Avanti (Avanti Polar Lipids, Alabaster, AL, USA), which included 1,2-dioleoyl-sn-glycero-3-phosphocholine (PC 18:1;18:1), 1,2-dieicosenoyl-sn-glycero-3-phosphocholine (PC 20:1;20:1), 1,2-dierucoyl-sn-glycero-3-phosphocholine (PC 22:1;22:1) and 1,2-dinervonoyl-sn-glycero-3-phosphocholine (PC 24:1;24:1). Unless otherwise specified, all other reagents were purchased from Sigma Aldrich, St. Louis, USA.

For the conversion of PC into glycerophosphoserine (PS), head-group substitution of PC was performed by a procedure based on the method of Comfurius and Zwaal (Comfurius and Zwaal 1977). In short, PC was dissolved in diethyl ether at a concentration of 5 mg/ml after which phospholipase D (10 U/ml) was added in an L-serine saturated acetate buffer (1 mL, 100 mM, pH 5.6) containing 100 mM CaCl₂. After continuous stirring for 3 hours at

37°C, the reaction was stopped by acidification by addition of 50 µl 6M HCL. Samples were spun down at 500g for 5 minutes, after which the ether phase was transferred to a new tube and dried under N₂. From the dried residue, lipids were extracted according to the method of Bligh and Dyer (Bligh and Dyer 1959). Subsequently, distinct classes of phospholipids (PS, PC and PA) were separated by column chromatography over a carboxymethyl cellulose CM-52 column (Serva, Heidelberg, Germany), essentially as described by Comfurius and Zwaal (Comfurius and Zwaal 1977).

Purified di-acyl-phospholipids were converted into mono-acyl phospholipids by enzymatic hydrolysis using phospholipase A₂ (20 U) in a two-phase system, consisting of 2 ml diethyl ether and 1 ml 100 mM TRIS-HCl, 4 mM CaCl₂, pH 7. After 90 min incubation the enzymatic conversion was stopped by acidification of the reaction medium by addition of 40 µl 1M HCl, which also induced the translocation of the mono-acyl phospholipids from the aqueous phase to the organic diethyl-ether phase of the incubation. After centrifugation for 5 min at 500g the organic phase was collected and transferred to a sterile tube containing a physiological salt solution (NaCl, 0.9% w/v). After continuous stirring for 1 min at 37°C followed by centrifugation for 5 min at 500g, the organic phase was slowly evaporated at 55°C, eventually yielding solubilized mono-acyl phospholipids in a physiological salt solution. Phospholipid concentrations were quantified by a phosphate assay as described by Rouser et al. (Rouser, Fleischer et al. 1970).

The synthesized phospholipids were characterized by two methods. To monitor the efficiency of the synthesis process by a quick and simple method, the phospholipid composition during the synthesis process was analyzed by thin layer chromatography (TLC) as described before by Skipski and Peterson (Skipski, Peterson et al. 1962). The synthesized endproducts were characterized in detail by matrix-assisted laser desorption ionization-time of flight mass spectrometry (MALDI-TOF/MS). For this analysis phospholipids were dissolved in MeOH: CHCl₃ (2:1); 0.5 µL of this solution was spotted on a stainless steel surface and overlaid with 0.5 µL of a matrix (2 mg alpha-cyano-4-hydroxycinnamic acid in 1 mL acetonitrile). MALDI-TOF spectra were recorded on an Ultraflex III MS (Bruker Daltonics) using the reflectron in both positive and negative ion modes as described in Ruttink et al. (Ruttink, Dekker et al. 2012). A laser repetition rate of 50 Hz was used and 1,000 shots (50 shots per raster spot) were accumulated. The laser power was chosen such that no signal saturation occurred after 50 shots at each raster spot.

Activation of Toll-Like Receptor 2 by synthesized phospholipids

To investigate whether the synthesized mono-acyl phospholipids were capable of activating TLR2, HEK-TLR2-Blue reporter cells were used according to the manufacturer's instructions (InvivoGen, San Diego, USA). These cells over-express TLR2, while having endogenous expression of TLR1 and TLR6. In these reporter cells, activation of TLR2 finally leads to $\text{Nf-}\kappa\text{B}$ dependent expression of secreted embryonic alkaline phosphatase, which can subsequently be quantified by measuring the alkaline phosphatase activity in the supernatant of the cell culture medium. For all assays 50,000 HEK-TLR2-Blue reporter cells per well were incubated in 280 μl culture medium with either the synthesized mono-acyl phospholipids in a range of 0-75 μM or the positive control compounds Pam2CGDHPKHSF (FSL-1, InvivoGen) (2.2 μM) or Pam3CysSerLys4 (Pam3CSK4, InvivoGen) (23 μM) for activation of the TLR2/6 and TLR2/1 heterodimers, respectively. After overnight incubation at 37°C the alkaline phosphatase activity in the culture medium was measured at 37°C using the HEK Blue detection kit according to the manufacturer's instructions. Negative controls were prepared by performing the complete biosynthesis process as described above, but without addition of PC in the first step of the biosynthesis process.

To determine the TLR2-heterodimer composition that is activated by the synthesized mono-acyl phospholipids, specific blocking-antibodies against TLR 1, TLR2 and/or TLR6 (InvivoGen, San Diego, USA) were added one hour before stimulation of reporter cells with the biosynthesized mono-acyl phospholipids or positive controls for TLR2/1 (Pam3CSK4) and TLR2/6 (FSL-1) activation. Blocking antibodies were used in equal volumes at a concentration of 1.5 mg/ml (TLR1 and TLR6) and 0.75 mg/ml (TLR2).

In silico modeling of 20:1 mono-acyl PS in the TLR2/6 heterodimer complex.

Ligand binding of 20:1 mono-acyl PS to the TLR2/6 heterodimer complex was modeled using AutoDock Vina (Trott and Olson 2010) and subsequently analyzed with Pymol (The PyMOL Molecular Graphics System, Version 2.0 Schrödinger, LLC). SMILES models (Weininger 1988) of 20:1 mono-acyl PS were created (see supplemental Fig 1A) and converted to a PDB-file. Subsequently, a model of the crystal structure of TLR2/6 with its ligand FSL-1 (Jin, Kim et al. 2007) was downloaded from rcsb.org using identifier 3A79. The FSL-1 ligand was removed, and the software was queried to calculate a possible fit for the earlier drawn SMILES model of 20:1 mono-acyl PS.

RESULTS

Synthesis of Lyso-PS

In order to provide conclusive evidence for the TLR2 activating capacity of mono-acyl phospholipids, which was so far based on the TLR2 activating capacity of purified lipid fractions derived from *S. mansoni* (Van der Kleij, Latz et al. 2002, Magalhaes, Almeida et al. 2010, Carneiro, Iaciura et al. 2013), we developed a method to synthesize mono-acyl PS species with various acyl chains, as well as the related mono-acyl phospholipids: phosphatidic acid (mono-acyl PA) and mono-acyl phosphatidylcholine (mono-acyl PC).

We used two consecutive enzymatic reactions to produce these compounds. First, commercially available PC was transphosphatidylated with phospholipase D in the presence of serine, which results in the formation of PS (Comfurius and Zwaal 1977). After purification on CM-cellulose, this PS was then treated with phospholipase A2 to obtain lyso-PS. Starting with, the commercially available, synthesized PC containing two identical fatty acid residues ensures that all formed lyso-PS molecules have one and the same fatty acid residue. As demonstrated by the MALDI-TOF/MS spectra (Fig. 1A), by this method highly pure mono-acyl phospholipids could be synthesized.

The first step, the transphosphatidylation, was highly effective, leaving no residual PC. Around 60 % of the PC was converted into PS, while the remainder was hydrolysed to PA. In the CM-52 column chromatography step, the first fractions containing PS also contain small amounts of PA. These fractions were discarded, which implied that approximately 50% of the PS produced, was used in the second step, the production of lyso-PS. In this step, the activity of phospholipase A2 used to obtain lyso-PS was enhanced by the use of a two-phase system of diethyl ether and water containing Ca^{++} ions (Misiowski and Wells 1974). The conversion of PS to lyso-PS occurred with 100% efficiency, and no residual PS remained after 90 minutes. Isolation of the resulting lysophospholipids from the reaction mixture by extraction from the diethyl ether phase, followed by transfer to an aqueous solution, had an efficiency of around 60%. The final yield of the complete procedure was around 18%. The above described procedure for the complete synthesis and purification of lyso-phospholipids can be completed within 6 hours.

20:1 mono-acyl PS activates TLR2

From the mono-acyl PS species that were examined for their TLR2 activating capacity at a concentration of 40 μM , 20:1 mono-acyl PS was found to be most effective in activating TLR2, whereas 18:1 mono-acyl PS, 22:1 mono-acyl PS and 24:1 mono-acyl PS hardly activated TLR2. (Fig. 1B). These results demonstrated that it is indeed 20:1

mono-acyl PS that activates TLR2, and that the structure of the acyl chain in the mono-acyl PS molecule is critical for TLR2 activation. Next, we examined the influence of the polar head-group in 20:1 mono-acyl PS by comparing its TLR2 activating capacity to that of synthesized 20:1 mono-acyl PC and 20:1 mono-acyl PA. These experiments showed that 20:1 mono-acyl PS activated TLR2 in a dose-dependent manner, whereas 20:1 mono-acyl PC and 20:1 mono-acyl PA did not activate TLR2 (Fig 1C). The range of concentrations in which these mono-acyl phospholipids were examined for their TLR2 activating capacity differed as the maximal concentrations that could be used were either limited by the maximal solubility in aqueous solutions (mono-acyl PA) or because higher concentrations (20:1 mono-acyl PS) lead to death of HEK-TLR2-Blue reporter-cells, a feature that has been reported for mono-acyl phospholipids before (Arouri and Mouritsen 2013). Taken together, these results are in agreement with the earlier observations by Van der Kleij et al. (Van der Kleij, Latz et al. 2002) confirming 20:1 mono-acyl PS as TLR2 agonist and ruling out the possibility that minor other compounds present in the schistosomal lipid fractions were the TLR2 activating ligands.

Mono-acyl PS activates the TLR-2/6 heterodimer

In contrast to most other activating ligands for TLR2 heterodimers, 20:1 mono-acyl PS only comprises a single acyl chain. For this reason we determined the TLR2 heterodimer composition that is activated by 20:1 mono-acyl PS. By addition of blocking antibodies against TLR1, TLR2 or TLR6 before the TLR agonist is added, it can be determined which TLR heterodimer composition is activated by which agonist. Blocking of TLR2 before addition of 20:1 mono-acyl PS reduced the TLR2 activation by 60%, which was similar to the observed reduction by blocking TLR2 before addition of the positive control ligands Pam3CSK4 for TLR2/1 and FSL-1 for TLR2/6 heterodimer activation (Fig. 1D). Blocking of TLR1 by blocking antibodies before addition of 20:1 mono-acyl PS did not reduce the TLR2 activation, whereas it did reduce the TLR2 activation induced by the well-known TLR2/1 heterodimer agonist Pam3CSK4 (Fig. 1D). Blocking of TLR6 before addition of 20:1 mono-acyl PS did result in inhibition of TLR2 activation, and this observed inhibition was similar to that of FSL-1, a well-known agonist of the TLR2/6 heterodimer (Fig. 1D). These results demonstrated that activation of TLR2 by 20:1 mono-acyl PS occurs via the TLR2/6 heterodimer. From these data, it can be concluded that 20:1 mono-acyl PS is a true agonist of the TLR2/6 heterodimer, and therefore, this heterodimer that is classically involved in the binding of di-acyl-lipopeptides, also accepts a mono-acyl phospholipid as a ligand.

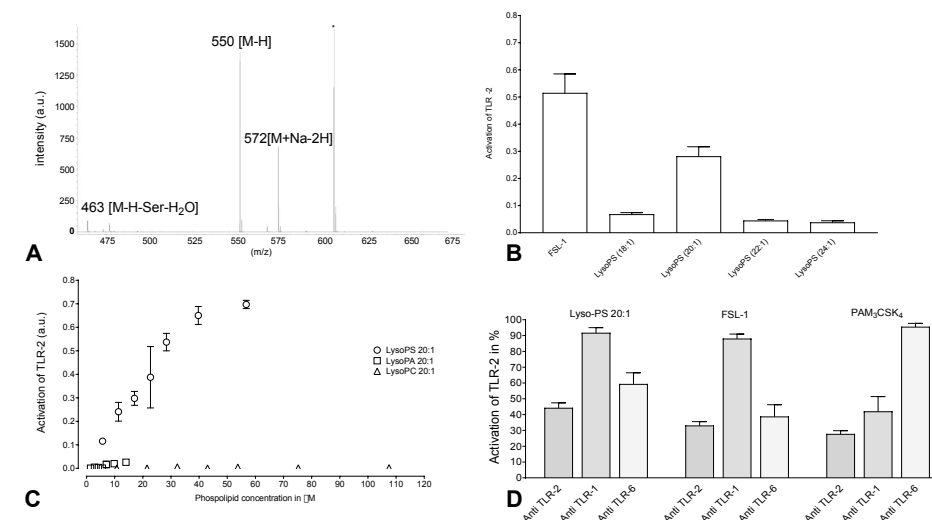


Figure 1. TLR2 activating properties of biosynthesized mono-acyl phospholipids.

Panel A shows the negative mode MALDI-TOF/MS spectrum of the synthesized 20:1 mono-acyl PS (predicted theoretical mass 551 amu). Peaks at 550 and 572 m/z correspond with 20:1 mono-acyl PS [M-H] and its sodium adduct [M+Na-H], respectively. The peak at 463 m/z corresponds with the mass of mono-acyl PS after neutral loss of the serine head-group [M-H-Ser-H₂O]. A matrix peak is indicated by *. Panel B shows the TLR2 activation of 20:1 mono-acyl PS (Lyso-PS) in comparison to other mono-acyl PS molecules with a different acyl-chain configuration. TLR2 activation was quantified by measuring the activity of TLR2-induced expression of NF-κB-SEAP after overnight incubation of HEK-TLR2-Blue with 25 μM synthesized mono-acyl PS 18:1, 20:1 mono-acyl PS, mono-acyl PS 22:1 or mono-acyl PS 24:1, FSL-1, 2.1 pM was added as positive control. Shown is the mean and standard deviation of 3 independent incubations. Panel C shows the TLR2 activation of 20:1 mono-acyl PS in comparison to mono-acyl PA 20:1 and mono-acyl PC 20:1 at the indicated concentrations. Shown is the mean and standard deviation of 3 independent incubations. Panel D. Selective blocking of TLR1, TLR2 or TLR6 reveals that mono-acyl PS is an agonist of the TLR2/6 heterodimer. HEK-Blue TLR2 cells were incubated with blocking antibodies against TLR1, TLR2 or TLR6 before 20:1 mono-acyl PS or the known agonists for TLR2/1 (PAM3CSK4, 23 pM) or TLR2/6 (FSL-1, 2.1 pM) were added. The TLR2 activation is expressed as the percentage of control incubations (no blocking antibodies). Shown is the mean and SD of 2 independent experiments, each performed in triplicate.

DISCUSSION

Although the general concept is that di- and tri-acylated compounds are ligands for the TLR2/6 and TLR2/1 heterodimer, respectively, three studies reported that lipid fractions derived from parasites containing mono-acyl phospholipids can activate TLR2 as well (Van der Kleij, Latz et al. 2002, Magalhaes, Almeida et al. 2010, Carneiro, Iacurra et al. 2013).

In order to prove the TLR2 activating capacity of mono-acyl phospholipids, we developed a method for the biosynthesis of several mono-acyl phospholipids. This biosynthetic approach has three advantages. First, it rules out the possibility that instead of mono-acyl PS, another minor compound present in the purified lipid fraction of *S. mansoni* was in fact the TLR2 activating compound. Second, the biosynthetic approach allows the preparation of several specific mono-acyl phospholipid variants, because mono-acyl phospholipids with distinct head-groups and/or acyl-chain can be synthesized. These synthesized specific mono-acyl phospholipid variants can then be used for structure-function analysis of TLR2 activation by mono-acyl phospholipid ligands. This is not possible using lipid fractions of schistosomes or other organisms, as those contain mixtures of different mono-acyl phospholipids. Third, the mono-acyl phospholipids that activate TLR2 can be synthesized in larger quantities than can be obtained purely by isolation from the parasite. Since our method resulted in the preparation of pure and large quantities of mono-acyl phospholipids, it allowed assessment of their TLR2 activating capacity in a cellular TLR2 reporter system. These experiments demonstrated that the biosynthesized 20:1 mono-acyl PS activated TLR2. This firmly confirms the earlier report in which a purified lipid fraction containing 20:1 mono-acyl PS from *S. mansoni* activated TLR2 (Van der Kleij, Latz et al. 2002).

TLR2-induced intracellular signaling requires the formation of heterodimers with TLR1 or TLR6 (Ozinsky, Underhill et al. 2000, van Bergenhenegouwen, Plantinga et al. 2013). The TLR2/1 and TLR2/6 heterodimers each have their preferred ligands and the classical ligands for the TLR2/6 heterodimer are di-acylated lipopeptides, while tri-acylated lipopeptides are the classical ligands for TLR2/1 heterodimer (Oliveira-Nascimento, Massari et al. 2012, van Bergenhenegouwen, Plantinga et al. 2013). Our experiments showed that 20:1 mono-acyl PS activates the TLR2/6 heterodimer and not the TLR2/1 heterodimer, which is consistent with the previous observations that activation of TLR2/1 heterodimer requires a ligand with multiple acyl chains of which one or two are inserted in the hydrophobic pocket in TLR2 and another acyl chain in TLR1 (Kang, Nan et al. 2009).

To gain more insight into the interaction between mono-acyl PS and the TLR2/6 heterodimer, we used the available crystal structure of TLR2/6 to generate an in silico model of the potential interaction of 20:1 mono-acyl PS and the TLR2/6 heterodimer. A search space was defined around the active site of the TLR2/6 heterodimer, after which automatic fits of 20:1 mono-acyl PS were calculated. The generated models are available as PyMol workspace (see supplemental data). In the optimal configuration in the in silico model, the hydrophobic acyl chain of 20:1 mono-acyl PS was positioned in the hydrophobic pocket of the TLR2 monomer such that it completely filled the pocket (Fig 2A and 2B), with a theoretical binding affinity of -34.3 kJ/mol. These results fit with the experimental data that showed that 20:1 mono-acyl PS was the most potent agonist for the TLR2/6 heterodimer. Figure 2B shows an overlay of 20:1 mono-acyl PS with FSL-1, the well-known agonist of TLR2/6 heterodimers that was also used to produce crystals for X-ray crystallography. This image shows that the acyl chain of 20:1 mono-acyl PS mainly follows the same configuration in the hydrophobic pocket of TLR2 as the lipid side chains of FSL-1. Finally, in the optimal configuration in the in silico model multiple hydrogen bonds are formed between the hydrophilic head-group of 20:1 mono-acyl PS and amino acids in the ligand binding pocket of the TLR2/6 heterodimer (Fig. 2C); amino acid residue D327 of TLR2 and the residues K321 and F319 of TLR6. Of these amino acid residues D327 of TLR2 and F319 of TLR6 are known to form hydrogen bonds with FSL-1 during ligand (Jin, Kim et al. 2007), and therefore, binding of 20:1 mono-acyl PS might stabilize the TLR2/6 heterodimer similar to stabilizing effect of FSL-1 binding to TLR2/6.

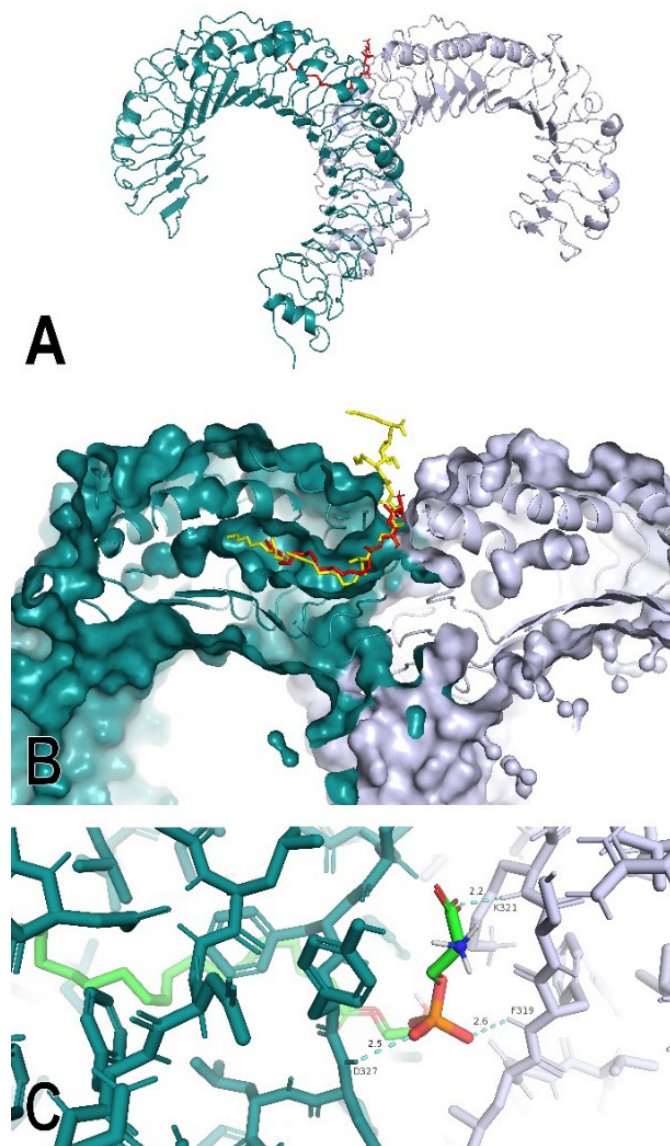


Figure 2. In silico modeling of the ligand-receptor interaction of 20:1 mono-acyl PS with the TLR2/6 heterodimer.

Panel A shows the interaction of 20:1 mono-acyl PS (red) with the TLR2/6 heterodimer (TLR2 green, TLR6 gray) in an in silico prepared model using VINA and PyMol. The best fit positioned the acyl-chain of 20:1 mono-acyl PS in the hydrophobic pocket of TLR2 and the serine head-group of mono-acyl PS interacting with amino acid residues of both TLR2 and TLR6. Panel B shows an identical projection compared to Panel A, but the TLR2/6 complex is now presented as a surface model and the ligands FSL-1 (yellow) and 20:1 mono-acyl PS (red) are shown in an overlay to visualize the similar position in the hydrophobic pocket of the TLR2 monomer of the acyl-chain of 20:1 mono-acyl PS compared to the acyl chains of FSL-1. Panel C shows the predicted hydrogen-bonds between 20:1 mono-acyl PS and residues D327 of TLR2, residues K321, F319 of TLR6, shown as dashed, cyan lines. Numbers indicate the distance in ångström.

Although mono-acylated ligands for TLR2 derived from pathogens seem to be scanty, many mono-acylated synthetic compounds have been prepared that can activate the TLR2/6 heterodimer (Agnihotri, Crall et al. 2011).

These results demonstrated that at least one acyl group and an appropriately orientated ester carbonyl group are essential for TLR2-agonistic activity (Agnihotri, Crall et al. 2011), which is consistent with our modelling results as well as the observed *in vitro* activation of the TLR2/6 heterodimer by 20:1 mono-acyl PS. However, the affinity of the TLR2/6 heterodimer for 20:1 mono-acyl PS seems low, as rather high concentrations (μM range) of 20:1 mono-acyl PS were required for TLR2/6 activation compared to the classical TLR2 ligands derived from bacteria (e.g. lipopeptides, such as FSL-1) and reported synthetic ligands for TLR2/6 (nM to pM range) (Jin, Kim et al. 2007). On the other hand, locally high concentrations of 20:1 mono-acyl PS might occur *in vivo* in *S. mansoni* infected hosts, as [1] the outer-surface membranes of adult *S. mansoni* worms were shown to be highly enriched in this mono-acyl PS species [2] adult schistosomes actively synthesize eicosaenoic acid (20:1) in high amounts (Brouwers, Smeenk et al. 1997), and [3] phospholipids in the outer-surface membranes of adult schistosomes have a high turnover rate (Brouwers, Skelly et al. 1999). Therefore, 20:1 mono-acyl PS could be a clinically relevant agonist for TLR2 that affects dendritic cells such that mature dendritic cells gained the ability to induce the development of IL-10-producing regulatory T-cells (Van der Kleij, Latz et al. 2002).

In short, our results conclusively demonstrated that 20:1 mono-acyl PS is a true agonist for the TLR2/6 heterodimer, and thereby it is the TLR2-activating compound in lipid fractions derived from *S. mansoni*. As 20:1 mono-acyl PS can now be prepared in higher quantities by the developed biosynthetic method, future studies can be performed to further assess the functions of 20:1 mono-acyl PS as an immunological mediator.

Funding/Conflict of interest

MB and AGMT were supported by the Dutch Organization for Scientific Research (NWO), grant STW 10725. All authors declare that they have no conflicts of interest with the contents of this article.

Supporting information

The prepared in silico models shown in Figure 2 are available as PyMol workspace. Panel A of Figure 2 is stored under F1, Panel B under F2 and Panel C under F3. A video-model is available at <https://www.youtube.com/user/Smansoni/videos>

REFERENCES

- Agnihotri, G., B. M. Crall, T. C. Lewis, T. P. Day, R. Balakrishna, H. J. Warshakoon, S. S. Malladi and S. A. David (2011). "Structure-Activity Relationships in Toll-Like Receptor 2-Agonists Leading to Simplified Monoacyl Lipopeptides." *Journal of Medicinal Chemistry* **54**(23): 8148-8160.
- Aroui, A. and O. G. Mouritsen (2013). "Membrane-perturbing effect of fatty acids and lysolipids." *Progress in Lipid Research* **52**(1): 130-140.
- Beutler B, Jiang Z, Georgel P, et al(2006);. Genetic analysis of host resistance: Toll-like receptor signaling and immunity at large. *Annual Reviews Immunology*. **24**:353-389.
- Beutler, B. A. (2009). "TLRs and innate immunity." *Blood* **113**(7): 1399-1407.
- Bligh, E. G. and W. J. Dyer (1959). "A rapid method of total lipid extraction and purification." *Canadian Journal of Biochemistry and Physiology* **37**(8): 911-917.
- Brouwers, J., P. J. Skelly, L. M. G. Van Golde and A. G. M. Tielens (1999). "Studies on phospholipid turnover argue against sloughing of tegumental membranes in adult *Schistosoma mansoni*." *Parasitology* **119**: 287-294.
- Brouwers, J., I. M. B. Smeenk, L. M. G. van Golde and A. G. M. Tielens (1997). "The incorporation, modification and turnover of fatty acids in adult *Schistosoma mansoni*." *Molecular and Biochemical Parasitology* **88**(1-2): 175-185.
- Carneiro, A. B., B. M. Iaciura, et al. (2013). "Lysophosphatidylcholine triggers TLR2- and TLR4-mediated signaling pathways but counteracts LPS-induced NO synthesis in peritoneal macrophages by inhibiting NF-kappaB translocation and MAPK/ERK phosphorylation." *PLOS ONE* **8**(9): e76233.
- Comfurius, P. and R. F. Zwaal (1977). "The enzymatic synthesis of phosphatidylserine and purification by CM-cellulose column chromatography." *Biochimica Biophysica Acta* **488**(1): 36-42.
- Jin, M. S., S. E. Kim, J. Y. Heo, M. E. Lee, H. M. Kim, S.-G. Paik, H. Lee and J.-O. Lee (2007). "Crystal structure of the TLR1-TLR2 heterodimer induced by binding of a tri-acylated lipopeptide." *Cell* **130**(6): 1071-1082.
- Kang, J. Y., X. Nan, et al. (2009). "Recognition of lipopeptide patterns by Toll-like receptor 2-Toll-like receptor 6 heterodimer." *Immunity* **31**(6): 873-884.
- Magalhaes, K. G., P. E. Almeida, G. C. Atella, C. M. Maya-Monteiro, H. C. Castro-Faria-Neto, M. Pelajo-Machado, H. L. Lenzi, M. T. Bozza and P. T. Bozza (2010). "Schistosomal-Derived Lysophosphatidylcholine Are Involved in Eosinophil Activation and Recruitment through Toll-Like Receptor-2-Dependent Mechanisms." *Journal of Infectious Diseases* **202**(9): 1369-1379.
- Misiorowski, R. L. and M. A. Wells (1974). "The activity of phospholipase A2 in reversed micelles of phosphatidylcholine in diethyl ether: effect of water and cations." *Biochemistry* **13**(24): 4921-4927.
- Oberg, H.-H., M. Juricke, D. Kabelitz and D. Wesch (2011). "Regulation of T cell activation by TLR ligands." *European Journal of Cell Biology* **90**(6): 582-592.
- Oliveira-Nascimento, L., P. Massari and L. M. Wetzler (2012). "The Role of TLR2 in Infection and Immunity." *Frontiers in Immunology* **3**: 79-79.
- Ozinsky, A., D. M. Underhill, J. D. Fontenot, A. M. Hajjar, K. D. Smith, C. B. Wilson, L. Schroeder and A. Aderem (2000). "The repertoire for pattern recognition of pathogens by the innate immune system is defined by cooperation between toll-like receptors." *Proceedings of the National Academy of Sciences of the United States of America* **97**(25): 13766-13771.
- Rouser, G., S. Fleischer and A. Yamamoto (1970). "Two dimensional thin layer chromatographic separation of polar lipids and determination of phospholipids by phosphorus analysis of spots." *Lipids* **5**(5): 494-496.
- Ruttink, P. J. A., L. J. M. Dekker, T. M. Luiders and P. C. Burgers (2012). "Complexation of divalent metal ions with diols in the presence of anion auxiliary ligands: zinc-induced oxidation of ethylene glycol to glycolaldehyde by consecutive hydride ion and proton shifts." *Journal of Mass Spectrometry* **47**(7): 869-874.
- Skipski, V. P., R. F. Peterson and M. Barclay (1962). "Separation of phosphatidyl ethanolamine, phosphatidyl serine, and other phospholipids by thin-layer chromatography." *Journal of Lipid Research* **3**(4): 467-470.
- Trott, O. and A. J. Olson (2010). "AutoDock Vina: Improving the speed and accuracy of docking with a new scoring function, efficient optimization, and multithreading." *Journal of Computational Chemistry* **31**(2): 455-461.
- Uematsu, S. and S. Akira (2006). "Toll-like receptors and innate immunity." *Journal of Molecular Medicine* **84**(9): 712-725.
- van Bergenhenegouwen, J., T. S. Plantinga, L. A. Joosten, M. G. Netea, G. Folkerts, A. D. Kraneveld, J. Garssen and A. P. Vos (2013). "TLR2 & Co: a critical analysis of the complex interactions between TLR2 and coreceptors." *Journal of Leukocyte Biology* **94**(5): 885-902.
- Van der Kleij, D., E. Latz, et al. (2002). "A novel host-parasite lipid cross-talk - Schistosomal lyso-phosphatidylserine activates Toll-like receptor 2 and affects immune polarization." *Journal of Biological Chemistry* **277**(50): 48122-48129.
- Weininger, D. (1988). "SMILES, a chemical language and information system. 1. Introduction to methodology and encoding rules." *Journal of Chemical Information and Computer Sciences* **28**(1): 31-36.



CHAPTER 5

Schistosoma mansoni infection affects the proteome and lipidome of circulating extracellular vesicles in the host

Michiel L. Bexkens ^a, Renske A. van Gestel ^b, Bas van Breukelen ^b, Rolf T. Urbanus ^c, Jos F. Brouwers ^{d,e}, Rienk Nieuwland ^{f,g}, Aloysius G.M. Tielens ^{a,d}, Jaap J. van Hellemond ^{a,*}

a. Department of Medical Microbiology and Infectious Diseases, Erasmus MC University Medical Center Rotterdam, Rotterdam, the Netherlands.

b. Biomolecular Mass Spectrometry & Proteomics, Utrecht Institute for Pharmaceutical Sciences and Bijvoet Center for Biomolecular Research, Utrecht University, Utrecht, the Netherlands

c. Department of Clinical Chemistry and Haematology, Center for Circulatory Health, University Medical Center Utrecht, Utrecht University, Utrecht, The Netherlands.

d. Department of Biochemistry and Cell Biology, Faculty of Veterinary Medicine, Utrecht University, Utrecht, the Netherlands.

e. Current address: Department of Molecular Cancer Research, Center for Molecular Medicine, University Medical Center Utrecht, Utrecht, the Netherlands.

f. Laboratory of Experimental Clinical Chemistry, Amsterdam UMC, University of Amsterdam, Amsterdam, The Netherlands.

g. Vesicle Observation Centre, Amsterdam UMC, University of Amsterdam, Amsterdam, The Netherlands.

ABSTRACT

Eggs, schistosomula and adult *Schistosoma* worms are known to release extracellular vesicles (EV) during *in vitro* incubations and these EVs are postulated to affect the host responses. So far only those EVs released during *in vitro* incubations of schistosomes have been studied and it is unknown whether in blood of infected hosts the schistosomal EVs can be detected amidst all the circulating EVs of the host itself. In this study we analyzed the protein as well as the phospholipid composition of EVs circulating in blood plasma of *S. mansoni* infected hamsters and compared those with the EVs circulating in blood of non-infected hamsters. Although neither proteins nor lipids specific for schistosomes could be detected in the circulating EVs of the infected hamsters, the infection with schistosomes had a marked effect on the circulating EVs of the host, as the protein as well as the lipid composition of EVs circulating in infected hamsters were different from the EVs of uninfected hamsters. The observed changes in the EV lipid and protein content suggest that more EVs are released by the diseased liver, the affected erythrocytes and activated immune cells.

Key words

Exosomes, cell-derived microparticles, schistosomiasis, host-parasite interactions, communicable diseases

Abbreviations

EVs, extracellular vesicles; PC, phosphatidylcholine; PCA, Principle Component Analysis; PE, phosphatidylethanolamine; PS, phosphatidylserine; PG, phosphatidylglycerol; PI, phosphatidylinositol; SM, sphingomyelin; TEM, transmission electron microscopy

INTRODUCTION

Extracellular vesicles (EVs) have been defined by the International Society for Extracellular Vesicles (ISEV) as the generic term for particles naturally released from the cell, that are delimited by a lipid bilayer and cannot replicate, i.e. do not contain a functional nucleus (Théry, Witwer et al. 2018). EVs vary substantially in size (ca. 30 to 1000 nm in diameter), density (ca. 1.13 to 1.19 g/ml) and biochemical composition (e.g. proteome, lipidome, DNA and RNA content, etc.) (Colombo, Raposo et al. 2014). EVs are released by most types of cells and organisms, including parasites (Gill, Forterre et al. 2018). Three types of EVs can be distinguished, 1) Exosomes are approximately 40-100 nm in diameter and are released by most cell types; they are formed within the endosomal network and their secretion is the result of inward budding and fusion of multi-vesicular bodies with the plasma membrane, 2) Microvesicles/microparticles can be difficult to distinguish from exosomes and can be up to 1 µm. They are formed by outward budding of the plasma membrane, incorporating lipids, proteins and other compounds before budding, 3) Apoptotic bodies are the largest vesicles with a size of 1 to 5 µm and they are formed as blebs of cells undergoing apoptosis (Yanez-Mo, Siljander et al. 2015). Were EVs first regarded to be involved in cellular waste management, EVs are now thought to be important as mediators of intercellular communication (Colombo, Raposo et al. 2014, Gill, Forterre et al. 2018, Théry, Witwer et al. 2018). In recent years, the knowledge on EVs has increased exponentially and it has been demonstrated that the plasma concentration of EVs changes during disease, and that EVs may function as biomarker for various diseases (Highton, Martin et al. 2018, Doyle and Wang 2019). In addition, there is accumulating evidence that the host immune system is affected by the lipids, nucleic acids and/or glycans contained in, or present on, pathogen derived EVs (Schorey, Cheng et al. 2015, Kuipers, Hokke et al. 2018).

From a host-pathogen interaction perspective, schistosomiasis is an intriguing disease as it is caused by blood-dwelling flukes. Despite the hostile environment that comprises all types of host immune cells and antibodies, the adult worm pairs have an average life-span of 5 to 10 years (Colley, Bustinduy et al. 2014). Adult worm pairs of *Schistosoma mansoni*, the best studied *Schistosoma* species, inhabit the mesenteric veins of the host and here the adult female produces up to 300 eggs per day. Eggs are either shed into the environment via the faeces, or are by chance retained in host tissues where they induce inflammation and subsequently granuloma formation (McManus, Dunne et al. 2018). Eggs as well as adult *S. mansoni* excrete factors that manipulate the host immune system and host haemostasis for their own survival (Dunne and Cooke 2005, Mebius, van Genderen et al. 2013, Costain, MacDonald et al. 2018). However, the mechanisms

applied by schistosomes in the interaction with their hosts, are not yet fully understood. Previous research has shown that *S. mansoni* schistosomula and adult worms release EVs during *in vitro* incubations and that these EVs contain microRNAs (miRNAs) and proteins (Nowacki, Swain et al. 2015, Sotillo, Pearson et al. 2016, Samoil, Dagenais et al. 2018). These reports demonstrated that schistosome derived EVs comprise common EV markers, such as heat shock proteins, enzymes involved in energy metabolism and cytoskeletal proteins. Furthermore, adult worms and eggs of *Schistosoma japonicum* are known to release EVs containing miRNAs and proteins during *in vitro* incubations (Zhu, Liu et al. 2016, Liu, Zhu et al. 2019). Analysis of the contents of these EVs suggests that schistosome-derived EVs may affect the host responses (Wang, Li et al. 2015, Cai, Gobert et al. 2016, Zhu, Liu et al. 2016).

So far only those EVs released during *in vitro* incubations of schistosomes have been studied and it is unknown whether in blood of infected hosts the schistosomal EVs can be detected amidst all the circulating EVs of the host itself. In our study we analyzed the protein as well as the phospholipid composition of EVs circulating in blood plasma of *S. mansoni* infected hamsters and compared those with the EVs circulating in blood of non-infected hamsters. In these investigations neither proteins nor lipids specific for schistosomes could be detected in the circulating EVs of the infected hamsters. However, infection with schistosomes had a marked effect on the circulating EVs of the host, as the protein as well as the lipid composition of EVs circulating in infected hamsters were different from the EVs of uninfected hamsters.

MATERIAL AND METHODS

Puerto Rican strain of *S. mansoni* was maintained in Golden hamsters (*Mesocricetus auratus*) for which animal ethics was approved (license EUR1860-11709). Animal care and maintenance was in accordance with institutional and governmental guidelines. In this study five hamsters infected with *S. mansoni* were used and five control hamsters, which were housed and fed identically to the infected hamsters. Blood was collected seven weeks after infection with approximately 600 cercariae per hamster. Infected and control hamsters were housed and fed identically. After seven weeks, the hamsters were anesthetized with isoflurane and whole blood was obtained by heart puncture and collected in tubes with trisodium citrate as an anticoagulant. Citrated platelet poor plasma was obtained by two-fold centrifugation of citrated blood at 2000g for 15 minutes at room temperature. Subsequently, EVs were isolated by a well-established method using size-exclusion chromatography with a cut-off of 70 nm as described

earlier (Böing, van der Pol et al. 2014). In short, platelet poor plasma was loaded on a Sepharose CL-2B column (30 mL, GE Healthcare; Uppsala, Sweden), that was washed with PBS containing 0.32% trisodium citrate (pH 7.4). Subsequently, fractions were eluted with PBS/0.32% citrate (pH 7.4). The collected fractions were further analyzed using electron microscopy after which the EV containing fractions were stored at -80°C until further analysis.

To determine the protein composition of EVs, 3 samples of infected and 3 samples of control hamsters and individually processed for proteome analysis. The proteins were first separated by SDS-PAGE, after which the lanes of the SDS-PAGE were subsequently divided into 10 slices and the proteins were then subjected to in-gel tryptic digestion as described by Shevchenko *et al.* (Shevchenko, Tomas et al. 2006). After digestion the samples were analyzed on an Orbitrap Q-Exactive (Thermo Fisher Scientific, Waltham, MA, USA) connected to a UHPLC Proxeon Easy-nLC 1000 (Thermo Fisher Scientific, Waltham, MA, USA). Peptides were trapped on a double-fritted trap column (Dr. Maisch Reprosil C18, 3 µm, 2 cm × 100 µm (Dr. Maisch HPLC GmbH, Ammerbuch-Entringen, Germany)) and separated on an analytical column (Agilent Zorbax SB-C18, 1.8 µm, 40 cm × 75 µm (Agilent, Santa Clara, CA, USA)). Solvent A consisted of 0.1 M acetic acid, solvent B of 0.1 M acetic acid in 80% acetonitrile. Samples were loaded at a pressure of 800 bar with 100% solvent A. Peptides were separated by a 30 min gradient of 10–30% buffer B followed by 30–100% B in 2 min, 100% B for 2.5 min at a flow rate of 150 nL/min. Full scan MS spectra were acquired in the Orbitrap (350–1500 m/z, resolution 35,000, AGC target 3e6, maximum injection time 250 ms). The 20 most intense precursors were selected for HCD fragmentation (isolation window 1.2 Da, resolution 17,500, AGC target 5e4, maximum injection time 120 ms, first m/z 100, NCE 33%, dynamic exclusion 60 s). The results were normalized on the Total Ion Count, then pooled for the 3 infected and the 3 control hamsters and subsequently filtered using Percolator (Käll, Storey et al. 2007, Spivak, Weston et al. 2009) to a false discovery rate (FDR) below 1%. We further only accepted peptides with at least six amino acid residues, a Mascot ion score of at least 20, and search engine rank of 1 and at least 2 identified peptides for protein identification. Scores (Mascot ion score) and peptide spectrum matches (PSM; total number of identified peptide spectra matched for the protein) were used to compare the samples. Analysis of the data to annotate the peptides was performed with Scaffold using the *S. mansoni* database (Schistosoma_mansoni_v5.2.fa, Wellcome Trust Sanger Institute, Hinxton, UK, accessible from: <ftp://ftp.sanger.ac.uk/pub/project/pathogens/Schistosoma/mansoni/Archive/S.mansoni/genome/>) and the genomic information available for the golden or Syrian hamster (*Mesocricetus auratus*) accessible from ftp://ftp.ncbi.nlm.nih.gov/genomes/all/GCF/000/349/665/GCF_000349665.1_MesAur1.0

The set of identified proteins in EVs derived from infected and control hamster plasma was normalized on the albumin score and further analyzed using the “FunRich” software package, which allows functional and comparative analysis with EV proteome data from other studies (Pathan, Keerthikumar et al. 2017). As FunRich does not contain hamster proteins, gene analogs coding for the identified proteins in hamsters were determined in the genome of *Mus musculus*. For 38 out of the 42 identified hamster proteins, gene homologues in the *M. musculus* genome could be automatically retrieved from the Uniprot database. The four remaining proteins were manually annotated by determining the most similar protein and its corresponding gene via BlastP analysis. The resulting 42 *M. musculus* genes (nomenclature according to NCBI gene) were used as a query in FunRich to identify whether the proteins encoded by these genes had been detected in earlier studies in EVs derived from blood plasma.

The phospholipid composition was determined at species level by Liquid Chromatography coupled to Mass Spectrometry (LC-MS). The extracted lipids were loaded on a hydrophilic interaction liquid chromatography (HILIC) column (2.6 μ m HILIC 100 Å, 50 x 4.6 mm, Phenomenex, Torrance, CA) and eluted at a flow rate of 1 mL/min with a gradient from acetonitrile/acetone (9:1, v/v) to acetonitrile/H₂O (7:3, v/v) with 10 mM ammonium formate. Both elution solutions also comprised 0.1% (v/v) formic acid. The column outlet of the LC was connected to a heated electrospray ionization (HESI) source of an LTQ-XL mass spectrometer (ThermoFisher Scientific, Waltham, MA). Full scan spectra were collected from m/z 450–1050 at a scan speed of 3 scans/s. For analysis the data were converted to mzXML format and analyzed using XCMS version 1.52.0 running under R version 3.4.3 (Smith, Want et al. 2006). Principle Component Analysis was provided by the R package PCA Methods (Stacklies, Redestig et al. 2007).

RESULTS

EVs were isolated from citrated plasma collected from either five control or five *S. mansoni* infected hamsters by size-exclusion chromatography as described earlier [22]. The presence of EVs was confirmed by transmission electron microscopy (TEM) imaging, as shown in Figure 1. The isolated vesicles range in size from about 50 nm to 150 nm, which is in agreement with the reported sizes of EVs released by schistosomes as well as of EVs isolated from plasma (Nowacki, Swain et al. 2015, Sotillo, Pearson et al. 2016, Samoil, Dagenais et al. 2018, Mathieu, Martin-Jaular et al. 2019).

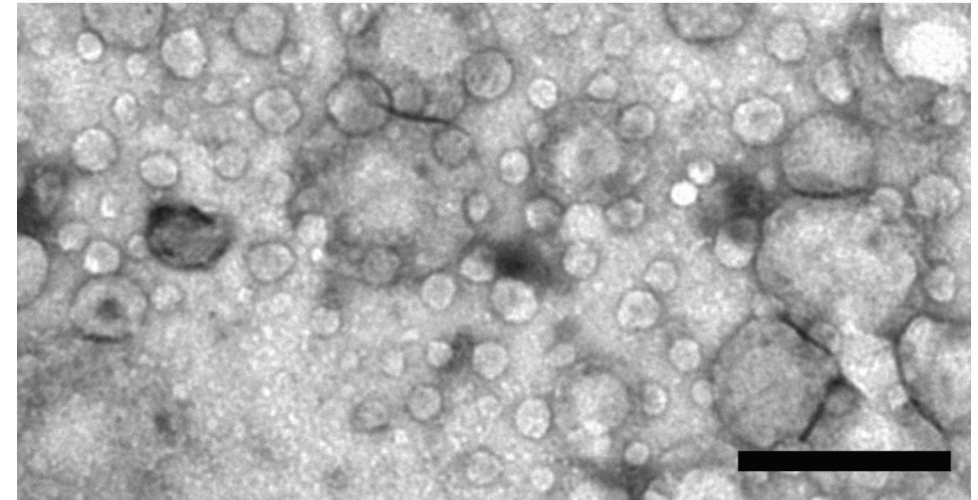


Figure 1. EM photograph of extracellular vesicles isolated from plasma of a hamster infected with *Schistosoma mansoni*. Visible are donut-shaped extracellular vesicle (EV)-like structures ranging in size from 50 to 150 nm. The scale bar denotes 200 nm.

The protein composition in the isolated EV fraction was determined by LC-MS/MS using a MASCOT database with hamster proteins as well as *S. mansoni* proteins. By this analysis no proteins of schistosomal origin were discovered and all identified proteins were of host origin (hamster) (Supplementary Table 1 and data are available via ProteomeXchange with identifier PXD019809). However, infection with *S. mansoni* had an effect on the protein content of the EVs of the host, as remarkable differences in protein composition were observed between the EVs of infected and non-infected hamsters (Fig. 2). In total 42 proteins were identified, of which 14 proteins were exclusively detected in EVs of *S. mansoni* infected hamsters, 7 proteins exclusively in EVs of control hamsters and 21 proteins were present in EVs of infected as well as control hamsters (Fig. 2). Of those 21 identified proteins present in EVs from the infected and from the control hamsters, three proteins were more than 2-fold enriched and two proteins were over 2-fold decreased in EVs of infected hamsters compared with the EVs of control hamsters (Supplementary Table 1).

In order to compare the set of EV proteins identified in our study with those identified in earlier studies, the FunRich software package was used (Pathan, Keerthikumar et al. 2017). FunRich does not contain hamster proteins, therefore gene analogs coding for the identified proteins in hamsters were determined in the genome of *Mus musculus* (see Materials and Methods for details). The resulting 42 *M. musculus* genes

(nomenclature according to NCBI gene) were used as a query in FunRich to identify whether the proteins encoded by these genes had been detected in EVs derived from blood plasma in earlier studies. This analysis showed that 36 out of these 42 proteins had been detected earlier in plasma-derived EVs (See Supplementary Table 1). In one of those nine studies (de Menezes-Neto, Saez et al. 2015) on EVs derived from plasma of healthy human volunteers, 30 of the 42 proteins of our study were identified (Supplementary Figure 1). In that de Menezes-Neto et al. study (de Menezes-Neto, Saez et al. 2015)(2015) a comparison was made between different EV isolation methods. That analysis revealed a core set of 17 proteins that were more frequently detected regardless of method or sample type. Of these 17 proteins, 11 (64.7%) were present in our EV preparation (Supplementary Figure 1).

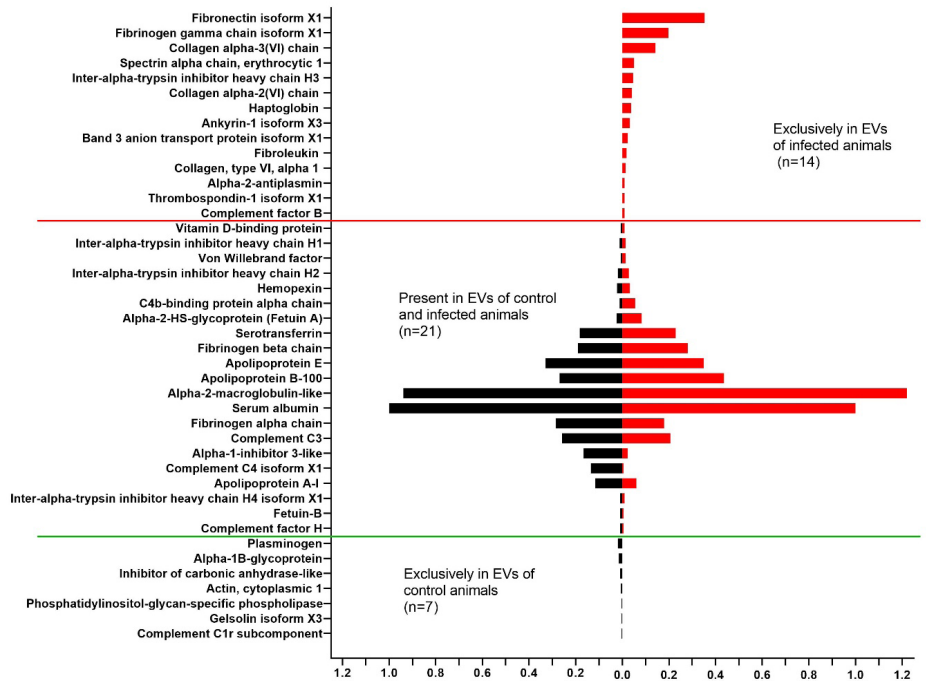


Figure 2. Infection with *S. mansoni* modifies the protein composition of extracellular vesicles in host blood plasma. Proteins identified by LC-MS/MS in extracellular vesicles (EVs) isolated from blood plasma from five non-infected control host (black bars) versus five infected host (red bars). Protein content in each sample was normalized to the serum albumin content and the relative abundance of identified proteins is given in comparison to serum albumin. The top part shows the proteins only detected in EVs from infected hosts, whereas the bottom part shows the proteins detected only in EVs of non-infected, control hosts. The center box shows proteins detected in EVs of control as well as infected hosts. Proteins exclusively in EVs of infected animals OR exclusively present in EVs of control animals are ordered from high to low based on their absolute abundance.

For proteins present in both samples, the ordering is centered around serum albumin (ratio=1 infected/control). Proteins with a ratio > 1 (infected/control) are ordered low to high (absolute abundance of proteins present in vesicles isolated from infected animals), proteins with a ratio < 1 are ordered high to low (based on absolute abundance of proteins present in vesicles isolated from control animals). Supplementary Table 1 contains these and other data on the proteins in question.

Table 1. Protein function and possible link with schistosomiasis of proteins exclusively detected in extracellular vesicles of *S. mansoni* infected animals.

	Proteins exclusively detected in infected animals	Functional process	Possible link with the disease schistosomiasis
1	fibronectin isoform X1	extra-cellular matrix protein	liver fibrosis
2	fibrinogen gamma chain isoform X1	blood coagulation	liver fibrosis & inflammatory response (acute phase reaction)
3	collagen alpha-3(VI) chain	extra-cellular matrix protein	liver fibrosis
4	spectrin alpha chain, erythrocytic 1	linking cytoskeleton to erythrocyte plasma membrane	anaemia
5	inter-alpha-trypsin inhibitor heavy chain H3	plasma protease inhibitor	inflammatory response
6	collagen alpha-2(VI) chain	extra-cellular matrix protein	liver fibrosis
7	haptoglobin	plasma protein binding free haemoglobin	inflammatory response (acute phase reaction)
8	ankyrin-1 isoform X3	linking cytoskeleton to erythrocyte plasma membrane	anaemia
9	band 3 anion transport protein isoform X1	transporter protein in erythrocyte plasma membrane	anaemia
10	fibroleukin	immune regulatory factor secreted by T-cells	host inflammatory response
11	collagen, type VI, alpha 1	extra-cellular matrix protein	liver fibrosis
12	alpha-2-antiplasmin	haemostasis	hypo-coagulable and hyper-fibrinolytic state during schistosomiasis
13	thrombospondin-1 isoform X1	haemostasis	hypo-coagulable and hyper-fibrinolytic state during schistosomiasis
14	complement factor B	complement system	complement system activation on the surface of schistosomes

Most of the identified EV proteins in our study are known blood plasma proteins, membrane proteins or proteins that are part of the cytoskeleton or extracellular matrix and they have a function in hemostasis, immunity or transport (Supplementary Table 1). Of the 14 proteins exclusively found in EVs derived from infected hamsters, four function in hemostasis (fibronectin, fibrinogen gamma chain, alpha-2 antiplasmin, thrombospondin-1), three are extracellular matrix proteins (collagen alpha-1, 2 and 3) and two are present in the cytoskeleton of erythrocytes (spectrin alpha chain, ankyrin-1). We analyzed not only the protein content of the EVs, but also the lipid content of EVs

derived from plasma of infected as well as control hamsters. This analysis demonstrated that the membranes of EVs of both infected and control hamsters comprised many distinct phospholipid species in all investigated major phospholipid classes: phosphatidylcholine (PC), phosphatidylethanolamine (PE), phosphatidylserine (PS), phosphatidylglycerol (PG) and phosphatidylinositol (PI) and sphingomyelin (SM) (Fig. 3 and Supplementary Data 1). Our earlier research demonstrated that the outer surface of adult *S. mansoni* contains several specific phospholipids, such as lyso-PS 20:1, PC 16:0/18:1 $\Delta 5$, PC 16:0/20:1, PI 16:0/18:0 and PI 18:0/20:1, that are not present in their mammalian host (Retra, deWalick et al. 2015). Not a single one of these schistosoma-specific lipids was detected in the EVs derived from infected or control hamsters. However, principal component analysis (PCA) of the top 150 lipid signals demonstrated that the membrane lipid composition of EVs derived from infected hamsters differed consistently from that of control hamsters (Fig. 3, top left panel). Clear differences in PC species were observed between EVs derived from infected and control hamsters, as PCs 36:4 and 33:0 were enriched in infected hamsters, while PCs 36:2, 36:3 and 34:2 were decreased compared to control hamsters (Fig. 3, bottom panel). However, the most striking difference was the relative increase in nearly all PS and SM species and decrease of most PI and lyso-phospholipid species in EV membranes derived from infected hamsters compared to control hamsters.

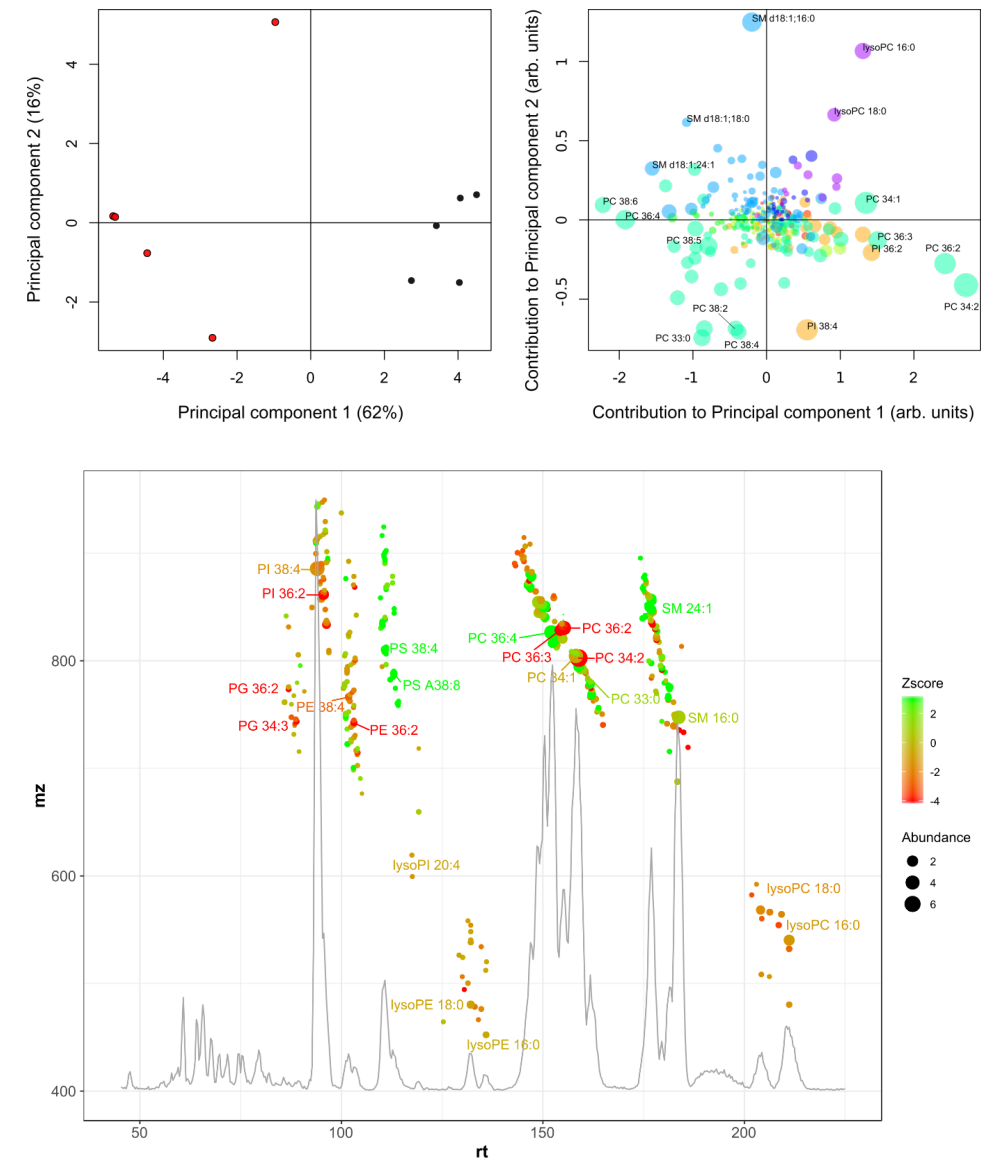


Figure 3. Infection with *S. mansoni* modifies the phospholipid composition of extracellular vesicles in host blood plasma. Complete phospholipid analysis of extracellular vesicles (EVs) isolated from blood-plasma of five infected versus five non-infected hosts. The top left panel shows the score plot of PCA of lipid content from vesicles isolated from infected hosts (red) versus non-infected hosts (black). The top right panel shows the corresponding loadings plot of the PCA; sizes of lipid species correspond to abundance, colors depict lipid class; green (PC), orange (PI), cyan (SM) and purple (lysoPC). Bottom panel shows an overlay of a contour plot and the base peak chromatogram as recorded during the analysis of EVs isolated from an infected host. Detected lipid species are shown at their corresponding retention time (rt, in seconds) and the color scale indicates the relative increased (green) or decreased (red) abundance in vesicles isolated from infected hosts compared to non-infected hosts.

DISCUSSION

Host-parasite interactions in schistosomiasis have been a subject of research for decades and recently several studies focused on a possible role for EVs in this interaction. It has been shown that adult schistosomes, schistosomula and eggs, three life cycle stages of *S. mansoni* that are present in the mammalian host, release EVs when they are cultured *in vitro*, outside the host (Nowacki, Swain et al. 2015, Sotillo, Pearson et al. 2016, Samoil, Dagenais et al. 2018).

Using exponential amplification via quantitative reverse transcription polymerase chain reaction of microRNAs (miRNAs) the presence of schistosomal miRNAs was demonstrated in the EV fraction harvested from sera of human patients infected with schistosomes (Meningher, Lerman et al. 2016). This shows that schistosomes release EVs not only during *in vitro* incubations but also when living in the bloodstream of the host. However, the effect of an *S. mansoni* infection on the composition of circulating EVs in blood of the host has not been investigated. It is not even known yet whether schistosomal proteins and lipids can be detected at all in EVs isolated from blood of a host infected with schistosomes, as amplification is not possible in those analyses in contrast to the analysis of miRNAs. Therefore, in this study we examined the EVs present in blood plasma of hamsters infected with *S. mansoni* and compared those with the EVs present in uninfected hamsters.

In our analysis of isolated EVs from plasma of *S. mansoni* infected hamsters no schistosome-specific proteins or lipids were found. Apparently, the presence in blood of the large number of EVs produced by the host (Arraud, Linares et al. 2014) completely overshadows in the proteome and lipidome analysis the presence of EVs produced by the parasite. This observation correlates with the fact that despite many attempts so far no specific protein nor lipid markers of cancer-derived exosomes have been detected in plasma derived EVs, except from melanoma (Jablonska, Pietrowska et al. 2019). Although no schistosome-specific compounds were detected in EVs circulating in blood of infected hamsters, the *S. mansoni* infection resulted in an altered plasma EV profile in the host, as a consistent difference in the EV protein and lipid composition was observed between infected and non-infected hamsters (Fig. 2, 3).

In our study we identified a relatively small number of proteins in the EV fractions compared to other studies (Gualdrón-López, Flannery et al. 2018, Karimi, Cvjetkovic et al. 2018). Compared to these studies many aspects of the protein identification method were similar to those used in our study, but two differences might explain the lower number of identified

proteins in our study. First, the lower number of identified proteins could be caused by a difference in the quality of the genome information available of the golden hamster (*Mesocricetus auratus*) compared to that of humans and mice, as the golden hamster genome has not been assembled and curated as thoroughly as the genomes of mice and humans. These differences could have limited the identification of EV proteins in our study compared to studies performed on humans or mice. In addition, in our study the proteins in the EV fraction were separated by SDS-PAGE prior to trypsin digestion, whereas the other studies digested the proteins directly. For samples with a low protein concentration the SDS-PAGE method might be less efficient as reduced protein digestion and peptide diffusion out the gel pieces could result in a lower peptide yield.

Lipid analysis of the isolated EV fractions demonstrated that the EVs derived from plasma of *S. mansoni* infected hamsters contained relatively more PS and SM and less PI and PG compared to those of control hamsters. Phospholipid classes PS and SM are both enriched in plasma membranes (Andreyev, Fahy et al. 2010, Leventis and Grinstein 2010) and the increased contribution of these two classes to the EVs of infected hamsters could reflect a shift from endosome- to plasma-membrane derived EVs, *i.e.* from exosomes to microvesicles. We also observed a shift in molecular species within the PC and PE classes. PC and PE are the two major phospholipid classes and contribute to all organelle membranes, albeit with different molecular species. In addition, a moderate decrease in lyso-PC content was observed in EVs derived from infected hamsters compared to control hamsters. However, lysophospholipids constitute only a minor, highly dynamic phospholipid fraction and are readily reacylated to their diacyl forms or further degraded to water soluble building blocks. Taken together, the lipidomic data clearly demonstrate a shift of systemic EV composition in response to the schistosome infection.

The most abundant proteins exclusively present (Table 1), or enriched in EVs of infected hamsters, were fibronectin, fibrinogen, and collagen. These proteins play a significant role in the formation of liver fibrosis, which is known to be induced by the deposition of *S. mansoni* eggs (Olveda, Olveda et al. 2014). Both fibronectin and fibrinogen were reported to be exclusively present or significantly increased in EV preparations of plasma from patients suffering from various liver diseases (Povero, Eguchi et al. 2014, Arbelaiz, Azkargorta et al. 2017). These results suggest that a substantial part of the circulating EVs in plasma of the *S. mansoni* infected host originate from the liver, probably as a response to tissue damage caused by egg deposition by the parasite.

Furthermore, the increased abundance of fibrinogen and haptoglobin could also result

from an inflammatory response induced by the *S. mansoni* infection, because both proteins are so-called acute phase proteins. The exclusive detection of fibroleukin (FGL2) in EVs of infected animals further supports the inflammatory response as a cause of the changed EV proteome, as FGL2 secreted by T-cells is an important immune regulator of both innate and adaptive responses (Marazzi, Blum et al. 1998).

Of the other identified proteins enriched, or exclusively found in EVs derived from *S. mansoni* infected hamsters, several function in hemostasis (fibronectin, fibrinogen gamma chain, alpha-2 antiplasmin, thrombospondin-1 and Von Willebrand Factor). Hemostasis is affected by an *S. mansoni* infection, as schistosomes excrete and/or expose several factors that interfere with primary and/or secondary hemostasis as well as with fibrinolysis (Mebius, van Genderen et al. 2013). In addition, in hepatosplenic schistosomiasis many hemostatic abnormalities occur, which include impaired coagulation, lower levels of platelets, coagulation and anticoagulation factors, as well as increased thrombin generation, fibrinolysis and Von Willebrand Factor levels (Tanabe 2003, Da'dara, de Laforcade et al. 2016, Mebius, Op Heij et al. 2018).

The coexistence of elevated thrombin and plasmin generation suggests a steady state of low-grade disseminated intravascular coagulation in hepatosplenic schistosomiasis, in which enhanced fibrin formation is coupled to enhanced fibrinolysis (Tanabe 2003). Since platelets are a major source of plasma EVs (Arraud, Linares et al. 2014), parasite induced enhanced coagulation and thrombocytopenia is expected to result in an increase in platelet-derived EVs in *S. mansoni* infected hamsters. Indeed a substantial number of proteins was identified in EVs of *S. mansoni* infected hamsters, that have previously been reported as proteins present in EVs formed by platelets (thrombospondin-1, fibrinogen, albumin, gelsolin and actin) (Milioli, Ibanez-Vea et al. 2015).

Also a relatively high number of complement system related proteins were identified in this study. Complement factor B and the C4b-binding protein, which has an inhibitory function, were exclusively detected, or enriched in EVs derived from *S. mansoni* infected hamsters, respectively. On the other hand complement factor C3, C4 and C1r were present in lesser amounts in EVs of infected hamsters compared to control hamsters. These results suggest that the complement system is activated by the *S. mansoni* infection, which fits with the earlier reported complement activation on the surface of adult schistosomes (Wilson 2012).

Finally, the detection of the specific erythrocyte plasma membrane proteins spectrin, ankyrin-1 and band 3 protein only in EVs isolated from infected animals suggests an

increase in erythrocyte-derived EVs during schistosomiasis. Schistosomiasis is often associated with anemia, for which several causes have been postulated including malnutrition, blood loss and restricted erythropoiesis due to inflammation (Nemeth, Rivera et al. 2004, Colley, Bustinduy et al. 2014). Thus, the increased formation of erythrocyte-derived EVs in *S. mansoni* infected animals suggests that during schistosomiasis more lysis of erythrocytes occurs and more improper erythrocytes are circulating, as EVs are thought to be shed by erythrocytes upon apoptosis or activation of cells by oxidative injury, endotoxin, cytokines, complement or high shear stress (Westerman and Porter 2016).

In conclusion, our results demonstrate that although *S. mansoni* eggs, schistosomula and adults are known to produce EVs, their relative contribution to the entire EV population circulating in plasma of their host is limited as no parasite-specific proteins nor lipids could be identified in EVs derived from plasma of infected hosts despite a relatively high infection dose. However, the *S. mansoni* infection does affect the EV composition in plasma of the host. Further research is necessary to determine the clinical relevance of these changes, and whether these changes are the result of the pathogenic effects of the infection or whether they have a function in the host-parasite interaction, or both.

Declaration of Competing Interest

None.

REFERENCES

- Andreyev, A. Y., E. Fahy, et al. (2010). "Subcellular organelle lipidomics in TLR-4-activated macrophages." *Journal of Lipid Research* **51**(9): 2785-2797.
- Arbelaiz, A., M. Azkargorta, et al. (2017). "Serum extracellular vesicles contain protein biomarkers for primary sclerosing cholangitis and cholangiocarcinoma." *Hepatology* **66**(4): 1125-1143.
- Arraud, N., R. Linares, S. Tan, C. Gounou, J. M. Pasquet, S. Mornet and A. R. Brisson (2014). "Extracellular vesicles from blood plasma: determination of their morphology, size, phenotype and concentration." *Journal of Thrombosis and Haemostasis* **12**(5): 614-627.
- Böing, A. N., E. van der Pol, A. E. Grootemaat, F. A. W. Coumans, A. Sturk and R. Nieuwland (2014). "Single-step isolation of extracellular vesicles by size-exclusion chromatography." *Journal of extracellular vesicles* **3**: 10.3402/jev.v3i403.23430.
- Cai, P., G. N. Gobert and D. P. McManus (2016). "MicroRNAs in Parasitic Helminthiasis: Current Status and Future Perspectives." *Trends in Parasitology* **32**(1): 71-86.
- Colley, D. G., A. L. Bustinduy, E. Secor and C. H. King (2014). "Human schistosomiasis." *Lancet* **383**(9936): 2253-2264.
- Colombo, M., G. Raposo and C. Théry (2014). "Biogenesis, Secretion, and Intercellular Interactions of Exosomes and Other Extracellular Vesicles." *Annual Review of Cell and Developmental Biology* **30**(1): 255-289.
- Costain, A. H., A. S. MacDonald and H. H. Smits (2018). "Schistosome egg migration: mechanisms, pathogenesis and host immune responses." *Frontiers in immunology* **9**: 3042.
- Da'dara, A. A., A. M. de Laforcade and P. J. Skelly (2016). "The impact of schistosomes and schistosomiasis on murine blood coagulation and fibrinolysis as determined by thromboelastography (TEG)." *Journal of Thrombosis and Thrombolysis* **41**(4): 671-677.
- de Menezes-Neto, A., M. J. Saez, I. Lozano-Ramos, J. Segui-Barber, L. Martin-Jaular, J. M. Ullate, C. Fernandez-Becerra, F. E. Borrás and H. A. Del Portillo (2015). "Size-exclusion chromatography as a stand-alone methodology identifies novel markers in mass spectrometry analyses of plasma-derived vesicles from healthy individuals." *Journal of Extracellular Vesicles* **4**: 27378.
- Doyle, L. M. and M. Z. Wang (2019). "Overview of Extracellular Vesicles, Their Origin, Composition, Purpose, and Methods for Exosome Isolation and Analysis." *Cells* **8**(7): 727.
- Dunne, D. W. and A. Cooke (2005). "A worm's eye view of the immune system: consequences for evolution of human autoimmune disease." *Nature Reviews Immunology* **5**: 420-426.
- Gill, S., P. Forterre and R. Catchpole (2018). "Extracellular membrane vesicles in the three domains of life and beyond." *FEMS microbiology reviews*.
- Gualdrón-López, M., E. L. Flannery, et al. (2018). "Characterization of *Plasmodium vivax* proteins in plasma-derived exosomes from malaria-infected liver-chimeric humanized mice." *Frontiers in Microbiology* **9**: 1271.
- Highton, P. J., N. Martin, A. C. Smith, J. O. Burton and N. C. Bishop (2018). "Microparticles and Exercise in Clinical Populations." *Exercise immunology review* **24**: 46-58.
- Jablonska, J., M. Pietrowska, S. Ludwig, S. Lang and B. K. Thakur (2019). "Challenges in the Isolation and Proteomic Analysis of Cancer Exosomes—Implications for Translational Research." *Proteomes* **7**(2): 22-33.
- Käll, L., J. D. Storey, M. J. MacCoss and W. S. Noble (2007). "Assigning significance to peptides identified by tandem mass spectrometry using decoy databases." *Journal of proteome research* **7**(01): 29-34.
- Karimi, N., A. Cvjetkovic, S. C. Jang, R. Crescitelli, M. A. H. Feizi, R. Nieuwland, J. Lötvald and C. Lässer (2018). "Detailed analysis of the plasma extracellular vesicle proteome after separation from lipoproteins." *Cellular and Molecular Life Sciences* **75**(15): 2873-2886.
- Kuipers, M. E., C. H. Hokke, H. H. Smits and E. N. M. Nolte (2018). "Pathogen-Derived Extracellular Vesicle-Associated Molecules That Affect the Host Immune System: An Overview." *Frontiers in Microbiology* **9**:2182.
- Leventis, P. A. and S. Grinstein (2010). "The distribution and function of phosphatidylserine in cellular membranes." *Annual review of biophysics* **39**: 407-427.
- Liu, J., L. Zhu, J. Wang, L. Qiu, Y. Chen, R. E. Davis and G. Cheng (2019). "Schistosoma japonicum extracellular vesicle miRNA cargo regulates host macrophage functions facilitating parasitism." *Plos Pathogens* **15**(6): e1007817.
- Marazzi, S., S. Blum, R. Hartmann, D. Gundersen, M. Schreyer, S. Argraves, V. von Fliedner, R. Pytela and C. Rüegg (1998). "Characterization of human fibroleukin, a fibrinogen-like protein secreted by T lymphocytes." *The Journal of Immunology* **161**(1): 138-147.
- Mathieu, M., L. Martin-Jaular, G. Lavieu and C. Théry (2019). "Specificities of secretion and uptake of exosomes and other extracellular vesicles for cell-to-cell communication." *Nature cell biology* **21**(1): 9-17.
- McManus, D. P., D. W. Dunne, M. Sacko, J. Utzinger, B. J. Vennervald and X. N. Zhou (2018). "Schistosomiasis." *Nature Review Disease Primers* **4**(1): 13.
- Mebius, M. M., J. M. J. Op Heij, A. G. M. Tielens, P. G. de Groot, R. T. Urbanus and J. J. van Hellemond (2018). "Fibrinogen and fibrin are novel substrates for *Fasciola hepatica* cathepsin L peptidases." *Molecular and Biochemical Parasitology* **221**: 10-13.
- Mebius, M. M., P. J. J. van Genderen, R. T. Urbanus, A. G. M. Tielens, P. G. de Groot and J. J. van Hellemond (2013). "Interference with the host haemostatic system by schistosomes." *Plos Pathogens* **9**(12): e1003781.
- Meningher, T., G. Lerman, N. Regev-Rudzki, D. Gold, I. Z. Ben-Dov, Y. Sidi, D. Avni and E. Schwartz (2016). "Schistosomal MicroRNAs Isolated From Extracellular Vesicles in Sera of Infected Patients: A New Tool for Diagnosis and Follow-up of Human Schistosomiasis." *The Journal of Infectious Diseases* **215**(3): 378-386.
- Milioli, M., M. Ibanez-Vea, S. Sidoli, G. Palmisano, M. Careri and M. R. Larsen (2015). "Quantitative proteomics analysis of platelet-derived microparticles reveals distinct protein signatures when stimulated by different physiological agonists." *Journal of Proteomics* **121**: 56-66.
- Nemeth, E., S. Rivera, V. Gabayan, C. Keller, S. Taudorf, B. K. Pedersen and T. Ganz (2004). "IL-6 mediates hypoferremia of inflammation by inducing the synthesis of the iron regulatory hormone hepcidin." *The Journal of clinical investigation* **113**(9): 1271-1276.
- Nowacki, F. C., M. T. Swain, et al. (2015). "Protein and small non-coding RNA-enriched extracellular vesicles are released by the pathogenic blood fluke *Schistosoma mansoni*." *Journal of extracellular vesicles* **4**: 28665.
- Olveda, D. U., R. M. Olveda, et al. (2014). "The chronic enteropathogenic disease schistosomiasis." *International*

Journal of Infectious Diseases **28**: 193-203.

- Pathan, M., S. Keerthikumar, et al. (2017). "A novel community driven software for functional enrichment analysis of extracellular vesicles data." Journal of Extracellular Vesicles **6**(1): 2597-2601.
- Povero, D., A. Eguchi, H. Li, C. D. Johnson, B. G. Papouchado, A. Wree, K. Messer and A. E. Feldstein (2014). "Circulating extracellular vesicles with specific proteome and liver microRNAs are potential biomarkers for liver injury in experimental fatty liver disease." PLOS ONE **9**(12): e113651.
- Retra, K., S. deWalick, M. Schmitz, M. Yazdanbakhsh, A. G. M. Tielens, J. F. H. M. Brouwers and J. J. van Hellemond (2015). "The tegumental surface membranes of *Schistosoma mansoni* are enriched in parasite-specific phospholipid species." International journal for parasitology **45**(9-10): 629-636.
- Samoil, V., M. Dagenais, V. Ganapathy, J. Aldridge, A. Glebov, A. Jardim and P. Ribeiro (2018). "Vesicle-based secretion in schistosomes: Analysis of protein and microRNA (miRNA) content of exosome-like vesicles derived from *Schistosoma mansoni*." Scientific reports **8**: 3286.
- Schorey, J. S., Y. Cheng, P. P. Singh and V. L. Smith (2015). "Exosomes and other extracellular vesicles in host-pathogen interactions." EMBO Reports **16**(1): 24-43.
- Shevchenko, A., H. Tomas, J. Havli, J. V. Olsen and M. Mann (2006). "In-gel digestion for mass spectrometric characterization of proteins and proteomes." Nature protocols **1**(6): 2856-2860.
- Smith, C. A., E. J. Want, G. O'Maille, R. Abagyan and G. Siuzdak (2006). "XCMS: processing mass spectrometry data for metabolite profiling using nonlinear peak alignment, matching, and identification." Analytical chemistry **78**(3): 779-787.
- Sotillo, J., M. Pearson, J. Potriquet, L. Becker, D. Pickering, J. Mulvenna and A. Loukas (2016). "Extracellular vesicles secreted by *Schistosoma mansoni* contain protein vaccine candidates." International journal for parasitology **46**(1): 1-5.
- Spivak, M., J. Weston, L. Bottou, L. Käll and W. S. Noble (2009). "Improvements to the percolator algorithm for Peptide identification from shotgun proteomics data sets." Journal of proteome research **8**(7): 3737-3745.
- Stacklies, W., H. Redestig, M. Scholz, D. Walther and J. Selbig (2007). "pcaMethods—a bioconductor package providing PCA methods for incomplete data." Bioinformatics **23**(9): 1164-1167.
- Tanabe, M. (2003). "Haemostatic abnormalities in hepatosplenic schistosomiasis mansoni." Parasitology International **52**(4): 351-359.
- Théry, C., K. W. Witwer, et al. (2018). "Minimal information for studies of extracellular vesicles 2018 (MISEV2018): a position statement of the International Society for Extracellular Vesicles and update of the MISEV2014 guidelines." Journal of extracellular vesicles **7**(1): 1535750.
- Wang, L., Z. Li, J. Shen, Z. Liu, J. Liang, X. Wu, X. Sun and Z. Wu (2015). "Exosome-like vesicles derived by *Schistosoma japonicum* adult worms mediates M1 type immune-activity of macrophage." Parasitology Research **114**(5): 1865-1873.
- Westerman, M. and J. B. Porter (2016). "Red blood cell-derived microparticles: an overview." Blood Cells, Molecules, and Diseases **59**: 134-139.
- Wilson, R. A. (2012). "Virulence factors of schistosomes." Microbes and Infection **14**(15): 1442-1450.
- Yanez-Mo, M., P. R. M. Siljander, et al. (2015). "Biological properties of extracellular vesicles and their

physiological functions." Journal of extracellular vesicles **4**: 27066.

- Zhu, L., J. Liu, J. Dao, K. Lu, H. Li, H. Gu, J. Liu, X. Feng and G. Cheng (2016). "Molecular characterization of *S. japonicum* exosome-like vesicles reveals their regulatory roles in parasite-host interactions." Scientific reports **6**:25885.



CHAPTER 6

Lipids are the preferred substrate
of the protist *Naegleria gruberi*,
relative of a human brain pathogen

Michiel L. Bexkens,¹ Verena Zimorski,² Maarten J. Sarink,¹ Hans Wienk,³ Jos F. Brouwers,⁴
Johan F. De Jonckheere,^{5,6} William F. Martin,² Fred R. Opperdoes,⁶ Jaap J. van Hellemond,¹
and Aloysius G.M. Tielens^{1,4}

¹Department of Medical Microbiology and Infectious Diseases, Erasmus MC, University Medical Center
Rotterdam, Rotterdam, the Netherlands

²Institute of Molecular Evolution, Heinrich-Heine-University, 40225 Düsseldorf, Germany

³NMR Spectroscopy, Bijvoet Center for Biomolecular Research, Department of Chemistry, Faculty of Science,
Utrecht University, Utrecht, the Netherlands

⁴Department of Biochemistry and Cell Biology, Faculty of Veterinary Medicine, Utrecht University, Utrecht,
the Netherlands

⁵Scientific Institute of Public Health, Brussels, Belgium

⁶de Duve Institute, Université catholique de Louvain, Brussels, Belgium

ABSTRACT

Naegleria gruberi is a free-living non-pathogenic amoeboflagellate and relative of *Naegleria fowleri*, a deadly pathogen causing primary amoebic meningoencephalitis (PAM). A genomic analysis of *N. gruberi* exists, but physiological evidence for its core energy metabolism or in vivo growth substrates is lacking. Here, we show that *N. gruberi* trophozoites need oxygen for normal functioning and growth and that they shun both glucose and amino acids as growth substrates. Trophozoite growth depends mainly upon lipid oxidation via a mitochondrial branched respiratory chain, both ends of which require oxygen as final electron acceptor.

Growing *N. gruberi* trophozoites thus have a strictly aerobic energy metabolism with a marked substrate preference for the oxidation of fatty acids. Analyses of *N. fowleri* genome data and comparison with those of *N. gruberi* indicate that *N. fowleri* has the same type of metabolism. Specialization to oxygen-dependent lipid breakdown represents an additional metabolic strategy in protists. We show that *N. gruberi* amoebae live preferably on lipids, for which they need oxygen, a lifestyle largely unknown among protists. This challenges existing views about its energy metabolism, with implications for treatment of its pathogenic relative, *N. fowleri*, the brain-eating agent of primary amoebic meningoencephalitis (PAM).

Keywords

Naegleria, fatty acid oxidation, aerobic energy metabolism, electron-transport chain, alternative oxidase, PAM

INTRODUCTION

Members of the genus *Naegleria* are cosmopolitan protists (De Jonckheere, 2002) that dwell in fresh water. The amoebic phagotrophic stage, or trophozoite, grows by division, feeds mainly on bacteria, and occupies habitats rich in organic matter such as mud, soil, rivers, lakes, and swamps (Fulton, 1970). Trophozoites can transform into a non-dividing flagellate with two flagella, but can also form dormant cysts, and can be cultured on non-bacterial food sources ranging from mammalian cell debris to non-particulate axenic culture media. By far the best known member of the genus is the thermotolerant amoeboflagellate, *Naegleria fowleri*, which causes primary amoebic meningoencephalitis (PAM) in humans, a severe and aggressive infection that usually leads to death. Cases of PAM are reported world-wide and are associated with swimming in warm waters, from which the pathogen gains access to the brain via the nasal mucosa (De Jonckheere, 2002). Trophozoites of *N. gruberi*, a nonpathogenic congener of *N. fowleri*, can be grown continuously in chemically defined media (Fulton et al., 1984). *N. gruberi* was earlier studied mainly as a model for transformation because the amoebae transform easily into flagellates but is nowadays also used as a model to study its pathogenic relative, *N. fowleri*. Pathways of energy metabolism (core ATP synthesis) in *Naegleria* are of interest as they might harbor targets for treatment of the pathogen. In 2010, the genome of the axenically cultured *N. gruberi* strain NEG-M was reported (Fritz-Laylin et al., 2010). The bioinformatic analyses of the genome indicated a capacity for both aerobic respiration and anaerobic metabolism with concomitant hydrogen production (Fritz-Laylin et al., 2010; Ginger et al., 2010; Oppendoes et al., 2011) and that *Naegleria*'s genome encodes features of an elaborate and sophisticated anaerobic metabolism (Fritz-Laylin et al., 2010). However, substrate and end-product studies are still lacking. Here, we investigate the ability to grow with and without oxygen of *N. gruberi* strain NEG-M and of an independent *N. gruberi* strain that was always fed with bacteria and was never grown in rich culture media. In addition, we studied the energy metabolic capacities of *N. gruberi* strain NEG-M mitochondria, its surprising spectrum of growth substrate preferences, and the pathways of ATP-production that it employs.

RESULTS AND DISCUSSION

To test the metabolic flexibility of *N. gruberi* and—based on its genome sequence (Fritz-Laylin et al., 2010; Ginger et al., 2010; Oppendoes et al., 2011)—its anticipated capacity to switch between aerobic and anaerobic modes of metabolism, we cultured the axenic *N. gruberi* strain NEG-M under various conditions (see STAR Methods).

Under aerobic conditions the oxygen consumption of *N. gruberi* NEG-M was avid, 2.5–10 nmol O₂ per min per 10⁶ amoebae (Figure 1A). Trophozoites did not grow under anaerobic conditions; they became moribund and stopped multiplying in the absence of oxygen (Figure S1) or when oxygen consumption was inhibited by blocking their electron transport chain (Figure 1). Of course, cells that are cultured for years in rich culture media can lose metabolic capacities. Therefore, we also investigated a wild-type strain of *N. gruberi* never grown in rich culture media (see below). This strain also stopped growing without oxygen, which shows that *N. gruberi* trophozoites need oxygen for normal functioning and growth and cannot rapidly switch between aerobic and anaerobic modes of metabolism. Genome analysis led to the suggestion that *N. gruberi* could use its putative metabolic flexibility during intermittent hypoxia in their environment (Fritz-Laylin et al., 2010).

Addition of cyanide inhibited respiration by 80% (Figure 1A, trace A), showing that mitochondrial complex IV (cytochrome *c* oxidase) was involved in aerobic growth, but also indicating that another route of oxygen consumption was operating as well. Subsequent addition of salicylhydroxamic acid (SHAM), an inhibitor of mitochondrial cyanide-insensitive plant-like alternative oxidases (AOX), resulted in a further inhibition of oxygen consumption (94%). When SHAM was added before cyanide, 14% inhibition of oxygen consumption was observed, and subsequent addition of cyanide resulted again in almost complete (94%) inhibition of the oxygen consumption (Figure 1A, trace B). SHAM inhibition indicates that *N. gruberi* trophozoites use a plant-like AOX that transfers electrons from reduced ubiquinone to oxygen involving a truly branched electron transport chain (Opperdoes et al., 2011). The observed difference in degree of inhibition by cyanide and SHAM shows that complexes III and IV have a higher capacity relative to the AOX branch. Addition of cyanide or SHAM to *N. gruberi* furthermore resulted in changes in morphology and a remarkable loss of pseudopodial movement (Videos S1, S2, and S3). Normal *N. gruberi* cell functions thus require both branches of the respiratory chain (see Figure 2).

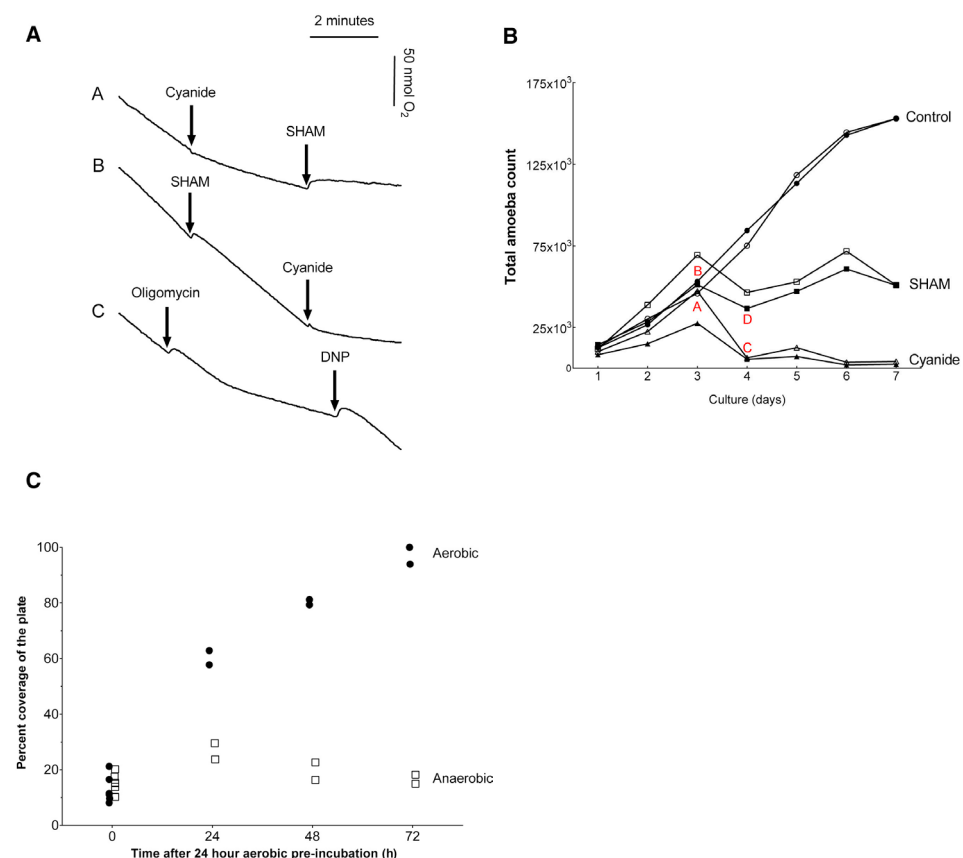


Figure 1. Oxygen Consumption and Growth under Aerobic and Anaerobic Conditions by *N. gruberi* Trophozoites (A) Oxygen consumption of *N. gruberi* NEG-M trophozoites was measured with a Clark-type electrode. SHAM (final concentration 1.5 mM), KCN (final concentration 1 mM), oligomycin (final concentration 5 mM), and dinitrophenol (DNP, final concentration 0.1 mM) were added at the indicated time points. See also Videos S1 and S2. (B) Growth curves of *N. gruberi* NEG-M trophozoites were measured in the presence or absence of respiratory chain inhibitors. Amoebae were cultured in PYNFH for 7 days. KCN (D, three filled boxes) or SHAM (open box, three filled boxes) was added on day 3, and controls (open circles, filled circles) were treated under identical conditions. Duplicates for each growth condition are shown (open and closed symbols). Representative images of the trophozoites under the various culture conditions marked here in Figure 1B with letters A–D are shown in the Supplemental Information (see Figure S2A–S2D; Video S3). (C) Growth of an *N. gruberi* field isolate was measured on plates covered with *E. coli* during incubations under aerobic (filled circle) or anaerobic (open box) conditions. Twelve plates were seeded with equal amounts of amoebae (as cysts), which were allowed to excyst for 24 hr under aerobic conditions at 37°C prior to the start of the experiment. After this aerobic pre-incubation, the plates were then further incubated (starting at *t* = 0) either aerobically or anaerobically for 24, 48, or 72 hr. The area covered by amoebae was recorded at the indicated time points.

To test cell viability under long-term respiratory inhibition, we cultured *N. gruberi* NEG-M in the presence of cyanide or SHAM. The presence of cyanide resulted in a reduction of viable trophozoites by about 90% within 24 hr (Figures 1B, S2A, and S2C),

while cells treated with SHAM grew slower and merely contained fewer intracellular vacuoles (Figures 1B, S2B, and S2D). This shows that inhibition of the AOX is less harmful to *Naegleria* than inhibition of complex IV, which inhibits ATP synthesis, while electron overflow via AOX is necessary for *Naegleria* vitality despite having no role in ATP formation. The observed direct decrease in movement and ultimate decline of the trophozoites in the presence of cyanide, which blocks the complex III and IV branch of their electron transport chain, indicates that the mitochondrial proton gradient is the cell's main source of ATP production. This is in agreement both with earlier observations that oxygen is essential for *N. gruberi* growth (Pittam, 1963; Weik and John, 1977b) and with our observation that oligomycin, an inhibitor of ATP synthase, strongly inhibited oxygen consumption (60%), which is again increased after addition of uncoupler (Figure 1A, trace C). Taken together, our oxygen consumption measurements and culture experiments show that *N. gruberi* trophozoites generate the bulk of their ATP via oxidative phosphorylation and that *N. gruberi* trophozoites require oxygen for homeostasis and growth, while providing no evidence for anaerobic energy metabolism.

Furthermore, we analyzed the quinone content of *N. gruberi* and demonstrated that the NEG-M as well as the wild-type strain contain exclusively ubiquinone and no rhodoquinone (Figure S3). Ubiquinone is used by aerobic mitochondria to transfer electrons to complex III, while rhodoquinone is used to donate electrons to a membrane-bound fumarate reductase. This reduction of fumarate to succinate is an essential reaction in malate dismutation, which is a true hallmark of the anaerobically functioning mitochondria of many eukaryotes (Tielens et al., 2002; van Hellemond et al., 1995).

To exclude the possibility that the observed strictly aerobic energy metabolism of the laboratory strain of *N. gruberi* is the result of culture-dependent metabolic losses, we also investigated the oxygen dependence of a wild-type strain that was more recently isolated from river sediment and was never grown in rich culture media, but was always fed with bacteria (see STAR Methods). For our aerobic-anaerobic growth experiment, the trophozoites of this field isolate were as ever cultured on plates covered with *Escherichia coli*, as *N. gruberi* field strains do not grow readily in liquid medium. Under aerobic conditions, the plates were fully covered with amoebae after 3 days, while under anaerobic conditions no further growth was observed after the initial 24-hr growth during an aerobic incubation (Figure 1C). Thus, a field isolate of *N. gruberi*, never grown in rich culture media, is also not able to grow in the absence of oxygen. This shows that the observed obligate aerobic growth and homeostasis of the NEG-M strain do not result from loss of anaerobic capacities during decades of axenic culturing in rich media.

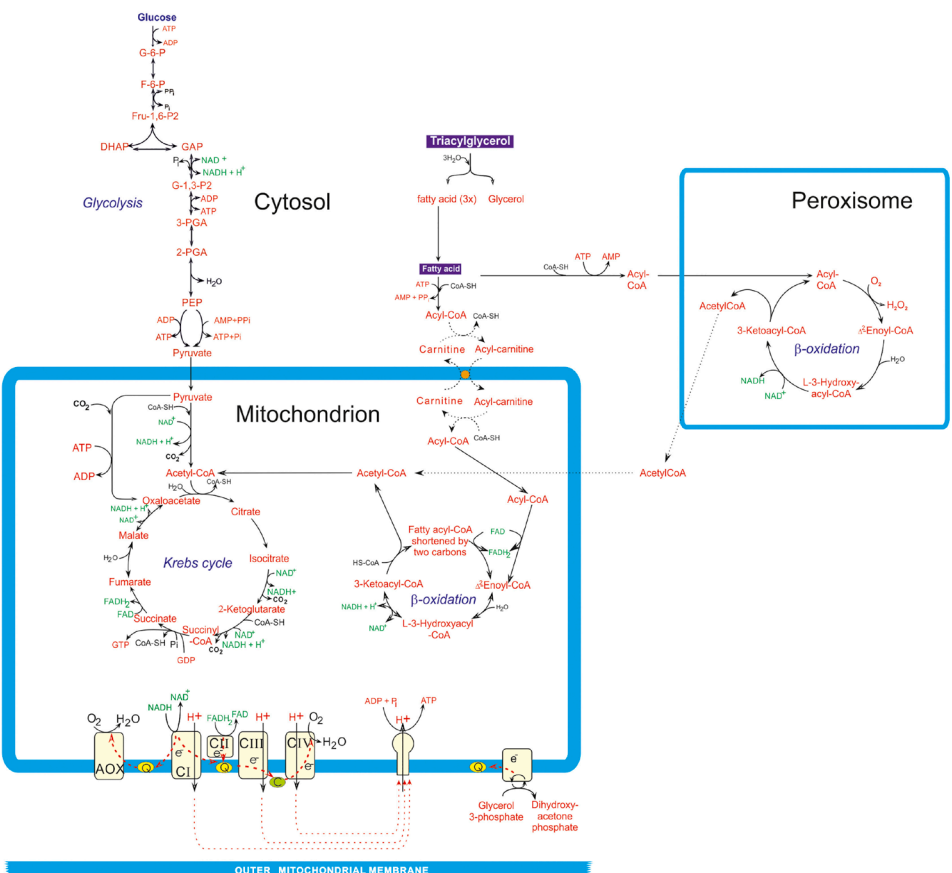


Figure 2. Main pathways of energy metabolism in *Naegleria gruberi* trophozoites *Naegleria* is able to oxidize fatty acids by a process of beta-oxidation, involving both peroxisomes and mitochondria, although it is not yet clear how the chain lengths of the fatty acids are distributed over the two organelle types. It is also unknown yet how the fatty acids enter the mitochondria as up to now no carnitine acyl-CoA transferase genes have been detected in its genome. AOX, alternative oxidase; CI–IV, complexes I–IV of the respiratory chain; DHAP, dihydroxyacetone- phosphate; FAD, flavine adenine dinucleotide; FADH₂, reduced FAD; F-6-P, fructose 6-phosphate; Fru-1,6-P₂, fructose 1,6-bisphosphate; GAP, glyceraldehyde 3-phosphate; G-1,3-P₂, glycerate 1,3-bisphosphate; G-6-P, glucose 6-phosphate; 3-PGA, glycerate 3-phosphate; 2-PGA, glycerate 2-phosphate; GTP, guanosine-triphosphate; GDP, guanosine-diphosphate; PEP, phosphoenolpyruvate. Dashed lines indicate uncertainties on the actual processes. See also Figure S3 and Tables S1 and S2.

An oxygen-consuming respiratory chain does not necessarily imply the presence of canonical Krebs cycle activity. African trypanosomes, for example, are obligate aerobes with a branched respiratory chain comparable to that of *N. gruberi*, but, despite their O₂ dependence, procyclics of *Trypanosoma brucei* feed on glucose and produce acetate and succinate as end products, rather than CO₂ and H₂O (Besteiro et al., 2005; van

Weelden et al., 2005). The existence in the *Naegleria* genome (Fritz-Laylin et al., 2010) of some enzymes considered to be typically used by eukaryotic anaerobes (Müller et al., 2012; Tielens et al., 2002), but also present in many O₂-producing algae (Atteia et al., 2013), is interesting from an evolutionary standpoint, but only the analysis of end products of energy metabolism can uncover how cells actually grow.

To investigate the energy metabolism of *N. gruberi*, trophozoites were incubated in the presence of [6-¹⁴C]-labeled glucose, a substrate that generates labeled ¹⁴CO₂ only if it is degraded via the Krebs cycle. These incubations released ¹⁴CO₂ (Table 1), while no significant amounts of any other labeled end products could be detected by anion-exchange chromatography (data not shown), demonstrating that the *N. gruberi* trophozoites degraded glucose via Krebs cycle activity without the help of fermentative pathways. The earlier genome annotations indicated already the capacity for aerobic degradation of substrates via the Krebs cycle as genes for all its enzymes are present (Fritz-Laylin et al., 2010; Ginger et al., 2010; Oppendoes et al., 2011).

Table 1. Analysis of Carbon Dioxide Produced from ¹⁴C-Labeled Substrates by *N. gruberi* NEG-M Trophozoites Incubated in PYNFH Medium, or PBS, Containing One of the Indicated ¹⁴C-Labeled Substrates

Labeled Substrates	Production of CO ₂ (nmol per Hr per 10 ⁶ Amoebae)		Calculated Production of ATP (nmol per Hr per 10 ⁶ Amoebae)	
	PYNFH	PBS	PYNFH	PBS
[6- ¹⁴ C]-glucose	7.1 ± 0.9 ^a	0.2 ^b	35 ± 5	1.0
[1- ¹⁴ C]-octanoic acid	35.9 ± 13.2 ^a	45.9 ± 18.8 ^a	224 ± 9	287 ± 118
[1- ¹⁴ C]-oleic acid	43.0 ± 7.6 ^a	not done	287 ± 20	not done
[1,2- ¹⁴ C]-acetic acid	372.1 ^c	96.2 ^d	1,674	433
¹⁴ C-labeled amino acids ^e	ND	not done	–	–

All values were corrected for blank incubations and are shown as mean ± SD. The amount of ATP produced was calculated from the measured production of carbon dioxide produced from the various labeled substrates. ND, not detectable.

^aAll values represent the mean and SD of at least 3 independent experiments.

^bMean of two independent experiments (0.19 and 0.22).

^cMean of two independent experiments (304.6 and 439.5).

^dMean of two independent experiments (142.2 and 50.2).

^e¹⁴C-labeled isoleucine, valine, lysine, threonine, or serine were added to PYNFH medium.

However, the production of CO₂ from glucose (7 nmol per hr per 10⁶ amoebae) accounted for only 1%–5% of the overall O₂ consumption, which was around 150–600 nmol per hr per 10⁶ amoebae (Figure 1A). Clearly, oxygen was mainly consumed by oxidation of substrates other than glucose present in the very rich PYNFH culture medium because

in standard aerobic degradation of glucose to carbon dioxide, O₂ consumption, and CO₂ production occur in 1:1 stoichiometry (glucose + 6 O₂ → 6 CO₂ + 6 H₂O).

To determine whether removal of alternative substrates could stimulate glucose consumption, we incubated the trophozoites in PBS with 5 mM glucose as the sole carbon source. Under these conditions, CO₂ production was even lower than in the rich PYNFH medium (Table 1). To see whether *N. gruberi* degrades proteins present in PYNFH medium for amino acid oxidation, the full set of enzymes for which is present in the *N. gruberi* genome (Oppendoes et al., 2011), we incubated trophozoites in PYNFH medium supplemented with one of the following ¹⁴C-labeled amino acids: isoleucine, valine, lysine, threonine, or serine. After 24 hr, no ¹⁴CO₂ release at all could be detected in any of these incubations (Table 1). Thus, amino acids are also not the amoeba's growth substrate. Incubations in the presence of ¹⁴C-labeled oleic acid (C_{18:1}) or octanoic acid (C_{8:0}) resulted in the production of ¹⁴CO₂ in amounts 5- to 6-fold higher than during the incubations with labeled glucose (Table 1). Analysis of the incubation medium by anion exchange chromatography revealed no significant amounts of metabolic end products other than CO₂. We also tested ¹⁴C-labeled acetate as a direct precursor for Krebs cycle activity. Acetate was rapidly degraded to ¹⁴CO₂ (Table 1), which confirms the activity of the Krebs cycle. The combined data indicate that *Naegleria* trophozoites prefer fatty acids to both glucose and amino acids as growth substrates. They oxidize fatty acids and degrade the resulting acetyl-CoA units via the Krebs cycle. In many eukaryotes, carbohydrates and most amino acids can be degraded by anaerobic fermentations to end products such as lactate, acetate, propionate, and succinate (Müller et al., 2012). Fatty acids are, however, non-fermentable substrates, and their oxidation requires the mitochondrial respiratory chain.

To more thoroughly exclude the possible use of other pathways and to independently confirm, via a different analytical technique, the use of fatty acids by *N. gruberi*, we incubated the NEG-M strain in the presence of ¹³C-octanoic acid and analyzed the resulting incubation medium by NMR spectroscopy (Figure 3). Comparison of the signal intensity of the peaks of [¹³C]-labeled carbon atoms 2, 3, and 4 of octanoic acid of the incubation that contained *N. gruberi* NEG-M amoebae (top graph) with the control incubation (bottom graph) showed that in the incubations containing trophozoites, octanoic acid was readily consumed (60% was degraded), while no ¹³C-labeled fermentation products such as acetate, propionate, or succinate could be detected (Müller et al., 2012), which is in full agreement with our ¹⁴C-labeled fatty acid incubations. Parasites are known to live on fermentation of sugars, whether they live in blood, organs, or the gut (Köhler and Tielens, 2008). Eukaryotic pathogens that invade human tissues

but do not live primarily on glucose have not been reported to date. *Naegleria* presents an interesting example of a human pathogenic protist that shuns glucose as a carbon and energy substrate. However, our observation that, when given a choice, lipids are the preferred substrate does not imply that other substrates, such as glucose, are not used to a lower extent at the same time, which is in fact what we observed (Table 1). Furthermore, the observation that lipids are the preferred substrate does not imply that *N. gruberi* cannot grow in its absence.

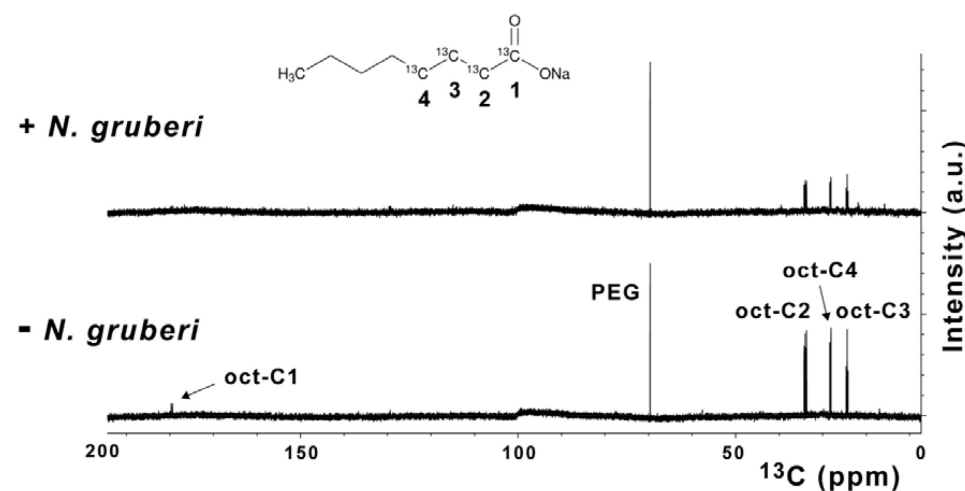


Figure 3. NMR Analysis of [^{13}C]-Labeled Octanoic Acid Degradation by *N. gruberi* Trophozoites were incubated in PBS containing 45 mM polyethylene glycol 6000 (PEG) plus 210 mM [$1,2,3,4\text{-}^{13}\text{C}$]-labeled octanoic acid. Identity of the peaks originating from the four labeled carbon atoms of octanoic acid is indicated by C1–C4.

The present findings allow us to propose a metabolic map for the energy metabolism of *N. gruberi* trophozoites that reflects the obligate aerobic nature of the growing organism and its reliance on lipid oxidation for energy metabolism (Figure 2). Though *N. gruberi* contains all the genes required for the metabolism of carbohydrates and amino acids (Opperdoo et al., 2011), when given the choice during growth it exhibits a clear preference for fatty acid oxidation as the main source for ATP production (Table 1). The genome encodes a full set of lipid-degrading enzymes, including lipases, phospholipases, and β -oxidation enzymes (Opperdoo et al., 2011) (Table S1) that underpin Figure 2. A close inspection of sequences of proteins involved in lipid degradation and the β -oxidation of the liberated free fatty acids that are encoded in the *N. gruberi* genome revealed that the genome contains many sequences with peroxisomal targeting signals (Opperdoo

et al., 2011) in addition to isofunctional homologs that carry a predicted mitochondrial transit sequence (Table S1). This suggests that both peroxisomes and mitochondria are involved in the oxidation of fatty acids.

Fatty acids can not, however, be the exclusive substrates for *Naegleria* growth, as degradation of acetyl-CoA to carbon dioxide requires the presence and occasional replenishment of Krebs cycle intermediates, and these cannot be made from fatty acids. This implies that complete oxidation of fatty acids to carbon dioxide requires a trickle of carbohydrate oxidation to pyruvate, which fits in the observed metabolism of glucose and fatty acids by *N. gruberi* (Table 1). The preferential use of lipids instead of carbohydrates is also reflected in the storage of substrates. Early histochemical studies of *N. gruberi* showed that spherical globules (0.4–1.0 μM) consisting of lipids are distributed throughout the cytoplasm, whereas glycogen is absent (Pittam, 1963). Parasites are known to obtain lipids from their host for usage as building blocks and increased expression of enzymes involved in lipid metabolism under certain conditions or in various life-cycle stages has also been observed in transcriptome and proteome studies (Atwood et al., 2005; Li et al., 2016; Roberts et al., 2003; Saunders et al., 2014; Trindade et al., 2016; Yichoy et al., 2011). Substrate and end-product studies are lacking, however, and the preferential use of lipids as the major bioenergetic substrate has not been shown for any eukaryotic pathogen to date. In nature, *N. gruberi*, like many other protists, feeds mainly on bacteria, a food source containing larger amounts of lipids than carbohydrates. Other phagotrophic protists might be found that exhibit a similar substrate preference for lipids. Furthermore, parasitic protists often encounter large variations in their menu during the life cycle, and the metabolism of many parasitic protists is therefore very flexible.

Based on our analysis of the genome content of *N. fowleri* and comparison with that of *N. gruberi* (Table S2), we suggest that the strong preference for lipids should also be found in the thermophilic congener, *N. fowleri*, which exhibits a strong tropism for the olfactory nerves of the nasal mucosa that it infects en route to the brain during PAM. The white matter of brain is rich in myelin sheets, which surround the axons of nerve cells and contain about 80% lipids by weight (O'Brien and Sampson, 1965). *N. fowleri* encodes a set of glycohydrolases, glycoside hydrolases, glucosyl ceramidase, sphingomyeline phosphodiesterase, and phospholipases, several present in multiple copies, that could channel myelin sheaths into its energy metabolism (Table S2). Acetate, here shown to be readily consumed by *Naegleria*, is also amply available in brain (Wyss et al., 2011). Though the preferred growth substrates of the “brain-eating amoeba” as the deadly and more difficult to culture pathogen *N. fowleri* is sometimes

called, have still not been directly shown, an earlier investigation suggested that they possibly are not carbohydrates (Weik and John, 1977a). The end products of glucose and fatty acid degradation reported here provide a clear picture for *N. gruberi* and make very specific predictions for *N. fowleri* in agreement with Weik and John (1977a) suggestion. Fatty acid oxidation in *Naegleria* uncovers a metabolic specialization in protists with evolutionary and medical significance and could point the way to improved treatments for PAM.

Supplemental information

Supplemental Information includes three figures, two tables, and three videos and can be found with this article online at <https://doi.org/10.1016/j.celrep.2018.09.055>.

Document S1. Figures S1–S3 and Table S1

Table S2. Identified Protein Sequences and Their Accession Numbers of Enzymes Involved in a Number of Metabolic Pathways of, Respectively, *Naegleria gruberi* and *N. fowleri*, Related to Figure 2

Identified protein sequences and their accession numbers of enzymes involved in a number of pathways of respectively *Naegleria gruberi* and *N. fowleri*. *N. gruberi* accessions numbers were taken from the Uniprot/TREMBL protein database (<https://www.uniprot.org/>). The protein sequences from the *N. fowleri* trophozoite transcriptome (Zysset-Burri et al., 2014) were downloaded from the AmoebaDB, release 25, 23 July 2015 (http://amoebadb.org/common/downloads/release-29/NfowleriATCC30863/fasta/data/AmoebaDB-29_NfowleriATCC30863_AnnotatedProteins.fasta). *N. fowleri* orthologs of *N. gruberi* enzyme sequences were identified by an “all against all” BLASTP search of *N. gruberi* sequences against the *N. fowleri* protein database. The expect E value represent the number of alignments expected at random. The lower the E value the less likely is a random similarity (Korf et al., 2003) Assignments of enzymes to either mitochondria or peroxisomes are based on the presence of identifiable mitochondrial transit sequences or peroxisomal targeting sequences. In several cases the assignment was based on the presence of a close relationship to an experimentally demonstrated mitochondrial or peroxisomal isoenzyme.

Video S1. *N. gruberi* Control Incubation, Related to Figure 1A Control, *N. gruberi* NEG-M trophozoites in PYNFH medium

Video S2. *N. gruberi* with KCN, Related to Figure 1A *N. gruberi* NEG-M trophozoites recorded immediately after addition of 1 mM KCN + 1.5 mM SHAM

Video S3. *N. gruberi* with KCN + SHAM, Related to Figure 1B *N. gruberi* NEG-M trophozoites after 24 hour exposure to 1 mM KCN. All movies were recorded at 20 s per frame, played back at 29 frames per second. The bar in the bottom right represents 200 μ m.

Document S2. Article plus Supplemental Information

Acknowledgments

We thank Matthias Wittwer (Spiez Laboratory, Federal Office for Civil Protection, Spiez, Switzerland) for making available the annotated transcriptome sequences of *Naegleria fowleri* ATCC 30863 trophozoites. W.F.M. thanks the ERC (grant 666053) for funding, and H.W. acknowledges financial support for the NMR experiments by NWO-Groot Grant 175.107.301.10.

Author contributions

M.L.B., J.J.v.H., and A.G.M.T. conceived and designed the experiments. M.L.B. and M.J.S. conducted the experiments. F.R.O., V.Z., and W.F.M. performed comparative genomic analyses. J.F.D.J. provided the field isolate of *N. gruberi* and know-how on amoebae. J.J.v.H. and J.F.B. developed and performed the quinone analyses. H.W. performed the NMR analysis. J.J.v.H. and A.G.M.T. supervised the project. M.L.B., F.R.O., W.F.M., and A.G.M.T. wrote the manuscript. All authors participated in discussion and commenting on and final approval of the manuscript.

Declaration of interests

The authors declare no competing interests.

Published: October 16, 2018

Supporting Citations

The following references appear in the Supplemental Information: Emanuelsson et al. (2000); Strijbis et al., (2008).

REFERENCES

- Atteia, A., R. van Lis, A. G. M. Tielens and W. F. Martin (2013). "Anaerobic energy metabolism in unicellular photosynthetic eukaryotes." *Biochimica et Biophysica Acta (BBA)-Bioenergetics* **1827**(2): 210-223.
- Atwood, J. A., 3rd, D. B. Weatherly, T. A. Minning, B. Bundy, C. Cavola, F. R. Oppendoes, R. Orlando and R. L. Tarleton (2005). "The *Trypanosoma cruzi* proteome." *Science* **309**(5733): 473-476.
- Besteiro, S., M. P. Barrett, L. Rivière and F. Bringaud (2005). "Energy generation in insect stages of *Trypanosoma brucei*: metabolism in flux." *Trends in Parasitology* **21**(4): 185-191.
- Bligh, E. G. and W. J. Dyer (1959). "A rapid method of total lipid extraction and purification." *Canadian Journal of Biochemistry and Physiology* **37**(8): 911-917.
- Chou, K.-C. and H.-B. Shen (2010). "A new method for predicting the subcellular localization of eukaryotic proteins with both single and multiple sites: Euk-mPLoc 2.0." *PLOS ONE* **5**(4): e9931.
- De Jonckheere, J. F. (2002). "A century of research on the amoeboflagellate genus *Naegleria*." *Acta Protozoologica* **41**(4): 309-342.
- De Jonckheere, J. F. (2007). "Molecular identification of free-living amoebae of the Vahlkampfiidae and Acanthamoebidae isolated in Arizona (USA)." *European Journal of Protistology* **43**(1): 9-15.
- De Jonckheere, J. F. (2014). "What do we know by now about the genus *Naegleria*?" *Experimental parasitology* **145**: S2-S9.
- Emanuelsson, O., H. Nielsen, S. Brunak and G. Von Heijne (2000). "Predicting subcellular localization of proteins based on their N-terminal amino acid sequence." *Journal of Molecular Biology* **300**(4): 1005-1016.
- Fritz-Laylin, L. K., S. E. Prochnik, et al. (2010). "The genome of *Naegleria gruberi* illuminates early eukaryotic versatility." *Cell* **140**(5): 631-642.
- Fulton, C. (1993). "*Naegleria* - A Research Partner For Cell And Developmental Biology." *Journal of Eukaryotic Microbiology* **40**(4): 520-532.
- Fulton, C., C. Webster and J. S. Wu (1984). "Chemically Defined Media For Cultivation Of *Naegleria gruberi*." *Proceedings of the National Academy of Sciences of the United States of America* **81**(8): 2406-2410.
- Ginger, M. L., L. K. Fritz-Laylin, C. Fulton, W. Z. Cande and S. C. Dawson (2010). "Intermediary metabolism in protists: a sequence-based view of facultative anaerobic metabolism in evolutionarily diverse eukaryotes." *Protist* **161**(5): 642-671.
- Korf, I., M. Yandell and J. Bedell (2003). *Blast*, "O'Reilly Media, Inc."
- Köhler, P., and Tielens, A.G.M. (2008). Energy Metabolism. In Encyclopedia of Parasitology, H. Mehlhorn, ed. (Springer-Verlag)
- Li, Y., S. Shah-Simpson, et al. (2016). "Transcriptome Remodeling in *Trypanosoma cruzi* and Human Cells during Intracellular Infection." *Plos Pathogens* **12**(4).
- Müller, M., M. Mentel, et al. (2012). "Biochemistry and evolution of anaerobic energy metabolism in eukaryotes." *Microbiology and Molecular Biology Reviews* **76**(2): 444-495.
- O'Brien, J. S. and E. L. Sampson (1965). "Lipid composition of the normal human brain: gray matter, white matter, and myelin." *Journal of Lipid Research* **6**(4): 537-544.
- Oppendoes, F. R., J. F. De Jonckheere and A. G. M. Tielens (2011). "*Naegleria gruberi* metabolism." *International journal for parasitology* **41**(9): 915-924.
- Oppendoes, F. R. and J.-P. Szikora (2006). "In silico prediction of the glycosomal enzymes of *Leishmania major* and trypanosomes." *Molecular and Biochemical Parasitology* **147**(2): 193-206.
- Pande, S. V. (1976). "Liquid Scintillation-Counting Of Aqueous Samples Using Triton-Containing Scintillants." *Analytical Biochemistry* **74**(1): 25-34.
- Pittam, M. D. (1963). "Studies of an Amoeboid-Flagellate, *Naegleria gruberi*." *Journal of Cell Science* **3**(68): 513-529.
- Roberts, C. W., R. McLeod, D. W. Rice, M. Ginger, M. L. Chance and L. J. Goad (2003). "Fatty acid and sterol metabolism: potential antimicrobial targets in apicomplexan and trypanosomatid parasitic protozoa." *Molecular and Biochemical Parasitology* **126**(2): 129-142.
- Saunders, E. C., W. W. Ng, J. Kloehn, J. M. Chambers, M. Ng and M. J. McConville (2014). "Induction of a Stringent Metabolic Response in Intracellular Stages of *Leishmania mexicana* Leads to Increased Dependence on Mitochondrial Metabolism." *Plos Pathogens* **10**(1).
- Strijbis, K., C. W. T. Van Roermund, et al. (2008). "Carnitine-dependent transport of acetyl coenzyme A in *Candida albicans* is essential for growth on nonfermentable carbon sources and contributes to biofilm formation." *Eukaryotic Cell* **7**(4): 610-618.
- Tielens, A. G. M., C. Rotte, J. J. van Hellemond and W. Martin (2002). "Mitochondria as we don't know them." *Trends in biochemical sciences* **27**(11): 564-572.
- Tielens, A. G. M., P. Van der Meer and S. G. Van den Bergh (1981). "The aerobic energy metabolism of the juvenile *Fasciola hepatica*." *Molecular and Biochemical Parasitology* **3**(4): 205-214.
- Trindade, S., F. Rijo-Ferreira, et al. (2016). "*Trypanosoma brucei* Parasites Occupy and Functionally Adapt to the Adipose Tissue in Mice." *Cell Host & Microbe* **19**(6): 837-848.
- Van Hellemond, J. J., M. Klockiewicz, C. P. H. Gaasenbeek, M. H. Roos and A. G. M. Tielens (1995). "Rhodoquinone and complex II of the electron transport chain in anaerobically functioning eukaryotes." *Journal of Biological Chemistry* **270**(52): 31065-31070.
- van Weelden, S. W. H., B. Fast, A. Vogt, P. Van Der Meer, J. Saas, J. J. Van Hellemond, A. G. M. Tielens and M. Boshart (2003). "Procyclic *Trypanosoma brucei* do not use Krebs cycle activity for energy generation." *Journal of Biological Chemistry* **278**(15): 12854-12863.
- Weik, R. R. and D. T. John (1977). "Agitated Mass Cultivation Of *Naegleria fowleri*." *Journal of Parasitology* **63**(5): 868-871.
- Weik, R. R. and D. T. John (1977). "Cell-Size, Macromolecular-Composition, And O₂ Consumption During Agitated Cultivation Of *Naegleria gruberi*." *Journal of Protozoology* **24**(1): 196-200.
- Wyss, M. T., P. J. Magistretti, A. Buck and B. Weber (2011). "Labeled acetate as a marker of astrocytic metabolism." *Journal of Cerebral Blood Flow & Metabolism* **31**(8): 1668-1674.
- Yichoy, M., T. T. Duarte, A. De Chatterjee, T. L. Mendez, K. Y. Aguilera, D. Roy, S. Roychowdhury, S. B. Aley and S. Das (2011). "Lipid metabolism in *Giardia*: a post-genomic perspective." *Parasitology* **138**(3):

267-278.

Zysset-Burri, D. C., N. Mueller, C. Beuret, M. Heller, N. Schuerch, B. Gottstein and M. Wittwer (2014).
“Genome-wide identification of pathogenicity factors of the free-living amoeba *Naegleria fowleri*.” *BMC genomics* **15**:496.

STAR ★ METHODS

Key Resources Table

REAGENT or RESOURCE	SOURCE	IDENTIFIER
Bacterial and Virus Strains		
<i>E. coli</i> Top10	Invitrogen	Cat# C404052
Chemicals, Peptides, and Recombinant Proteins		
Peptone	BD	Cat#211693
Yeast Extract	BD	Cat#R6625
Nucleic Acid	Sigma	Cat#R6625; CAS Number: 63231-63-0
Folic Acid	Sigma	Cat#F7876; CAS Number: 59-30-3
Hemin	Sigma	Cat#52180; CAS Number: 16009-13-5
Fetal Bovine Serum	GIBCO	Cat#10270
D-[6- ¹⁴ C] glucose	Amersham	Cat#CFA351
[1- ¹⁴ C] octanoic acid	DuPont NEN	Cat#NEC 092H
[1- ¹⁴ C] oleic acid	Perkin-Elmer	Cat#NEC 317
[1,2- ¹⁴ C] acetic acid	Perkin-Elmer	Cat#NEC 553050UC
L-[U- ¹⁴ C] isoleucine	Amersham Biosciences	Cat#CFB 68
L-[U- ¹⁴ C] valine	Amersham Biosciences	Cat#CFB 75
L-[U- ¹⁴ C] lysine	Amersham Biosciences	Cat#CFB 69
L-[U- ¹⁴ C] threonine	MP Biomedicals	Cat#0110126E50
L-[3- ¹⁴ C] serine	Pharmacia Biotech	CFA 151
[1,2,3,4 - ¹³ C] octanoic acid	Cambridge Isotope Laboratories	CLM-3876-0.25
LumaGel Safe	Perkin-Elmer	Cat#3077
Experimental Models: Organisms/Strains		
<i>N. gruberi</i> strain NEG-M	ATCC	Cat#30224
<i>N. gruberi</i> field isolate	Personal collection	(De Jonckheere, 2007)
Software and Algorithms		
Cell^F Software	Olympus	Version 3.1.1275
Analyst	AB Sciex	Version 1.5.1
Target P	Emanuelson et al., 2000	http://www.cbs.dtu.dk/services/TargetP/
Euk-mPloc 2.0	Chou and Shen, 2010	http://www.csbio.sjtu.edu.cn/bioinf/euk-multi-2/
PTS1	Opperdoes and Szikora, 2006	

Contact for reagent and resource sharing

Further information and requests for resources and reagents should be directed to and will be fulfilled by the Lead Contact, Aloysius G.M. Tielens (a.tielens@erasmusmc.nl).

METHOD DETAILS

Naegleria strains

Naegleria gruberi strain NEG-M (ATCC® 30224) was cultured at 25°C while shaking at 50 rpm in PYNFH medium, which contains Peptone, Yeast extract, Nucleic acid, Folic acid, Hemin and 10% heat-inactivated fetal bovine serum (ATCC medium 1034). This

medium was supplemented with 40 mg/ml gentamicin, 100 units/ml penicillin and 100 mg/ml streptomycin. A field isolate of *N. gruberi* was obtained from sediment in Rio Verde, Tuzigoot, Arizona, USA (De Jonckheere, 2007). This field isolate has the same ITS rDNA sequence as strain NEG-M, indicating that it is the same species (De Jonckheere, 2014). Since its isolation from the field this *N. gruberi* isolate (FI trophozoites) was always cultured on non-nutrient agar plates coated with *Escherichia coli* and this strain was never cultured in any of the culture media that are used to grow the NEG-M strain. For our experiments the amoebae were cultured at 37°C on non-nutrient agar plates seeded with Top10 *E. coli* (ThermoFisher Scientific). Amoebae were counted using Differential Interference Contrast (DIC) microscopy and images taken were analyzed using Cell[^] Software (Olympus).

Trophozoite culture of *N. gruberi* NEG-M in the absence of oxygen or in the presence of inhibitors of respiration

To investigate the anaerobic capacity of *N. gruberi* NEG-M, trophozoites were seeded at a density of 30,000 trophozoites per ml in 5 mL PYNFH medium containing 40mM ascorbate (anaerobic incubations) or 40mM NaCl (aerobic incubations). In aerobic incubations the gas phase was air. For anaerobic incubations the medium was degassed, flasks were flushed for 5 min with nitrogen and prior to closing the bottles, ascorbate oxidase (100 U) was added to the anaerobic incubations to remove any remaining oxygen (Tielens et al., 1981).

To determine the effects of respiratory chain inhibitors on the cell growth of *N. gruberi* NEG-M, trophozoites were seeded in PYNFH medium at a density of 30,000 trophozoites per ml. Upon reaching log growth (day 3) respiratory chain inhibitors were added, KCN was added to the culture in a final concentration of 1 mM, SHAM was dissolved in 96% ethanol and added to the culture at a final concentration of 1.5 mM SHAM, 0.5% ethanol. Control incubations contained 0.5% ethanol. Throughout cell growth experiments, the medium was changed daily, and KCN and SHAM were added fresh daily.

Anaerobic trophozoite culture of *N. gruberi* field isolate

Fresh NN-plates were inoculated by placing a circular slice (9 mm in diameter) of an agar plate covered uniformly with *N. gruberi* cysts upside down on the center of the plate. These inoculated plates were then pre-incubated aerobically for 24 hours at 37°C to allow excystment of amoebae. After this aerobic pre-incubation the amoebic growth perimeter was marked and recorded, and the plates were then further incubated aerobically or anaerobically for 72 hours. Anaerobic conditions were created by placing the plates in gas-tight jars in which the air was replaced by a mixture of 85% N₂, 10%

CO₂, 5% H₂ using an Anoxomat (Mart Microbiology, Drachten, the Netherlands), aerobic plates were incubated under normal atmospheric conditions in identical jars. After 24, 48 and 72 hours an anaerobic and an aerobic jar, each containing two plates, were opened and the perimeter of growth on the anaerobic and aerobic plates was recorded.

Respiration of *N. gruberi* NEG-M

Oxygen consumption by *N. gruberi* NEG-M trophozoites was determined using a Clark-type electrode at 25°C in 2 mL oxygen-saturated fresh medium. KCN and SHAM were used at a final concentration of 1 mM and 1.5 mM, respectively.

Quinone-composition of *N. gruberi* NEG-M

N. gruberi NEG-M was cultured in PYNFH medium and harvested during logarithmic growth. Lipids were isolated by a chloroform/methanol extraction procedure (Bligh and Dyer, 1959). Ubiquinone and rholoquinone content was analyzed by a Liquid Chromatography-Mass Spectrometry (LC-MS) method as described before (van Hellemond et al., 1995). Quinones from *Fasciola hepatica* were isolated using the same method and analyzed as a positive control. The quinone composition of the *N. gruberi* field isolate was analyzed using the same procedure.

Metabolism of *N. gruberi* NEG-M

Trophozoites were harvested during logarithmic growth and 3.5 × 10⁶ trophozoites were transferred to a sealed 25 mL erlenmeyer flask containing either 5 mL PYNFH medium or phosphate buffered saline (PBS). The incubation was started by addition of one of the labeled substrates (all supplied by PerkinElmer, Boston, MA, USA): D-[6-¹⁴C] glucose (5 mM, 5 μCi), [1-¹⁴C] octanoic acid (210 mM, 5 μCi), [1-¹⁴C] oleic acid (210 mM, 5 μCi), [1,2-¹⁴C] acetic acid (5 mM, 5 μCi), [U-¹⁴C] isoleucine (5 μCi), [U-¹⁴C] valine (5 μCi), [U-¹⁴C] lysine (5 mCi), [U-¹⁴C] threonine (5 μCi) and [3-¹⁴C] serine (5 μCi). Blank incubations without trophozoites were started simultaneously. All samples were incubated at 22°C while shaking gently at 125 rpm. After 18–24 hours the incubations were terminated and end products were analyzed as described before (van Weelden et al., 2003). In short, 100 μL NaHCO₃ (25 mM) was added and the incubation was ended by addition of 6 M HCl, lowering the pH to 2.5. Carbon dioxide was trapped in a series of four scintillation vials, each filled with 1 mL of 0.3 M NaOH and 15 mL of Tritisol scintillation fluid (Pande, 1976). Thereafter the radioactivity in this fraction was counted in a scintillation counter. After this removal of carbon dioxide, the acidified supernatant was separated from the cells by centrifugation (4°C for 10 min at 500 × g) and neutralized by the addition of NaOH. The labeled end-products were analyzed by anion-exchange chromatography (Tielens et al., 1981). Fractions were collected

and radioactivity was measured in a scintillation counter after addition of LUMA-gel (Lumac*LCS, Groningen, the Netherlands).

NMR spectroscopy was used to analyze samples that had been incubated in phosphate buffered saline (PBS) containing 45 mM polyethylene glycol 6000 (PEG) plus 210 mM ^{13}C -labeled [1,2,3,4- ^{13}C]-labeled octanoic acid (Cambridge Isotope Laboratories, Andover, MA, USA) for 24 hr at 22°C while shaking gently at 125 rpm. After the incubations the cells were spun down (4°C for 10 min at 500 × *g*) and 500 µL of the supernatants were analyzed. NMR experiments were performed at 25°C on a 600 MHz Bruker Avance spectrometer equipped with cryogenically cooled TCI-probe for extra sensitivity. ^{13}C experiments were recorded from 0–200 ppm employing power-gated proton decoupling. 16k FIDs were accumulated with inter-scan delay of 2 s, and acquisition times of 0.5 s (32k complex points). Processing was performed with exponential multiplication and Fourier Transformation, followed by base-line correction.

QUANTIFICATION AND STATISTICAL ANALYSIS

Quantification

Mass spectrometry data processing, peak detection and peak area quantification for detection and quantification of quinones were performed using Analyst software, version 1.5.1; AB Sciex, Foster City, CA, USA.

Statistical Analysis

Replicate numbers are indicated in the legend of Table 1 and Figures 1 and S1. Standard deviations (SD) were calculated and are shown in Table 1.



CHAPTER 7

Summarizing discussion

SUMMARIZING DISCUSSION

Energy metabolism and parasites

All work requires energy. Within the biological realm, energy requirements are most often fulfilled by adenosine triphosphate (ATP), the universal energy currency used by all cells. After its use, ATP can be (re)generated from ADP and phosphate by oxidation of the carbon in fuel (food), such as glucose and fats. In aerobic organisms, the final electron acceptor is oxygen and the oxidation product is carbon dioxide. In an anaerobic energy metabolism, another final electron acceptor than oxygen is used and the end product is not carbon dioxide but partly oxidized fermentation products, such as lactate, succinate and acetate.

Parasites have different stages in their life cycles and variations in the external conditions force the parasite to adapt its energy metabolism. Important variations in this respect are the availability of food and oxygen. Free-living stages of parasitic helminths have to provide for their own food and use their endogenous glycogen stores for energy metabolism. They often use Krebs cycle activity, producing carbon dioxide as end product, thereby obtaining as much ATP as possible from their substrates. Parasitic stages, on the other hand, consume substrates they obtain from the host and have a less efficient, fermentative metabolism. As they are surrounded by food, there is little need for economy. These parasitic stages obtain their nutrients and many of their structural elements from the host. However, although the host supplies the food, parasites have to use their own metabolism and machinery to produce ATP. Therefore, a greater understanding of these processes in parasites holds great potential for the identification of possible drug targets, especially where the energy metabolism or the machinery of the parasite is different from that of the host. In this thesis, investigations are presented on the energy metabolism and related processes of two different parasites, *Schistosoma mansoni* and *Naegleria gruberi/fowleri*.

Energy metabolism in *S. mansoni*

The parasitic flatworm *S. mansoni* has various stages in its lifecycle, each having its own metabolism. The free-living stages of *S. mansoni* rely on an aerobic metabolism and ATP is generated for a large part via the efficient Krebs cycle. The parasitic stages of *S. mansoni* on the other hand, have a mostly fermentative metabolism, in which pyruvate is converted to lactate by the enzyme lactate dehydrogenase (LDH) (Bueding, 1950; Mansour and Bueding, 1953; Tielens et al., 1991; Tielens et al., 1992). This means that in *S. mansoni* pyruvate will either be transported into the mitochondria and ultimately degraded to carbon dioxide, or be converted to lactate in the cytosol by LDH,

depending on the life-cycle stage of the parasite. Anaerobic processing of glucose, i.e. glycolysis followed by the conversion to lactate, yields two ATP, while processing of pyruvate via the Krebs cycle will yield about 30 ATP per glucose molecule degraded. For the free-living stages, it is in the interest of schistosomes not to ferment pyruvate to lactate, but to degrade pyruvate to carbon dioxide inside the mitochondria. In that way they can produce more ATP from their endogenous glycogen substrates, and therefore, they will live longer and have more chance to find a new host that can be infected.

Earlier studies have shown that the switch from aerobic energy metabolism in free-living cercariae to anaerobic energy metabolism in the mammalian stages can occur quickly after penetration of the final host (Horemans et al., 1992). This study showed that just after transformation of the free-living cercariae into schistosomula, *S. mansoni* adapts its energy metabolism to the external glucose concentration; from an aerobic energy metabolism producing carbon dioxide in the absence of external glucose to an anaerobic energy metabolism mainly producing lactate in presence of 5 mM glucose. This metabolic switch was shown to be reversible and not coupled to life-cycle stage transformation (Horemans et al., 1992). As the metabolic fluxes towards lactate production and Krebs cycle activity are determined by the external glucose concentration, the kinetic properties of the enzymes involved in the metabolic pathways are apparently such that this metabolic switch is facilitated. In addition, the involved enzymes thereby also differ from those of the host, because an external-glucose-concentration induced metabolic switch does not occur in mammals. As the metabolic flux from glucose to carbon dioxide and lactate separates after pyruvate formation by glycolysis, lactate dehydrogenase (LDH) is probably a key enzyme in regulating lactate production since it converts pyruvate into lactate.

Lactate dehydrogenase of *S. mansoni*

The *S. mansoni* genome comprises three genes that encode LDH; Smp_033040, Smp_038950, Smp_038960 (Protasio et al., 2012; Howe et al., 2017; Lu et al., 2017). The sequence similarity between the proteins encoded by these genes is high and in case of Smp_038950 and Smp_038960 this is above 95% (Lu et al., 2017). Normalized gene expression analysis showed that Smp_038950 was the most abundantly expressed LDH gene in cercariae (Protasio et al., 2012), which suggests that the LDH encoded by the Smp_038950 gene plays a role in the metabolic switch that occurs after the cercariae penetrate their new host.

In a previous investigation of *S. mansoni* LDH (SmLDH) by our group, the serendipitous discovery was made that the enzyme had altered kinetic properties in the presence

of fructose 1,6 biphosphate (FBP), an intermediate of glycolysis (Tielens, 1997 “Biochemistry of Trematodes” in Fried and Graczyk, 1997). Although allosteric activation by FBP is highly unusual for LDH in eukaryotes, many prokaryote NADH-dependent L-LDHs are allosterically activated by FBP (Garvie, 1980; Iwata and Ohta, 1993; Fushinobu et al., 1996). The allosteric regulation of L-LDHs of prokaryotes has been studied extensively and these LDHs all consist of four identical monomers arranged around what are conventionally known as the P, Q and R axes (Adams et al., 1973). Each monomer has one active site and the tetramer has two allosteric FBP-binding sites, each situated at the interface between two monomers, which correspond to the so-called anion-binding sites of the vertebrate enzymes (Grau et al., 1981; Wigley et al., 1992). As only a few preliminary findings of FBP-sensitivity of LDH in eukaryotes were reported (Brennan et al., 1995; Lloyd, 1983; Tielens, 1997), we performed a comprehensive study on the kinetic properties of SmLDH, its 3-dimensional structure and its function in regulation of metabolic fluxes (**Chapter 2**).

The kinetic properties (including ATP inhibition and FBP activation) of LDH of *S. mansoni* were investigated experimentally using purified LDH of adult *S. mansoni* worms (SmLDH) as well as purified SmLDH that was recombinant expressed in *Escherichia coli* (rSmLDH). In addition, for comparison with host LDH a commercially available purified rabbit muscle LDH was used. This revealed that whereas rabbit LDH was unaffected by FBP and ATP, both SmLDH and rSmLDH were strongly inhibited by ATP and stimulated by FBP, the latter especially in the presence of ATP inhibition. In fact, FBP increased the affinity of SmLDH for pyruvate (and lowered the K_m for pyruvate), whereas ATP resulted in the opposite effect.

Since the kinetic properties of SmLDH differed from those of their host, we studied the structure of SmLDH in more detail. Sequence alignment of SmLDH with both eukaryotic and prokaryotic LDHs revealed a striking feature in the anion pocket of SmLDH. While all eukaryotic LDHs have a cysteine and tryptophan residue at position 187 and 190, respectively, SmLDH has a valine and tyrosine at those positions similar to the FBP-activated prokaryotic LDHs. Modelling studies of the 3-dimensional structure of SmLDH suggested that the anion binding pocket of SmLDH can bind both FBP as well as ATP. Altogether these results suggested that FBP might release the inhibition by ATP by direct competition for the allosteric anion binding pocket of SmLDH. These structural differences between SmLDH and LDH of the mammalian host might be exploitable for drug design aimed to interfere with this crucial enzyme in the energy metabolism of adult schistosomes. X-ray crystallography of SmLDH in the presence of ATP and or FBP can provide further direct evidence to these interactions.

***In silico* modeling of energy metabolism of *S. mansoni*.**

SmLDH is not the only allosterically regulated enzyme in the metabolic pathway that converts glucose into lactate. Hexokinase, which catalyses the conversion of glucose into glucose-6-phosphate at the expense of ATP, is substantially inhibited by its product glucose-6-phosphate in mammals and most other eukaryotes (Litwack, 2018). However, hexokinase of *S. mansoni* is inhibited by glucose-6-phosphate to a limited extend only (Tielens et al., 1994). Therefore, the kinetic properties of both LDH and hexokinase of *S. mansoni* differ from those of their mammalian host. In addition, these kinetic differences might facilitate the observed metabolic switch upon a sudden increase in external glucose concentrations.

To further investigate this issue, i.e. how the glycolytic flux is controlled in *S. mansoni*, an *in silico* kinetic model was produced. This model was not generated from scratch, but rather created by changing the kinetic properties of the well-defined models of glycolysis from the yeast *Saccharomyces cerevisiae* (Heerden et al., 2014) and *Trypanosoma brucei* (Haanstra et al., 2008) In the developed *S. mansoni* model, all available kinetic properties of known *S. mansoni* glycolytic enzymes were entered, as well as a functional Krebs cycle and oxidative phosphorylation. Explicitly, the SmLDH activity was modeled to be affected by FBP and ATP. In order to investigate the importance of SmLDH inhibition by ATP and activation by FBP separately, three model versions were prepared; the ‘wild type’-model in which SmLDH is both inhibited by ATP and activated by FBP, the ‘FBP-model’ in which SmLDH is only activated by FBP, and the ‘ATP-model’ in which SmLDH is only inhibited by ATP. Subsequently, using these models we explored what would happen to the metabolic fluxes towards lactate and carbon dioxide upon a sudden increase in the glucose concentration in the presence or absence of these regulatory mechanisms. The results from these simulations showed that schistosomes need an adapted LDH to cope with fluctuating external glucose concentrations. SmLDH requires both inhibition by ATP and activation by FBP, as ATP inhibition of SmLDH prevents a wasteful fermentative metabolism in the free-living stages, while the FBP activation is required to increase lactate formation when a sudden increase in external glucose concentration will boost the glycolytic flux, which is in schistosomes not sufficiently inhibited by the glucose-6-phosphate inhibition of hexokinase. To this end, the LDH of *S. mansoni* prevents a disbalance of substrates and co-factors in the glycolytic pathway. One can envision the ATP-inhibited, FBP-stimulated LDH of *S. mansoni* as an emergency flotation device that deploys when required; in conditions in which the external glucose concentration suddenly increases.

Lipid metabolism in *S. mansoni*

At first glance, it can be considered remarkable that the free-living stages of *S. mansoni* have glycogen stores, rather than lipid stores. Triacylglycerol stores have an energy density of about 9 kcal g⁻¹ (38 kJ g⁻¹), in contrast to only 4 kcal g⁻¹ (17 kJ g⁻¹) for carbohydrates and protein (Berg et al., 2015). Hypothetically, if we were to replace glycogen by lipids in the free-living stages of *S. mansoni*, the energy density of the free-living stages would be six times as high (accounting for the hydration of glycogen and anhydrous storage of lipids). The absence of lipid stores for ATP production in free-living stages of *S. mansoni* is consistent with the view that schistosomes rely entirely on carbohydrate catabolism for their energy metabolism (Van Oordt et al., 1989; Tielens, 1994). In addition, fatty acid oxidation was never demonstrated directly in *S. mansoni*, nor in any other parasitic trematode (Meyer et al., 1970; Rumjanek and Simpson, 1980; Frayha and Smyth, 1983). However, the dogma of the inability of *S. mansoni* to oxidize fatty acids was recently challenged by Huang et al. (2012), who concluded that “fatty acid oxidation is essential for egg production in *S. mansoni*”. This report even inspired others to investigate the enzymes suggested to be involved in the postulated lipid catabolism in *S. mansoni* in more detail (Buro et al., 2013; Edwards et al., 2015; Oliveira et al., 2016; Timson, 2016) or to include this novel observation in general reviews on *S. mansoni* (Colley et al., 2014; Guigas and Molofsky, 2015). The first scientific claim that fatty acid oxidation might occur in *S. mansoni* was proposed by Berriman et al. (Berriman et al., 2009) in their paper in which the authors postulated the presence of genes encoding beta-oxidation enzymes in the draft genome of *S. mansoni*. However, at that time most of those genes were annotated automatically, a method prone to annotation errors (Schnoes, Brown et al. 2009). Therefore, it was unclear whether fatty acid oxidation does occur in schistosomes and, if so, whether the fatty acid oxidation pathway could be a good target for anti-schistosomal drug design.

In **Chapter 3** the results are described of a comprehensive study on the lipid metabolism in *S. mansoni* cercariae, adult worms and eggs. These investigations comprised *in vitro* experiments in which the metabolic fate of radioactively labelled fatty acids was examined in combination with careful manual gene annotations of published draft genomes of multiple model organisms. In our metabolic assays we demonstrated that radioactively labelled fatty acids were taken up by the parasites and used for biosynthetic purposes, but we could not detect any carbon dioxide production originating from the labeled fatty acid substrates. On the other hand, in parallel incubations containing radioactively labelled carbohydrates (glucose), we detected carbon dioxide production which demonstrated that carbohydrates were, in contrast to fatty acids, completely oxidized to carbon dioxide. These results demonstrated that eggs, cercariae and adult stages of *S.*

mansoni metabolize fatty acids, but do not oxidize them.

In addition, from nine different model organisms we retrieved the genes known to be involved in fatty acid oxidation and these were subsequently used to identify their closest homolog in the genome database of *S. mansoni*. The thereby identified genes in *S. mansoni* were manually annotated by reversed BLAST analysis and the results from this genome analysis demonstrated that the genes identified by the forward BLAST in the genome of *S. mansoni* were only weakly similar to the genes known to encode fatty acid oxidation enzymes in the 9 model organisms. In addition, the reversed BLAST analysis showed that the identified *S. mansoni* genes demonstrated more sequence similarity to genes encoding enzymes involved in other processes than fatty acid oxidation. Therefore, the genes that were postulated to encode beta-oxidation enzymes, encoded enzymes with another function. Hence, our genome analysis demonstrated that *S. mansoni* lacks the genes encoding proteins involved in fatty oxidation and this conclusion was recently confirmed in the updated analysis of the *S. mansoni* genome annotation (Coghlan et al., 2019). Altogether these results demonstrated that schistosomes do not and cannot oxidize fatty acids.

Although schistosomes do not and cannot oxidize fatty acids, fatty acids are essential for egg production. These lipids are required for biosynthetic processes, but not for ATP production, as was suggested by Huang et al. (Huang et al., 2012). The experiments described in **Chapter 3** showed that newly produced, immature eggs contain large amounts of lipids. To elucidate the role of these lipid stores, we tracked the composition of lipids during maturation of the eggs. These experiments demonstrated that the large lipid stores in immature eggs mainly consisted of neutral lipids, mostly triacylglycerol (TAG). These neutral lipids were subsequently used by the developing larvae for phospholipid biosynthesis, which is required for membrane synthesis during the generation of new cells in the developing miracidium in the egg. The results from our experiments and the experimental results of Huang et al. do not contradict each other, but the interpretation should be different; the large lipid stores within the vitelline-cells of female *S. mansoni* worms serve as precursors to be used by the developing miracidium in the egg but not as substrates for ATP production.

Lipids of *S. mansoni* and host-pathogen interaction.

Lipids are not only essential to schistosomes for biosynthetic reasons, they also play a role in immune-evasion by the parasite. One of the reasons why *S. mansoni* is successful in immune-evasion is related to the tegument, which covers the entire outer surface of adult *S. mansoni* worms. This structure consists of two adjacent lipid bilayers which have

a high turnover rate, as these membranes are renewed every 6 hours (de Oliveira et al., 2013). The tegument, and more specifically the shedding of it, provides an interesting mechanism for the parasite to affect host responses and it has been shown that the lipid composition of the tegument is quite distinct both from other membranes in the parasite as well as from membranes of host blood cells (Van Hellemond et al., 2006; Retra et al., 2015). One of the most striking differences is the specific enrichment of 20:1 lyso-phosphatidylserine (lyso-PS) in the tegument (Retra et al. 2015). Interestingly, purified lyso-PS fractions of schistosomes were earlier shown to activate the TLR2 receptor on dendritic cells, which thereby affects their immunological response (Van der Kleij et al., 2002). These results suggest that 20:1 lyso-PS could function as an immune modulating factor in schistosomiasis.

In **Chapter 4**, the results of a study on the interaction of 20:1 lyso-PS and TLR2 are described. Instead of isolating 20:1 lyso-PS from *S. mansoni* as was previously done (Van der Kleij et al., 2002), a method was developed to synthesize 20:1 lyso-PS under controlled circumstances. This biosynthetic method to produce 20:1 lyso-PS has a number of advantages compared to isolation of this compound from worms. First, any fraction purified from a biological source, in this case homogenized parasites, can comprise minor (barely detectable) compounds that could be responsible for activation of cellular receptors and subsequent intracellular signaling. Second, the developed biosynthetic method allows the synthesis of multiple lyso-phospholipids variants that contain distinct acyl chains or polar head-group moieties, which is useful in studies on the structure-function relations in the ligand-receptor interaction. Third, the developed biosynthetic method allowed the synthesis of much larger amounts of 20:1 lyso-PS, without the use of costly and difficult to obtain parasites. The synthesized lyso-phospholipids were examined for their TLR2 activating capacity using a recombinant TLR2 reporter cell line. It was shown that 20:1 lyso-PS indeed activated TLR2, whereas other synthesized lyso-phospholipid variants did not. These results demonstrated that both the acyl-chain and the polar head group of 20:1 lyso-PS are important for TLR2 activation. In addition, using specific TLR blocking antibodies, we showed that 20:1 lyso-PS activated the TLR2/6 heterodimer and not the TLR2/1 heterodimer. Classically, the TLR2/1 heterodimer has been described to be activated by ligands with 3 acyl-chains attached, while ligands of the TLR2/6 heterodimer contain two acyl chains (Ozinsky et al., 2000; Beutler et al., 2006; Oliveira-Nascimento et al., 2012; van Bergenhenegouwen et al., 2013). However, in **Chapter 4** we now unambiguously showed that 20:1 lyso-PS, a mono-acyl phospholipid, activates TLR2/6 heterodimers.

To gain further insight in the ligand-receptor interaction between 20:1 lyso-PS and

TLR2/6 an *in silico* model was generated, using the already determined crystal structure of TLR2/6 with its classical ligand PAM3CSK4 (FSL-1) (Kang et al., 2009). This model was used to fit 20:1 lyso-PS in the hydrophobic pocket of the TLR2/6 heterodimer, which resulted in a structure in which 20:1 lyso-PS interacted with similar amino-acid residues of the receptor compared to FSL-1. In conclusion, the experiments described in **Chapter 4** demonstrated that 20:1 lyso-PS activates the TLR2/6 heterodimer and our developed method to synthesize 20:1 lyso-PS now allows more complex experiments in which the effects of 20:1 lyso-PS on host immune cells can be examined.

Extracellular vesicles and host-parasite interactions during schistosomiasis.

As described above the turnover rate of the outer membranes of adult schistosomes is very high and components of the tegument are shed into the environment (de Oliveira et al., 2013). Relatively recently it was shown that adult schistosomes secrete extracellular vesicles (EVs) containing proteins, lipids and RNA molecules that have been linked to immune regulation (Wang et al., 2015; Sotillo et al., 2016; Zhu et al., 2016; Samoil et al., 2018). EVs are small vesicles released by cells and they play an important role in intercellular communication by delivering payloads such as cytosolic proteins, lipids, and RNA (Raposo and Stoorvogel, 2013; Yanez-Mo et al., 2015). *S. mansoni* is not the only helminth that produces EVs and other parasites, such as *Fasciola hepatica* (Marcilla et al., 2012; Cwiklinski et al., 2015), *S. japonicum* (Wang et al., 2015; Zhu et al., 2016) and *Opisthorchis viverrini* (Chaiyadet et al., 2015) have been shown to excrete EVs as well. So far most studies on EVs produced by parasites have been performed on EVs isolated from *in vitro* incubated parasites (Nowacki et al., 2015; Wang et al., 2015; Sotillo et al., 2016; Zhu et al., 2016). Although culture conditions for *in vitro* maintenance of parasites have greatly increased over the last few years (Wang et al., 2019), parasites in culture will eventually become moribund. This raises the following question when investigating parasites under *in vitro* conditions; are the actual processes of the parasite being investigated or merely the effects of a dying parasite and related events? The absence of a host under these culture conditions is also an issue, as there is no active complement system present nor other components of the immune system to which the parasite has to respond. To circumvent this biased approach, we investigated the lipid and protein composition of EVs circulating in the infected host (in this case, *Mesocricetus auratus*, Syrian Gold Hamster) in comparison to the non-infected controls in order to determine whether EVs of schistosomal origin can be detected in host plasma.

As described in **Chapter 5** we used a well-established size exclusion chromatography method to isolate EVs from plasma (Böing et al., 2014). Size exclusion chromatography is one of several accepted methods currently in use for the isolation of EVs (Baranyai et

al., 2015; Serrano-Pertierra et al., 2019). Protein analysis of the isolated EVs revealed that all identified proteins were from the host and no proteins from *S. mansoni* could be detected under these experimental settings. However, the protein composition of the EVs isolated from infected hamsters was markedly different from that of EVs isolated from non-infected control hamsters. These EV protein profiles suggested the activation (and in-activation) of the complement and coagulation system and the presence of an enhanced primary immune response in the *S. mansoni* infected hamsters. Comparison of the lipid composition of EVs isolated from infected versus those from non-infected hamsters showed similar results, as no specific lipids of *S. mansoni* were detected in EVs of infected hamsters. However, the lipid composition of EVs of infected hamsters differed consistently from that of EVs of non-infected control hamsters, as relatively large differences in (lyso-)phosphatidylcholine (PC), PS and phosphatidylinositol (PI) composition and/or abundance were detected.

Although we were not able to detect EVs produced by schistosomes in the peripheral blood of an experimental host by our methods, evidence for schistosomal EVs in host blood plasma has however been provided by Meninger et al. who isolated EVs from the blood of schistosomiasis patients and detected schistosome-specific microRNA's in these samples (Meninger et al., 2016). In addition, Magalhães (Magalhães et al., 2010; Magalhães et al., 2019) postulated a role for lysophospholipids in schistosomal EVs and suggested that EVs might protect the bio-active lyso-phospholipids from enzyme degradation (Magalhães et al., 2019). These authors suggested that EVs would allow targeted delivery of immune-modifying lipids rather than just having a local effect near the parasite. Altogether these results, when corroborated independently, suggest that EVs containing schistosome specific lipids may circulate in patients' blood, and that these EVs have a function in the complex host-parasite interaction during schistosomiasis.

Energy metabolism of *Naegleria gruberi*; the model organism for *Naegleria fowleri*

In addition to schistosomes most other parasites have a deviant energy metabolism when compared to their host, because parasites do not fully oxidize their nutrients. In this respect the interpretation of the characterized core genome of *Naegleria gruberi* was of interest. *N. gruberi* is not a parasite, but it is an extensively studied model organism for the facultative parasite *N. fowleri*. In this case, facultative means that *N. fowleri* can have a complete free-living life cycle, which does not require a host at any stage, but *N. fowleri* can also infect mammals. In case of uptake of infected water in the nose, the amoeba can penetrate the mucosa and migrate to the brain where they cause primary amoebic meningoencephalitis (PAM). The amoeba then feed on brain cells and cause a severe inflammatory response (Cervantes-Sandoval et al., 2008). The mortality rate of

this fulminant infection is over 95% and so far no proper treatment has been determined. Fritz-Laylin et al. (Fritz-Laylin et al., 2010) characterized the core genome of *N. gruberi* and from this information the authors concluded that this amoeba had “the capacity for both aerobic respiration and anaerobic metabolism with concomitant hydrogen production, with fundamental implications for the evolution of organelle metabolism”. Since the postulated mixture of aerobic respiration and hydrogen production is quite special and because the postulated deviant energy metabolism might harbor targets for drug development against the pathogen, we performed a comprehensive analysis of the energy metabolism of *N. gruberi* in a similar manner as we investigated the (lipid) metabolism of *S. mansoni*, though with very different results (**Chapter 6**).

First we determined the conditions under which *N. gruberi* could survive and multiply. We demonstrated that both a laboratory strain (NEG-M) and a wild-type strain cannot grow under anaerobic conditions or when respiration was blocked by cyanide and salicyl hydroxamic acid (SHAM). Subsequently, the presence of ubiquinone and rhodoquinone in *N. gruberi* trophozoites was investigated. Ubiquinone is used in mitochondria during aerobic respiration to transfer electrons from complex I and II to complex III, while rhodoquinone is used to transfer electrons from complex I to a membrane-bound fumarate reductase. Rhodoquinone is essential in organisms with anaerobically functioning mitochondria (Van Hellemond et al., 1995; Müller et al., 2012), and Fritz-Laylin et al. postulated the presence of rhodoquinone in *N. gruberi* (Fritz-Laylin et al., 2011). However, our analysis demonstrated the presence of ubiquinone in both the NEG-M laboratory strain and the wild-type strain, but rhodoquinone could not be detected in *N. gruberi*. The absence of RQ in combination with the absence of growth under the anaerobic conditions indicates that *N. gruberi*, cannot function anaerobically and, thus, depends on aerobic respiration.

Second, we examined which substrates are preferably used by this amoeba for its energy metabolism. To answer this question, trophozoites were incubated with radioactively labeled substrates (either glucose, fatty acids or amino acids). To our great surprise, lipids were the preferred substrate for energy metabolism, as both long and short chain fatty acids were preferably and completely oxidized to carbon dioxide. Since fatty acids are non-fermentable substrates and their oxidation requires aerobic mitochondrial respiration, this observation further substantiated our earlier conclusion that *N. gruberi* is a strictly aerobic functioning amoeba. Of course, the energy metabolism of *N. gruberi* does not rely on lipids only, as carbohydrates (glucose) and amino acids were also used for energy metabolism, but only to a limited extend. From a biochemical perspective this is also an absolute requirement, because intermediates of the Krebs cycle have to be

replenished regularly using pyruvate originating from glycolysis. In other words, lipids burn in a flame of carbohydrates (Rosenfeld 1895, cited by Ringer, 1914) (Ringer, 1914).

Finally, a genomic comparison was made between *N. gruberi* and *N. fowleri* in order to investigate whether analogs of the genes involved in lipid catabolism in *N. gruberi* are also present in the genome of *N. fowleri*. Our analysis demonstrated that for all the investigated *N. gruberi* genes, an analog could be identified in the genome of *N. fowleri*, which suggests that *N. fowleri* has the same metabolic capacity and most likely also thrives on lipids as a nutrient source. Although this genomic comparison is not a perfect approach, the two species are closely related, and therefore, likely to have a similar metabolism. Furthermore, in nature both *Naegleria* species feed mostly on bacteria, which constitute a source rich in lipids.

As described above, the porte d'entrée of an *N. fowleri* infection is the nasal mucosa of the olfactory nerve. This nasal mucosa is covered in a layer of lipid-secrections, which contain odorant binding proteins that capture and transport odorant molecules to olfactory chemoreceptors of nerve cells. Whether *N. fowleri* recognizes these lipids remains to be investigated, but an alternative option could be the recognition of gangliosides on nerve cells (Ang et al., 2004). After traversing the olfactory nerve, the trophozoites end up in the forebrain. The white matter of the brain is rich in myelin sheets, which surround the axons of nerve cells and contain about 80% lipids by weight (O'Brien and Sampson, 1965). The *N. fowleri* genome encodes a set of glycoside hydrolases, glucosyl-ceramidases, sphingomyelin phosphodiesterases and phospholipases, that could function in the degradation of myelin sheaths into substrates for energy metabolism (Zysset-Burri et al., 2014). Another substrate for *N. fowleri* present in the brain is acetate, which is normally used by astrocytes as a substrate for energy metabolism (Wyss et al., 2011). Altogether the results described in **Chapter 6** demonstrated that *N. gruberi* preferably uses lipids for its energy metabolism, which uncovered a so far unprecedented metabolic specialization in protists with evolutionary and medical significance that could point the way to improved treatments for PAM.

Concluding remarks and future perspectives

In the introduction of this thesis, several questions were asked in relation to the lipid and energy metabolism of parasites and how the adaptations of the parasites might be exploited to improve treatment of parasitic diseases.

Both **Chapters 2 and 3** highlighted the importance of carbohydrates for the energy metabolism of *S. mansoni*, but via different approaches. **Chapter 2** provided insight to the

mechanism involved in regulation of the glycolytic flux in different stages of *S. mansoni*. The enzyme lactate dehydrogenase (LDH) plays an important role in the metabolism of *S. mansoni* and also in the other *Schistosoma* species, and therefore, can be considered a good target for drug development. Our results suggest that adaptations in SmLDH are essential for the parasite during the instant transition from low to high glucose conditions when the parasite infects its mammalian host. Possibly, specific SmLDH inhibitors could be used as a prophylactic drug to prevent *Schistosoma* infections, which is of clinical use as such a drug has not been found yet. In addition, by the recombinant expression method for SmLDH described in **Chapter 2**, large amounts of rSmLDH can be produced that could be used for high throughput screening of compound libraries to identify inhibitors of SmLDH. It is likely that such an inhibitor is present in these libraries, as inhibitors for mammalian LDH have been developed to target cancer cells, as cancer cells have often replaced the slow process of oxidative phosphorylation by anaerobic glycolysis (Liberti and Locasale, 2016). Further investigations to identify lead components that would specifically inhibit SmLDH are therefore worthwhile and could lead to the identification of new (prophylactic) drugs to treat schistosomiasis.

The results described in **Chapter 3** showed that beta-oxidation of lipids does not occur in *S. mansoni*, nor in any other *Schistosoma* species. Hence, this process may not be a prime target for drug intervention for schistosomiasis. However, lipid metabolism is essential for egg production by female worms, and, therefore, interfering with lipid metabolism could still be an interesting drug target as it will limit both transmission and disease pathology caused by schistosomes. In addition, the results described in **Chapter 4** showed that lipids synthesized by schistosomes have an important function in immune modulation of the host. Lyso-PS 20:1 was shown to activate the TLR2/6 heterodimer, which is present on dendritic cells of the host and is involved in the induction of a regulatory T-cell response. So far the physiological role of lyso-PS 20:1 has been difficult to delineate, but since lyso-PS 20:1 can now be synthesized in larger quantities more complex *in vitro* experiments can be performed to assess the potential of lyso-PS 20:1 as an immune modulating factor that could be of use to reduce allergic immune responses.

The study described in **Chapter 5** demonstrated that the schistosome specific lipid 20:1 lyso-PS could not be detected in extracellular vesicles (EVs) in circulating blood of an experimentally infected host. Furthermore, no other schistosome specific lipids nor protein were detected in the peripheral blood of these animals. However, the substantial difference in the protein as well as in the lipid composition of EVs derived from *S. mansoni* infected hosts compared to non-infected hosts, suggests that EVs play an important

role in the host-parasite interaction and/or disease progression during schistosomiasis. More studies in infected versus non-infected human hosts are needed to confirm these preliminary findings.

Finally, the studies on the energy metabolism of *N. gruberi* described in **Chapter 6** showed that lipids are the preferred nutrients of this amoeba. This observation is clinically relevant as it provided us with valuable insights in the energy metabolism of this close relative of the parasite *N. fowleri*. It seems that the lipids within our brains provide ideal conditions for *N. fowleri*. A currently performed follow-up study in our research group aims to identify compounds that inhibit fatty acid oxidation and thereby the growth of *N. fowleri*. Several drugs of which it is known that they inhibit fatty acid oxidation and that are already used in clinical practice, were found to inhibit or completely block the replication of *N. gruberi* *in vitro*. These observations support targeting the energy metabolism in these amoeba and specifically fatty acid oxidation in *Naegleria* for drug interventions.

REFERENCES

- Agnihotri, G., B. M. Crall, T. C. Lewis, T. P. Day, R. Balakrishna, H. J. Warshakoon, S. S. Malladi and S. A. David (2011). "Structure-Activity Relationships in Toll-Like Receptor 2-Agonists Leading to Simplified Monoacyl Lipopeptides." *Journal of Medicinal Chemistry* **54**(23): 8148-8160.
- Ang, C. W., B. C. Jacobs and J. D. Laman (2004). "The Guillain-Barre syndrome: a true case of molecular mimicry." *Trends in Immunology* **25**(2): 61-66.
- Baranyai, T., K. Herczeg, et al. (2015). "Isolation of Exosomes from Blood Plasma: Qualitative and Quantitative Comparison of Ultracentrifugation and Size Exclusion Chromatography Methods." *PLOS ONE* **10**(12): e0145686.
- Berg, J. M., L. Stryer, J. L. Tymoczko and G. J. Gatto (2015). *Biochemistry*, Macmillan Learning.
- Berriman, M., B. J. Haas, et al. (2009). "The genome of the blood fluke *Schistosoma mansoni*." *Nature* **460**(7253): 352-U365.
- Böing, A. N., E. van der Pol, A. E. Grootemaat, F. A. W. Coumans, A. Sturk and R. Nieuwland (2014). "Single-step isolation of extracellular vesicles by size-exclusion chromatography." *Journal of extracellular vesicles* **3**: 10.3402/jev.v3403.23430.
- Bueding, E. (1950). "Carbohydrate metabolism in *Schistosoma mansoni*." *The Journal of General Physiology* **33**(5): 475-495.
- Buro, C., K. C. Oliveira, Z. G. Lu, S. Leutner, S. Beckmann, C. Dissous, K. Cailliau, S. Verjovski-Almeida and C. G. Greveling (2013). "Transcriptome Analyses of Inhibitor-treated Schistosome Females Provide Evidence for Cooperating Src-kinase and TGF beta Receptor Pathways Controlling Mitosis and Eggshell Formation." *Plos Pathogens* **9**(6): e1003448.
- Cervantes-Sandoval, I., J. d. J. Serrano-Luna, E. García-Latorre, V. Tsutsumi and M. Shibayama (2008). "Characterization of brain inflammation during primary amoebic meningoencephalitis." *Parasitology International* **57**(3): 307-313.
- Chaiyadet, S., J. Sotillo, et al. (2015). "Carcinogenic Liver Fluke Secretes Extracellular Vesicles That Promote Cholangiocytes to Adopt a Tumorigenic Phenotype." *Journal of Infectious Diseases* **212**(10): 1636-1645.
- Coakley, G., J. L. McCaskill, et al. (2017). "Extracellular Vesicles from a Helminth Parasite Suppress Macrophage Activation and Constitute an Effective Vaccine for Protective Immunity." *Cell Reports* **19**(8): 1545-1557.
- Colley, D. G., A. L. Bustinduy, W. E. Secor and C. H. King (2014). "Human schistosomiasis." *Lancet* **383**(9936): 2253-2264.
- Cwiklinski, K., E. de la Torre-Escudero, et al. (2015). "The Extracellular Vesicles of the Helminth Pathogen, *Fasciola hepatica*: Biogenesis Pathways and Cargo Molecules Involved in Parasite Pathogenesis." *Molecular & Cellular Proteomics* **14**(12): 3258-3273.
- de Oliveira, C. N. F., R. N. de Oliveira, T. F. Frezza, V. L. G. Rehder and S. M. Allegretti (2013). Tegument of *Schistosoma mansoni* as a therapeutic target. *Parasitic Diseases-Schistosomiasis*, IntechOpen.
- Edwards, J., M. Brown, E. Peak, B. Bartholomew, R. J. Nash and K. F. Hoffmann (2015). "The Diterpenoid 7-Keto-Sempervirol, Derived from *Lycium chinense*, Displays Anthelmintic Activity against both

- Schistosoma mansoni* and *Fasciola hepatica*." *PLoS neglected tropical diseases* **9**(3): e0003604
- Frayha, G. J. and J. D. Smyth (1983). Lipid Metabolism in Parasitic Helminths. *Advances in Parasitology*. J. R. Baker and R. Muller, Academic Press. **22**: 309-387.
- Fritz-Laylin, L. K., M. L. Ginger, C. Walsh, S. C. Dawson and C. Fulton (2011). "The *Naegleria* genome: a free-living microbial eukaryote lends unique insights into core eukaryotic cell biology." *Research in microbiology* **162**(6): 607-618.
- Fritz-Laylin, L. K., S. E. Prochnik, et al. (2010). "The genome of *Naegleria gruberi* illuminates early eukaryotic versatility." *Cell* **140**(5): 631-642.
- Garvie, E. I. (1980). "Bacterial lactate dehydrogenases." *Microbiological reviews* **44**(1): 106.
- Guigas, B. and A. B. Molofsky (2015). "A worm of one's own: how helminths modulate host adipose tissue function and metabolism." *Trends in Parasitology* **31**(9): 435-441.
- Heerden, J. H. V., M. T. Wortel, et al. (2014). "Fatal attraction in glycolysis: how *Saccharomyces cerevisiae* manages sudden transitions to high glucose." *Microbial Cell* **1**(3): 103-106.
- Horemans, A. M. C., A. G. M. Tielens and S. G. van den Bergh (1992). "The reversible effect of glucose on the energy metabolism of *Schistosoma mansoni* cercariae and schistosomula." *Molecular and Biochemical Parasitology* **51**(1): 73-79.
- Howe, K. L., B. J. Bolt, M. Shafie, P. Kersey and M. Berriman (2017). "WormBase ParaSite - a comprehensive resource for helminth genomics." *Molecular and Biochemical Parasitology* **215**: 2-10.
- Huang, S. C.-C., T. C. Freitas, E. Amiel, B. Everts, E. L. Pearce, J. B. Lok and E. J. Pearce (2012). "Fatty Acid Oxidation Is Essential for Egg Production by the Parasitic Flatworm *Schistosoma mansoni*." *Plos Pathogens* **8**(10): e1002996.
- International Helminth Genomes, C. (2019). "Comparative genomics of the major parasitic worms." *Nature genetics* **51**(1): 163-174.
- Kang, J. Y., X. Nan, et al. (2009). "Recognition of lipopeptide patterns by Toll-like receptor 2-Toll-like receptor 6 heterodimer." *Immunity* **31**(6): 873-884.
- Liberti, M. V. and J. W. Locasale (2016). "The Warburg effect: how does it benefit cancer cells?" *Trends in Biochemical Sciences* **41**(3): 211-218.
- Litwack, G. (2018). Chapter 14 - Metabolism of Fat, Carbohydrate, and Nucleic Acids. *Human Biochemistry*. G. Litwack. Boston, Academic Press: 395-426.
- Lu, Z., F. Sessler, N. Holroyd, S. Hahnel, T. Quack, M. Berriman and C. G. Grevelding (2017). "A gene expression atlas of adult *Schistosoma mansoni* and their gonads." *Scientific data* **4**: 170118.
- Magalhães, K. G., P. E. Almeida, G. C. Atella, C. M. Maya-Monteiro, H. C. Castro-Faria-Neto, M. Pelajo-Machado, H. L. Lenzi, M. T. Bozza and P. T. Bozza (2010). "Schistosomal-Derived Lysophosphatidylcholine Are Involved in Eosinophil Activation and Recruitment through Toll-Like Receptor-2-Dependent Mechanisms." *Journal of Infectious Diseases* **202**(9): 1369-1379.
- Magalhães, K. G., T. Luna-Gomes, F. Mesquita-Santos, R. Corrêa, L. S. Assunção, G. C. Atella, P. F. Weller, C. Bandeira-Melo and P. T. Bozza (2019). "Schistosomal Lipids Activate Human Eosinophils via Toll-Like Receptor 2 and PGD2 Receptors: 15-LO Role in Cytokine Secretion." *Frontiers in immunology* **9**(3161).
- Mansour, T. E. and E. Bueding (1953). "Kinetics of lactic dehydrogenases of *Schistosoma mansoni* and of rabbit muscle." *British Journal of Pharmacology* **8**(4): 431-434.
- Marcilla, A., M. Trelis, et al. (2012). "Extracellular Vesicles from Parasitic Helminths Contain Specific Excretory/Secretory Proteins and Are Internalized in Intestinal Host Cells." *PLOS ONE* **7**(9): e45974.
- Meningher, T., G. Lerman, N. Regev-Rudzki, D. Gold, I. Z. Ben-Dov, Y. Sidi, D. Avni and E. Schwartz (2016). "Schistosomal MicroRNAs Isolated From Extracellular Vesicles in Sera of Infected Patients: A New Tool for Diagnosis and Follow-up of Human Schistosomiasis." *The Journal of Infectious Diseases* **215**(3): 378-386.
- Meyer, F., H. Meyer and E. Bueding (1970). "Lipid metabolism in the parasitic and free-living flatworms, *Schistosoma mansoni* and *Dugesia dorotocephala*." *Biochimica et biophysica acta* **210**(2): 257-266.
- Müller, M., M. Mentel, et al. (2012). "Biochemistry and evolution of anaerobic energy metabolism in eukaryotes." *Microbiology and Molecular Biology Reviews* **76**(2): 444-495.
- Nowacki, F. C., M. T. Swain, et al. (2015). "Protein and small non-coding RNA-enriched extracellular vesicles are released by the pathogenic blood fluke *Schistosoma mansoni*." *Journal of extracellular vesicles* **4**: 28665.
- O'Brien, J. S. and E. L. Sampson (1965). "Lipid composition of the normal human brain: gray matter, white matter, and myelin." *Journal of Lipid Research* **6**(4): 537-544.
- Oliveira, M. P., J. B. Correa Soares and M. F. Oliveira (2016). "Sexual Preferences in Nutrient Utilization Regulate Oxygen Consumption and Reactive Oxygen Species Generation in *Schistosoma mansoni*: Potential Implications for Parasite Redox Biology." *PLOS ONE* **11**(7): e0158429.
- Raposo, G. and W. Stoorvogel (2013). "Extracellular vesicles: Exosomes, microvesicles, and friends." *The Journal of Cell Biology* **200**(4): 373-383.
- Retra, K., S. deWalick, M. Schmitz, M. Yazdanbakhsh, A. G. M. Tielens, J. F. H. M. Brouwers and J. J. van Hellemond (2015). "The tegumental surface membranes of *Schistosoma mansoni* are enriched in parasite-specific phospholipid species." *International journal for parasitology* **45**(9-10): 629-636.
- Ringer, A. I. (1914). "Studies In Diabetes I. Theory Of Diabetes, With Consideration Of The Probable Mechanism Of Antiketogenesis And The Cause Of Acidosis." *Journal of Biological Chemistry* **17**(2): 107-119.
- Rumjanek, F. D. and A. J. G. Simpson (1980). "The incorporation and utilization of radiolabelled lipids by adult *Schistosoma mansoni* in vitro." *Molecular and Biochemical Parasitology* **1**(1): 31-44.
- Salunke, D. B., S. W. Connelly, N. M. Shukla, A. R. Hermanson, L. M. Fox and S. A. David (2013). "Design and Development of Stable, Water-Soluble, Human Toll-like Receptor 2 Specific Monoacyl Lipopeptides as Candidate Vaccine Adjuvants." *Journal of Medicinal Chemistry* **56**(14): 5885-5900.
- Samoil, V., M. Dagenais, V. Ganapathy, J. Aldridge, A. Glebov, A. Jardim and P. Ribeiro (2018). "Vesicle-based secretion in schistosomes: Analysis of protein and microRNA (miRNA) content of exosome-like vesicles derived from *Schistosoma mansoni*." *Scientific reports* **8**: 3286.
- Serrano-Pertierra, E., M. Oliveira-Rodríguez, M. Rivas, P. Oliva, J. Villafani, A. Navarro, M. C. Blanco-López and E. Cernuda-Morollón (2019). "Characterization of Plasma-Derived Extracellular Vesicles Isolated by Different Methods: A Comparison Study." *Bioengineering* **6**(1): 8.

- Sotillo, J., M. Pearson, J. Potriquet, L. Becker, D. Pickering, J. Mulvenna and A. Loukas (2016). "Extracellular vesicles secreted by *Schistosoma mansoni* contain protein vaccine candidates." *International journal for parasitology* **46**(1): 1-5.
- Tielens, A. G. M. (1997). Biochemistry of trematodes. *Advances in Trematode Biology*. B. Fried and T. K. Graczyk, CRC Press, Boca Raton, Florida: 309-343.
- Tielens, A. G., J. M. Van den Heuvel, H. J. Van Mazijk, J. E. Wilson and C. B. Shoemaker (1994). "The 50-kDa glucose 6-phosphate-sensitive hexokinase of *Schistosoma mansoni*." *Journal of Biological Chemistry* **269**(40): 24736-24741.
- Tielens, A. G. M., A. M. C. Horemans, R. Dunnewijk, P. van der Meer and S. G. van den Bergh (1992). "The facultative anaerobic energy metabolism of *Schistosoma mansoni* sporocysts." *Molecular and Biochemical Parasitology* **56**(1): 49-57.
- Tielens, A. G. M., F. A. M. van de Pas, J. M. van den Heuvel and S. G. van den Bergh (1991). "The aerobic energy metabolism of *Schistosoma mansoni* miracidia." *Molecular and Biochemical Parasitology* **46**(1): 181-184.
- Timson, D. J. (2016). "Metabolic Enzymes of Helminth Parasites: Potential as Drug Targets." *Current Protein & Peptide Science* **17**(3): 280-295.
- Van der Kleij, D., E. Latz, et al. (2002). "A novel host-parasite lipid cross-talk - Schistosomal lysophosphatidylserine activates Toll-like receptor 2 and affects immune polarization." *Journal of Biological Chemistry* **277**(50): 48122-48129.
- Van Hellemond, J. J., K. Retra, J. F. H. M. Brouwers, B. W. M. van Balkom, M. Yazdanbakhsh, C. B. Shoemaker and A. G. M. Tielens (2006). "Functions of the tegument of schistosomes: Clues from the proteome and lipidome." *International Journal For Parasitology* **36**(6): 691-699.
- Van Oordt, B. E. P., A. G. M. Tielens and S. G. Van den Bergh (1989). "Aerobic to anaerobic transition in the carbohydrate-metabolism of *Schistosoma mansoni* cercariae during transformation in vitro." *Parasitology* **98**: 409-415.
- Wang, J., R. Chen and J. J. Collins Iii (2019). "Systematically improved in vitro culture conditions reveal new insights into the reproductive biology of the human parasite *Schistosoma mansoni*." *PLoS biology* **17**(5): e3000254.
- Wang, L., Z. Li, J. Shen, Z. Liu, J. Liang, X. Wu, X. Sun and Z. Wu (2015). "Exosome-like vesicles derived by *Schistosoma japonicum* adult worms mediates M1 type immune- activity of macrophage." *Parasitology Research* **114**(5): 1865-1873.
- Wyss, M. T., P. J. Magistretti, A. Buck and B. Weber (2011). "Labeled acetate as a marker of astrocytic metabolism." *Journal of Cerebral Blood Flow & Metabolism* **31**(8): 1668-1674.
- Yanez-Mo, M., P. R. M. Siljander, et al. (2015). "Biological properties of extracellular vesicles and their physiological functions." *Journal of extracellular vesicles* **4**: 27066.
- Žárský, V. and J. Tachezy (2015). "Evolutionary loss of peroxisomes – not limited to parasites." *Biology Direct* **10**: 74.
- Zhu, L., J. Liu, J. Dao, K. Lu, H. Li, H. Gu, J. Liu, X. Feng and G. Cheng (2016). "Molecular characterization of

S. japonicum exosome-like vesicles reveals their regulatory roles in parasite-host interactions." *Scientific reports* **6**.

- Zysset-Burri, D. C., N. Müller, C. Beuret, M. Heller, N. Schürch, B. Gottstein and M. Wittwer (2014). "Genome-wide identification of pathogenicity factors of the free-living amoeba *Naegleria fowleri*." *BMC genomics* **15**(1): 496.



APPENDICES

Dutch summary/
Nederlandstalige samenvatting
CV
PhD Portfolio
List of publications
Dankwoord

DUTCH SUMMARY NEDERLANDSTALIGE SAMENVATTING

Introductie over parasieten/parasitisme

Parasieten vindt men overal. In de biomedische wetenschap wordt de volgende definitie voor parasieten gehanteerd: "zich in stand houdend in of op een gastheer van een andere soort, van waar voedingsstoffen worden onttrokken, ter betering van zichzelf". Uiteraard voldoen ziekteverwekkers zoals bacteriën, virussen en schimmels ook aan deze definitie, maar tot de groep "parasieten" rekenen we enkel protozoa (eencellige eukaryoten) en metazoa (multi-cellulaire eukaryoten). In contact komen met parasieten is voor de mens onvermijdelijk, maar een infectie wordt niet altijd opgemerkt. Maar liefst 90% van de bevolking raakt geïnfecteerd met één of meerdere parasieten gedurende zijn of haar leven. Op dit moment zijn er maar liefst 350 verschillende soorten parasieten beschreven welke de mens kunnen infecteren. In deze groep valt bijvoorbeeld de protist *Giardia lamblia*, slechts 10 micron groot, de runderlintworm *Taenia saginata*, die wel 20 meter lang kan worden, maar ook ecto-parasieten zoals teken en luizen. Humane parasitaire infecties zijn wijdverbreid, het wordt geschat dat jaarlijks wereldwijd meer dan 1 miljoen mensen overlijden als gevolg van parasitaire ziektes.

Het verminderen van deze aantallen blijkt een complexe taak. Er zijn maar een beperkt aantal anti-parasitaire middelen bekend, en de beschikbaarheid hiervan in (arme) endemische gebieden is erg beperkt.

Een universeel medicijn tegen parasieten is waarschijnlijk een brug te ver, hiervoor is de groep die we parasieten noemen, te divers. Er is echter wel een universeel thema dat alle parasieten verbindt, dat is namelijk de gastheer. Zonder deze gastheer kunnen parasieten niet overleven, deze is namelijk de bron van alle voedingsstoffen.

Vanuit de gastheer onttrekt de parasiet onder andere voedingsstoffen voor het energie-metabolisme, zoals glucose, maar ook bouwstoffen voor structurele componenten, zoals lipiden en eiwitten. Bouwstoffen worden door de meeste parasieten zo min mogelijk gemodificeerd en direct verwerkt vanuit de gastheer. Hierdoor spelen dergelijke biosynthetische processen naar verhouding een kleinere rol in parasieten dan in andere (vrijlevende) organismes, en zijn daardoor een minder interessant doelwit voor interventie. Het essentiële energie-metabolisme van de parasiet is echter een zeer interessant doelwit. De parasiet kan verschillende voedingsstoffen zoals suikers, vetten en eiwitten verkrijgen van de gastheer, maar zal vervolgens zelf adenosine trifosfaat (ATP) moeten (re)genereren. Dit essentiële molecuul kan immers niet verkregen worden vanuit de gastheer.

Processen om ATP te (re)genereren in parasieten wijken vaak sterk af van de processen aanwezig in de (humane) gastheer. Het humane energie-metabolisme is (voornamelijk) aerob, voor de regeneratie van ATP is zuurstof vereist maar het energie-metabolisme van parasieten is vaker anaerob. Een dergelijk verschil in metabolisme is een ideaal doelwit voor de ontwikkeling van potentiële medicinale interventies die parasitaire processen kunnen verstoren. Het doel van het onderzoek beschreven in dit proefschrift is het verschaffen van meer inzicht in de betreffende unieke (metabole) processen en het achterhalen welke rol deze spelen in de gastheer-parasiet interactie, maar ook welke processen dermate belangrijk zijn voor de parasiet, dat verstoring van deze processen zou kunnen helpen in het bestrijden van parasitaire infecties. We hebben ons geconcentreerd op het energie-metabolisme en gerelateerde processen van twee belangrijke parasieten, *Schistosoma mansoni* en *Naegleria fowleri*.

Onderzoek naar het metabolisme van *S. mansoni*

De parasitaire worm *Schistosoma* komt voor in grote delen van de wereld, voornamelijk in het Sub-Sahara gebied van Afrika, en in grote delen van Azië. Infectie met *Schistosoma*, Schistosomiasis, zorgt voor ongeveer 100.000 doden per jaar, er bevinden zich meer dan 200 miljoen mensen in de risicogroep voor infectie. In dit proefschrift is het metabolisme van een bepaalde soort, *Schistosoma mansoni*, uitgebreid onderzocht. Een infectie met *Schistosoma mansoni* kan worden opgelopen na contact met door *Schistosoma*-larven besmet water. Deze larven, cercariën genaamd, penetreren de huid op zoek naar een bloedvat. Vervolgens migreert de larve via de bloedsomloop naar de bloedvaten rondom de darm. Tijdens deze migratie transformeert de larve tot een juveniele worm. Hier vormen een mannelijke en vrouwelijke worm samen een wormpaartje, een belangrijke stap in de maturatie van de juveniele worm. Uiteindelijk vestigen de volwassen wormpaartjes zich in de mesenteriale vaten, hier leggen de vrouwtjes per stuk zo'n 300 eieren per dag. Deze eieren komen via de bloedvatwand in de darm terecht, om zo met de ontlasting mee het lichaam te verlaten. Wanneer deze eieren weer in zoetwater terecht komen, komt het er uit het ei een miracidium, welke infectieus is voor de zoetwaterslak (geslacht *Biomphalaria* of *Oncomelania*). Na penetratie vinden enkele transformaties plaats, en vervolgens komen uit deze slak weer de cercariën, de eerder beschreven larven. Deze kunnen weer een nieuwe (humane) gastheer besmetten om zo de cyclus rond te maken. Tijdens de levenscyclus van *Schistosoma* wisselt het energie-metabolisme van de parasiet enkele malen; grof gezegd is het energie-metabolisme in de gastheer voornamelijk anaerob en daarbuiten voornamelijk aerob. Volwassen wormen fermenteren vooral, zij zetten pyruvaat (verkregen uit anaerobe glycolyse van glucose) om naar lactaat via lactaat dehydrogenase (LDH). De vrijlevende stadia hebben een overwegend aerob metabolisme, waarin pyruvaat wordt getransporteerd

naar het mitochondrion waar dit wordt verwerkt via de citroenzuurcyclus en oxidatieve fosforylering, op deze manier gaan de aerobe cercariën efficiënter om met hun (beperkte) energievoorraad. Uit eerder onderzoek was reeds bekend dat het LDH een centrale rol speelt in deze wisseling van het energie-metabolisme in *S. mansoni*. Dit maakt LDH een interessant enzym om verder te onderzoeken en de vraag te beantwoorden: hoe zorgt LDH er voor dat pyruvaat op de juiste manier wordt verwerkt in de verschillende stadia van *S. mansoni*?

In **Hoofdstuk 2** is het *Schistosoma mansoni* LDH enzym (SmLDH) onderzocht. Het enzym is hiervoor opgezuiverd uit volwassen wormen, maar ook recombinant tot expressie gebracht. Vervolgens hebben we de kinetiek van deze enzymen vergeleken met die van LDH geïsoleerd uit spierweefsel van een konijn. Dit liet zien dat het *S. mansoni* LDH duidelijk afwijkt van konijnen-LDH. Dit is bijzonder voor een enzym dat normaliter vrij sterk geconserveerd is tussen verschillende (dier)soorten. Het enzym uit de parasiet werd geremd door adenosine trifosfaat, en gestimuleerd door fructose 1,6 bisfosfaat (FBP), een intermediair uit de glycolyse. Dit stimulerende effect van FBP was het sterkste als SmLDH reeds geremd was door ATP. Om dit alles beter te begrijpen is er een simulatie gemaakt van de glycolyse en citroenzuurcyclus van *S. mansoni*. Hieruit werd duidelijk dat deze unieke ATP-geremde, FBP gestimuleerde LDH de spil is van de schakeling van het energie-metabolisme van *S. mansoni*. Het energie-metabolisme van Schistosomen wordt klassiek beschouwd als een anaeroob metabolisme, met als belangrijkste voedingsbron koolhydraten in de vorm van glucose/glycogeen. Recent werd dit dogma in twijfel getrokken door andere onderzoekers, zij voorzagen een belangrijke rol voor lipiden binnen het energie-metabolisme van *S. mansoni*. Dit was voor onze onderzoeksgroep aanleiding voor het onderzoek in **Hoofdstuk 3** waarin het lipide-katabolisme van *S. mansoni* aan grondig onderzoek is onderworpen. De resultaten uit dit onderzoek waren ondubbelzinnig, uit onze experimenten bleek dat *S. mansoni* geen lipiden gebruikt om ATP mee te kunnen (re)genereren. Uit vergelijking met 9 verschillende genomen bleek dat het *S. mansoni* genoom niet de vereiste genen bevatte. Hiermee hebben we laten zien dat *S. mansoni* lipiden niet afbreekt en dit ook niet kan. Uit verdere analyse van de eieren van *S. mansoni* bleek dat lipiden in het ei een belangrijke rollen spelen tijdens de biosynthese van membranen van het ontwikkelende miracidium. Op deze manier is het lipide-metabolisme van *S. mansoni* wellicht een interessant doelwit voor het onderbreken van de levenscyclus.

De rol van lipiden en gastheer-parasiet interactie

Hoewel de rol van lipiden binnen het energie-metabolisme van *S. mansoni* verwaarloosbaar bleek te zijn, betekent dit niet automatisch dat lipiden geen enkele rol spelen voor *S.*

mansoni. Het tegument is een lipide-rijke structuur aan de buitenzijde van *S. mansoni* en bestaat uit twee gefuseerde lipiden bi-lagen, een viervoudige lipidenstructuur dus. Verversing van deze lipiden-buitenlaag draagt bij aan de ontwijking van detectie door het immuunsysteem van de gastheer. Een van de lipiden waaruit het tegument bestaat is 20:1 lyso-fosfatidylserine (lyso-PS), een mono-acyl fosfolipide. In eerder onderzoek is aangetoond dat dit molecuul kan binden aan een receptor van het immuunsysteem van de gastheer, Toll-like receptor 2, en de initiële immuunrespons tegen *S. mansoni* kan onderdrukken. In **Hoofdstuk 4** hebben we dit molecuul en zijn interactie met het immuunsysteem nader onderzocht. Er is een methode ontwikkeld voor de biochemische synthese van 20:1 lyso-fosfatidylserine. Met dit synthetische product is vervolgens achterhaald dat bij de moleculaire interactie tussen 20:1 lyso-PS en TLR2, ook TLR6 betrokken is. Via een computermodel is deze interactie tussen 20:1 lyso-PS en TLR2/6 verder in kaart gebracht. Hieruit werd duidelijk dat deze interactie veel overeenkomsten vertoont met een reeds gepubliceerd model van een bewezen TLR2/6 activator, FSL-1.

De resultaten van de volgende studie in **Hoofdstuk 5** sluiten nauw aan op dit onderzoek, hier is onderzoek gedaan naar de effecten van een *S. mansoni* infectie op de samenstelling van extracellulaire vesicles (EVs), kleine druppels van slechts 100 nanometers groot, gevuld met lipiden, eiwitten of DNA, die een belangrijke rol spelen in intercellulaire communicatie. Uit *in vitro* onderzoek is gebleken dat *S. mansoni* ook zelf EVs aanmaakt, deze data waren echter nog niet ondersteund door *in vivo* data.

In **Hoofdstuk 5** zijn de resultaten te vinden van een studie naar de samenstelling van EVs geïsoleerd uit het bloed van hamsters geïnfecteerd met *S. mansoni*. We hebben specifiek gezocht naar eiwitten en lipiden van *S. mansoni* in de geïsoleerde EVs. Hoewel we die schistosomen-specifieke lipiden niet hebben gevonden, waren er wel duidelijk verschillen te vinden in de samenstelling van EVs geïsoleerd uit besmette of onbesmette hamsters. Uit de analyse van de samenstelling van EVs, bleek dat *S. mansoni* infectie ervoor had gezorgd dat bepaalde stollingseiwitten nu aanwezig waren in de EVs. Ook was de lipide-samenstelling van de EV's flink veranderd. De implicaties hiervan moeten nader onderzocht worden.

Onderzoek naar het metabolisme van *Naegleria gruberi*

Het laatste experimentele hoofdstuk van dit proefschrift, **Hoofdstuk 6**, beschrijft de resultaten van een uitgebreid onderzoek naar het energie-metabolisme van *N. gruberi*. Hoewel deze amoebe zelf geen parasiet is, wordt deze beschouwd als model-organisme voor de parasiet *Naegleria fowleri*. *N. fowleri* is een unieke parasiet, een die kan overleven zonder gastheer. Deze amoebe komt met name voor

in warmwaterbronnen met een temperatuur tussen de 26 en 46° Celsius. Men kan besmet worden door nasale blootstelling aan dit water, bijvoorbeeld door te zwemmen in een geïnfecteerd meer. Andere risicofactoren zijn nasale irrigatie, met als doel het uitspoelen van de sinussen. Ook tijdens bepaalde religieuze reinigingsrituelen schrijft men nasale opname van water voor. Mocht dit water besmet zijn met *N. fowleri* en raakt men geïnfecteerd dan is dit in meer dan 95% van gevallen dodelijk. Deze ziekte, waarbij *N. fowleri* de hersenen infecteert en hierbij grote gaten maakt in het hersenweefsel, wordt primaire amoeben meningo-encephalitis (PAM) genoemd en kenmerkt zich door koorts, hoofdpijn, stijve nek, en overgeven. Door deze combinatie van symptomen is PAM moeilijk te diagnosticeren, deze symptomen komen overeen met de veel vaker voorkomende bacteriële meningitis. De behandeling is uiteraard niet hetzelfde. Er zijn momenteel weinig efficiënte middelen bekend die snel werkzaam zijn tegen *N. fowleri*. Nieuwe middelen voor een betere behandeling zijn nodig.

In **Hoofdstuk 6** zijn de resultaten te vinden van het onderzoek naar het energie-metabolisme van het model-organisme voor *N. fowleri*, *N. gruberi*. In een eerder onderzoek door een andere groep is de suggestie gewekt dat *N. gruberi* potentieel een anaeroob metabolisme zou hebben. Dit zou implicaties kunnen hebben voor een eventuele (nieuw te ontwikkelen) behandelingsmethode. We hebben daarom van twee verschillende *N. gruberi* stammen onderzocht of deze konden groeien onder aerobe en/of anaerobe omstandigheden. Deze resultaten van beide stammen waren hetzelfde en eenduidig, *N. gruberi* kan niet groeien onder anaerobe omstandigheden. Uit deze experimenten werd duidelijk dat *N. gruberi* enkel kan functioneren in aanwezigheid van zuurstof. De volgende vraag was dan ook, welk substraat wordt verbruikt door *N. gruberi*? Hiervoor werden amoeben geïncubeerd tezamen met suikers, lipiden, of aminozuren. Tot onze grote verbazing bleek hieruit dat *N. gruberi* een sterke voorkeur heeft voor het verbranden van vetten. Bij een gelijk aanbod, worden lipiden veel meer verbrand dan suikers of aminozuren. Dit resultaat ondersteunde onze eerdere conclusie, betreffende het aerobe karakter van *N. gruberi*, lipiden kunnen immers alleen verbrand worden in de aanwezigheid van zuurstof, en kunnen niet (anaeroob) gefermenteerd worden. Om deze resultaten te vertalen naar een relevante klinische situatie, hebben we de genomen van *N. gruberi* en *N. fowleri* met elkaar vergeleken. Hieruit bleek dat alle relevante eiwitten voor een lipide metabolisme aanwezig waren in zowel *N. gruberi* als in *N. fowleri*. Dit zou betekenen dat *N. fowleri* in staat is om lipiden te metaboliseren, en daarom is het lipide-metabolisme dus een erg interessant doelwit voor medicinale interventie.

Conclusie

De onderzoeken beschreven in dit proefschrift hebben nieuwe inzichten gegeven in

het (energie) metabolisme van twee belangrijke humane parasieten, *S. mansoni* en *N. fowleri*. Er zijn nieuwe doelwitten geïdentificeerd voor mogelijke toekomstige medicinale interventies. Zowel voor LDH (een potentieel doelwit in *S. mansoni*) als voor het lipide-metabolisme (een doelwit in *N. fowleri*), bestaan al verschillende goedgekeurde medicijnen voor gebruik bij andere ziektes. Maar deze zijn echter nog niet onderzocht voor hun werkzaamheid tegen parasieten. Dit zou een belangrijke interventie kunnen worden. Voor onderzoeken van medicijnen effectief tegen LDH van *S. mansoni* is een *in vitro* testsysteem ontwikkeld, dat geautomatiseerd zou kunnen worden. Verder zijn de observaties gedaan in dit proefschrift ten aanzien van de gastheer-parasiet interactie zijn een aanvulling op de huidige literatuur betreffende immuun-ontwijking en immuun-modulatie door *S. mansoni*.

CURRICULUM VITAE

Michiel Leendert Bexkens was born on the 18th of February 1986 in Breda, The Netherlands. After secondary school, he enrolled at the Academy for the Technology of Health and Environment in Breda to study Biology and Medical Laboratory Research. In the third year of his education (2006), he moved to Sydney, Australia, to perform research on stem cells in the lab of Prof. Dr. T. Chan-Ling and Dr. M. W. Weible II. Specifically, the effects of noggin and BMP4 on oligo-dendrocytic lineage elaboration in spinal-cord derived neural precursor cells were studied. After finishing his research in Australia, he sold his surfboard and returned to The Netherlands in 2007, to complete his bachelor thesis at Alloksys Life Sciences in Utrecht under the guidance of Dr. R. Brands and Professor Dr. W. Seinen. Here he was first introduced to the wonderful world of enzyme kinetics, studying the protective effects of prophylactic treatment with alkaline phosphatase prior to cardiac surgery. After obtaining his B.Sc. (2008) he started as a research-technician at the department of Medical Microbiology and Infectious Diseases, to support the newly formed Host-Parasite interaction research group of Dr. J.J. van Hellemond and Prof. Dr. A.G.M. Tielens. In 2011 he started his Ph.D. on “Biochemical adaptations in host-parasite interactions”, of which this thesis is now the result. Since 2017, he works in the same department where he investigates the early detection of pathogens and rapid detection of antimicrobial resistance by using mass-spectrometry and related techniques.

Ph.D. PORTFOLIO

Candidate:	Michiel Leendert Bexkens
Institute:	Erasmus MC
Department:	Medical Microbiology and Infectious Diseases
Research school:	Molecular Medicine postgraduate school
Promotors:	Prof. Dr. H.A. Verbrugh, Prof. Dr. A.G.M. Tielens
Co-promotor:	Dr. J.J. van Hellemond

Courses followed	Year
Article 12, certified as animal technician	2009
Basic course on R	2010
Biomedical English writing	2013
Photoshop and Illustrator CS5	2013
Research Integrity	2015
Workshop on Ensembl	2016
Programming with Python	2016
Conferences/presentations	
NVP, Spring Meeting of the Netherlands Society for Parasitology	2012-2016
NVMM , Dutch Society for Medical Microbiology, <i>poster presentation</i>	2012
Gordon Research Conference, Rhode Island, USA, <i>poster presentation</i>	2016
TU Delft/Erasmus MC convergence seminar, Rotterdam	2018
NVML, Zwolle, <i>invited speaker</i>	2019
ECCMID, Amsterdam	2019
Teaching	
Teaching assistant, course on Infectious Diseases.	2011-2020
Supervision of internships	2013-2020
Course on antibiotic resistance	2018-2019
Grants received	
NVP travel grant	2016
Erasmus Trust fund travel grant	2016
Gordon Conference attendance Grant	2016

LIST OF PUBLICATIONS

deWalick, S., **M. L. Bexkens**, B. W. M. van Balkom, Y.-P. Wu, C. H. Smit, C. H. Hokke, P. G. de Groot, A. J. R. Heck, A. G. M. Tielens and J. J. van Hellemond (2011). "The proteome of the insoluble *Schistosoma mansoni* eggshell skeleton." *International Journal for Parasitology* **41**(5): 523-532.

deWalick, S., P. J. Hensbergen, **M. L. Bexkens**, C. Grosserichter-Wagener, C. H. Hokke, A. M. Deelder, P. G. de Groot, A. G. M. Tielens and J. J. van Hellemond (2014). "Binding of von Willebrand factor and plasma proteins to the eggshell of *Schistosoma mansoni*." *International Journal for Parasitology* **44**(5): 263-268.

Bexkens, M. L., V. Zimorski, M. J. Sarink, H. Wienk, J. F. Brouwers, J. F. De Jonckheere, W. F. Martin, F. R. Opperdoes, J. J. van Hellemond and A. G. M. Tielens (2018). "Lipids Are the Preferred Substrate of the Protist *Naegleria gruberi*, Relative of a Human Brain Pathogen." *Cell Reports* **25**(3): 537-543

Bexkens, M. L., M. M. Mebius, M. Houweling, J. F. Brouwers, A. G. M. Tielens and J. J. van Hellemond (2019). "*Schistosoma mansoni* does not and cannot oxidise fatty acids, but these are used for biosynthetic purposes instead." *International Journal for Parasitology* **49**(8): 647-656.

Foudraine, D. E., L. J. M. Dekker, N. Strepis, **M. L. Bexkens**, C. H. W. Klaassen, T. M. Luider, W. H. F. Goessens. (2019) "Accurate detection of the four most prevalent carbapenemases in *E. coli* and *K. pneumoniae* by high-resolution mass spectrometry". *Frontiers in Microbiology*. **26**; 10:2760.

Normand, A. C., G. Frederic, C. Cassange, N. Bourgeois, A. Huguenin, P. Chauvin, D. DeGeyter, **M. L. Bexkens**, E. Rubio, M. Hendrickx, S. Ranque, R. Piarroux.(2020) "Optimization of MALDI-ToF mass spectrometry for yeast identification: a multicentric study" *Medical Mycology*. **58**(5):639-649

Bexkens, M. L., R. A. van Gestel, A. Böing, B. van Breukelen, R. T. Urbanus, J. F. Brouwers, R. Nieuwland, A. G. M. Tielens and J. J. van Hellemond (2020) "*Schistosoma mansoni* affects the proteome and lipidome of circulating extracellular vesicles in the host. *Molecular and Biochemical Parasitology*. **238** P111296

Bexkens, M.L., M. Houweling, P. C. Burgers, T. M. Luider, A. G. M. Tielens and J. J. van Hellemond. "A mono-acyl phospholipid (20:1 lyso-PS) activates Toll-Like Receptor 2/6 hetero-dimer". *Submitted for publication*

Bexkens, M. L., O.M.F Martin, J. M. van den Heuvel, M. G .J. Schmitz, B. Teusink, J.R. Haanstra, J. J. van Hellemond, M.D. Walkinshaw and A.G.M. Tielens. "The unusual properties of lactate dehydrogenase of *Schistosoma mansoni* play a distinct role in metabolic adaptations that occur during the life cycle of this parasite". *In preparation*

DANKWOORD

Een woord van dank. Is één woord genoeg vraag ik me dan af voor zo'n heel proefschrift? Nee waarschijnlijk niet, dan toch maar een dank-manuscript schrijven? Moet je dat dank-manuscript dan ook laten peer-reviewen? Waarbij reviewer #1 je wijst op een paar pijnlijke type/schrijffouten. Maar verder noemt hij het een prima dankwoord, zo publiceren. Maar reviewer #2, die gaat los. Blijkbaar zijn dankwoorden helemaal zijn ding, hij is gepromoveerd op dankwoorden. Zijn eerste vraag: Hoe je het in je hoofd haalt om je dankwoord niet te beginnen met je familie, en bovendien die paragraaf over “de lieve Heer die vogeltjes doet fluiten terwijl hij niet bestaat” (H. van Veen, S. Rosenberg, N. Rosenberg, N. Rosenberg) staat hem zeer zeker niet aan. Zelden heeft hij zo'n slecht dankwoord gelezen...

Maar dan zie je het, in zijn repliek, één zinsnede die je eerder hebt gelezen, ergens in oud manuscript, lang geleden, en je weet ineens wie reviewer #2 is. Je leest je dankwoord nog eens na, woord voor woord. En inderdaad, je bent reviewer #2 vergeten te bedanken. Vlug naar de baas, die het dank-manuscript eerder (wellicht terecht) “een omgevallen boekenkast” had genoemd. Of hij nog een keer wil meekijken. Hij is het met je eens, reviewer #2 heeft je tuk. Wat je ook zegt of doet, bij reviewer #2 heb je het verpest, je dank-manuscript is niet meer te redden. Nee dat lijkt me niks, dan probeer ik het maar kort te houden.

Jaap en Lodewijk, bedankt voor al jullie steun en harde werk tijdens dit promotie-traject. Lodewijk, bedankt voor je hartelijke ontvangst op je lab in Utrecht, en wat vind ik het inspirerend om te zien dat je nu nog steeds graag de labjas aan trekt, en nog “even” een “proefje” inzet. Wat heb ik genoten van de “vrijdagmiddag-experimenten” en de ruimte om buiten het gebaande pad te lopen, om nóg maar eens een “wild goose chase” in te zetten. Ik ben erg blij dat we in al die jaren ook een aantal vette ganzen hebben mogen vangen, in het bijzonder het *Naegleria gruberi* verhaal. De uren/dagen achter de kolommen zie ik nu als een mooi leermoment, duizend potjes, honderden fracties, maar gelukkig allemaal niet voor niks. Ook bedankt voor je generous criticism op al het schrijfwerk wat ik bij je heb ingeleverd, je lessen zijn zeker blijven hangen, nu het toepassen nog! Jaap, in deze promotie was je een onmisbare partner, zo wel voor mij als voor Lodewijk denk ik. Het probleem met de vrijdagmiddag-experimenten is dat ze vaak meer vragen opleverden dan antwoorden. Meer dan eens stonden we met het spreekwoordelijke schaamrood op de kaken aan je bureau om uit te leggen dat we nog één heel klein proefje wilden doen, en dan was het echt klaar. Als ik er zo eens op terug kijk, is het wellicht een hele vrijdagmiddag-promotie geweest, maar met erg mooie

resultaten. Bedankt voor je overkoepelende visie en sturing, om mij terug op het pad te krijgen/houden/brengen! Prof. Verbrugh, Henri, bedankt voor het gestelde vertrouwen en het aanbieden van deze promotie-plek. De contacten die we hebben gehad tijdens deze promotie heb ik als kostbaar en nuttig ervaren. Aan mijn commissieleden, bedankt voor jullie tijd, en de commentaren op het voorstel voor het proefschrift, jullie adviezen hebben bijgedragen aan het geheel te verbeteren!

Ad, Wil, Annelies, bedankt voor alle ruimte die ik gekregen heb om mijn proefschrift af te werken, ik ervaar onze samenwerking altijd als heel prettig, en hoop dat dit in de toekomst nog lang door mag gaan! Aan alle co-auteurs, grote dank voor jullie mooie toevoegingen. Jos, Martin, Marjon, verdeeld over de gehele periode stonden jullie altijd klaar in Utrecht, om “even” een veel te lang experiment in te zetten, een kolommetje te draaien, of iets “over de massa te gooien”, super, dank jullie wel. Aan al mijn Rotterdamse collega's, wat houden jullie het al lang met me uit. Carla, Ger, Marian dank jullie wel voor al het klaarzet, bestel en afmaak werk, jullie weten altijd precies wat ik nodig heb! Sanne, blijkbaar werken we hier al weer 12 jaar, wat fijn dat je naast me staat als paranimf.

Aan alle anderen die mij hebben geholpen maar nog niet genoemd zijn, graag nodig ik u uit om langs te komen, dan zal ik mijn dank persoonlijk aan u uitspreken. Het is nu namelijk de hoogste tijd om hier “een nietje door heen te jassen”.

